EARLY PALEOZOIC POST-BREAKUP MAGMATISM ALONG THE CORDILLERAN MARGIN OF WESTERN NORTH AMERICA: NEW GEOCHRONOLOGICAL AND GEOCHEMICAL RESULTS FROM THE KECHIKA GROUP, YUKON, CANADA

By © Roderick William Campbell

A Thesis submitted to the School of Graduate Studies

in partial fulfilment of the requirements for the degree of

Master of Science, Department of Earth Sciences

Memorial University of Newfoundland

August 2018

St. John's   Newfoundland and Labrador

Abstract

Lower Paleozoic igneous rocks were emplaced along the Cordilleran margin of western North America following lithospheric breakup. Several competing rift models have been proposed to explain the significance of this magmatism to Cordilleran passive margin evolution. New field and laboratory studies of the Kechika group, south-central Yukon, were conducted to test these rift models and constrain the timing and tectonic setting of post-breakup magmatism. The Kechika group contains vent-proximal and sediment-sill facies that developed outboard of continental margin shelf and trough basins. Zircon U-Pb dates indicate that Kechika group rocks crystallized during the late Cambrian (488-483 Ma) and Early Ordovician (473 Ma). Whole-rock trace element and Nd-Hf isotope results are consistent with the low-degree partial melting of a lithospheric mantle source during margin-scale extension. Post-breakup rocks emplaced along the magma-poor North Atlantic margins, including the Orphan Knoll and Galicia Bank crustal blocks, are likely modern analogues for the Kechika group.

Acknowledgments

Table of Contents

List of Tables

Chapter 2

List of Figures

Chapter 1

Chapter 2

Chapter 3

List of Abbreviations

Back. R.	Backbone Ranges
CA-TIMS	Chemical Abrasion – Thermal Ionization Mass Spectrometry
CGVP	Charlie Gibbs volcanic province
CHUR	Chondritic Uniform Reservoir
CP	Cassiar platform
CT	Cassiar terrane
DR	Data repository
EBA	Eagle Bay assemblage
EBG	Eagle Bay greenstone
Fm	Formation (formal)
fm	formation (informal)
FZ	Fracture zone
GEM	Geo-mapping for Energy and Minerals
Gp	Group (formal)
gp	group (informal)
GSC	Geological Survey of Canada
GSSZ	Great Slave Lake Shear Zone
HFSE	High field strength elements
HREE	Heavy rare earth elements
HR-ICPMS	High resolution – Inductively coupled plasma-mass spectrometry
KP	Kakwa platform

KT	Kootenay trough
LIP	Large igneous province
Lk	Lake
LOI	Loss on ignition
LREE	Light rare earth elements
MCE	Misty Creek embayment
MC-ICPMS	Multi-collector - Inductively Coupled Plasma Mass Spectrometer
Mid-	Middle
MORB	Mid-ocean ridge basalt
MP	McEvoy platform
MP	MacDonald platform
MRE	Meilleur River embayment
MSWD	Mean square of weighted deviates
Mtns.	Mountains
NSERC	Natural Sciences and Engineering Research Council
NTS	National Topographic System
NWT	Northwest Territories
OA	Ogilvie Arch
OE	Ospika embayment
OIB	Ocean island basalt
PA	Purcell arch
RT	Richardson Trough

SEDEX	Sedimentary exhalative
Sil	Silurian
T_{DM}	Depleted mantle model age
Vol	Volcanics
WRE	White River embayment
YEG	Yukon Exploration and Geology
YTT	Yukon-Tanana terrane

List of Appendices

Appendix 1 – Compilation of Ediacaran-early Paleozoic magmatic ages and stratigraphic relationships

Appendix 2 – CA-TIMS zircon U-Pb isotope results

Appendix 3 – Whole-rock major and trace element geochemical results, and additional major-element geochemistry plots (TAS and AFM).

Appendix 4 – Whole-rock Nd-Hf isotope geochemical results

Chapter 1 Introduction and purpose of study

1.1 Introduction

The western or Cordilleran margin of ancestral North America formed after protracted Tonian-Ediacaran rifting and Ediacaran-Cambrian breakup of the supercontinent Rodinia (Stewart, 1972; Colpron et al., 2002; Li et al., 2008; Macdonald et al., 2012; Yonkee et al., 2014). Several rift-related rock units of uncertain tectonic significance outcrop within the Cryogenian-lower Paleozoic succession of western North America (e.g., Goodfellow et al., 1995), including Cambrian to Ordovician volcanic rocks that post-date the inferred rift to post-rift transition in southern British Columbia and Utah by up to 40 m.y. (Bond et al., 1985; Devlin and Bond, 1988; Hein and McMechan, 1994). These rocks are volumetrically minor compared to most large igneous provinces associated with continental breakup, which suggests that a plume-related origin is unlikely (e.g., Goodfellow et al., 1995). The oldest rocks that record the initiation of east-dipping subduction under the western Cordilleran margin are Late Devonian (e.g., Piercey et al., 2004, 2006) and possibly as old as Late Ordovician-Silurian in some of the outboard peri-Laurentian terranes (e.g., Pecha et al., 2016). Processes related to the establishment of the Cordilleran passive margin therefore appear the most likely cause of Cambrian to mid-Ordovician extension and magmatism along western North America. However, the processes responsible for producing these syn- to post-breakup volcanic rocks (Fig. 1-1) are poorly understood and not fully examined in published pure-shear and simple-shear rift models for the development of the Cordilleran margin (e.g., Goodfellow et al., 1997; Lund, 2008).

The primary objectives of this thesis are to constrain the physical volcanology, crystallization age, and mantle-crustal source of lower Paleozoic magmatic rocks of the Kechika group, south-central Yukon, Canada. These igneous rocks are representative

examples of post-breakup magmatism in the Canadian Cordillera (Goodfellow et al., 1997; Tempelman-Kluit, 2012). These new results, in addition to published data from coeval units in western North America, enable the examination of whether published pure-, simple-shear, and magma-poor rift scenarios for Cordilleran passive margin development (Fig. 1-2; e.g., Bond et al., 1985; Cecile et al., 1997; Yonkee et al., 2014; Beranek, 2017) can suitably explain post-breakup volcanism. The following sections provide a brief overview of the history of geological research in the central Pelly Mountains of south-central Yukon, the Neoproterozoic to early Paleozoic stratigraphy of western North America, and previously published rift models for the Cordilleran rifted margin.
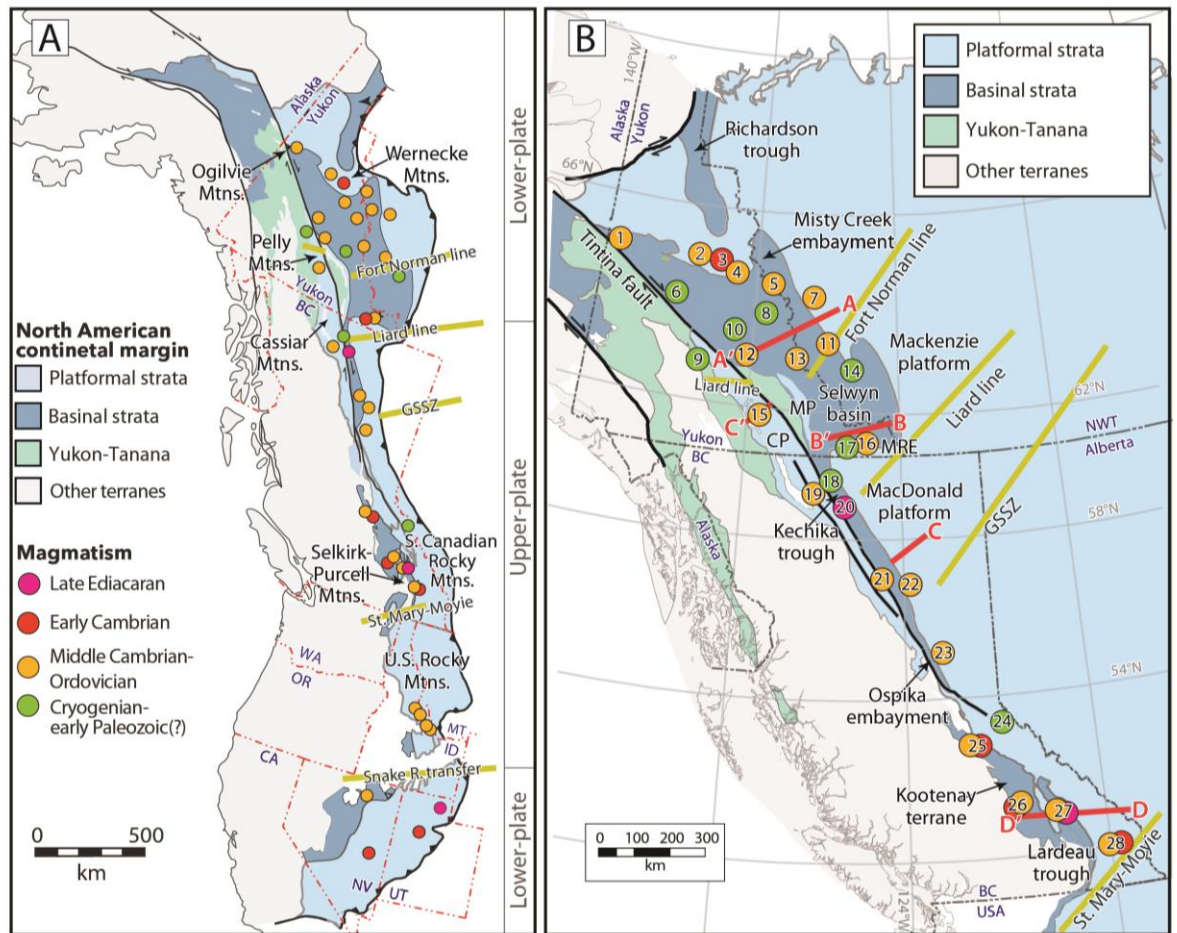
Figure 1-1(A) *Ediacaran to early Paleozoic magmatic rocks, tectonic elements, and crustal lineaments of the North American Cordillera adapted from Goodfellow et al. (1995), Lund (2008), and Colpron and Nelson (2009). Lower- and upper-plate divisions are from Lund (2008). (B) Map of the Canadian Cordillera highlighting the locations of Ediacaran to early Paleozoic magmatic rocks and key paleogeographic features. Numbers from 1-28 are references for Cordilleran margin magmatism provided in Appendix 1. CP - Cassiar platform, MP - McEvoy platform, MRE - Meilleur River embayment, Mtns. - Mountains, MP - McEvoy platform, R. - river.*

3
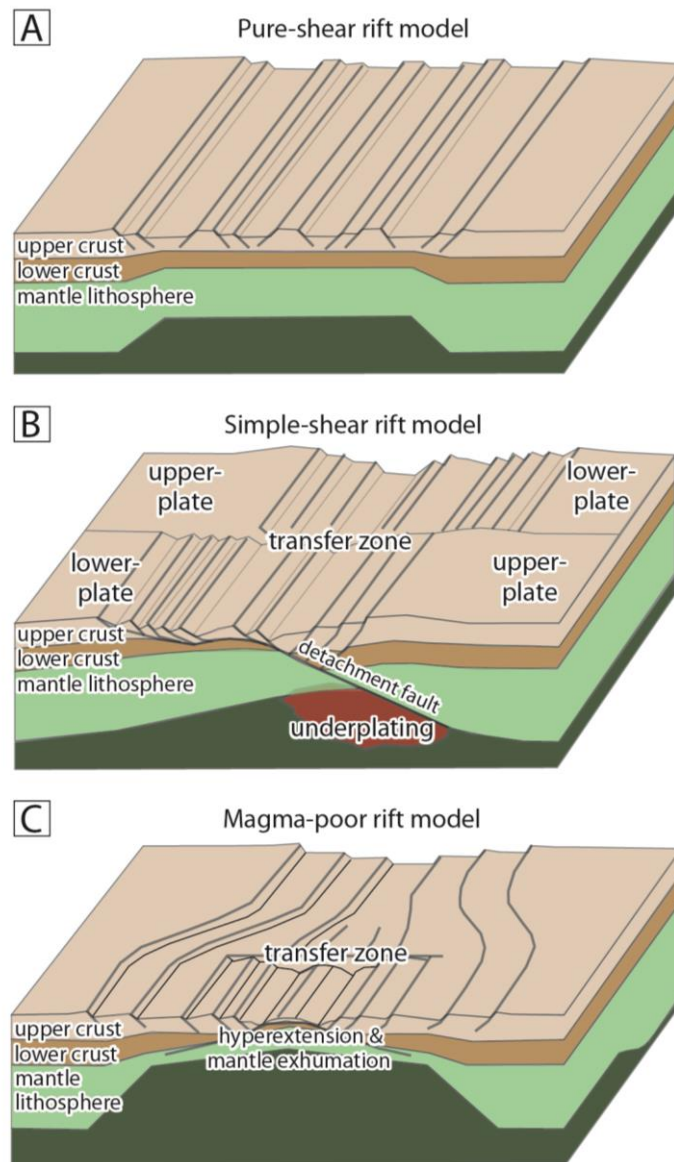
Figure 1-2 *Simplified kinematic models for Cordilleran rift evolution adapted from Yonkee et*

al. (2014). ***(A)*** *Pure-shear rift model with uniform, homogeneous thinning of crust and*

mantle based on McKenzie (1978). Margins that form through mostly pure-shear rifting

display very limited evidence for post-rift magmatism when contrasted with evidence for syn-

rift magmatism. ***(B)*** *Simple-shear rift model with heterogeneous thinning of upper and lower*

lithosphere based on Lister et al. (1986, 1991). Magmatism in the simple-shear model mostly

occurs beneath upper-plate margins during the syn- to post-rift phase. ***(C)*** *Magma-poor rift*

model with depth-dependent lithospheric thinning and necking based on Davis and Kusznir

(2004). This figure represents the period after lithospheric thinning but prior to lithospheric breakup. Syn-breakup magmatism is more voluminous in outboard areas where it is dominated by tholeiitic volcanism sourced from the depleted asthenospheric mantle. In contrast post-breakup magmatism occurs across the nascent plate boundary including throughout the rifted margin and is represented by low volume alkaline volcanism, derived from enriched mantle sources.

1.2 Geological Background

1.2.1 Cordilleran margin development

The cratonic basement of paleocontinent Laurentia (ancestral North America) formed as a result of the collision of Archean microcontinents, early Proterozoic island arcs, and related oceanic terranes around 1.96-1.81 Ga (Hoffman, 1988). The western Laurentian craton likely extends beneath the eastern half of the Yukon and British Columbia Cordillera (e.g., Nelson et al., 2013). This hypothesis is consistent with geophysical evidence for lithospheric scale lineaments that extend as far west as the Denali fault in southwestern Yukon (Hayward, 2015).

Rifting associated with the development of the Cordilleran margin began during Tonian-Cryogenian time (e.g., Christie-Blick and Levy, 1989; Yonkee et al., 2014). These early rift episodes thinned and weakened Cordilleran lithosphere (Yonkee et al., 2014) and were likely associated with strike-slip deformation in some regions of western Laurentia (Strauss et al., 2015). Within the Canadian Cordillera, initial rifting was represented by the Gunbarrel magmatic event (ca. 780 Ma; Harlan et al., 2003; Sandeman et al., 2014) and deposition of the 723-716 Ma Windermere Supergroup (e.g., Stewart, 1972; Link et al., 1993; Nelson et al., 2013). Rifting along the western Laurentian margin was contemporaneous with the emplacement of the Franklin magmatic event along the ancestral northern margin of North America (ca. 723 Ma; Heaman et al., 1992; Macdonald et al., 2010). Magmatic activity continued through the Cryogenian (ca. 720-640 Ma) in southeastern Yukon (Pigage and Mortensen, 2004), northern British Columbia (Ferri et al., 1999), and western United States (Lund et al., 2003, 2010; Fanning and Link, 2004).

Ediacaran to lower Cambrian siliciclastic and volcanic strata within southwestern Canada and western United States, including rift-related 570 Ma alkalic volcanic rocks (Colpron et al., 2002) of the Hamill Group in southeastern British Columbia, represent the

renewal of rifting along western Laurentia (e.g., Bond et al., 1985; Devlin and Bond, 1988). Bond and Kominz (1984) calculated thermal subsidence trends associated with crustal thinning from platformal strata along western North America as initiating around the Ediacaran-Cambrian boundary. These results led Bond et al. (1984, 1985) to conclude that this final short-lived rift phase at the Ediacaran-Cambrian boundary resulted in the breakup of Rodinia and opening of the Panthalassa Ocean.

1.2.2 Pure-shear rift models

Bond and Kominz (1984) and Bond et al. (1984, 1985) used the pure-shear rift model (Fig. 1-2A) of McKenzie (1978) to estimate subsidence patterns within stable shelf strata from the inner Cordilleran margin and therefore make predictions about the timing of lithospheric breakup along western North America. Pure-shear scenarios predict uniform homogenous lithospheric extension as per McKenzie (1978) that results in symmetric conjugate margins with syn-rift magmatism invoked to reduce lithospheric strength (e.g., Buck, 2004). Bond et al. (1985) concluded that lithospheric breakup was indicated by an inferred rift to post-rift transition between Ediacaran-Cambrian rift-related strata and the lower Paleozoic platformal strata that record thermal subsidence. The transition lies near the Cambrian Stage 2 (late Terreneuvian) to Cambrian Stage 3 (early Series 2) boundary in southeastern British Columbia and within Cambrian Stage 2 in the western United States (time scale of Cohen et al., 2017; e.g., Bond et al., 1985; Magwood and Pemberton, 1988; Hein and McMechan, 1994).

1.2.3 Simple-shear rift models

Christie-Blick and Levy (1989) concluded that heterogeneous deformation and/or detachment faults may be required to explain the contrast between the calculated subsidence

patterns of Bond et al. (1984) and the relative lack of field evidence for late Ediacaran-early Cambrian crustal extension. The postulated role of detachment faulting and recognition of asymmetry along western North America led to comparisons with the simple-shear or asymmetric rift scenarios of Lister et al. (1986, 1991) to explain the development of the Cordilleran margin (e.g., Cecile et al., 1997; Lund, 2008).

Lister et al. (1986; 1991) predicted various simple-shear rift scenarios that share several consistent characteristics (e.g., Fig. 1-2B). Within these rift scenarios intracontinental rifting and subsequent breakup are asymmetric because a detachment fault separates the upper- and lower-plate regions of a conjugate margin. At depth the detachment fault acts as a shallow-angle shear zone that allows for heterogeneous deformation between the upper crust and lower crust-lithospheric mantle. In this manner the asymmetric nature of lithospheric breakup leads to the upper-plate containing a greater proportion of cool, low-density upper crust. In contrast, the lower-plate margin has a greater proportion of hotter, high-density lower crust and lithospheric mantle.

Breakup occurs where asthenospheric uplift is greatest, usually beneath the upper-plate (Lister et al., 1991). Movement along the detachment fault separates the upper-plate from much of its lithospheric mantle and places it against hot lithospheric and asthenospheric mantle. This results in extension and contributes to thermal buoyancy along the margin (recorded as marginal plateaux/seamounts; Lister et al., 1991). Steeply dipping normal faults connect to the transfer and transform faults and may also connect to the shallow-dipping detachment fault close to the margin (Lister et al., 1986; Lund, 2008). Basaltic underplating occurs at the base of the crust due to partial melting of upwelling asthenospheric mantle (Lister et al., 1991). 'Passive margin' mountains are predicted as a surface expression of underplating and associated thermal uplift (Lister et al., 1991). The upper-plate contains areas

of localized extension, such as in the outer portion of the margin, but overall significantly less extension than the corresponding lower-plate (Lister et al., 1986).

The lower-plate comprises the footwall of the detachment fault (Lister et al., 1991) and may experience initial uplift associated with the removal of crustal material. However, the lower-plate features a much greater level of subsidence and significant crustal attenuation. Progressive extension leads to the rotation of crustal fault blocks (Lister et al., 1986; Cecile et al., 1997). Such extension and the lack of shallow crustal cover may expose crystalline rocks at the surface. The greater degrees of crustal extension may allow for long-lived marine basins to develop.

Simple-shear models predict that upper- and lower-plate margins create a zigzag geometry of promontories and embayments divided by transform and transfer faults (Lister et al., 1986, 1991). As these structures represent the locus of lithospheric extension, it is feasible that they are important for controlling the timing and locations of mafic magmatism and massive sulphide mineralization (e.g., Lund, 2008).

Published simple-shear rift models (e.g., Lister et al., 1986; 1991) do not specifically detail the expected timing and geochemical composition of igneous rocks within upper- and lower-plate margins. Lund (2008) concluded that transfer-transform zones may localize subsequent magmatism and that alkalic volcanism is characteristic of the upper-plate margin. However, lower Paleozoic alkalic volcanic rocks occur on both sides of the major crustal lineaments that are inferred to represent transfer-transform zones along the Cordilleran margin (Fig. 1-1). Furthermore, published simple-shear rift models do not provide a mechanism that can explain post-breakup volcanism.

1.2.4 Magma-poor rift models

Yonkee et al. (2014) and Beranek (2017) proposed magma-poor rift scenarios, comparable to those for the modern Newfoundland-Iberia rift system, to explain the development of the Cordilleran margin. Magma-poor rift margins (Fig. 1-2C) are characterized by extreme lithospheric thinning related to slow protracted extension, lithospheric rupture prior to breakup, and limited syn-rift volcanism (e.g., Peron-Pinvidic et al., 2013; Doré and Lundin, 2015). Although Figure 1-2C displays two symmetric rift margins these rift margins are often asymmetric in nature. The protracted rift history and minor syn-rift magmatism prior to lithospheric breakup have been related to the inability to produce sufficient magma at shallow crustal levels (e.g., Manatschal et al., 2015). The initial rift phase comprises a depth-dependent 'stretching' phase that can heat and weaken the lithosphere but does not lead to extensive lithospheric thinning (e.g., Peron-Pinvidic et al., 2013). This is succeeded by the 'thinning' phase where the lithosphere is thinned through detachment faulting in a manner comparable to the asymmetric, simple-shear rift scenario of Lister et al. (1986, 1991). Lithospheric thinning eventually reaches a point termed hyperextension where the entire crust is thinned to <10 km and is incapable of ductile deformation (e.g., Peron-Pinvidic et al., 2013). This enables faults to penetrate the crust and result in the exhumation of continental lithospheric mantle (e.g., Peron-Pinvidic et al., 2013). Lithospheric breakup is associated with the emplacement of a major magmatic pulse (e.g., Bronner et al., 2011; Eddy et al., 2017) and the generation of a lithospheric breakup surface (e.g., Soares et al., 2012). During the subsequent initiation of seafloor spreading, basin-wide alkalic magmatism can occur for at least 30 m.y. (e.g., Eddy et al., 2017) and be associated with the deposition of breakup-related clastic successions that preserve the transition from breakup to thermal subsidence (Soares et al., 2012).

Yonkee et al. (2014) suggested that the Tonian-early Paleozoic polyphase rift history of western North America was related to depth-dependent extension and lithospheric thinning

and necking. A magma-poor rift origin is supported by the recognition of exhumed mantle lithosphere beneath accreted terranes in northwestern Canada (e.g., Hayward, 2015) and similarities between the clastic breakup successions of the ancient Cordilleran and modern North Atlantic margins (Beranek, 2017). Therefore, post-breakup volcanic rocks emplaced along the modern Newfoundland-Iberia margins, including the Cretaceous Orphan seamount, offshore Newfoundland (e.g., Pe-Piper et al., 2013), may provide suitable modern analogues for early Paleozoic volcanism along the ancestral North American margin (Beranek, 2017).

1.2.5 Cambrian-Ordovician margin architecture

Ediacaran to Ordovician marine successions deposited along western North America are parts of a long-lived, proto-Pacific passive margin (e.g., Bond et al., 1985; Aitken, 1993b). Paleogeographic features aligned parallel to the coast along the length of the Cordilleran margin, including arches and basins, are terminated by a series of north- to northeast-trending crustal lineaments (Fig. 1-1; Cecile et al., 1997). Many of these crustal lineaments are ancient basement structures that were reactivated as transfer-transform or strike-slip fault zones during the creation of the margin, including the northeast-trending Liard line near southeastern Yukon and northeastern British Columbia (Fig. 1-1; Cecile et al., 1997). Cecile et al. (1997) concluded that the Liard line represents a first-order tectonic division that separates the Canadian Cordillera into a southern upper-plate margin and northern lower-plate margin (Fig. 1-1).

The southern upper-plate margin includes the deep-water Kechika trough, shallow-water Macdonald platform, most of the parautochthonous Cassiar terrane, and various other elements of the ancestral margin in southern and central British Columbia (Fig. 1-1; e.g., Cecile et al., 1997). Margin-parallel displacement of the Cassiar terrane occurred in the Cretaceous to Eocene with the 430 km of dextral movement along the Tintina fault (Gabrielse

et al., 2006). The continuation of crustal lineaments beyond the Tintina fault is indicated by gravity and magnetic studies in southwest Yukon (Hayward, 2015), consistent with previous suggestions that the Liard line extended through the northern part of the Cassiar terrane (Cecile et al., 1997). Lower Cambrian and Upper Ordovician-Silurian strata suggest that the Cassiar terrane represents lesser-extended continental crust that originated outboard of the Kechika trough (Fig. 1-1; e.g., Cecile and Norford, 1993; Cecile et al., 1997; Hayward, 2015). Cecile et al. (1997) suggested that the Cassiar platform was originally joined to the MacDonald platform at the southern edge of the Kechika trough by the shallow-water Kakwa platform. This southern boundary of the Kechika trough generally relates to the trace of the Hay River and Great Slave Lake fault systems (e.g., Cecile et al., 1997). Broad areas of positive relief and early Paleozoic unconformities along the southeastern Canadian Cordillera could be related to thermal uplift associated with igneous underplating (e.g., Lister et al., 1986, 1991).

The northern lower-plate margin includes the deep-water Selwyn basin and shallow-water Mackenzie platform that underlie central Yukon and western Northwest Territories (e.g., Fig. 1-1; Gordey and Anderson, 1993; Cecile et al., 1997). In addition to being wider than time-equivalent basins in the southern Canadian Cordillera, these elements typically contain complex, local paleogeographic features such as the Misty Creek embayment, Meilleur River embayment, Ogilvie arch, and McEvoy platform (e.g., Cecile et al., 1997; Gordey, 2013). A heterogenous style of rifting (e.g., Cecile et al., 1997), which may include detachment faulting, preserved blocks of relatively thicker continental crust represented by outboard platforms, arches and highs.

The Liard line exerted significant control on the pre-rift lithospheric architecture of northwestern Canada (Lund, 2008). Reactivation of the Liard line during Neoproterozoic-early Cambrian rifting is indicated by a change in the dominant trend of margin-

perpendicular structures from north to northeast and the asymmetry of outboard marginal

basins (e.g., Cecile et al., 1997). However, the extent of later reactivation is uncertain. Cecile

et al. (1997) concluded that varied preservation of lower Paleozoic rocks across the Liard line

is as much controlled by early Paleozoic tectonics and paleogeography, including extensional

faulting, as it is influenced by younger erosional factors.

1.2.6 Cambrian to Ordovician extension

The outer continental basins of the Cordilleran margin developed through periodic,

heterogeneous crustal extension rather than purely thermal subsidence (Fig. 1-1; e.g., Cecile

and Norford, 1993; Goodfellow et al., 1995; Cecile et al., 1997; Pyle and Barnes, 2003;

Pigage, 2004; Lund, 2008; Pigage et al., 2015). The Cambrian and Ordovician periods are

generally associated with regional facies changes throughout the northern Cordillera.

Transgressive cycles (MacIntyre, 1998) inferred by calcareous shale/argillaceous limestone

units overlain by black shale (typically associated with turbidite and/or chert units) are

recognized within the Kechika Formation to lower Road River Group in the Kechika trough

(Ferri et al., 1995; Pyle and Barnes, 2003), parts of the Lardeau Group in the Selkirk

Mountains (Logan and Colpron, 2006), and Rabbitkettle to Duo Lake formations of the

Selwyn basin (Gordey and Anderson, 1993). The Misty Creek embayment, which forms an

entrant of Selwyn basin into the Mackenzie platform, comprises Middle to Upper Ordovician

strata with a steer's-head rift profile and associated mafic alkaline volcanic rocks (Cecile et

al., 1997). A change from a broad transitional ramp to narrow Middle Ordovician platform is

also observed in the southern Canadian Cordillera (Cecile et al., 1997). Extensional faulting

was likely important for the development of second-order euxinic basins that were sites for

syngenetic and epigenetic sediment-hosted base-metal deposits in western Canada (e.g., the

Anvil District of central Yukon, Goodfellow, 2007). The scale and spatial extent of early

Paleozoic crustal extension and its importance on the development of Ordovician-Silurian architecture are uncertain.

1.2.7 Cambrian-Ordovician magmatism

The majority of early Paleozoic basins along the Cordilleran margin contain minor accumulations of mafic lava flows, sills, and related volcaniclastic rocks (Fig. 1-1; Appendix 1; e.g., Ospika Volcanics, Index Formation, Menzie Creek formation; Goodfellow et al., 1995). These pulses of magmatism have been linked to intermittent extension along the rifted margin (e.g., Lund et al., 2010; Millonig et al., 2012; Pyle, 2012; Nelson et al., 2013). This is evidenced by the spatial association of volcanic rocks with local normal faults (e.g., the Menzie Creek formation of central Yukon, Pigage, 2004; and the Crow Formation, southeastern Yukon; Pigage et al., 2015) and reactivated transfer-transform zones (e.g., Big Creek-Beaverhead belt and Snake River transfer fault, central Idaho; e.g., Link et al., 2017). These faults allowed volumetrically limited, incompatible element-enriched, low-degree partial melts to rise into the upper crust (e.g., Sykes, 1978; Goodfellow et al., 1995).

Cambrian-Ordovician volcanic rocks are herein divided into four geochemical groups. The majority are alkali basalt with OIB-like (ocean island basalt) geochemical signatures that mostly occur west of the continental margin platform-to-basin transition (e.g., Fig. 1-1; Goodfellow et al., 1995), either in the basin itself (e.g., Selwyn basin) or within embayments into the western platform (e.g., Misty Creek embayment). Highly incompatible element-enriched magmatic rocks are observed within extensional basins along the eastern Canadian Cordillera, including ultrapotassic to alkalic diatremes in eastern Yukon and western NWT (e.g., Mountain diatreme, Goodfellow et al., 1995), various alkalic – carbonatite diatremes in southeastern British Columbia (e.g., Mt. Dingley Diatreme, Norford and Cecile, 1994; Millonig et al., 2012), and alkaline intrusive rocks in Idaho (e.g., Big Creek-Beaverhead belt,

Lund et al., 2010). Cambrian tholeiites with MORB-like (mid-ocean ridge basalt) signatures underlie or are laterally equivalent to Cambrian-Ordovician alkali basalts with OIB-like signatures within the Lardeau Group and the Eagle Bay assemblage of the Kootenay terrane of southeastern British Columbia (e.g., Logan and Colpron, 2006; Paradis et al., 2006). Volumetrically limited felsic volcanic rocks occur within central and southeast Yukon in association with alkali basalts (e.g., Pigage et al., 2015).

1.2.8 Geology of the Pelly Mountains, south-central Yukon

The Hudson Bay Company funded the first geological fieldwork in the Pelly Mountains during the 1850s (Tempelman-Kluit, 2012). From this initial work until the 1950s, the understanding of central Yukon geology was based upon limited route transects. In the 1950s, the GSC commissioned a broader survey throughout central Yukon named Operation Pelly. The current stratigraphic nomenclature within the Pelly Mountains arose mostly through 1:50 000 and 1:250 000 scale mapping during the 1970s in the Quiet Lake and Finlayson Lake map areas (NTS 105 F & G; Gordey, 1981; Tempelman-Kluit, 2012). Paleozoic rock units in the Pelly Mountains were defined prior to the North American Stratigraphic Code and have not been correlated with potentially equivalent strata of the Kechika, McEvoy, and Cassiar Mountain groups in British Columbia. The Paleozoic stratigraphy of the Pelly Mountains defined by Templeman-Kluit (2012) is illustrated in Figure 1-3 and from bottom to top consists of four regional units.

The Ketza group comprises mostly shallow-water, upper Neoproterozoic(?) to lower Cambrian rocks that are the oldest exposed units of the Cassiar terrane in Yukon. The basal Pass Peak formation consists of quartzite and fine-grained siliciclastic rocks, whereas the overlying McConnell River formation contains calcareous to pyritic mudstone and carbonate lenses with archaeocyathid-bearing mounds (Read, 1980; Tempelman-Kluit, 2012).

Upper Cambrian to Ordovician strata of the Kechika group sit unconformably on the Ketza group (Tempelman-Kluit, 2012). The Kechika group consists of four formations that Tempelman-Kluit (2012) described as "laterally equivalent" and "interfingered". The four formations from NE to SW (Fig. 1-4A, B) are the Ram, Cloutier, Groundhog, and Gray Creek formations (Tempelman-Kluit, 2012). These units are discontinuously capped by the Magundy formation, which contains an almost complete sequence of Ordovician graptolites (Gordey, 1981; Tempelman-Kluit, 2012). Limited Cambrian to Ordovician fossil ages within the Kechika group are the only pre-existing constraints on the timing of mafic magmatism (Tempelman-Kluit, 2012).

The Cloutier formation consists of at least 500 m of basalt and volcaniclastic rocks that are intercalated with variably metamorphosed grey to black argillaceous shale, silty limestone, and tuffaceous shale. Primary volcanic facies include 2-20 m-thick units of vesicular to amygdaloidal massive flows, pillow lavas, and sediment-matrix basalt breccia. Sediment-matrix basalt breccia units typically contain amoeboid to angular lapilli-sized clasts and are interpreted as fluidal peperite units (e.g., Skilling et al., 2002). The volcaniclastic facies includes at least 60 m thick units of lapilli tuff, tuffaceous sandstone, monomictic basalt breccia, and volcanic conglomerate. The monomictic basalt breccias feature lapilli to bomb-sized clasts. Tempelman-Kluit (2012) inferred that the concentration of eruptive components in the Cloutier formation represented a volcanic centre that decreased to the northeast and southwest and transitioned laterally into the Groundhog and Ram formations.

The Groundhog formation is at least 800 m thick and contains fine-grained argillaceous and calcareous shale and siltstone units that are intercalated with minor volcanic and volcaniclastic rocks. Volcanic and volcaniclastic facies include tuffaceous sandstone, shale, and vesicular to amygdaloidal basalt flows. Pyroxene gabbro sills and stocks (1 to 30 m thick) intrude these layered units throughout the Pelly Mountains. The Groundhog

formation features large mafic stocks and sills, but volcanic facies comparable to the Cloutier

formation only occur within the upper Groundhog formation (Tempelman-Kluit, 2012).

The regionally extensive Magundy formation mostly contains black, graptolite-

bearing shale, but also contains minor quartz sandstone, greenstone, and tuff units that are

comparable with those of the Cloutier formation (Gordey, 1981).

The Ram formation is bounded by the Tintina and St. Cyr faults and contains

calcareous slate with local minor limestone. The Gray Creek formation consists of

greenstone, biotite quartz schist, and black graphitic muscovite siltstone that Tempelman-

Kluit (2012) correlated with more metamorphosed equivalents of the Cloutier and Pass Peak,

formations, respectively (Tempelman-Kluit, 2012).

The Harvey group is named for poorly understood, variably deformed and

metamorphosed siliciclastic, carbonate, and volcanic rocks that crop out between the Tintina

and St. Cyr faults (Fig. 1-4). Tempelman-Kluit (2012) proposed that the lower two units

(Canyon and Danger formations) correlate with Kechika and Askin group strata, respectively

(Fig. 1-3).

Shallow-water sedimentary rocks and volumetrically limited volcanic strata of the

Silurian Askin group overlie the Kechika group. Within the Pelly Mountains, the basal Askin

group (Orange Volcanics member, Platy Siltstone formation of Tempelman-Kluit, 2012)

contains mafic to intermediate lava flows, volcanic breccia, and tuff (Campbell and Beranek,

2017). The Askin group, along with the Sandpile Formation in the Cassiar Mountains,

comprises part of the Silurian-Devonian Cassiar platform (Gabrielse, 1963, 1998; Cecile et

al., 1997; Tempelman-Kluit, 2012).
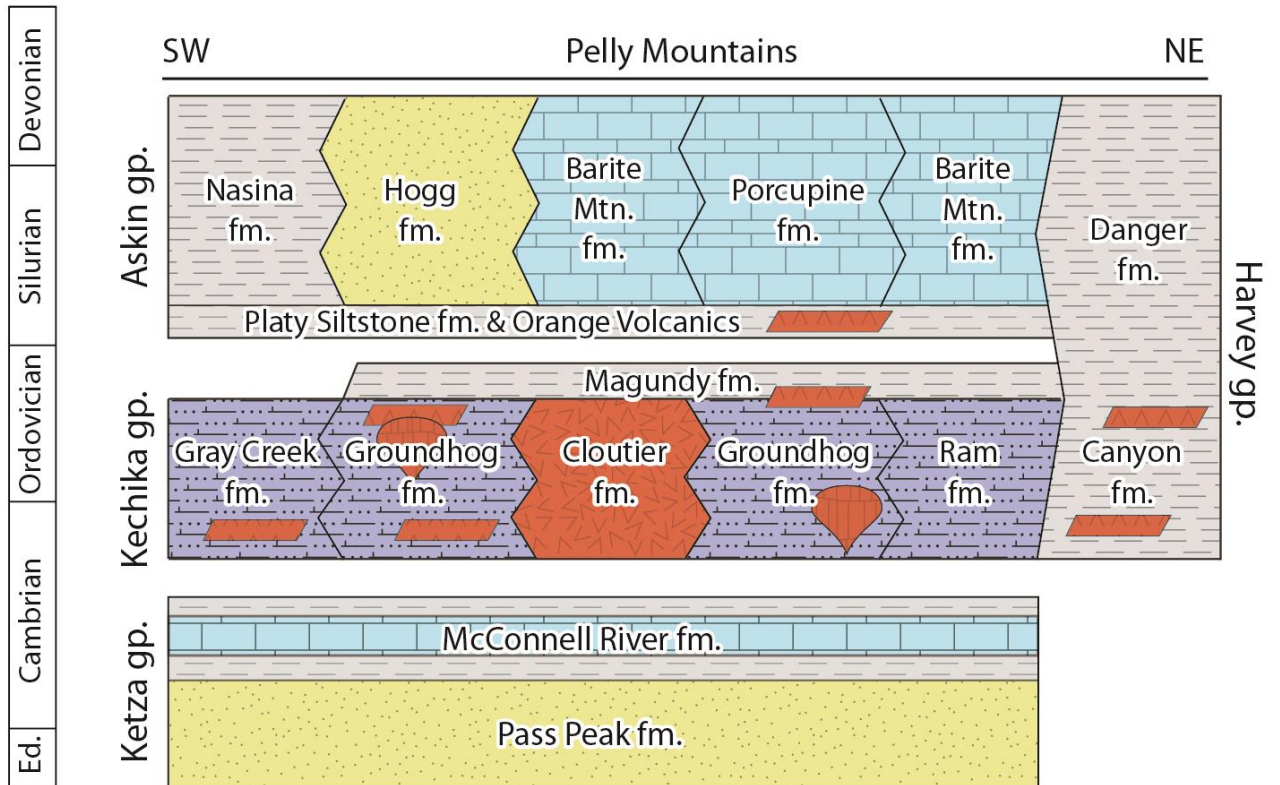
Figure 1-3 Paleozoic stratigraphy of the Pelly Mountains compiled by Tempelman-Kluit (2012). Abbreviations: Ank = Ankerite; Ed = Ediacaran; fm = formation; gp = group; Miss = Mississippian; Mtn = mountain; Sil = Siliceous; and Sl = Slate. Grey polygons in Kechika group represent mafic sills.
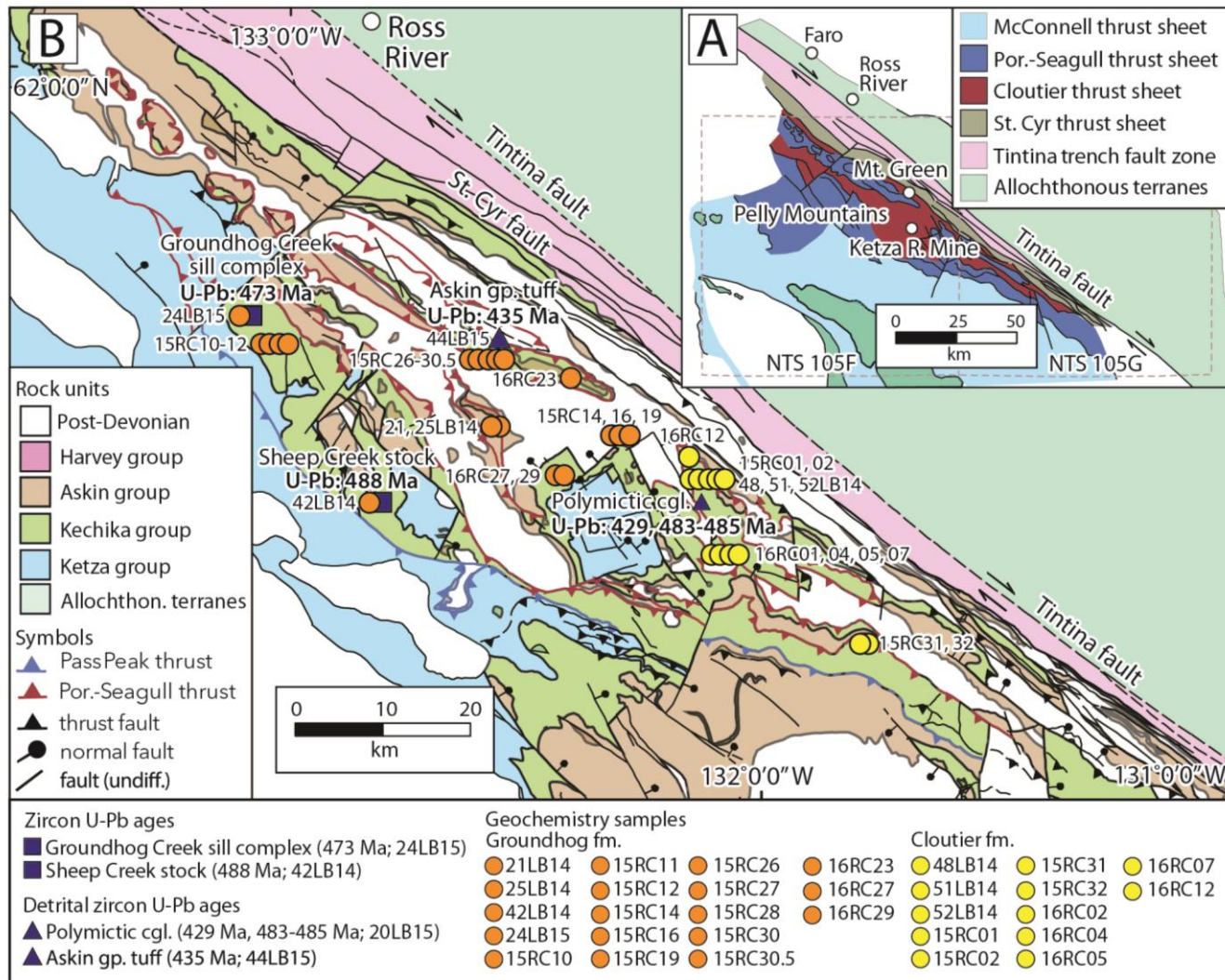
Figure 1-4 (a) *Distribution of thrust sheets within the Quiet Lake (NTS 105F) and Finlayson Lake (NTS 105G) map areas, Pelly Mountains, south-central Yukon (modified from Tempelman-Kluit, 2012).* *(b)* *Distribution of Ketza, Kechika and Askin group rocks in the Pelly Mountains (modified from Tempelman-Kluit, 2012). Numbers refer to localities where samples were collected for geochronology and geochemistry, and are referenced in Appendix 2, 3, and 4.*

1.3 Thesis Objectives

The aim of this thesis is to constrain the precise timing, depositional environment, and lithogeochemistry of Kechika group volcanic rocks and intrusive equivalents. New field and laboratory results, in conjunction with a review of available data on coeval volcanic strata, provide opportunities to test and develop ideas for early Paleozoic rifting and post-breakup volcanism along the Cordilleran margin. The following points highlight the field and analytical objectives for this study:

1) Constrain the physical stratigraphy and depositional setting of Kechika group using lithofacies observations and facies relationships (e.g., Cas and Wright, 1988). This objective was completed by field analysis of Groundhog and Cloutier formation stratigraphy in the central Pelly Mountains during the summers of 2015 and 2016. These field results were published in *Yukon Exploration and Geology 2016* (Campbell and Beranek, 2017) and appear in modified form in Chapter 2.

2) Constrain the petrogenesis, tectonic setting, and timing of Kechika group magmatism. This objective was achieved through high-precision CA-TIMS zircon U-Pb geochronology, whole-rock major and trace element lithogeochemistry, whole-rock Hf-Nd isotope geochemistry, and thin section petrography.

3) Use the available data to examine the published rift models for western North America and hypotheses for post-breakup magmatism and sedimentation in the Canadian Cordillera. This analysis required a detailed understanding of potentially analogous post-breakup strata emplaced along modern rifted margins for the process of comparison.

4) Write, submit, and publish a peer-reviewed, international journal article that encompasses the objectives listed in points 2 and 3. The submitted version of the manuscript appears as Chapter 3 of this thesis.

1.4 Methods

1.4.1 Fieldwork and sample collection

Helicopter-supported fieldwork and sample collection in the Pelly Mountains of south-central Yukon, ~20-50 km south and southeast of Ross River (Fig. 1-4), were completed during July 2015 and June 2016. The first field season focused on contact relationships, primary lithofacies, and the collection of rock samples for whole-rock geochemistry and thin section petrography. The second field season allowed for the construction of detailed stratigraphic logs and further sample collection of Groundhog and Cloutier formation facies.

1.4.2 CA-TIMS zircon U-Pb geochronology

Zircons from five rock samples, selected to characterize the precise timing of Kechika group magmatism, were analysed by CA-TIMS U-Pb geochronology at the Pacific Centre for Isotopic and Geochemical Research, University of British Columbia, following the procedures outlined in Scoates and Friedman (2008). Three Kechika group intrusive rocks were selected to determine the timing and duration of Kechika group magmatism and two detrital zircon samples were selected to constrain the maximum depositional age of uppermost Kechika group-lowermost Askin group strata (Appendix 2; see Fig. 1-4 for sample locations).

Zircon crystals were concentrated from rock samples using standard crushing, gravimetric, and magnetic separation methods, handpicked in alcohol under the binocular microscope, and annealed in quartz glass crucibles at 900ºC for 60 hours. Annealed zircons were rinsed in ultrapure acetone and water, transferred into screwtop beakers, and chemically abraded in ultrapure HF and HNO_3 at ~175ºC for 12 hours. The remaining zircon crystals were separated from the leachate, rinsed, weighed, and dissolved in HF and HNO_3 at ~240ºC for 40 hours. Ion-exchange column techniques were used to separate and purify Pb and U. Isotopic ratios were measured with a modified single-collector VG-54R thermal ionization mass spectrometer equipped with analog Daly photomultipliers. U-Pb isotopic data were calibrated by replicate analyses of the NBS-982 reference material and values recommended by Thirwall (2000). Data reduction was completed with the Microsoft Excel software of Schmitz and Schoene (2007). The Isoplot program of Ludwig (2003) was used to make Wetherill concordia diagrams and calculate weighted mean averages and MSWD (mean square of weighted deviates) values.

1.4.3 Major, trace and Nd isotope geochemistry

Thirty samples were collected from intrusive, volcanic, and volcaniclastic units of the Groundhog and Cloutier formations for whole-rock major- and trace-element geochemical analysis (Appendix 3). Samples were photographed, washed, and trimmed with a rock saw to remove weathered material. Major element oxide concentrations were acquired at Activation Laboratories in Ancaster, Ontario, by fused-bead x-ray fluorescence. Trace element concentrations for six samples were acquired at the Pacific Centre for Isotopic and Geochemical Research by HR-ICPMS (Element 2, Thermo Finnigan, Germany), whereas twenty-four samples were analyzed at Activation Laboratories using a research grade analytical package (4LITHO RESEARCH package).

Eight of the samples were selected for whole-rock Nd and Hf isotope geochemistry (Appendix 4). Isotopic analyses were carried out at the Pacific Centre for Isotopic and Geochemical Research on a Nu Plasma II MC-ICP-MS (Nu Instruments Ltd, UK). Sample introduction followed the methods described in Weis et al. (2006, 2007) and occurred under dry plasma conditions using a membrane desolvator (DSN-100). For each analytical session, the standard solution JDNi (for Nd analyses) yielded average values of $^{143}Nd/^{144}Nd = 0.512088 \pm 0.000008$ ($n = 24$), and $^{143}Nd/^{144}Nd = 0.282157 \pm 0.000011$ ($n = 41$) for 2014 and 2015 samples, respectively. The JMC 475 standard solution (for Hf analyses) yielded average values of $^{176}Hf/^{177}Hf = 0.282156 \pm 0.000004$ ($n = 11$), and $^{176}Hf/^{177}Hf = 0.282157 \pm 0.000011$ ($n = 41$) for 2014 and 2015 samples, respectively. The results were corrected for instrumentation mass fractionation by exponentially normalizing to $^{146}Nd/^{144}Nd = 0.7219$ (O'Nions et al., 1979), and $^{179}Hf/^{177}Hf = 0.7325$ (Patchett and Tatsumoto, 1981).

1.5 Co-Authorship Statement

Roderick W. Campbell:

The fieldwork portion of this thesis was completed with the assistance of Luke Beranek and Stephen Piercey. I am the lead author of both manuscripts (Chapters 2 and 3) and the project itself benefited from continuous discussion and constructive criticism from my supervisor Luke Beranek. Co-authors Luke Beranek, Stephen Piercey, and Richard Friedman reviewed and provided edits for the Chapter 3 manuscript.

Luke Beranek:

Luke Beranek designed this M.Sc. project, assisted with fieldwork and sample collection, and provided commentary and guidance throughout all aspects of this thesis.

Beranek was the primary editor on the two manuscripts, wrote parts of the zircon U-Pb results in Chapter 3, and aided the completion of this project.

Stephen Piercey:

Steve Piercey assisted with fieldwork and sample collection, provided insight on the physical stratigraphy and geochemistry of basalt units, and aided Chapter 3 through discussion and review.

Richard Friedman:

Richard Friedman completed the zircon U-Pb analysis at the Pacific Centre for Isotopic and Geochemical Research, University of British Columbia, and provided edits for the Chapter 3 manuscript.

1.6 Thesis presentation

This thesis consists of four chapters and four appendices. Chapter 1 presents a brief geological background on the Cordilleran margin, pre-existing rift models, previous work on lower Paleozoic rocks in the central Pelly Mountains, an overview of the purpose of the thesis and the methods used in this study.

Chapter 2 is a modified version of a geological fieldwork article that was published in *Yukon Exploration and Geology 2016* by Campbell and Beranek (2017). This article reported results from two field seasons and included detailed descriptions of observed lithofacies and stratigraphic logs.

Chapter 3 is intended for publication in an international peer-reviewed journal with the author list being Campbell, Beranek, Piercey, and Friedman. This chapter presents new geochronological and geochemical results from the Kechika group and provides a detailed

overview of the Cordilleran margin and published rift models. This chapter discusses the validity of published rift models to explain the origin of Kechika group magmatic rocks and post-breakup tectonism along the Cordilleran margin.

Chapter 4 presents a summary of the thesis results and outlines some unanswered questions and areas for future research.

The appendices include new compilations and supporting data for the thesis. Appendix 1 contains a compilation of Ediacaran-early Paleozoic magmatic ages and stratigraphic relationships along the Cordilleran margin. Appendix 2 contains the CA-TIMS zircon U-Pb isotope results from five rocks in the Pelly Mountains. Appendix 3 contains whole-rock major and trace element geochemical results of 30 rock samples. Appendix 4 contains the whole-rock Nd-Hf isotope geochemical results from eight rock samples.

Chapter 2 Volcanic stratigraphy of the Cambrian-Ordovician Kechika group, Pelly Mountains, south-central Yukon*

2.1 Abstract

Volcanic rocks occur throughout the lower Paleozoic passive margin successions of western Canada. The tectonic significance of post-breakup magmatism is uncertain; however, some volcanic rocks are spatially associated with margin-parallel normal faults. At the plate-scale, such magmatism is consistent with asymmetric rift models for passive margins, including those with lineaments or transform-transfer zones that form at high angles to the rifted margin. A two-year project was conducted to define the stratigraphy of post-breakup volcanism in the Pelly Mountains, south-central Yukon, and test genetic relationships with the adjacent Liard line lineament. Field studies targeted Cambrian-Ordovician volcanic strata of the Kechika group in the Quiet Lake map area (NTS 105F). Observed lithofacies are indicative of submarine volcanic edifices and sediment-sill complexes that develop during continental extension. Analogous margin-parallel extension is recognized along the length of the Canadian Cordillera, but the influence of the Liard line on Cambrian-Ordovician magmatism requires further testing.

2.2 Introduction

The ancestral Pacific margin of western North America (Fig. 2-1) was created during the protracted rifting of Rodinia (e.g., Bond et al., 1984, 1985). An initial Neoproterozoic rifting event in the Canadian Cordillera is in part recorded by the Franklin LIP and Windermere Supergroup (Heaman et al., 1992; Colpron et al., 2002). The Hamill and Gog groups are the inferred products of the final stage of continental breakup within the southern Canadian Rocky Mountains and the Selkirk and Purcell Mountains, southeastern British Columbia (Fig. 2-1; e.g., Bond et al., 1985; Devlin and Bond, 1988; Nelson et al., 2013). In this region, the timing of final rifting is constrained by late Ediacaran (ca. 570 Ma) volcanic rocks of the Hamill Group (Colpron et al., 2002). The rift to post-rift transition did not occur until at least the early Cambrian based on Tommotian to Atdabanian (Terreneuvian to Cambrian Series 2) fossils in the Gog Group and McNaughton Formation (Bond et al., 1985; Magwood and Pemberton, 1988; Hein and McMechan, 1994) and thermal subsidence trends (e.g., Bond and Kominz, 1984). Ediacaran to lower Cambrian strata similarly record the establishment of shallow-water Mackenzie platform and deep-water Selwyn basin in eastern Yukon and adjacent Northwest Territories (Fig. 2-1; e.g., Gordey and Anderson, 1993; Moynihan, 2014).
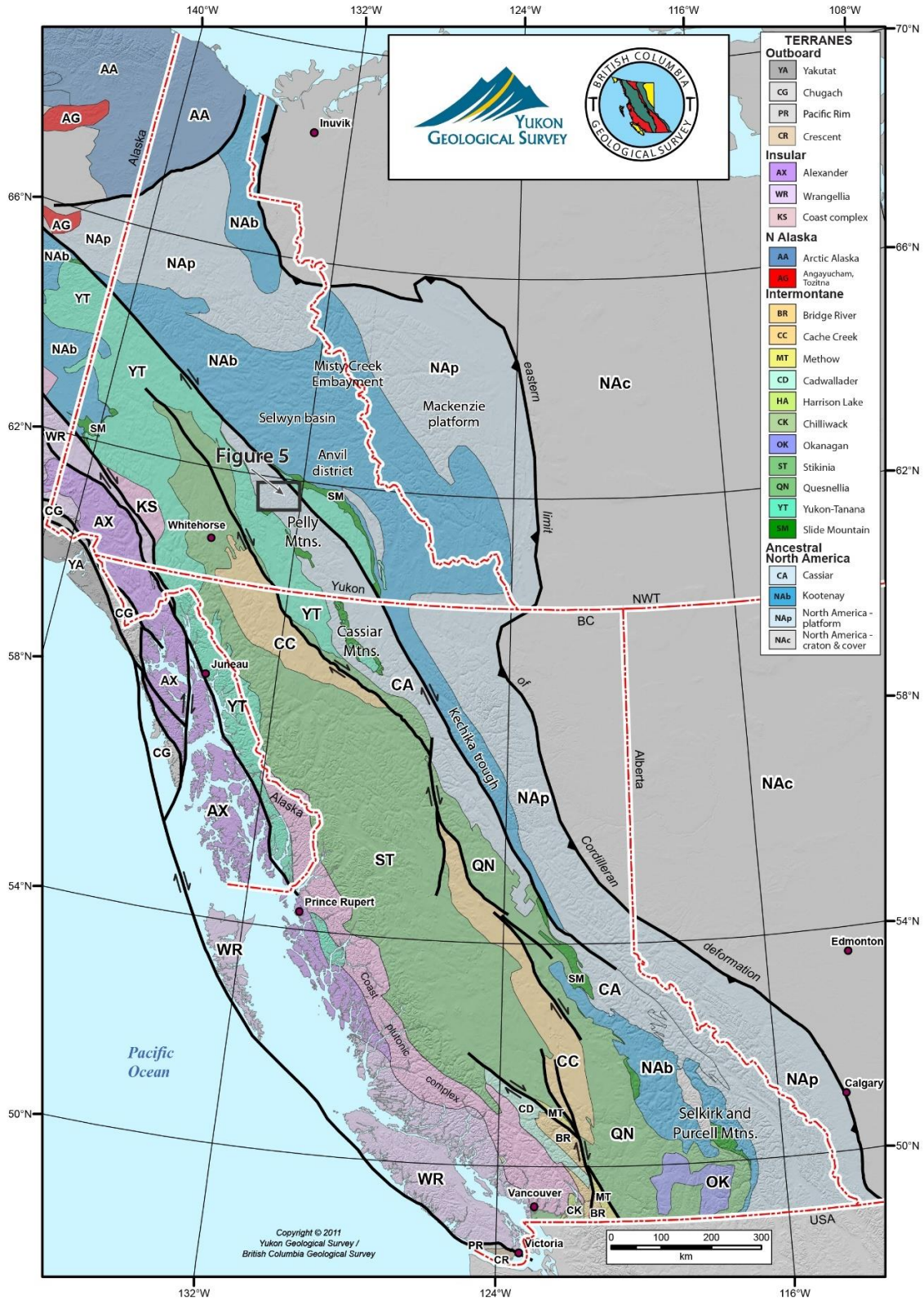
Figure 2-1 Terrane map of the Canadian Cordillera (modified from Colpron and Nelson,

2011).

Magmatism along the western Laurentian margin did not cease with continental breakup and remains an outstanding problem in Cordilleran geology. For example, upper Cambrian-Ordovician volcanic rocks observed along the length of the North American Cordillera (e.g., Goodfellow et al., 1995; Lund et al., 2010; Millonig et al., 2012; Pigage et al., 2012) are seemingly inconsistent with simplistic models for post-breakup, passive margin sedimentation (e.g., Aitken, 1993). Goodfellow et al. (1995) suggested a spatial association between lower Paleozoic volcanic rocks and margin-parallel normal faults that define the western extent of the basin to the basin-platform transition zone (2- 2; Hayward, 2015). Early Paleozoic volcanism in the region has therefore been linked to periodic extension (e.g., Fritz et al., 1991; MacIntyre, 1998; Pyle and Barnes, 2003). For example, Marmot Formation rocks in the Misty Creek embayment, Northwest Territories (Fig. 2-1) are associated with a "steer's head" rift profile (Cecile et al., 1982, 1997; Leslie, 2009). Menzie Creek formation volcanic rocks in the Anvil District, central Yukon (Fig. 2-1), are adjacent to sedimentary exhalative (SEDEX) base-metal deposits (Faro, Grum, Vangorda and others) and probably related to local faulting (e.g., Pigage, 2004; Cobbett, 2016). Early Paleozoic faults allowed volumetrically small, incompatible element-enriched, low degree partial mantle melts to erupt onto the surface or crystallize in the upper crust (Goodfellow et al., 1995; Millonig et al., 2012).

The inferred volume of early Paleozoic magmatism is minor compared to that associated with continental breakup and no other major tectonic event is recorded within Cambrian-Ordovician rocks along the ancient Pacific margin (e.g., Bond et al., 1984; Devlin and Bond, 1988; Cecile and Norford, 1993). Periodic, late Cambrian to Ordovician volcanism is therefore unlikely to result from subduction or plume-related magmatism. Instead, post-breakup magmatism is consistent with asymmetric rift models for passive continental margins (e.g., Lister et al., 1986, 1991). Such models combine

lithospheric-scale detachment faults and related low-angle shear zones with crustal thinning to achieve continental breakup. In most versions of this model, the hanging wall of the detachment fault, termed the upper-plate, undergoes less extension and is dominated by upper crust. Conversely the footwall, termed the lower-plate, undergoes a greater degree of extension and is more dominated by lower and middle crust (Fig. 2-3; e.g., Lister et al., 1986). In some of these rift scenarios the majority of the lithospheric mantle is removed from beneath the upper-plate margin and replaced with asthenospheric mantle (e.g., Lister et al., 1991). Along the length of a rifted margin, upper and lower-plate segments are separated by lithospheric-scale transform-transfer faults (e.g., Lister et al., 1986). Such structural zones may provide a pathway for mantle-derived melts (e.g., Corti et al., 2002). Asymmetric rifting processes have been applied to the Paleozoic Cordilleran margin to explain the control of lithospheric-scale structures on extension and regional paleogeography (Fig. 2-2; e.g., Cecile et al., 1997; Lund, 2008).

In order to understand the implications of post-breakup magmatism along the Cordilleran margin, a field project was designed to characterize the physical stratigraphy of Cambrian-Ordovician volcanic rocks in the Pelly Mountains, south-central Yukon. These rocks form part of the Cassiar terrane, a parautochthonous fragment of ancestral North America (Fig. 2-1) that underwent at least 430 km of dextral displacement along the Tintina fault (Gabrielse et al., 2006). Our fieldwork targeted outcrops of the Kechika group (informal) in the Pass Peak (105F/9) and Cloutier Creek (105F/10) map areas of the Quiet Lake 1:250 000 sheet, south of the Tintina Trench and community of Ross River. Cecile et al. (1997) interpreted that a northeast-trending, transform-transfer zone named the Liard line is present in the Pelly Mountains, placing most of the southern Cassiar terrane within an upper- plate setting (Fig. 2-2). The Liard line is likely a

reactivated ancient basement structure (Hayward, 2015) that also controlled the northern margin of the Proterozoic Muskwa basin (Lund, 2008) and recent neotectonic activity in the northern Cordillera (Audet et al., 2016). Because the Liard line is spatially associated with Neoproterozoic and Eocene alkaline magmatism in southeastern Yukon (Pigage and Mortensen, 2004), it is important to consider its influence on Kechika group volcanism in the Pelly Mountains.
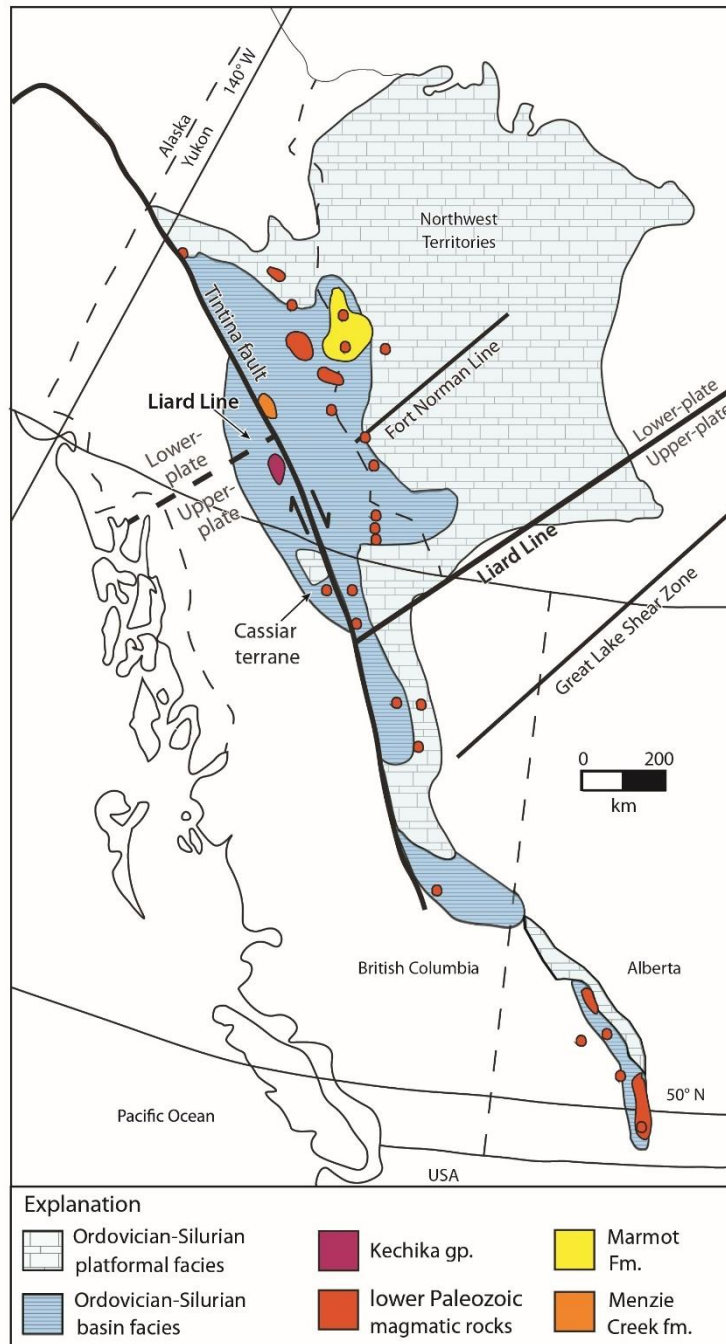
Figure 2-2 *Distribution of major faults, lower Paleozoic igneous rocks and Ordovician-Silurian paleogeography in the Canadian Cordillera (modified from Goodfellow et al., 1995; Cecile et al., 1997). The division between the northern lower-plate and the southern upper-plate is an inferred ancestral transfer fault, the Liard line, which is offset in the west due to dextral movement along the Tintina fault.*
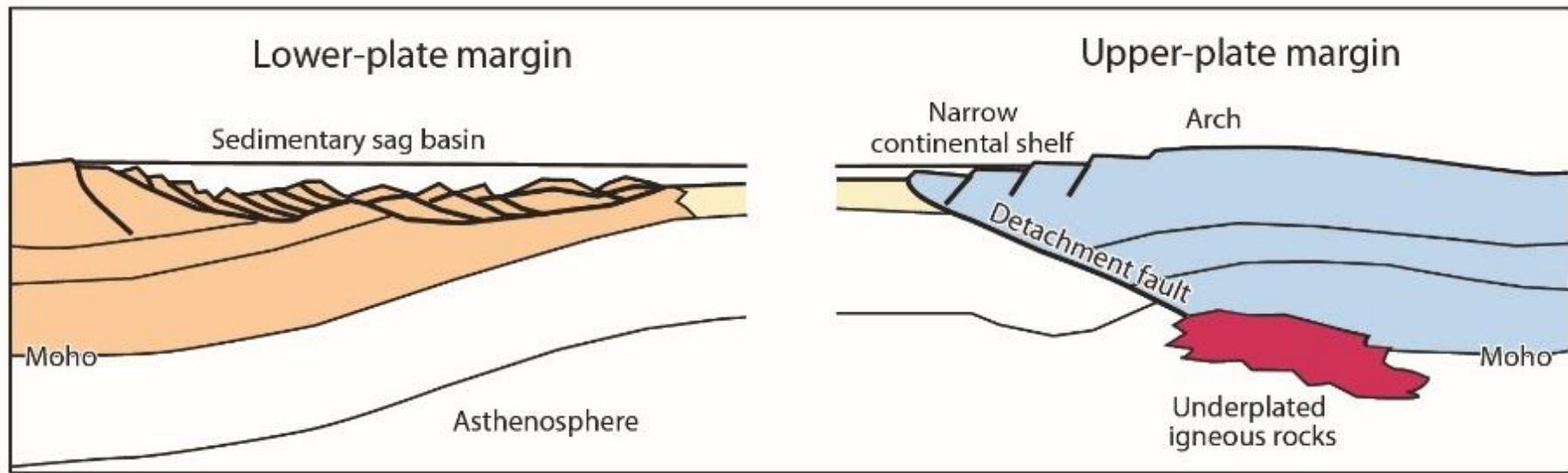
Figure 2-3 *Schematic cross section of an asymmetric rift system (modified from Lister et al., 1991; Lund, 2008).*

2.3 Geological framework

2.3.1 Ketza group

The Ketza group consists of upper Neoproterozoic to lower Cambrian rocks that are the oldest exposed units of the Cassiar terrane in the Quiet Lake map area (Figs. 2-4 and 2-5a; Tempelman-Kluit, 2012). The basal Pass Peak formation is 200-700 m thick and comprises green to tan shale, siltstone, and quartzite. The overlying McConnell River formation is 600-800 m-thick and consists of calcareous mudstone and siltstone, carbonate lenses with archaeocyathid-bearing mounds, and black pyritic slate (Tempelman-Kluit, 2012). The late early Cambrian archaeocyathid mounds are also recognized within post- rift successions of the southern Canadian Cordillera (e.g., Devlin, 1989). In the Cloutier Creek map area, the upper contact of the Ketza group near the Ketza River Mine (Fig. 2-5b) is poorly exposed and structurally deformed. A distinct mid-Cambrian fossil gap between upper Ketza and lower Kechika group strata suggests the presence of an unconformity (Tempelman-Kluit, 2012). A similar mid-Cambrian unconformity has been inferred within the Cassiar terrane of the Cassiar Mountains and the Kechika trough of the northern Canadian Rocky Mountains (Fig. 2-1; e.g., Gabrielse, 1963; Taylor and Stott, 1973; Gabrielse et al., 2006). In the Cassiar Mountains, the contact between the lower Cambrian Rosella Formation and upper Cambrian to Ordovician Kechika group is obscured by faulting (Gabrielse, 1963; Fritz et al., 1991). In the Canadian Rockies, mid- to late Cambrian deposition occurred within an active horst and graben system named the Kechika graben (e.g., Gabrielse and Taylor, 1982; Post and Long, 2008). This graben later evolved into the Kechika trough (Post and Long, 2008).
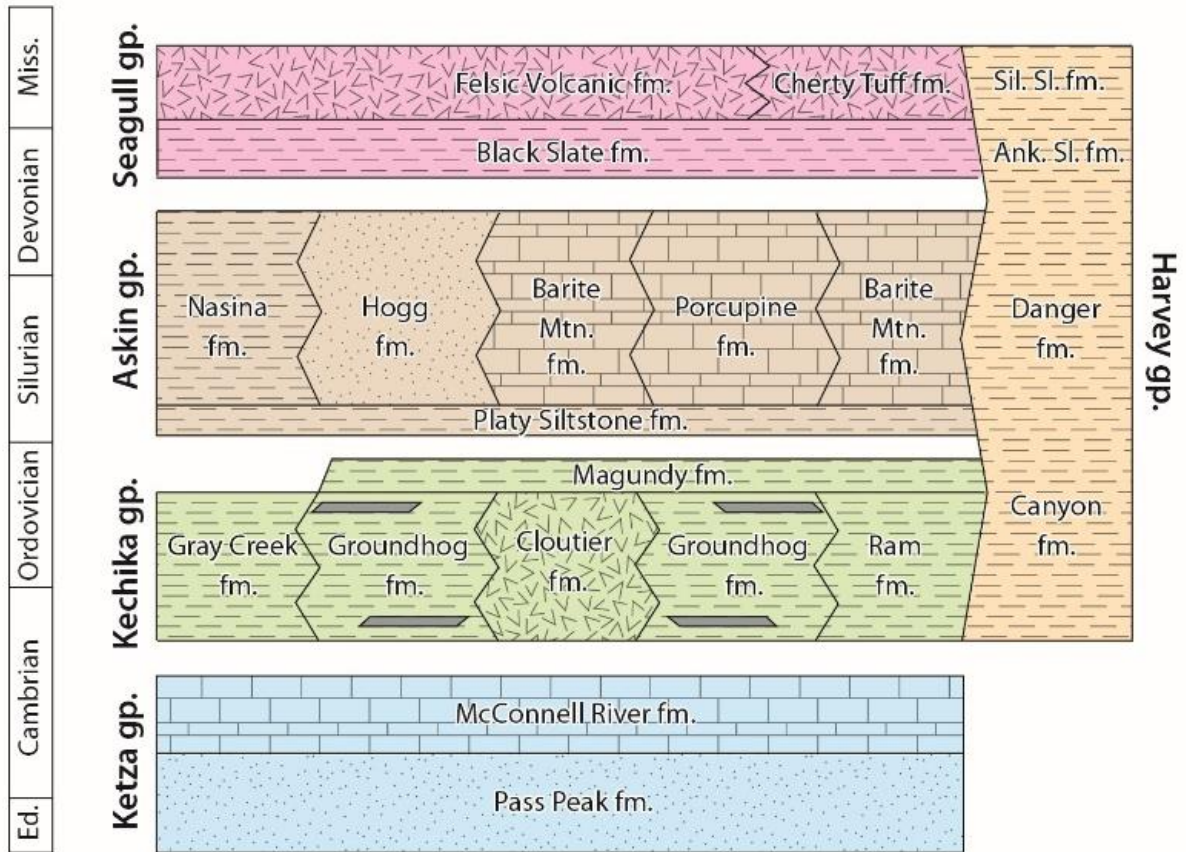
Figure 2-4 *Paleozoic stratigraphy of the Pelly Mountains compiled by Tempelman-Kluit*
(2012). Abbreviations: Ank = Ankerite; Ed = Ediacaran; fm = formation; gp = group; Miss
= Mississippian; Mtn = mountain; Sil = Siliceous; and Sl = Slate. Grey polygons in Kechika
group represent mafic sills.
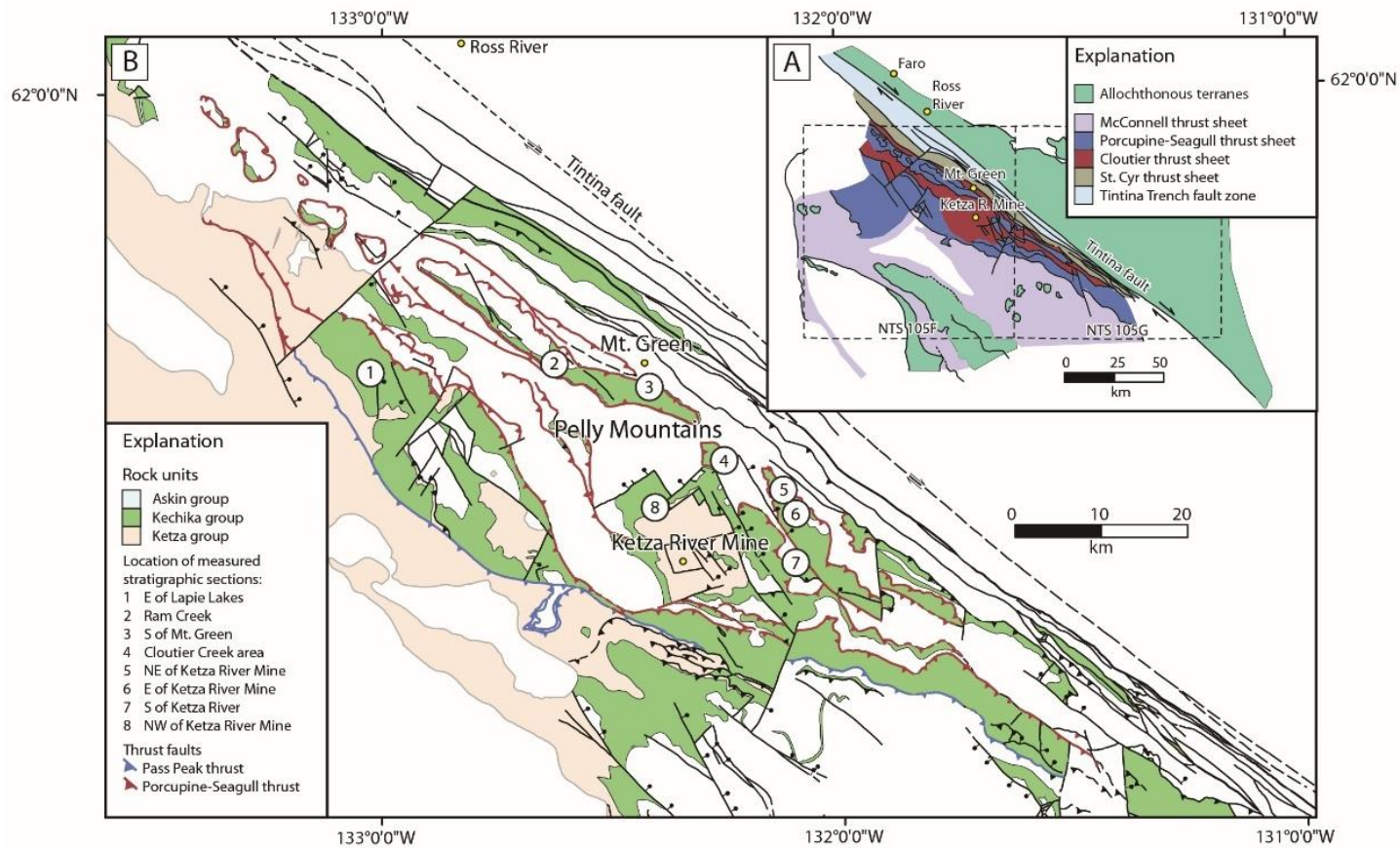
Figure 2-5 (a) *Distribution of thrust sheets within the Quiet Lake (NTS 105F) and Finlayson Lake (NTS 105G) map areas, Pelly Mountains,*

south-central Yukon (modified from Tempelman-Kluit, 2012). **(b)** *Distribution of Ketza, Kechika and Askin group rocks in the Pelly Mountains*

(modified from Tempelman-Kluit, 2012). Measured stratigraphic sections on map are displayed in Figure 2-6.

2.3.2 Kechika group

The Kechika group (Fig. 2-4; Beranek et al., 2016) is an upper Cambrian to Ordovician succession of four formations that Tempelman-Kluit (2012) described as laterally equivalent and interfingered. The four formations from northeast to southwest (Fig. 2-5a, b) comprise the Ram, Cloutier, Groundhog, and Gray Creek formations (Tempelman-Kluit, 2012) and occur as narrow, northwest- trending, discontinuous belts across the Pelly Mountains. The Groundhog, Cloutier and Ram formations are discontinuously capped by the Magundy formation (Fig. 2-4).

Tempelman-Kluit (2012) defined the Groundhog formation as at least 800 m-thick and consisting of thinly bedded, "darker, non-calcareous phyllite or slate" as opposed to the "orange or buff platy limestone and phyllite" of the Ram formation and the volcanic tuff of the Cloutier formation. Our fieldwork has instead shown that Groundhog formation strata are characterized by interbedded argillaceous shale, silty limestone, tuffaceous shale (phyllite) to sandstone, and lapilli tuff. Silty limestone occurs throughout the Groundhog formation, but tuffaceous rocks are generally restricted to the middle to upper part of the sequence.

Massive basalt and gabbro sills that are 0.5 to 30 m-thick occur throughout the Groundhog formation and typically show intrusive contacts with enclosing fine-grained clastic rocks. Up to 20 m-thick sections of volcanic and volcaniclastic rocks occur within the Groundhog and Magundy formations in the northern Quiet Lake map area, especially near Ram Creek and south of Mt. Green (Fig. 2-5b). Volcanic and volcanogenic sedimentary lithofacies include massive amygdaloidal basalt, lapilli tuff, monomictic volcanic breccia, sediment-matrix (volcanic and sedimentary lithic) breccia, and polymictic (volcanic and sedimentary clast) conglomerate (Table 2-1).

The Cloutier formation is 500 to 1000 m-thick and comprises resistant, mafic volcanic and volcaniclastic rocks that vary in lateral extent (Tempelman-Kluit, 2012). Primary volcanic facies include massive vesicular to amygdaloidal basalt, pillow basalt, and sediment-matrix basalt breccia (Table 2-1). Volcanogenic sedimentary facies include lapilli tuff, tuffaceous shale (phyllite) to sandstone, monomictic volcanic breccia, monomictic volcanic conglomerate and polymictic (volcanic and sedimentary clast) conglomerate (Table 2-1). These facies are intercalated with fine-grained argillaceous and calcareous rocks (comparable to those that define the Groundhog and Ram formations, respectively) and black shale (Table 2-1).

The Magundy formation is up to 400 m-thick and mostly consists of recessive graphitic shale with minor quartz sandstone, massive basalt, and tuff comparable with those of the Cloutier formation (Gordey, 1981; Tempelman-Kluit, 2012). Ordovician graptolites provide an upper age constraint for the Magundy formation (Gordey, 1981; Tempelman-Kluit, 2012).

The Ram formation is at least 1000 m-thick and crops out between the Tintina and St. Cyr faults. The depositional age of the Ram formation is constrained by late Cambrian and Early Ordovician trilobite fossils (Tempelman-Kluit, 2012). The Gray Creek formation is a 400 m-thick unit that consists of greenstone, quartz mica schist, and siltstone that Tempelman-Kluit (2012) related to more metamorphosed equivalents of the Cloutier, Pass Peak, and Nasina formations (Askin group), respectively.

Equivalents of the magmatic rocks of the Groundhog and Cloutier formations in the Pelly Mountains are recognized elsewhere in the Cassiar terrane. In the Cassiar Mountains, Gabrielse (1963) mapped greenstone units that are similar to the mafic sills within the Quiet Lake map area (Tempelman-Kluit, 2012). In the Glenlyon area of central

Yukon, minor amphibolite has been interpreted as high-grade equivalents of the Kechika group sills (e.g., Black et al., 2003; Gladwin et al., 2002).

2.3.3 Askin group

Shallow-marine strata of the Askin group (Fig. 2-4) comprise part of the Silurian and Early Devonian Cassiar platform (e.g., Gabrielse, 1963; Cecile et al., 1997; Tempelman-Kluit, 2012). A basal 100-500 m-thick unit of dolomitic siltstone (Platy Siltstone formation) locally contains mafic to intermediate volcanic rocks (Orange Volcanics member). Our field observations suggest that the Orange Volcanics member near Ram Creek and Mt. Green (Fig. 2-5b) contains pillow basalt and intermediate volcanic breccia. This basal unit is overlain by four formations (Porcupine, Barite Mountain, Hogg and Nasina formations; Fig. 2-4) with gradational to angular discordant contacts and rapid facies and thickness changes (Tempelman-Kluit, 2012). The Grey Limestone formation caps these four formations.

2.4 Field studies

Lower Paleozoic rocks of the Pelly Mountains crop out within four structural-stratigraphic zones that from west to east comprise the McConnell, Porcupine-Seagull, Cloutier, and St. Cyr thrust sheets (Fig. 2-5a). Seven of the stratigraphic sections (Figs. 2-6.1 to 2-6.7) discussed below occur within the Porcupine-Seagull thrust sheet, whereas one stratigraphic section (Fig. 2-6.8) occurs within the overlying Cloutier thrust sheet. The locations of field sites are shown in Figure 2-5b and sequentially numbered therein from northeast to southwest. Facies associations and estimated thicknesses are documented through stratigraphic measurement and description. Volcanic and intrusive rocks were systematically sampled for whole-rock geochemistry, Nd-Hf isotope

geochemistry, and zircon U-Pb geochronology to constrain the genesis and crustal-mantle sources of early Paleozoic magmatism.
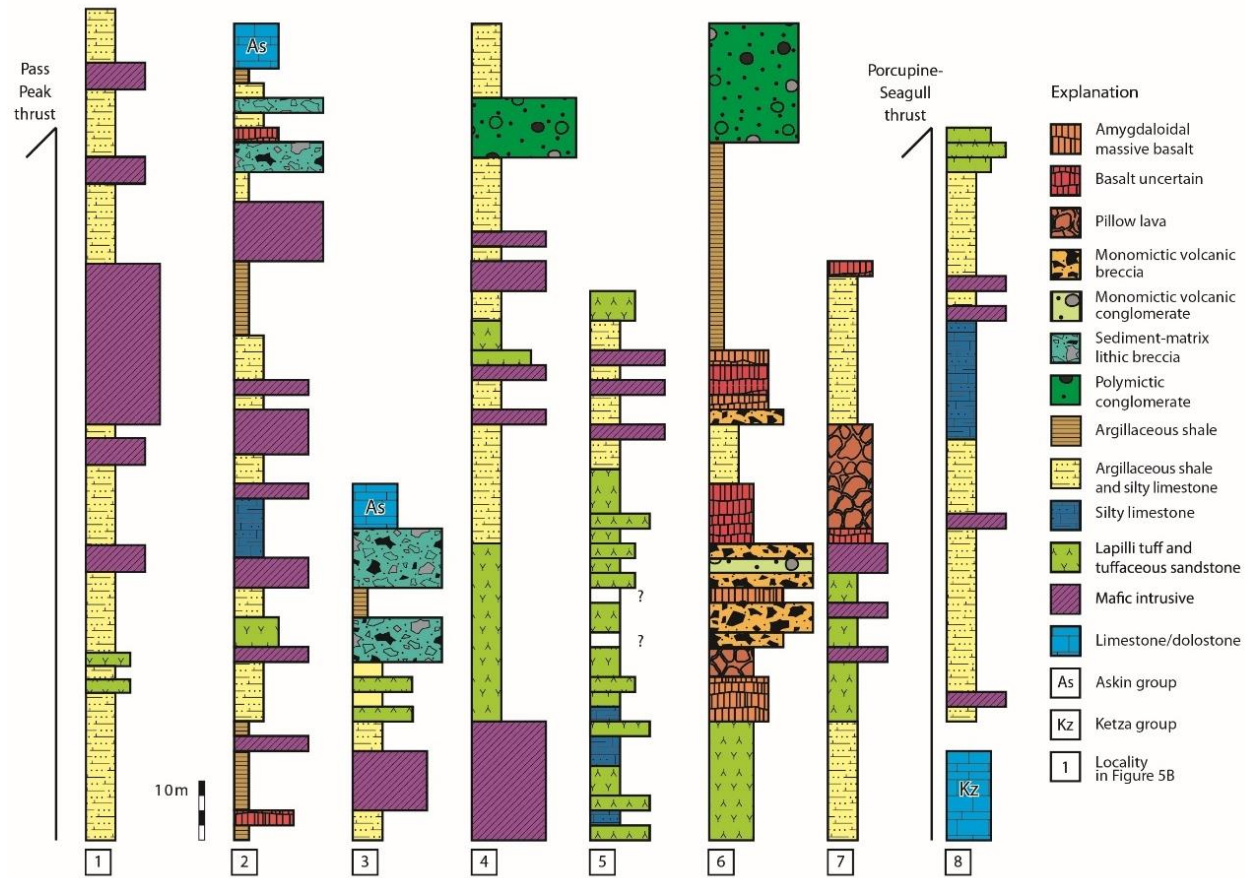
Figure 2-6 *Measured stratigraphic sections of the Kechika group, Pass Peak and Cloutier Creek map areas, Pelly Mountains, south-central*

Yukon.

2.4.1 Groundhog formation stratigraphy

East of Lapie Lakes - Figure 2-6, location 1

This section is exposed along a series of northeast-trending ridges immediately east of Lapie Lakes and the South Canol Road in the western Pass Peak map area (base of section: zone 08V 603248E 6843697N NAD83). Although exposure is patchy and complex folding is common, 50% of the outcrop throughout >200 m-thick section consists of interbedded steel-grey argillaceous and calcareous shale (phyllite; Fig. 2-7a, b) with rare 5-30 cm fine sandstone beds. Approximately 40% of the exposure consists of resistant, 1 to >30 m thick basaltic to gabbroic sills. Rare (<10% of outcrop), up to 2 m-thick lapilli tuff beds form resistant units within the shale.

Ram Creek - Figure 2-6, location 2

Exposures of the upper Groundhog formation were examined along a northwest-trending ridge near the headwaters of Ram Creek in the northern Pass Peak map area (base of section: zone 08V 626236E 6844619N NAD83). The section is >130 m-thick and features two distinct components. The basal 60% of the section consists of steel grey to black argillaceous and tuffaceous shale (phyllite), with medium-bedded silty limestone and 1 to >10 m-thick massive amygdaloidal basalt, and gabbroic sills (Fig. 2-7c). Volcanic and volcaniclastic rocks are intercalated within the upper 40% of the section and mostly consist of massive basalt, monomictic volcanic breccia, and sediment-matrix (volcanic and sedimentary lithic) breccia (Fig. 2-7d-f). These rocks are interbedded with metre-thick units of grey shale, limestone and poorly exposed black shale of the Magundy formation. The overlying Askin group at this location consists of volcaniclastic breccia and dolomitic sandstone of the Orange Volcanics member of the Platy Siltstone formation.

South of Mt. Green - Figure 2-6, location 3

Groundhog and Magundy formation strata were examined along a northeast-trending ridge ~3 km south of Mt. Green in the northwest Cloutier Creek map area. The basal contact of the Groundhog formation is a thrust fault that places Kechika group rocks on top of the Devonian- Mississippian Black Slate formation (base of section: zone 08V 0636780E 6843033N NAD83). This section is at least 50 m-thick and lithologically similar to that exposed in the Ram Creek area. The basal 50% consists of interbedded steel-grey argillaceous and calcareous shale (phyllite) and >10 m-thick gabbro intrusion. The upper 50% consists of monomictic volcanic breccia, sediment-matrix (volcanic and sedimentary lithic) breccia (Fig. 2-7g) and lapilli tuff (Fig. 2-7h).

Cloutier Creek area - Figure 2-6, location 4

Groundhog formation rocks were examined ~8 km north of the Ketza River Mine, along a northwest-trending ridge between Cloutier Creek and the Ketza River, in the central Cloutier Creek map area (base of section: zone 08V 645712E 6834820N NAD83). This section is at least 150 m-thick and consists of a gabbroic stock (mapped as Cloutier formation) that intrudes >20 m of interbedded tuffaceous shale (Fig. 2-8a), thin to medium- bedded silty limestone (Fig. 2-8b), tuffaceous sandstone (Fig. 2-8c), and interbedded steel-grey argillaceous to calcareous shale (phyllite). Several metre-thick gabbroic sills occur throughout the succession. The erosional top of the section consists of green, polymictic (volcanic and limestone clast) conglomerate.

Northwest of Ketza River Mine - Figure 2-6, location 8

A succession of Groundhog formation strata overlies the Ketza group ~6 km northwest of the Ketza River Mine in the southern Cloutier Creek map area (base of the Groundhog formation: 08V 637814E 6829108N NAD83). Ketza group strata at this location comprise archaeocyathid-bearing limestone, silty limestone and pyritic mudstone. The contact with the overlying Groundhog formation is poorly exposed and the Ketza group shows evidence of structural duplication and local faulting. The Groundhog formation is >100 m-thick and consists of interbedded steel-grey shale and silty limestone units (Fig. 2-8d, e) that are intruded by 0.5-2 m-thick, typically amygdaloidal, basalt to gabbroic sills (Fig. 2-8f; >10% of the total outcrop). Strongly deformed and complexly folded tuffaceous green phyllitic shale and lesser fine-grained sandstone comprise the top of the section (<10% of sequence).

2.4.2 Cloutier formation stratigraphy

Northeast of Ketza River Mine - Figure 2-6, location 5

This section is >90 m-thick and exposed along a ridge ~6 km northeast of the Ketza River Mine, near peak 6762 in the eastern Cloutier Creek map area (base of the section: 08V 652511E 6831507N NAD83). The basal 70% of the section consists of tuffaceous shale (phyllite), normally graded beds of coarse to fine-grained volcanic sandstone (Fig. 2-8g), and lapilli tuff (Fig. 2-8h). The tuffaceous rocks are locally intercalated with medium-bedded limestone. The upper 30% of the section consists of complexly folded, massive metre-scale amygdaloidal basalt sills that are intercalated with steel-grey argillaceous and calcareous shale (phyllite) and lapilli tuff.

East of Ketza River Mine - Figure 2-6, location 6

This 140 m-thick section is exposed along a southwest- trending ridge ~10 km east of the Ketza River Mine (base of section: zone 08V 654218E 6829014N NAD83). The basal part of the sequence consists of 2 to 10 m-thick units of vesicular to amygdaloidal massive basalt (Fig. 2-9a), vesicular pillow basalt (Fig. 2-9b), sediment-matrix basalt breccia (Fig. 2-9c), and up to 8 m-thick units of monomictic volcanic breccia (Fig. 2-9d) and monomictic volcanic conglomerate (Fig. 2-9e). The top of the succession is variably deformed and consists of black shale, limestone and up to 2 m-thick massive basalt lava flows that are capped by granule to cobble polymictic (mafic-intermediate volcanic and limestone clast) conglomerate (Fig. 2-9f).

South of Ketza River - Figure 2-6, location 7

At least 90 m of Cloutier formation strata are exposed along a north-trending ridge at the headwaters of the Ketza River in the southern Cloutier Creek map area (base of section: zone 08V 654352E 6823223N NAD83). The basal 70% of this sequence consists of interbedded steel-grey argillaceous and calcareous shale (phyllite), 1 to 3 m-thick basalt to gabbro sills, and up to 3 m-thick beds of lapilli tuff. The upper 30% consists of a 20 m-thick sequence of pillow basalt (Fig. 2-9g, h) and sheared mafic rocks that are intercalated with silty limestone and argillaceous shale.

Figure 2-7 *Field photographs of Kechika group units. **(a)** tight folding of grey-shale, east of Lapie Lakes, Pass Peak map area; **(b)** steel-grey argillaceous shale; **(c)** resistant 8 m-thick gabbroic sill within shale, Ram Creek, Cloutier Creek map area; **(d)** sediment-matrix lithic (limestone and tuffaceous rock) breccia; **(e)** massive amygdaloidal basalt in contact with sediment-matrix volcanic and sedimentary lithic breccia (contact outlined in yellow) **(f)** sediment-matrix volcanic and sedimentary lithic breccia; **(g)** sediment-matrix lithic (limestone, shale, mafic tuff, amygdaloidal basalt) breccia, south of Mt. Green, Cloutier Creek map area; and **(h)** lapillistone to lapilli tuff with rounded lapilli clasts.*
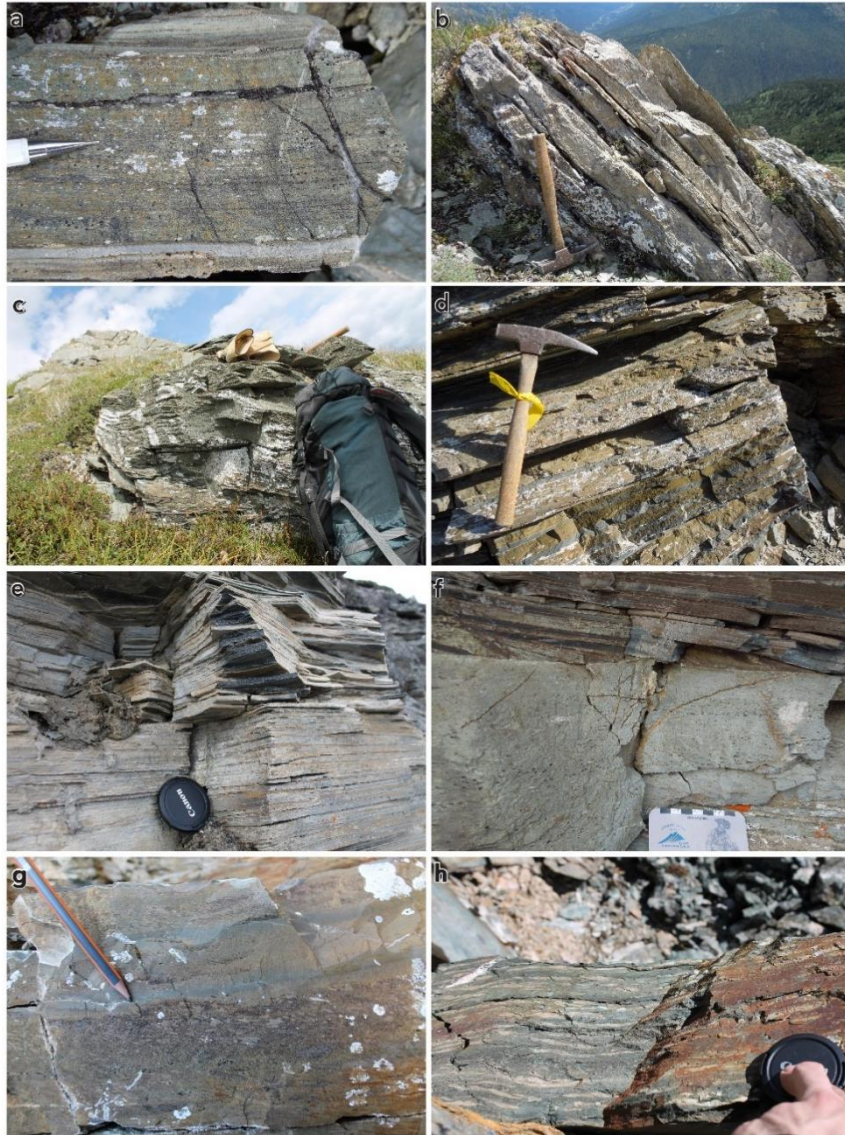
Figure 2-8 *Field photographs of Kechika group units. (a) Interbedded tuffaceous shale and silty limestone, near Cloutier Creek, Cloutier Creek map area (b) medium-bedded silty limestone; (c) green tuffaceous sandstone; (d) interbedded steel-grey argillaceous shale and silty limestone, northwest of Ketza River Mine, Cloutier Creek map area; (e) thin to medium-bedded silty limestone; (f) intrusive contact of 2 m-thick amygdaloidal basalt sill; (g) irregular lapilli clasts in graded tuffaceous sandstone and shale, northeast of Ketza River, Cloutier Creek map area; and (h) lapilli tuff with elongate lapilli clasts.*
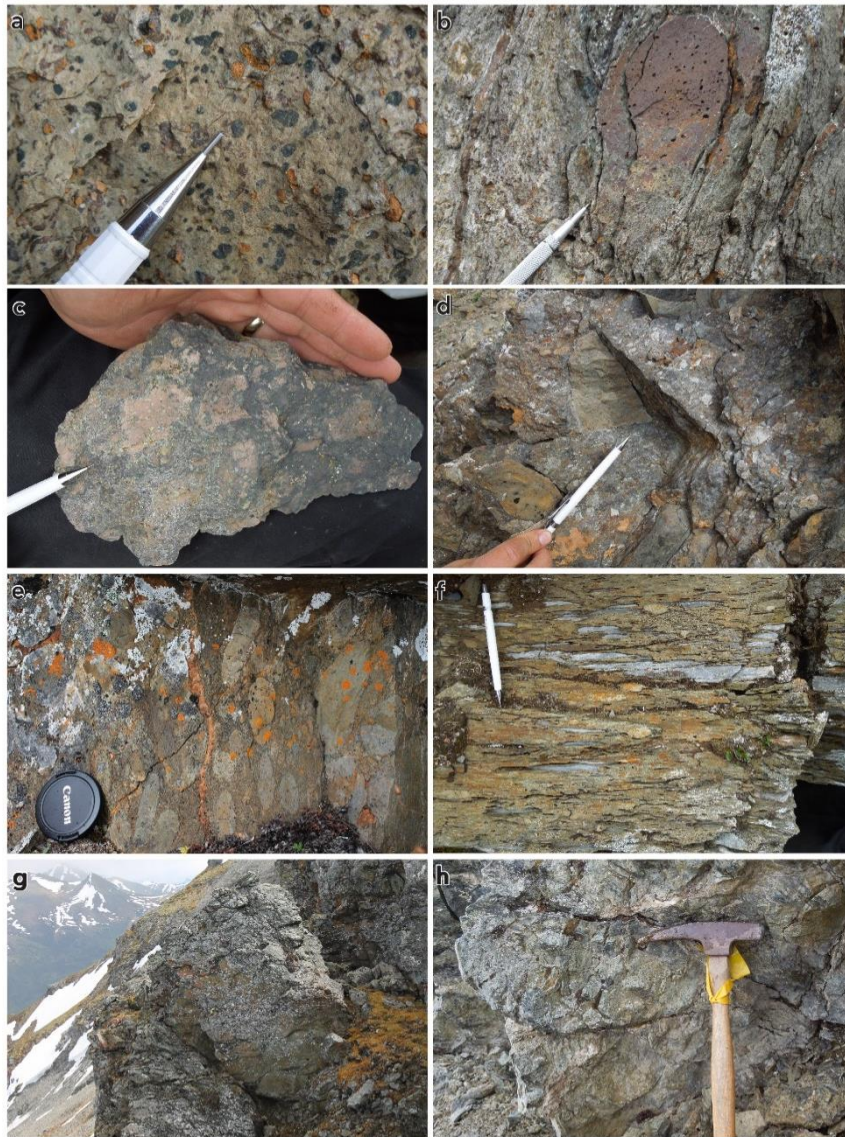
Figure 2-9 Field photographs of Kechika group units. *(a)* Amygdaloidal (chlorite) massive basalt, east of Ketza River Mine, Cloutier Creek map area; *(b)* vesicular pillow basalt; *(c)* sediment-matrix basalt breccia (fluidal peperite) consisting of amoeboid to angular-shaped, lapilli-sized fragments in volcaniclastic matrix *(d)* monomictic basalt breccia (hyaloclasite) with angular, lapilli to bomb sized fragments in volcaniclastic matrix; *(e)* monomictic volcanic conglomerate; *(f)* sheared polymictic limestone and mafic-intermediate volcanic conglomerate; *(g)* part of a 20 m-thick sequence of pillow basalt, south of Ketza River, Cloutier Creek map area; and *(h)* pillow basalt.

2.5 Preliminary analytical results

Preliminary lithogeochemical results indicate that Kechika group rocks have ocean island basalt-like (OIB) affinities (Fig. 2-10a; Sun and McDonough, 1989) that are typical of some alkali basalt to foidite rocks in the Canadian Cordillera (Fig. 2-10b) and around the globe (Winchester and Floyd 1977; Sykes, 1978; Pearce 1996). High-precision zircon U-Pb studies have determined late Cambrian and Early Ordovician crystallization ages for gabbro in the Pass Peak map area (work in progress).
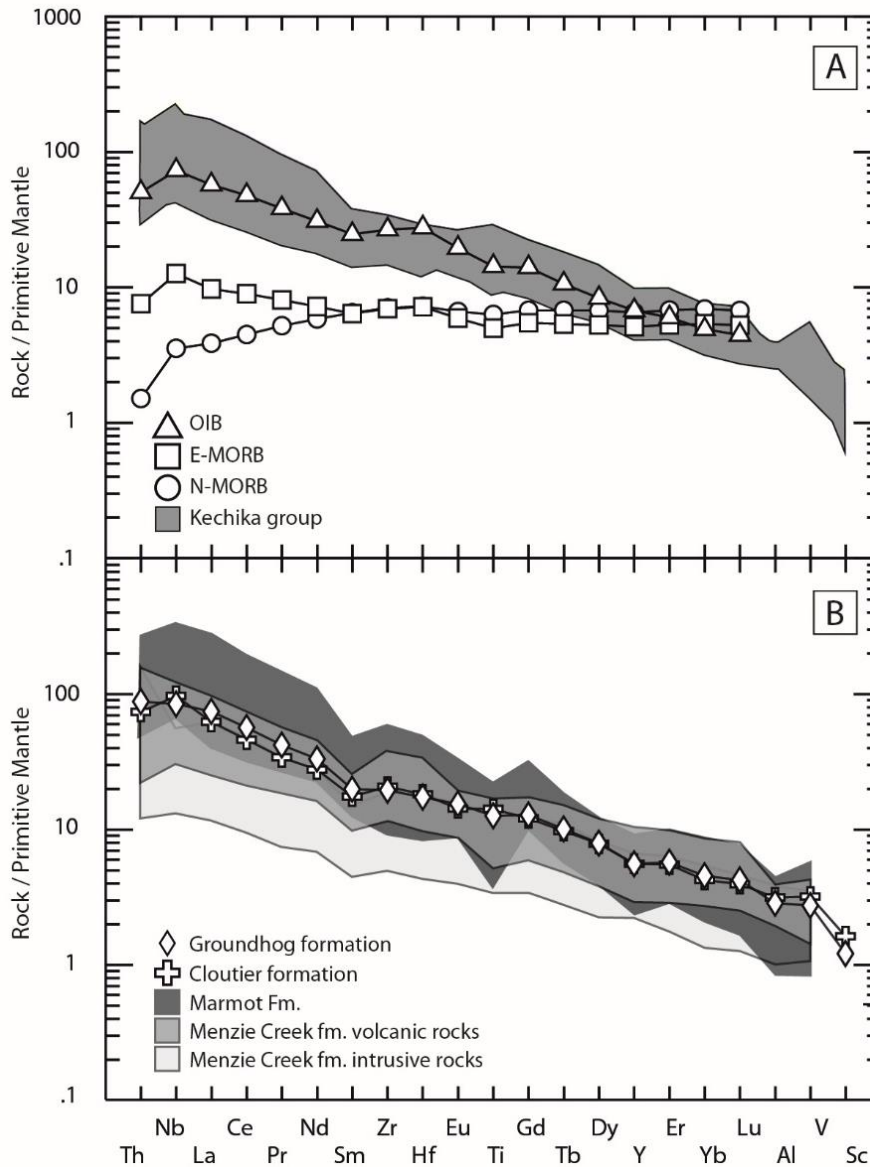
Figure 2-10 *Primitive mantle-normalized multi-element plots of mafic rocks from the Kechika group and global magmatic system.* ***(a)*** *Range of values from Kechika group (this study) and the global averages of ocean-island basalt (OIB), normal and enriched mid-ocean ridge basalt (E-MORB and N-MORB; Sun and McDonough, 1989); and* ***(b)*** *average values of Cloutier and Groundhog formation (this study), range of values from the Marmot Formation (Leslie, 2009) and range of values from the Menzie Creek formation (Pigage, 2004). Primitive-mantle normalising values are from Sun and McDonough (1989) and McDonough and Sun (1995).*

2.6 Stratigraphic interpretation

Four principal lithofacies (basaltic, volcanogenic sedimentary, limestone-argillite, intrusive rock) are recognized within the Cloutier and Groundhog formations (Table 2-1). Volcanic and proximal volcanogenic lithofacies of the middle to upper Cloutier formation and parts of the upper Groundhog and lower Magundy formations are consistent with a submarine vent proximal succession. The lower Cloutier formation and much of the Groundhog formation may comprise part of a sediment- sill complex based on the prevalence of concordant mafic rocks that intruded into, or were erupted onto, wet marine sediment (e.g., Einsele, 1986; Batiza and White, 2000).

2.6.1 Basaltic facies association

The basaltic facies association is related to the eruption of primary volcanic products. Basaltic lithofacies consist of massive amygdaloidal to vesicular basalt, pillowed basalt and peperite (Table 2-1). The massive amygdaloidal to vesicular basalts are predominantly sills, but some lava flows are locally recognized. Pillowed lava flows are consistent with subaqueous volcanism and most common within low effusivity systems (Moore, 1975; Batiza and White, 2000). Sediment-matrix basalt breccia lithofacies, with lapilli-sized, amoeboid to angular-shaped clasts, are interpreted as fluidal peperite units that formed through the interaction of basaltic lava and fluid-saturated sediment during emplacement (e.g., Skilling et al., 2002).

2.6.2 Volcanogenic sedimentary facies association

Volcanogenic sedimentary rocks are interpreted to have formed by the reworking of primary volcanic units. Volcanogenic sedimentary facies mostly include monomictic volcanic breccia, monomictic volcanic conglomerate, sediment-matrix volcanic and

sedimentary lithic breccia, polymictic volcanic and limestone clast conglomerate, lapilli

tuff and tuffaceous shale to sandstone (Table 2-1).

Monomictic volcanic breccia units consist of lapilli to bomb-sized, irregular-

shaped, basaltic clasts. These strata likely represent resedimented hyaloclastite units that

form due to the rapid cooling and fragmentation of basaltic lava during interaction with

water (e.g., Batiza and White, 2000; Simpson and McPhie, 2001). Fragmentation

processes can also occur due to the expansion of volatiles (Fisher and Schminke, 1984).

Hyaloclastite units with bomb-sized fragments occur adjacent to pillow basalt and are

inferred to represent pillow breccia, a deposit formed by the gravitational or mechanical

detachment of pillows (e.g., Batiza and White, 2000; Simpson and McPhie, 2001).

Hyaloclastite units are typical of shallow-water deposits and/or within areas of steep

relief such as seamount flanks (Batiza and White, 2000).

Sediment-matrix lithic breccia and polymictic conglomerate units contain rock

fragments that are representative of underlying volcanic, volcaniclastic, and marine

sedimentary strata. For example, the limestone-bearing conglomerate units have clasts

that are comparable to exposures of blue-grey carbonate and limy clastic rocks within the

Cloutier and Groundhog formations. The large clast sizes and locally sourced material

indicate proximal reworking and deposition with limited transport. These coarse-grained

units were likely caused by slope collapse processes and may be unrelated to volcanic

processes (e.g., McPhie and Cas, 2015).

Tuffaceous rocks are inferred to record both pyroclastic and epiclastic processes

(e.g., Fisher and Schmincke, 1984). Tuffaceous sandstone and shale are indicative of

epiclastic processes, especially when beds show evidence for normally graded bedding

(e.g., Cas and Wright, 1988). Tuffaceous shale, often interbedded with argillaceous and

calcareous layers, likely formed through the deposition of "relatively dilute suspensions

of ash" in the water column during periods of low volcanic activity (e.g., McPhie and
Cas, 2015).

2.6.3 Limestone-argillite facies association

The limestone-argillite facies likely resulted from the suspension sedimentation of
mud, silty carbonate and volcanic ash below wave-base. Interbedded steel-grey argillaceous
shale and blue-grey to tan silty limestone are the most common facies. Black shale with rare
limestone occurs near the top of the Groundhog and Cloutier formations. Metre-thick,
medium-bedded limestone units are intercalated within the tuffaceous-rich successions. Silty
limestone predominates over argillaceous shale for tens of metres near the base of the
Kechika group.

2.6.4 Intrusive rocks

Intrusive rocks of the Kechika group are associated with the emplacement of
magma within shallow or unconsolidated sedimentary strata. The intrusive rocks consist
of tabular, 1 to 30 m-thick basaltic to gabbroic rocks that are concordant with bedding.
Gabbroic rocks are dark grey to green, with coarse porphyritic pyroxene (altered to
chlorite) and more rarely plagioclase. The intrusive contacts are typically irregular and
often display chilled margins and baked contacts with enclosing shale units that are 10s
of centimetres thick.

The geochemical similarities of Kechika group units support the interpretation
that intrusive rocks (mostly in the Groundhog formation) were subvolcanic feeders to
coeval extrusive rocks (mostly in the Cloutier formation). Metre-thick to tens of metres
thick sills within the Groundhog and lower Cloutier formations are inferred to represent
part of a sill-sediment complex (e.g., Einsele, 1986). Such complexes occur in areas of

thick unconsolidated (wet) sediment, although intrusive, not peperite contacts, predominate within the Kechika group sills. Sill-sediment complexes can form during the rifting of thinned continental crust and are frequently associated with transform-transfer zones (e.g., Einsele, 1986; Naylor et al., 1999).

2.7 Regional correlations and future work

Based on the available geochemical results (Fig. 2-10a), our working hypothesis calls for Kechika group magmatism to have resulted from the low-degree partial melting of a mantle source with fertile components (e.g., Fitton, 1987; Pearce 1996; Niu et al., 2011), perhaps due to periodic extensional faulting along the Cordilleran margin. Although no direct field evidence is yet recognized for Cambrian-Ordovician faults in the Pelly Mountains (Tempelman-Kluit, 2012), the Kechika group is characterized by lithofacies and geochemical signatures that are analogous to coeval mafic rocks within the Selwyn basin and Misty Creek embayment (Fig. 2-10b), which are demonstrably linked to local extension (e.g., Pigage, 2004; Leslie, 2009). These correlations imply that similar post-breakup, rift-related processes occurred to the north and south of the Liard line during the early Paleozoic. Similar to the Kechika group, Menzie Creek formation rocks in the Anvil District are overlain by younger volcanic rocks that may be related to the reactivation of pre-existing structures along the Cordilleran margin (Beranek et al., 2016; Cobbett, 2016). The influence of the Liard line on Paleozoic magmatism in south-central Yukon remains an open question and requires future testing.

Potential analogues for Kechika group volcanism include syn to post-breakup rocks associated with the Orphan, Fogo, and Newfoundland Seamounts in the Grand Banks area, offshore Newfoundland (Pe-Piper et al., 2007, 2013). The Newfoundland continental margin is a magma-poor, hyperextended, asymmetric rift margin that evolved

from Late Triassic to mid-Cretaceous time (e.g., Peron-Pinvidic et al., 2007; Brune et al., 2014). This margin has volcanic centres with OIB-like, alkaline mafic rocks that were emplaced into extended continental crust (Jagoutz et al., 2007; Pe-Piper et al., 2013). The seamounts are generally linear features that are bounded by margin-parallel extensional faults. In the case of the Orphan and Fogo Seamounts, volcanic centres are spatially associated with the Charlie Gibbs fracture zone and Southwest Grand Banks transform margin, respectively (Pe-Piper et al., 2007). These structures are major transfer zones that are at high angles to the rifted margin, analogous to the Liard line in the Canadian Cordillera.

2.8 Acknowledgements

2.9 References

Aitken, J.D., 1993, Cambrian and lower Ordovician-Sauk sequence, *in* Stott, D.F., and Aitken, J.D., eds., Sedimentary Cover of the North American Craton in Canada: Geological Survey of Canada, Geology of Canada, v. 5, p. 96-124, doi:10.4095/192360.

Audet, P., Sole, C. and Schaeffer, A.J., 2016, Control of lithospheric inheritance on neotectonic

    activity in northwestern Canada?: Geology, v. 44, p. 807-810, doi:10.1130/G38118.1

Batiza, R., and White, J.D.L., 2000, Submarine lavas and hyaloclastite, *in* Sigurdsson, H., ed.,

    Encyclopedia of Volcanics: Academic, San Diego, California, p. 361-381.

Beranek, L.P., Piercey, S.J., Campbell, R., and Wawrzonkowski, P., 2016, Paleozoic

    stratigraphy, tectonics and metallogeny of the Pelly Mountains, Quiet Lake and

    Finlayson Lake map areas (NTS 105F and G), central Yukon: Project outline and

    preliminary field results, *in* MacFarlane, K.E., and Nordling, M.G., eds., Yukon

    Exploration and Geology 2015: Yukon Geological Survey, p. 17-28.

Black, R., Gladwin, K., and Johnston, S.T., 2003, Geology and metamorphic conditions in rocks of

    the Cassiar terrane, Glenlyon map area (105L/1), south-central Yukon, *in* Emond, D.S., and

    Lewis, L.L., eds., Yukon Exploration and Geology 2002: Exploration and Geological

    Services Division, Yukon Region, Indian and Northern Affairs Canada, p. 65-76.

Bond, G.C., and Kominz, M.A., 1984, Construction of tectonic subsidence curves for the early

    Paleozoic miogeocline, southern Canadian Rocky Mountains: Implications for subsidence

    mechanisms, age of breakup, and crustal thinning: Geological Society of America Bulletin, v.

    95, p. 155-173, doi:10.1130/0016-7606(1984)95<155:cotscf>2.0.co;2.

Bond, G.C., Nickeson, P.A., and Kominz, M.A., 1984, Breakup of a supercontinent between 625 Ma

    and 555 Ma: new evidence and implications for continental histories: Earth and Planetary

    Science Letters, v. 70, p. 325-345, doi:10.1016/0012-821x(84)90017-7.

Bond, G.C., Christie-Blick, N., Kominz, M.A., and Devlin, W.J., 1985, An Early Cambrian rift to post-rift transition in the Cordillera of western North America: Nature, v. 315, p. 742-746, doi:10.1038/315742a0.

Brune, S., Heine, C., Pérez-Gussinyé, M., and Sobolev, S.V., 2014, Rift migration explains continental margin asymmetry and crustal hyper-extension: Nature Communications, v. 5, p. 1-9, doi:10.1038/ncomms5014.

Cas, R.A.F., and Wright, J.V., 1988, Volcanic successions, Modern and Ancient: A geological approach to processes, products and successions: Allen and Unwin, London 528 p.

Cecile, M.P., Fritz, W.H., Norford, B.S. and Tipnis, R.S., 1982. The Lower Paleozoic Misty Creek embayment, Selwyn Basin, Yukon and Northwest Territories. Geological Survey of Canada, Bulletin 335, 78 p.

Cecile, M.P., Norford, B.S., Stott, D.F., and Aitken, J.D., 1993, Ordovician and Silurian, *in* Stott, D.F., and Aitken, J.D., eds., Sedimentary cover of the craton in Canada: Geology of Canada: Geological Survey of Canada, v.5, p.125-149, doi:10.1130/dnag-gna-d1.125.

Cecile, M.P., Morrow, D.W., and Williams, G.K., 1997, Early Paleozoic (Cambrian to Early Devonian) tectonic framework, Canadian Cordillera: Bulletin of Canadian Petroleum Geology, v. 45, p. 54-74.

Cobbett, R., 2016, Preliminary observations on the geology of Tay Mountain Area (parts of NTS
105K/12 and 13, 105L/09 and 16), central Yukon, *in* MacFarlane, K.E., and Nordling, M.G.,
eds., Yukon Exploration and Geology 2015: Yukon Geological Survey, p. 79-98.

Colpron, M., Logan, J.M., and Mortensen, J.K., 2002, U-Pb zircon age constraint for late
Neoproterozoic rifting and initiation of the lower Paleozoic passive margin of western
Laurentia: Canadian Journal of Earth Sciences, v. 39, p. 133-143, doi:10.1139/E01-069.

Colpron, M., and Nelson, J.L., 2011, A Digital Atlas of Terranes for the Northern Cordillera. Yukon
Geological Survey, <www.geology.gov.yk.ca> [accessed November 2016].

Corti, G., Bonini, M., Mazzarini, F., Boccaletti, M., Innocenti, F., Manetti, P., Mulugeta, G.,
and Sokoutis, D., 2002, Magma-induced strain localization in centrifuge models of
transfer zones: Tectonophysics, vol. 348, p. 205-218, doi:/10.1016/s0040-1951(02)00063-
x.

Devlin, W.J., 1989, Stratigraphy and Sedimentology of the Hamill Group in the northern Selkirk
Mountains, British Columbia: evidence for latest Proterozoic-Early Cambrian extensional
tectonism: Canadian Journal of Earth Sciences, v. 26, p. 515-533, doi:10.1139/e89-044.

Devlin, W.J., and Bond, G.C., 1988, The initiation of the early Paleozoic Cordilleran miogeocline:
evidence from the uppermost Proterozoic-Lower Cambrian Hamill Group of southeastern
British Columbia: Canadian Journal of Earth Sciences, v. 25, p. 1-19, doi:10.1139/e88-001.

Einsele, G., 1986, Interaction between sediments and basalt injections in young Gulf of California-type spreading centers: Geologische Rundschau, v. 75, p. 197-208, doi:10.1007/bf01770188.

Fisher, R.V., and Schmincke, H.U., 1984, Pyroclastic rocks: Springer-Verlag, Berlin, 472 p, doi:10.1007/978-3-642-74864-6.

Fitton, J.G., 1987, The Cameroon line, West Africa: a comparison between oceanic and continental alkaline volcanism, *in* Fitton, J.G., and Upton B.G.J., eds., Alkaline Igneous Rocks: Geological Society, London, Special Publications, v. 30, p. 273-291, doi:10.1144/gsl.sp.1987.030.01.13.

Fritz, W.H., Cecile, M.P., Norford, B.S., Morrow, D.W., and Geldsetzer, H.H.J., 1991, Cambrian to Middle Devonian assemblages, *in* Gabrielse, H., and Yorath, C.J., eds., The Cordilleran Orogen: Canada: Geological Survey of Canada, Geology of Canada, no. 4, p. 151-218, doi:10.4095/134087

Gabrielse, H., 1963, McDame map area, Cassiar District, British Columbia: Geological Survey of Canada, Memoir 319, 138 p, doi:10.4095/100546.

Gabrielse, H., and Taylor, G.C., 1982, Geological maps and cross-sections of the Cordillera from near Fort Nelson, British Columbia to Gravina Island, southeastern Alaska: Geological Survey of Canada, Open File 864, doi:10.4095/129756.

Gabrielse, H., Murphy, D.C., and Mortensen, J.K., 2006, Cretaceous and Cenozoic dextral orogen-parallel displacements, magmatism, and paleogeography, northcentral Canadian Cordillera, *in*

Haggart, J.W., Enkin, R.J., and Monger, J.W.H., eds., Paleogeography of the North American Cordillera: evidence for and against large-scale displacements: Geological Association of Canada, Special Paper, 46, p. 255-276.

Gladwin, K., Colpron, M., Black, R., and Johnston, S.T., 2003, Bedrock geology at the boundary between Yukon-Tanana and Cassiar terranes, Truitt Creek map area (NTS 105L/1), south central Yukon, *in* Emond, D.S., and Lewis, L.L., eds., Yukon Exploration and Geology 2002: Exploration and Geological Services Division, Yukon Region, Indian and Northern Affairs Canada, p. 135-148.

Goodfellow, W.D., Cecile, M.P., and Leybourne, M.I., 1995, Geochemistry, petrogenesis, and tectonic setting of lower Paleozoic alkalic and potassic volcanic rocks, Northern Canadian Cordilleran Miogeocline: Canadian Journal of Earth Sciences, v. 32, p. 1236-1254, doi:10.1139/e95-101.

Gordey, S.P., 1981, Stratigraphy, structure, and tectonic evolution of the southern Pelly Mountains in the Indigo Lake area, Yukon Territory: Geological Survey of Canada, Bulletin 318, 44 p, doi:10.4095/111359.

Gordey, S.P., and Anderson, R.G., 1993, Evolution of the northern Cordilleran miogeocline, Nahanni map area (105 I), Yukon and Northwest Territories: Geological Survey of Canada, Memoir 428, 214 p, doi:10.4095/183983.

Hayward, N., 2015, Geophysical investigation and reconstruction of lithospheric structure and its control on geology, structure, and mineralization in the Cordillera of northern Canada and eastern Alaska: Tectonics, v. 34, doi:10.1002/2015TC003871.

Heaman, L.M., LeCheminant, A.N., and Rainbird, R.H., 1992, Nature and timing of Franklin igneous events, Canada: implications for a Late Proterozoic mantle plume and the break-up of Laurentia: Earth and Planetary Science Letters, v. 109, p.117-131, doi:10.1016/0012-821X(92)90078-A.

Hein, F.J., and McMechan, M.E., 1994, Proterozoic and Lower Cambrian strata of the Western Canada sedimentary basin, *in* Mossop, G.D., and Shetsen, I., eds., Geological Atlas of the Western Canada Sedimentary Basin: Canadian Society of Petroleum Geologists and Alberta Research Council, p. 57-67.

Jagoutz, O., Munterer, O., Manatschal, G., Rubatto, D., Peron-Pinvidic, G., Turrin, B.D., and Villa, I.M., 2007, The rift-to-drift transition in the North Atlantic: A stuttering start of the MORB machine?: Geology, v. 35, p. 1087-1090, doi:10.1130/G23613A.1.

Leslie, C.D., 2009, Detrital zircon geochronology and rift-related magmatism: central Mackenzie Mountains, Northwest Territories [M.Sc. thesis] University of British Columbia, 224 p.

Lister, G.S., Etheridge, M.A., and Symonds, P.A., 1986, Detachment faulting and the evolution of passive continental margins: Geology, v. 14, p. 246-250, doi:10.1130/0091-7613(1986)14<246:dfateo>2.0.co;2.

Lister, G.S., Etheridge, M.A., and Symonds, P.A., 1991, Detachment models for the formation of passive continental margins: Tectonics, v. 10, p. 1038-1064, doi:10.1029/90tc01007.

Lund, K., 2008, Geometry of the Neoproterozoic and Paleozoic rift margin of western Laurentia: Implications for mineral deposit settings: Geosphere, v. 4, p. 429-444, doi:10.1130/GES00121.1.

Lund, K., Aleinikoff, J.N., Evans, K.V., Dewitt, E.H., and Unruh, D.M., 2010, SHRIMP U-Pb dating of recurrent Cryogenian and Late Cambrian–Early Ordovician alkalic magmatism in central Idaho: Implications for Rodinian rift tectonics: Geological Society of America Bulletin, v. 122, p. 430-453, doi:10.1130/B26565.1.

MacIntyre, D.G., 1998, Geology, geochemistry and mineral deposits of the Akie River Area, northeast British Columbia: British Columbia, Ministry of Energy and Mines, Bulletin 103, p. 1-91.

Magwood, J.P.A., and Pemberton, S.G., 1988, Trace fossils of the Gog Group, a lower Cambrian tidal sand body, Lake Louise, Alberta, *in* Landing, E., Narbonne, G.M., and Myrow, P., eds., Trace fossils, small shelly fossils and the Precambrian-Cambrian boundary-proceedings: New York State Museum Bulletin 463, 14 p.

McDonough, W.F., and Sun, S.S., 1995, The composition of the Earth: Chemical Geology, vol. 120, p. 223-253, doi:10.1016/0009-2541(94)00140-4.

McPhie, J., and Cas, R., 2015, Volcanic Successions Associated with Ore Deposits: Facies Characteristics and Ore–Host Relationships, Chapter 49, *in* Sigurdsson, H., ed., The Encyclopedia of Volcanoes (Second Edition): Academic Press, Amsterdam, p. 865-879, doi:10.1016/b978-0-12-385938-9.00049-3.

Millonig, L.J., Gerdes, A., and Groat, L.A., 2012, U–Th–Pb geochronology of meta-carbonatites and meta-alkaline rocks in the southern Canadian Cordillera: a geodynamic perspective: Lithos, v. 152, p. 202-217, doi:10.1016/j.lithos.2012.06.016.

Moore, J.G., 1975, Mechanism of formation of pillow lava: pillow lava, produced as fluid lava cools underwater, is the most abundant volcanic rock on earth, but only recently have divers observed it forming: American Scientist, vol. 63, no. 3, p. 269-277.

Moynihan, D., 2014, Bedrock Geology of NTS 106B/04, Eastern Rackla Belt, *in* MacFarlane, K.E., Nordling, M.G., and Sack, P.J., eds., Yukon Exploration and Geology 2013: Yukon Geological Survey, p. 147-167.

Naylor, P.H., Bell, B.R., Jolley, D.W., Durnall, P., and Fredsted, R., 1999, Palaeogene magmatism in the Faeroe–Shetland Basin: influences on uplift history and sedimentation, *in* Fleet, A.J., and Boldy, S.A.R., eds., Petroleum Geology of Northwest Europe: Proceedings of the 5th Conference: Geological Society, London, p. 545-558, doi:10.1144/0050545

Nelson, J.L., Colpron, M., and Israel, S., 2013, The Cordillera of British Columbia, Yukon, and Alaska: Tectonics and metallogeny, *in* Colpron, M., Bissing, T., Rusk, B.G., and Thompson, J.F.H., eds., Tectonics, Metallogeny, and Discovery: The North American Cordillera and

Similar Accretionary Settings: Society of Economic Geologists Special Publication 17, p. 53-109.

Niu, Y., Wilson, M., Humphreys, E.R., and O'Hara, M.J., 2011, The origin of intra-plate ocean island basalts (OIB): the lid effect and its geodynamic implications: Journal of Petrology, v. 52, p. 1443-1468, doi:10.1093/petrology/egr030.

Pe-Piper, G., Piper, D.J.W., Jansa, L.F., and de Jonge, A., 2007, Early Cretaceous opening of the North Atlantic Ocean: Implications of the petrology and tectonic setting of the Fogo Seamounts off the SW Grand Banks, Newfoundland: Geological Society of America Bulletin, v. 119, p. 712-724, doi:10.1130/B26008.1.

Pe-Piper, G., Meredyk, S., Zhang, Y., Piper, D.J., and Edinger, E., 2013, Petrology and tectonic significance of seamounts within transitional crust east of Orphan Knoll, offshore eastern Canada: Geo-Marine Letters, v. 33, p. 433-447, doi:10.1007/s00367-013-0342-2.

Pearce, J.A., 1996, A user's guide to basalt discrimination diagrams. Trace element geochemistry of volcanic rocks: applications for massive sulphide exploration: Geological Association of Canada, Short Course Notes, v. 12, 113 p.

Peron-Pinvidic, G., Manatschal, G., Minshull, T.A., and Sawyer, D.S., 2007, Tectonosedimentary evolution of the deep Iberia-Newfoundland margins: Evidence for a complex breakup history: Tectonics, v. 26, doi:10.1029/2006TC001970.

Pigage, L.C., 2004, Bedrock geology compilation of the Anvil District (parts of NTS 105K/2, 3, 4, 5, 6, 7 and 11), central Yukon: Yukon Geological Survey, Bulletin 15, 103 p.

Pigage, L.C., and Mortensen, J.K., 2004, Superimposed Neoproterozoic and early Tertiary alkaline magmatism in the La Biche River area, southeast Yukon Territory: Bulletin of Canadian Petroleum Geology, v. 52, p. 325-342, doi:10.2113/52.4.325.

Pigage, L.C., Crowley, J.L., Pyle, L.J., Abbott, J.G., Roots, C.F., and Schmitz, M.D., 2012, U–Pb zircon age of an Ordovician tuff in southeast Yukon: implications for the age of the Cambrian–Ordovician boundary: Canadian Journal of Earth Sciences, v. 49, p. 732-741, doi:10.1139/e2012-017.

Post, R.T., and Long, D.G., 2008, The middle Cambrian Mount Roosevelt Formation (new) of northeastern British Columbia: evidence for rifting and development of the Kechika graben system: Canadian Journal of Earth Sciences, v. 45, p. 483-498, doi:10.1139/E08-014.

Pyle, L.J., and Barnes, C.R., 2003, Lower Paleozoic stratigraphic and biostratigraphic correlations in the Canadian Cordillera: implications for the tectonic evolution of the Laurentian margin: Canadian Journal of Earth Sciences, v. 40, p. 1739-1753, doi:10.1139/e03-049.

Simpson, K., and McPhie, J., 2001, Fluidal-clast breccia generated by submarine fire fountaining, Trooper Creek Formation, Queensland, Australia: Journal of Volcanology and Geothermal research, vol. 109, p. 339-355, doi:10.1016/s0377-0273(01)00199-8.

Skilling, I.P., White, J.D.L., and McPhie, J., 2002, Peperite: a review of magma-sediment mingling: Journal of Volcanology and Geothermal Research, v. 114, p. 1-17, doi:10.1016/s0377-0273(01)00278-5.

Sun, S.S., and McDonough, W.S., 1989, Chemical and isotopic systematics of oceanic basalts: implications for mantle composition and processes: Geological Society, London, Special Publications, v. 42, p. 313-345, doi:10.1144/gsl.sp.1989.042.01.19.

Sykes, L.R., 1978, Intraplate seismicity, reactivation of preexisting zones of weakness, alkaline magmatism, and other tectonism postdating continental fragmentation: Reviews of Geophysics, v. 16, p. 621-688, doi:10.1029/rg016i004p00621.

Taylor, G.C., and Stott, D.F., 1973, Tuchodi Lakes map-area, British Columbia (94K): Geological Survey of Canada, Memoir 373. 37 p, doi:10.4095/102437.

Tempelman-Kluit, D.J., 2012, Geology of Quiet Lake and Finlayson Lake map areas, south-central Yukon: An early interpretation of bedrock stratigraphy and structure: Geological Survey of Canada, Open File 5487, 103 p, doi:10.4095/291931.

Winchester, J.A., and Floyd, P.A., 1977, Geochemical discrimination of different magma series and their differentiation products using immobile elements: Chemical Geology, v. 20, p. 325-343, doi:10.1016/0009-2541(77)90057-2

Table 2-1 *Principal lithofacies of Kechika group, Pass Peak and Cloutier Creek map areas, Pelly Mountains, south-central Yukon.*

Lithofacies	Thickness and lateral extent	Characterisation	Contact/relationship and associated lithofacies	Interpretation
Basaltic facies association				
Amygdaloidal massive basalt	1-5 m-thick	Aphyric to 25% porphyritic (dark green 1- 5 mm), up to 25% vesicular-amygdaloidal (1 mm-5 mm quartz-chlorite-carbonate).	Conformable contacts with overlying pillow basalt; intercalated and overlain by other volcanic and volcanogenic facies; irregular, baked contacts with enclosing shale.	Coherent basalt lava; mostly sills represented by upper and lower baked contacts +/- rare sediment-matrix basalt breccia (peperite). Rare lava flows likely also present (e.g. Batiza and White, 2000).
Pillow lava	2-20 m-thick	50% aphyric, 50% porphyritic (dark green 1-5mm); rarely vesicular; 0.1-0.5 m lobes closely-loosely packed.	Conformably overlies or grades into massive basalt; locally interpillow matrix of shale; overlain at outcrop scale by monomictic volcanic breccia or shale.	Subaqueous pillowed lava flows (e.g. Moore, 1975), most common within low effusivity magmatic systems (Batiza and White, 2000).
Sediment-matrix basalt breccia	Limited extent	>25% lapilli sized amoeboid to angular basalt clasts; very poorly sorted, massive.	Intercalated with massive basalt and monomictic to sediment-matrix volcanic breccia.	Fluidal to blocky peperite; in-situ disintegration of coherent magma due to mingling with unconsolidated to poorly consolidated sediment (Skilling et al., 2002).
Volcanogenic sedimentary facies association				

Table 2-1 (continued)

Monomictic volcanic breccia	Up to 8 m-thick	>30% lapilli- to bomb-sized, angular basalt clasts (1 cm to 16 cm); very poorly sorted, massive.	Overlies massive and pillow basalt facies; intercalated with volcanic breccia and conglomerate.	In-situ to wholly to partly resedimented hyaloclasite (Batiza and White, 2000); +/- pillow basalt breccia due to detachment of pillows by mechanical/gravitational means (e.g. Simpson and McPhie, 2001).
Monomictic volcanic conglomerate	Up to 2 m-thick	Rounded to sub-angular, granule- to cobble-sized volcanic clasts (25%); very poorly sorted, massive.	Intercalated within monomictic volcanic breccia and sediment-matrix lithic breccia.	Resedimented volcanic conglomerate formed by proximal reworking and transport of unstable volcanic facies.
Sediment-matrix volcanic and sedimentary lithic breccia	20 m-thick	Up to 70% angular to subrounded, granule- to cobble-sized (0.5 cm to >20 cm) clasts of amygdaloidal basalt, dark green (chloritic) tuff, grey-black shale and blue-grey limestone; very poorly sorted, massive.	Underlain by tuff, shale and sills; intercalated with black shale; irregular contacts with massive basalt.	Resedimented volcanic breccia formed through gravity-driven collapse of volcanic facies and erosion of underlying sedimentary facies.
Polymictic volcanic and limestone clast conglomerate	20 m-thick	Up to 30% granule- to boulder-sized, rounded to subangular; blue-grey limestone and mafic-intermediate volcanic clasts based on colour index.	Intercalated with volcanic strata and shale of the Cloutier formation and tuff, sills and shale of the Groundhog formation.	Reworking and transport of underlying volcanic and sedimentary facies.

Table 2-1 *(continued)*

Lapilli tuff	0.1 m- to 3 m-thick beds and lenses	Up to 30% pale to dark green (chlorite) lapilli clasts; often elongate, irregular to wispy to rounded (0.1-3 cm); within dark grey, resistant, sandy to phyllitic volcaniclastic matrix; 1 m-thick beds of normally graded lapillistone.	Forms solitary beds within limestone-argillite facies and tuffaceous sequences.	Formed through pyroclastic processes and/or epiclastic processes (e.g. Fisher and Schminke, 1984).
Tuffaceous shale to sandstone	>50 m-thick sequences; laterally continuous over 10s of meters	Mostly green-orange, tuffaceous shale-siltstone and rare fine-medium sandstone; finely laminated to thinly bedded; normally graded beds of sandstone.	Intercalated with >3 m-thick, laminated to thinly bedded limestone, m-thick (steel-grey) phyllite and lapilli tuff.	Suspension and turbidity current sedimentation of volcanic-derived and limestone-argillite units, most likely below wave base.
Limestone-argillite facies association				
Argillaceous shale	<1 m- to >2 m-thick	Finely laminated, grey-steel to black argillaceous shale.	Typically interbedded with silty limestone; dominates lower and middle parts of Groundhog and Cloutier formations.	Suspension sedimentation of clay and volcanic ash; likely below wave base.
Silty limestone	<1 m- to >2 m-thick	Finely laminated to medium-bedded, blue-grey to tan limestone.	Typically interbedded with argillaceous shale; m-thick beds intercalated with tuffaceous shale and sandstone.	Suspension sedimentation of silt and carbonate mud.

Table 2-1 (continued)

Intrusive rocks				
Mafic intrusive	0.5 m- to 30 m-thick; continuous over 100's of meters	Coherent, dark grey-green, fine- (basalt) to coarse-grained (gabbro) intrusive rocks; tabular, concordant bodies; contacts are irregular and baked; coarse porphyritic chlorite/pyroxene and more rarely plagioclase in thicker intrusions; 0.1 - 0.5 mm quartz-chlorite amygdales found in m-thick bodies.	Predominantly emplaced within limestone-argillite facies.	Concordant and tabular nature of bodies infers they are sills; may be comparable to sediment-sill complexes where thick packages of unconsolidated sediment prevent coherent magma movement through fracture propagation, therefore resulting in magma spreading laterally through the sediment (Einsele, 1986; Batiza and White, 2000).

Chapter 3 Early Paleozoic post-breakup magmatism along the Cordilleran margin of western North America: new geochronological and geochemical results from the Kechika group, Yukon, Canada*

3.1 Abstract

Lower Paleozoic volcanic rocks occur throughout the Cordilleran passive margin successions of western North America. These volcanic rocks were deposited after Ediacaran-Cambrian lithospheric breakup and several competing pure-shear, simple-shear, and magma-poor rift models have been proposed to explain the significance of early Paleozoic magmatism to Cordilleran tectonic evolution. New zircon U-Pb age and whole-rock geochemical studies were conducted on the lower Paleozoic Kechika group (informal), south-central Yukon, to test these rift models and constrain the timing, mantle source, and tectonic setting of post-breakup magmatism in the Canadian Cordillera. The Kechika group consists of vent-proximal and sediment-sill complexes within the Cassiar platform, a linear paleogeographic high that developed outboard of continental shelf and trough basins. Chemical abrasion (CA-TIMS) U-Pb dates indicate that Kechika group mafic rocks were generated during the late Cambrian (488-483 Ma) and Early Ordovician (473 Ma). Whole-rock trace element and Nd-Hf isotope results are consistent with the low-degree partial melting of an enriched lithospheric mantle source, likely during margin-scale extension. Coeval volcanic rocks with similar geochemical signatures occur throughout continental shelf and trough strata from Yukon to Nevada and are spatially associated with transfer-transform zones and faults that were episodically reactivated during Cordilleran rift evolution. We

propose that post-breakup rocks emplaced along the North Atlantic margins, such as those in the Orphan and Newfoundland basins, are modern analogues of the Kechika group. This magma-poor rift scenario calls for the release of in-plane tensile stresses and off-axis, post-breakup magmatism along the nascent plate boundary, after lithospheric breakup, but prior to the onset of seafloor spreading.

3.2 Introduction

The western or Cordilleran margin of ancestral North America (Laurentia) is widely assumed to be the result of Tonian-Ediacaran rifting and Ediacaran-Cambrian fragmentation of supercontinent Rodinia (e.g., Stewart, 1972; Colpron et al., 2002; Li et al., 2008; Macdonald et al., 2012). Despite several decades of research on Cordilleran margin development, there remain many open questions about the precise age and paleogeographic setting of Neoproterozoic to lower Paleozoic rift-related rock units that crop out in the western United States and western Canada. Of particular interest are poorly dated, Cambrian-Ordovician volcanic and intrusive rocks (Fig. 3-1A, 1B) that postdate the rift to drift transition and onset of passive margin sedimentation along western North America by up to 40 m.y. (e.g., Souther, 1991; Goodfellow et al., 1995; Cecile et al., 1997; Lund, 2008). The processes responsible for Cordilleran post-breakup magmatism are uncertain and the presence of lower Paleozoic magmatic rocks within the passive margin successions of western North America are not easily reconciled with published scenarios for Ediacaran-Cambrian lithospheric breakup and subsequent thermal subsidence (e.g., Bond et al., 1985). The purpose of this article is to re-examine the Tonian-early Paleozoic rift evolution of western North America and test published models for Cordilleran margin development through new, targeted studies of post-breakup volcanic strata in Yukon, Canada.
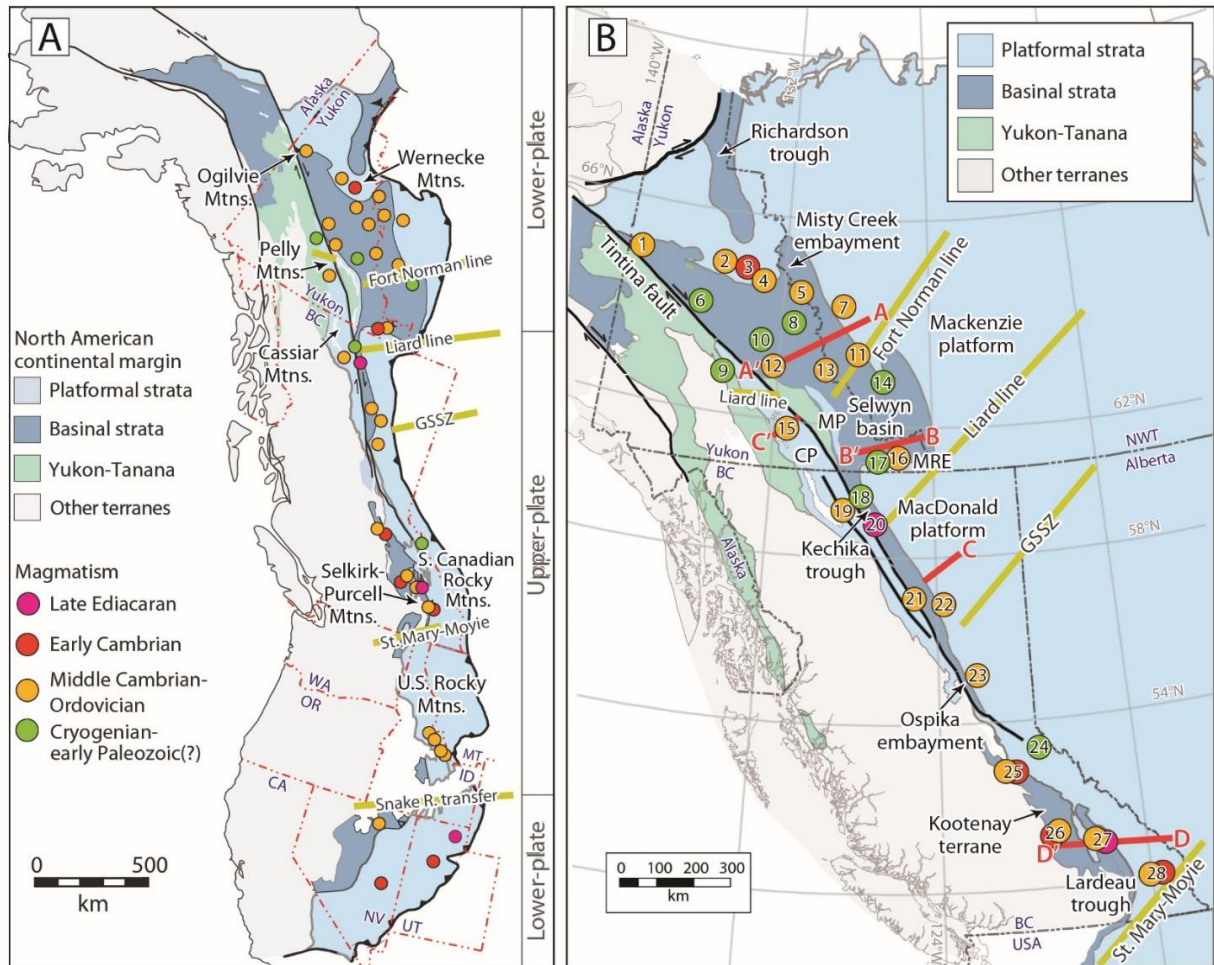
Figure 3-1(A) *Ediacaran to early Paleozoic magmatic rocks, tectonic elements, and crustal lineaments of the North American Cordillera adapted from Goodfellow et al. (1995), Lund (2008), and Colpron and Nelson (2009). Lower- and upper-plate divisions are from Lund (2008).* ***(B)*** *Map of the Canadian Cordillera highlighting the locations of Ediacaran to early Paleozoic magmatic rocks and key paleogeographic features. Numbers from 1-28 are references for Cordilleran margin magmatism provided in Appendix 1. CP - Cassiar platform, MP - McEvoy platform, MRE - Meilleur River embayment, Mtns. - Mountains, R. - river.*

The Gunbarrel magmatic event (780 Ma; e.g., Harlan et al., 2003; Sandeman et al., 2014) and deposition of the Windermere Supergroup (e.g., Stewart, 1972; Link et al., 1993) record the Tonian-Cryogenian stages of Cordilleran rift evolution. These early rift episodes thinned and weakened Cordilleran lithosphere (Yonkee et al., 2014) and were likely associated with strike-slip deformation in some regions of western Laurentia (Strauss et al., 2015). Magmatic activity continued through the Cryogenian (ca. 720-640 Ma) in southeastern Yukon (Pigage and Mortensen, 2004), northern British Columbia (Ferri et al., 1999; Eyster et al., 2018), and western United States (Lund et al., 2003, 2010; Fanning and Link, 2004). Ediacaran (ca. 570 Ma) volcanic rocks and Ediacaran-lower Cambrian siliciclastic strata were deposited after a period of thermal subsidence and are considered to be the products of a second rift phase that resulted in lithospheric breakup (e.g., Devlin and Bond, 1988; Devlin, 1989; Lickorish and Simony, 1995; Warren, 1997; Colpron et al., 2002). Siliciclastic strata of this second rift phase unconformably overlie rocks of the Cryogenian rift episode throughout western North America (e.g., Stewart and Suczek, 1977; Aitken, 1993; Prave, 1999; Lund, 2008) and are spatially associated with volcanic rocks in parts of southern British Columbia and northern Utah (Fig. 3-1A; Christie-Blick, 1997; Colpron et al., 2002; Ferri and Schiarizza, 2006).

An early Paleozoic age for lithospheric breakup is predicted from the thermal subsidence trends of upper Cambrian to Lower Ordovician platformal strata in the southern Canadian and U.S. Rocky Mountains (Armin and Mayer, 1983; Bond and Kominz, 1984; Bond et al., 1985; Levy and Christie-Blick, 1991). The inferred rift to post-rift transition is typically associated with an unconformity between coarse, locally feldspathic rocks and mature, shallow-water quartz sandstone (Bond et al., 1985; Devlin and Bond, 1988; Hein and McMechan, 1994). The transition lies near the Cambrian Stage 2 (late Terreneuvian) to Cambrian Stage 3 (early Series 2) boundary in southeastern British Columbia and within

Cambrian Stage 2 in the western United States (time scale of Cohen et al., 2017; e.g., Bond et al., 1985; Magwood and Pemberton, 1988; Hein and McMechan, 1994). Post-rift, lower Cambrian carbonate strata with archaeocyathid-bearing horizons overlie this syn-rift, siliciclastic sequence (Read, 1980; Fritz et al., 1991; Paradis et al., 2006). Lower Cambrian successions also include poorly dated mafic volcanic rocks with OIB- (ocean island basalt) to N-MORB-like (normal mid-ocean ridge basalt) geochemical signatures in Yukon (e.g., Murphy, 1997; Abbott, 1997; Milidragovic et al., 2006), southern British Columbia (e.g., Kubli and Simony, 1992; Ferri and Schiarizza, 2006; Logan and Colpron, 2006; Paradis et al., 2006), and western United States (e.g., Morris and Lovering, 1961; Kellogg, 1963).

Post-breakup volcanism is not a predicted outcome of pure- or simple-shear rift scenarios that have populated the Cordilleran literature since the early 1980s. For example, Bond and Kominz (1984) and Bond et al. (1984, 1985) used the pure-shear rift model of McKenzie (1978) to estimate subsidence patterns within stable Cordilleran shelf strata (Fig. 3-2A). Pure-shear scenarios predict uniform lithospheric extension that results in symmetric conjugate margins, with syn-rift magmatism invoked to reduce lithospheric strength (e.g., Buck, 2004). The simple-shear rift models of Lister et al. (1986, 1991) were subsequently used to explain the asymmetry of the Cordilleran margin (Fig. 3-2B) and continued reactivation of lithospheric-scale lineaments during the Paleozoic (e.g., Christie-Blick and Levy, 1989; Hansen et al., 1993; Cecile et al., 1997; Tosdal et al., 2000; Lund, 2008). Simple-shear models predict that detachment faults separate the rifted margin into conjugate, upper- and lower-plate margin pairs, with transfer-transform zones bounding different plate-margin segments (Fig. 3-2B). These zones of lithospheric weakness offset contrasting structural domains and provide focal points for mantle-derived magmatism (Thomas, 2006). Upper-plate regions undergo less crustal extension and result in narrow margins with syn-rift uplift being accommodated by magmatic underplating. The lower-plate undergoes a greater

degree of extension, which results in a wide area of lithospheric thinning and highly attenuated continental crust. Whereas alkaline volcanism is inferred to characterize upper-plate margins (e.g., Lund, 2008), the role of volcanism along lower-plate margins is uncertain.

Yonkee et al. (2014) and Beranek (2017) proposed magma-poor rift scenarios (Fig. 3-2C) with lithospheric thinning and necking that are broadly comparable to modern North Atlantic passive margin development. Magma-poor rift processes accommodate depth-dependent extension and decoupling of upper and lower lithosphere, which can result in hyperextension of continental crust and exhumation of continental mantle (Braun and Beaumont, 1989; Davis and Kusznir, 2004; Peron-Pinvidic et al., 2007; Brune et al., 2014). North Atlantic rift models suggest that lithospheric breakup is fundamentally linked to asthenosphere-derived magmatism across the nascent plate boundary, with magmatic activity being most voluminous in outboard regions (Bronner et al., 2011). Off-axis, alkaline magmatism may subsequently occur across an embryonic plate boundary after breakup (Jagoutz et al., 2007), coincident with the deposition of breakup-related clastic successions that preserve the transition from breakup to thermal subsidence (Soares et al., 2012). Beranek (2017) hypothesized that these North Atlantic rift scenarios best explain the origins of post-breakup, Cambrian-Ordovician rocks along the Cordilleran margin of western North America.
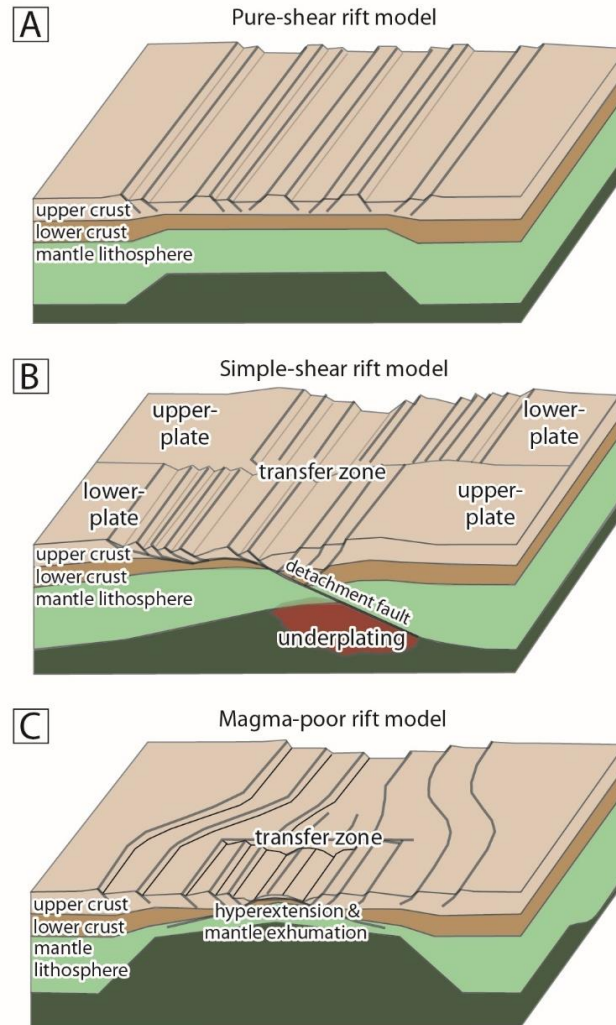
Figure 3-2 *Simplified kinematic models for Cordilleran rift evolution adapted from Yonkee et al. (2014).* ***(A)*** *Pure-shear rift model with uniform, homogeneous thinning of crust and mantle based on McKenzie (1978). Margins that form through mostly pure-shear rifting display very limited evidence for post-rift magmatism when contrasted with evidence for syn-rift magmatism.* ***(B)*** *Simple-shear rift model with heterogeneous thinning of upper and lower lithosphere based on Lister et al. (1986, 1991). Magmatism in the simple-shear model mostly occurs beneath upper-plate margins during the syn- to post-rift phase.* ***(C)*** *Magma-poor rift model with depth-dependent lithospheric thinning and necking based on Davis and Kusznir (2004). This figure represents a snapshot of the period after extensive lithospheric thinning but prior to lithospheric breakup. Syn-breakup magmatism is more voluminous in outboard*

areas where it is dominated by tholeiitic volcanism sourced from the depleted asthenospheric mantle. In contrast post-breakup magmatism occurs across the nascent plate boundary including throughout the rifted margin and is represented by low volume alkaline volcanism, derived from enriched mantle sources.

New high-precision analytical studies of Cambrian-Ordovician igneous rocks are required to establish the significance of post-breakup magmatism in the North American Cordillera. In this article, we use a combination of CA-TIMS (chemical abrasion-thermal ionization mass spectrometry) zircon U-Pb geochronology and whole-rock trace element and Nd-Hf isotope geochemistry to constrain the precise age and origin of the Kechika group, an aerially extensive volcanic-sedimentary succession in south-central Yukon that is representative of post-breakup magmatism in the Canadian Cordillera (Goodfellow et al., 1995; Tempelman-Kluit, 2012). The new results allow us to test the three end-member rift scenarios for the Cordilleran margin and develop new working models for the Neoproterozoic-early Paleozoic evolution of western North America.

3.3 Lower Paleozoic Stratigraphy of the Northern Cordillera

3.3.1 Overview

The Cordilleran margin during Cambrian Series 2 to Ordovician time consisted of broad carbonate platforms that passed seaward into deep-water embayments and margin-parallel troughs (e.g., Fritz et al., 1991; Cecile and Norford, 1991; Nelson et al., 2013). Several paleogeographic highs, defined by areas with a history of non-deposition and/or thin shallow-water strata, periodically emerged during the early Paleozoic and include the long-lived Peace River arch of western Alberta (e.g., McMechan, 1990; Norford, 1990; Cecile and Norford, 1993; Cecile et al., 1997). The outer continental margin basins developed through periodic, heterogeneous early Paleozoic crustal extension rather than purely thermal subsidence and locally have abundant volcanic deposits (Fig. 3-3; Cecile and Norford, 1993; Cecile et al., 1997; Lund, 2008; see also stratigraphic compilation and volcanic rock occurrences in Appendix 1). Coeval volcanism is also recognised within inner continental margin areas, although it is volumetrically restricted and represented by ultrapotassic and

alkaline rocks and carbonatites (Pell, 1987, 1994; Mott, 1989; Norford and Cecile, 1994; Goodfellow et al., 1995; Leslie, 2009; Lund et al., 2010; Millonig et al., 2012).

Lithospheric-scale lineaments, including the northeast-trending Snake River transfer zone and the Liard line (Figs. 3-1A, 3-1B), border most of the significant Cambrian-Ordovician basins (Abbott et al., 1986; Turner et al., 1989; Roots and Thompson, 1992; Cecile and Norford, 1991; MacIntyre, 1998; Pyle and Barnes, 2003; Lund, 2008; Pigage, 2009; McMechan, 2012; Hayward, 2015). The spatial association of these transfer-transform faults with Proterozoic, Paleozoic, and Cenozoic volcanic rocks implies that these structures represent long-lived, leaky zones that were continually reactivated (Goodfellow et al., 1995; MacIntyre, 1998; Lund, 2008; McMechan, 2012; Millonig et al., 2012; Audet et al., 2016; Cobbett, 2016). The Liard line is the most prominent lineament in the Canadian Cordillera and subdivides a wide, lower-plate margin from a narrow, upper-plate margin (Cecile et al., 1997).

Several margin-parallel basins were established within the upper-plate region of western Canada during the early Paleozoic. The Kechika graben of northern British Columbia (Figs. 3-1B, 3-2) was a precursor to the Kechika trough that developed during middle to late Cambrian extensional faulting and local uplift (e.g., Douglas et al., 1970; Fritz et al., 1991; Ferri et al., 1999; Post and Long, 2008; Pyle, 2012). Late Cambrian to Early Ordovician extension was associated with regional volcanism in the Ospika embayment (Fig. 3-1B) and adjacent MacDonald platform (MacIntyre, 1998; Ferri et al., 1999; Pyle and Barnes, 2000, 2003). The parautochthonous Kootenay terrane of southeastern British Columbia contains a Cambrian-Ordovician deep-water rift basin, the Lardeau trough (Fig. 3-1B), that developed adjacent to the St. Mary-Moyie transfer-transform zone and hosts at least three pulses of tholeiitic to alkalic magmatism (Smith and Gehrels, 1992; Ferri and Schiarizza, 2006; Logan and Colpron, 2006; Paradis et al., 2006; Nelson et al., 2013). East of the Kootenay terrane,

Cambrian-Ordovician (ca. 500 Ma) diatremes and alkaline lavas were emplaced in the White River trough (Fig. 3-1B; Godwin and Price, 1986; Pell, 1987; Parrish and Reichenbach, 1991; Kubli and Simony, 1992; Norford and Cecile, 1994; Millonig et al., 2012).

Syn- to post-breakup volcanic rocks are associated with the development of the Selwyn basin (Figs. 3-1B, 3-2) and related embayments in the lower-plate region of northwestern Canada (Cecile and Norford, 1991; Pyle and Barnes, 2003). Alkalic to ultrapotassic volcanic centers, sill complexes, dikes, and diatremes along the lower-plate margin were episodically emplaced during the early Paleozoic (Hart, 1986; Roots, 1988; Abbott, 1997; Murphy, 1997; Cecile, 2000; Thorkelson et al., 2003; Pigage et al., 2015). Some volcanic rocks, such as the middle Cambrian Dempster volcanics in the Ogilvie Mountains of western Yukon (Fig. 3-1B; Roots, 1988; Abbott, 1997; Murphy, 1997; Cecile, 2000), are adjacent to Proterozoic growth faults (Thompson and Roots, 1982; Roots and Thompson, 1992). In areas such as the Misty Creek embayment (Fig. 3-1B), Middle Ordovician alkali basalts and foidites of the Marmot Formation are intercalated with basinal rocks that display a "steer's head" rift profile (Cecile et al., 1982, Goodfellow et al., 1995; Leslie, 2009). The Meilleur River embayment (Liard depression) of southeastern Yukon contains >5.5 km of lower to mid-Paleozoic strata that were likely deposited during the reactivation of the adjacent Liard line (Cecile and Norford, 1991; Cecile et al., 1997). These strata overlie upper Cambrian to Middle Ordovician alkaline basalt and rhyolite of the Crow, Rabbitkettle, and Sunblood Formations that erupted during regional extension (Fig. 3-3; Gabrielse et al., 1973; Pigage, 2009; Pigage et al., 2012, 2015).

Middle Cambrian to Ordovician post-breakup magmatism in the western United States is represented by Covada Group and Bradeen Hill assemblage mafic rocks in the Kootenay terrane of Washington (e.g., Smith and Gehrels, 1992), alkaline plutons of the Big Creek-Beaverhead belt in Idaho (Lund et al., 2010), and mafic alkaline rocks of the Roberts

Mountain allochthon in Nevada (e.g., Watkins and Browne, 1989). Volcanic rocks in the southern Kootenay terrane and Roberts Mountain allochthon were probably deposited in an outer continental margin setting that underwent extensional or transtensional faulting (e.g., Turner et al., 1989). Late Cambrian detrital zircons with intermediate to evolved Hf isotope compositions occur in the upper Cambrian St. Charles Formation of Idaho and likely indicate the uplift of the Lemhi arch and erosion of the Big Creek-Beaverhead belt during reactivation of Snake River transfer fault (Link et al., 2017).

Early Paleozoic crustal extension resulted in local hydrothermal activity and massive sulfide occurrences along the length of the Cordilleran margin (e.g., Goodfellow and Jonasson, 1986; Jennings and Jilson, 1986; Logan and Colpron, 2006). For example, mafic volcanic rocks and sills in the Anvil district of central Yukon (Menzie Creek and Vangorda formations, Fig. 3-3) overlie sedimentary exhalative base-metal deposits that were likely cogenetic with local normal faulting (Allen et al., 2000; Pigage, 2004; Cobbett, 2016). In southeastern British Columbia, the Cu-Zn Goldstream deposit is intercalated with post-breakup volcanic rocks of the Index Formation (Fig. 3-3; Logan and Colpron, 2006). Similar base-metal occurrences are associated with Ordovician strata in the Roberts Mountain allochthon (e.g., Turner et al., 1989). Intrusive rocks and diatremes within the platform and adjacent craton are also linked with enrichments of rare earth elements and other critical metals in southern British Columbia and micro-diamonds in northern Yukon (Godwin and Price, 1986; Pell, 1987; Norford and Cecile, 1994; Goodfellow et al., 1995; Leslie, 2009; Millonig et al., 2012).
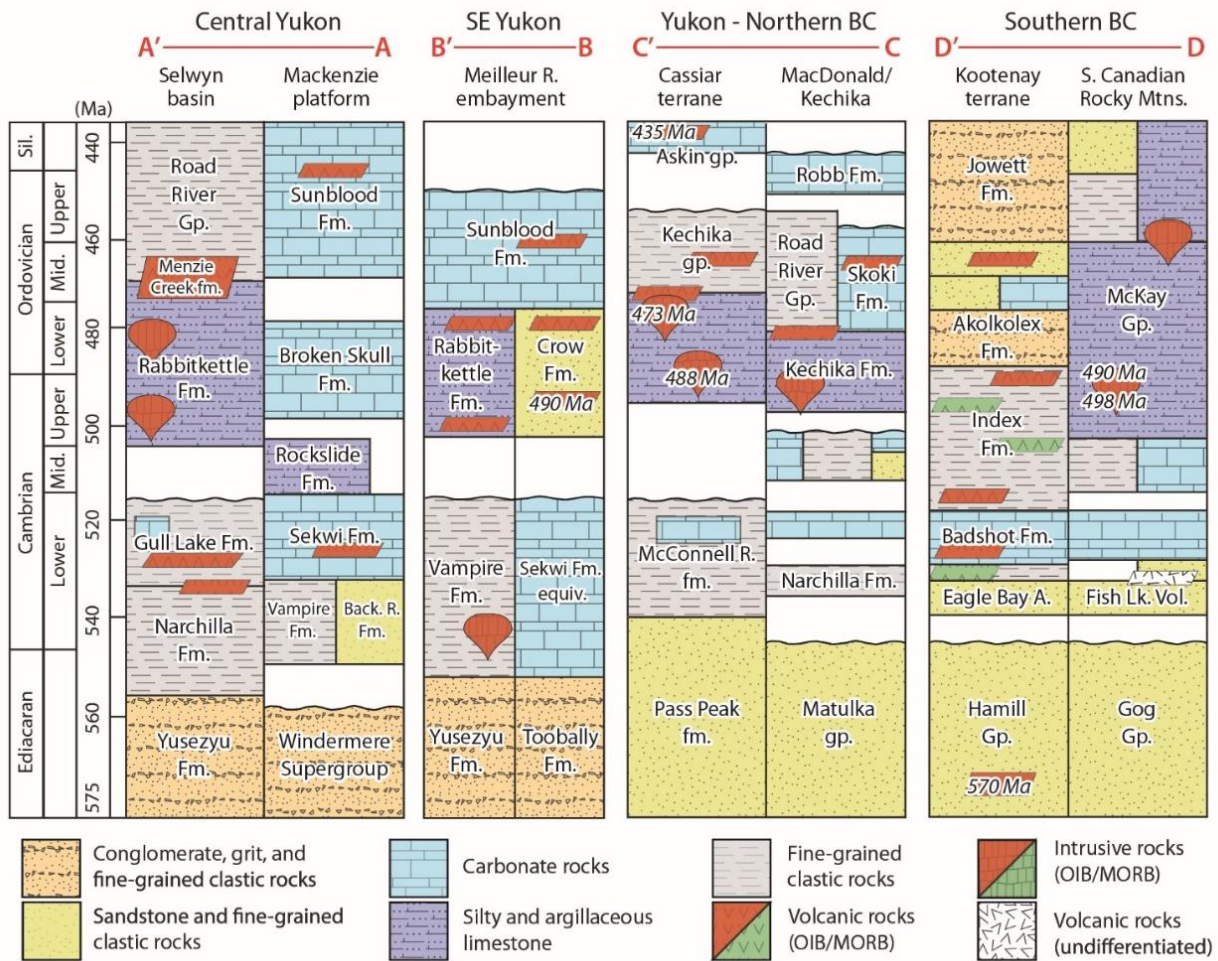
Figure 3-3 *Simplified Ediacaran to lower Silurian stratigraphy of the Canadian Cordillera from central Yukon to southern British Columbia (see lines A-A', B-B', C-C', and D-D' in Figure 1B). Italicized numbers are zircon U-Pb crystallization ages for igneous or tuffaceous rock units*

in the Hamill Group (569.6 ± 5.3 Ma; Colpron et al.., 2002), Crow Formation (490.04 ± 0.13 Ma; Pigage et al., 2012), Kechika group (488.25 ± 0.45 Ma and 472.99 ± 0.70 Ma, this study), Askin group (ca. 435 Ma, this study), and southern Canadian Rocky Mountains (497.6 ± 2 Ma and 489.7 ± 8.4 Ma; Millonig et al., 2012). Stratigraphic compilations: Selwyn basin-Mackenzie platform (Gabrielse et al., 1973; Gordey and Anderson, 1993; Narbonne and Aitken, 1995; Pigage, 2004; Gordey, 2013; Ootes et al., 2013; Pigage et al., 2015; Cobbett, 2016), Meilleur River embayment (Pigage et al., 2015), Cassiar terrane (Tempelman-Kluit, 2012), Kechika trough-MacDonald platform (Fritz et al., 1991; Ferri et al., 1999; Pyle and Barnes, 2003; Pyle, 2012), Kootenay terrane (Hein and McMechan, 1994; Colpron et al., 2002; Ferri and Schiarizza, 2006; Logan and Colpron, 2006; Paradis et al., 2006), southern Canadian Rocky Mountains (Bond and Kominz, 1984; Hein and McMechan, 1994; Millonig et al., 2012; Nelson et al., 2013). A. - assemblage, Back. R. - Backbone Ranges, Fm - Formation (formal), fm. formation (informal), Gp. - Group (formal), gp. - group (informal), Lk. - Lake, Mid. - Middle, MORB - mid-ocean ridge basalt, Mtns. - Mountains, OIB - ocean island basalt, R. - River, S. - Southern, Sil. - Silurian, Vol. – Volcanics.

3.3.2 Pelly Mountains, south-central Yukon

The lower Paleozoic stratigraphy of the Pelly Mountains (Figs. 3-4, 3-5), south-central Yukon, consists of four depositional successions that from oldest to youngest are the Ketza, Kechika, Askin, and Harvey groups (all units informal, Tempelman-Kluit, 2012). The Pelly Mountains region is mostly underlain by the Cassiar terrane, a parautochthonous block of the ancestral North American margin that underwent at least 430 km of post-Cretaceous dextral displacement along the Tintina fault (Gabrielse et al., 2006). Lower Paleozoic strata of the Cassiar terrane comprise part of a linear paleogeographic feature named the Cassiar or Pelly-Cassiar platform (CP in Fig. 3-1B, Gabrielse, 1967; Fritz et al., 1991) or Pelly high (Cecile and Norford, 1993) that was located to the west of inboard elements such as the Selwyn basin, Kechika trough, and MacDonald platform. Allochthonous units of the pericratonic Yukon-Tanana and Slide Mountain terranes that evolved to the west of the North American margin occur in faulted contact with the Cassiar terrane along its western edge and as overlying klippen (e.g., Gordey, 1981). The western extent of the Liard line, which is offset by the Tintina fault, apparently transects the Pelly Mountains region and places most of the Cassiar terrane within an upper-plate setting (Fig. 3-1B; Cecile et al., 1997; Hayward, 2015).
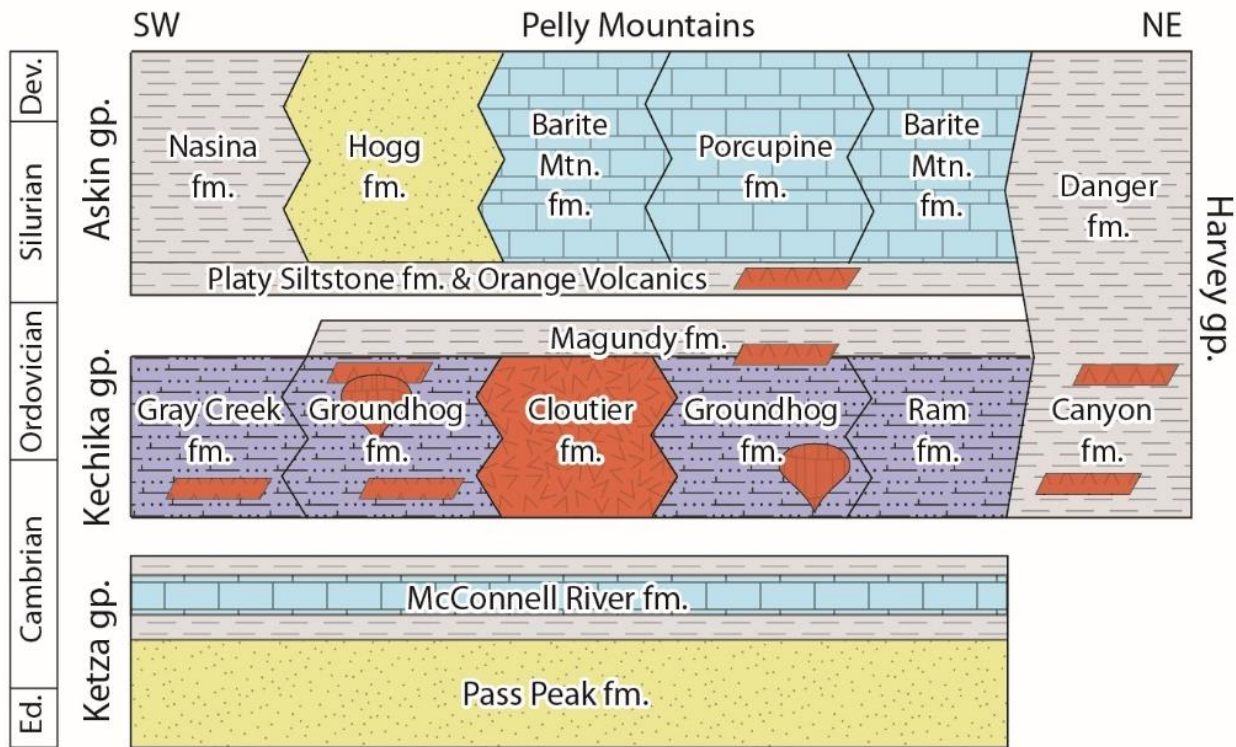
Figure 3-4 *Paleozoic stratigraphy of the Pelly Mountains compiled by Tempelman-Kluit (2012). Abbreviations: Ank = Ankerite; Ed = Ediacaran; fm = formation; gp = group; Miss = Mississippian; Mtn = mountain; Sil = Siliceous; and Sl = Slate. Red polygons in Kechika group represent mafic sills.*
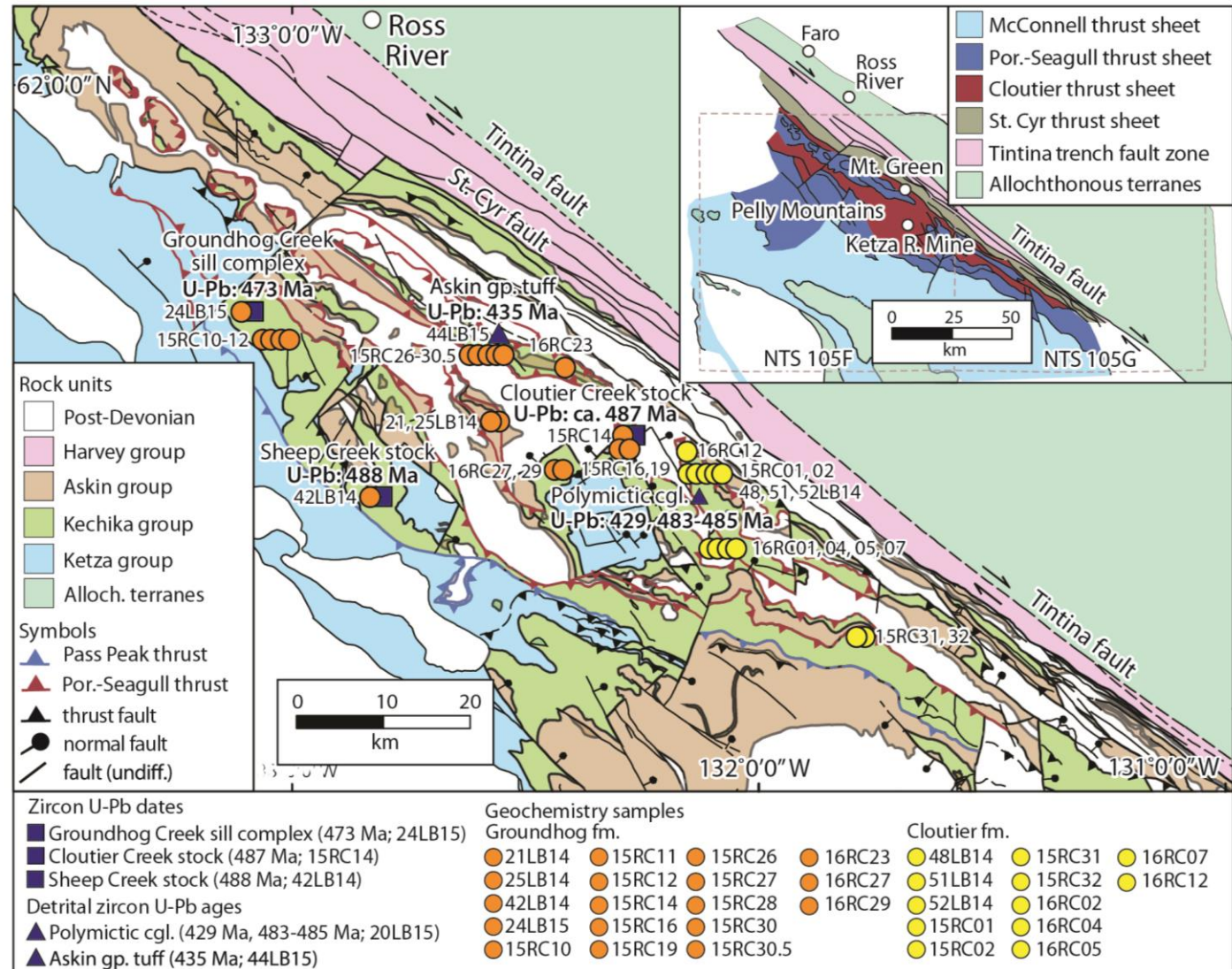
Figure 3-5 (a) *Distribution of thrust sheets within the Quiet Lake (NTS 105F) and Finlayson Lake (NTS 105G) map areas, Pelly Mountains, south-central Yukon (modified from Tempelman-Kluit, 2012).* *(b)* *Distribution of Ketza, Kechika and Askin group rocks in the Pelly Mountains (modified from Tempelman-Kluit, 2012). Numbers refer to localities where samples were collected for geochronology and geochemistry, and are referenced in Appendix 2, 3, and 4.*

Ketza group

Upper Neoproterozoic(?) to lower Cambrian rocks of the Ketza group represent the oldest exposed Cassiar terrane units in Yukon. The basal Pass Peak formation consists of quartzite and fine-grained siliciclastic rocks, whereas the overlying McConnell River formation contains calcareous to pyritic mudstone and carbonate lenses with archaeocyathid-bearing mounds (Read, 1980; Tempelman-Kluit, 2012). The contact between the Ketza group and overlying Kechika group is poorly exposed and typically obscured by faulting (Campbell and Beranek, 2017). A middle Cambrian fossil gap in the Pelly Mountains region, however, suggests the presence of an unconformity (Tempelman-Kluit, 2012); a mid-Furongian unconformity is similarly inferred within the Cassiar terrane of northern British Columbia (Gabrielse, 1963, 1998; Taylor and Stott, 1973; Pyle and Barnes, 2001). The lower Cambrian Rosella Formation in the Cassiar Mountains, northern British Columbia, is correlative to the McConnell River formation and locally intruded by m-thick mafic sills (Gabrielse, 1998).

Kechika group

The Kechika group, the focus of the present study, is an upper Cambrian to Ordovician succession that includes the Cloutier, Groundhog, Ram, and Gray Creek formations (Fig. 3-4; Tempelman-Kluit, 2012; Campbell and Beranek, 2017). Tempelman-Kluit (2012) defined these four formations as being laterally equivalent and interfingered. A fifth stratigraphic unit, the Magundy formation, discontinuously caps the Groundhog, Cloutier, and Ram formations. Kechika group strata generally occur as narrow, northwest-trending, discontinuous belts across the Pelly Mountains (Fig. 3-5).

The Groundhog formation mostly consists of argillaceous to tuffaceous shale, silty limestone, and mafic tuff (Tempelman-Kluit, 2012). Basaltic to gabbroic sills occur throughout the unit, whereas subordinate volcanic and volcaniclastic rocks occur locally

within the upper parts of the formation and overlying Magundy formation (Campbell and Beranek, 2017). The correlative Cloutier formation contains mafic volcanic and volcaniclastic rocks that vary in lateral extent (Tempelman-Kluit, 2012). Volcanic and volcaniclastic lithofacies within the Kechika group include pillow lava, sediment-matrix basalt breccia, and monomictic basalt breccia (Campbell and Beranek, 2017). These lithofacies are overlain by undated polymictic conglomerate and intermediate tuff at several localities (Campbell and Beranek, 2017). The Magundy formation consists of black shale with minor quartz sandstone, basalt, and mafic tuff (Gordey, 1981; Tempelman-Kluit, 2012). Ordovician graptolites provide an upper age constraint for the Magundy formation (Gordey, 1981; Tempelman-Kluit, 2012). The upper Cambrian to Lower Ordovician Ram formation contains platy limestone and lesser shale that is comparable to the calcareous sections of the Groundhog formation. It is restricted to areas between the Tintina and St. Cyr faults (Fig. 3-5; Tempelman-Kluit, 2012). Greenstone, quartz mica schist, and siltstone of the Gray Creek formation may be metamorphosed equivalents of other Kechika group units (Tempelman-Kluit, 2012).

Basinal strata of the lower Kechika group are comparable to those of the Kechika Formation in the southern Cassiar terrane and Kechika trough and Rabbitkettle Formation in the Selwyn basin (Fig. 3-2; Cecile and Norford, 1991; Fritz et al., 1991; Gabrielse, 1998). Magundy formation black shale units are similarly analogous to lower Road River group strata within the Selwyn basin and Kechika trough (Fig. 3-2; Pyle, 2012). Magmatic rocks that are likely correlative with the Kechika group occur in the southern Cassiar Mountains (Gabrielse, 1963; Tempelman-Kluit, 2012), Glenlyon area of central Yukon (Gladwin et al., 2002; Black et al., 2003), and northern Rocky Mountains of British Columbia (Ferri et al., 1999).

Askin group

The Askin group, along with the Sandpile Formation in the Cassiar Mountains, comprises part of the Silurian-Devonian Cassiar platform (Figs. 3-2, 3-4; Gabrielse, 1963, 1998; Cecile et al., 1997; Tempelman-Kluit, 2012). The McEvoy platform of eastern Yukon (EP in Fig. 3-1B) consists of similar shallow-water strata and likely represents a northern equivalent to the northeast of the Tintina fault (Gordey, 2013). Within the Pelly Mountains, the basal Askin group (Orange Volcanics member, Platy Siltstone formation of Tempelman-Kluit, 2012) contains mafic to intermediate lava flows, volcanic breccia, and tuff (Campbell and Beranek, 2017). Ordovician to Silurian shallow-water strata of the Sunblood and Haywire Formations are intercalated with similar volcanic rocks in the Meilleur River embayment area of southeastern Yukon (Fig. 3-2; Goodfellow et al., 1995; Pigage et al., 2015). The significance of the Silurian volcanism is beyond the scope of this paper but may be related to early convergent margin tectonism along northwestern Laurentia (e.g., Pecha et al., 2016).

Harvey group

The Harvey group is named for poorly understood, variably deformed and metamorphosed siliciclastic, carbonate, and volcanic rocks that crop out between the Tintina and St. Cyr faults. Tempelman-Kluit (2012) proposed that the lower two units (Canyon and Danger formations) correlate with Kechika and Askin group strata, respectively (Fig. 3-5).

3.4 Methods

3.4.1 CA-TIMS zircon U-Pb geochronology

Zircons from five rock samples that represent the broad regional extent of early Paleozoic magmatism in the Pelly Mountains were analyzed for CA-TIMS U-Pb

geochronology (Appendix 2) at the Pacific Centre for Isotopic and Geochemical Research (Vancouver, British Columbia) following procedures outlined in Scoates and Friedman (2008). U-Pb dating studies of three gabbro units within the Groundhog formation were conducted to determine the precise timing of Kechika group magmatism, whereas detrital zircons from two volcaniclastic rock samples were examined to constrain the depositional ages of upper Kechika group – lower Askin group strata (see Fig. 3-5 for sample locations). Zircon crystals were concentrated from rock samples using standard crushing, gravimetric, and magnetic separation methods, handpicked in alcohol under the binocular microscope, and annealed in quartz glass crucibles at 900ºC for 60 hours. Annealed zircons were rinsed in ultrapure acetone and water, transferred into screwtop beakers, and chemically abraded in ultrapure HF and HNO_3 at ~175ºC for 12 hours. The remaining zircon crystals were separated from the leachate, rinsed, weighed, and dissolved in HF and HNO_3 at ~240ºC for 40 hours. Ion-exchange column techniques were used to separate and purify Pb and U. Isotopic ratios were measured with a modified single-collector VG-54R thermal ionization mass spectrometer equipped with analog Daly photomultipliers. U-Pb isotopic data were calibrated by replicate analyses of the NBS-982 reference material and values recommended by Thirwall (2000). Data reduction was completed with the Microsoft Excel software of Schmitz and Schoene (2007). The Isoplot program of Ludwig (2003) was used to make Wetherill concordia diagrams and calculate weighted mean averages and MSWD (mean square of weighted deviate) values.

3.4.2 Whole-rock lithogeochemistry

Thirty mafic volcanic and intrusive rocks from the Kechika group were analyzed for whole-rock major- and trace-element geochemistry (Appendix 3). Major element oxide concentrations were acquired at Activation Laboratories (Ancaster, Ontario) by fused-bead x-

ray fluorescence. Trace element concentrations for six samples were acquired at the Pacific

Centre for Isotopic and Geochemical Research by HR-ICPMS (Element 2, Thermo Finnigan,

Germany), whereas twenty-four samples were analysed at Activation Laboratories using a

research grade analytical package (4LITHO RESEARCH).

Eight of the samples were selected for whole-rock Nd and Hf isotope geochemistry

(Appendix 4). Isotopic analyses were carried out at the Pacific Centre for Isotopic and

Geochemical Research on a Nu Plasma II MC-ICP-MS (Nu Instruments Ltd, United

Kingdom). Sample introduction followed the methods described in Weis et al. (2006, 2007)

and occurred under dry plasma conditions using a membrane desolvator (DSN-100). For each

analytical session, the standard solution JDNi (for Nd analyses) yielded average values of

^{143}Nd/^{144}Nd = 0.512088 ± 0.000008 (n = 24), and ^{143}Nd/^{144}Nd = 0.282157 ± 0.000011 (n =

41) for 2014 and 2015 samples, respectively. The JMC 475 standard solution (for Hf

analyses) yielded average values of ^{176}Hf/^{177}Hf = 0.282156 ± 0.000004 (n = 11), and

^{176}Hf/^{177}Hf = 0.282157 ± 0.000011 (n = 41) for 2014 and 2015 samples, respectively. The

results were corrected for instrumentation mass fractionation by exponentially normalising to

^{146}Nd/^{144}Nd = 0.7219 (O'Nions et al., 1979), and ^{179}Hf/^{177}Hf = 0.7325 (Patchett and

Tatsumoto, 1981).

Sampling and alteration

Rocks that preserve primary volcanic and intrusive textures were preferentially

selected for geochemical analysis, whereas those containing veining, alteration, and textures

associated with extensive fluid-rock interaction were avoided to limit post-crystallization

geochemical modification. Fluid-rock interaction can lead to the mobility of elements that are

otherwise thought to be immobile such as P_2O_5 and Y during the alteration of volcanic glass

to clays (e.g., Price et al., 1991; Murton et al., 1992). Kechika group rock samples typically

feature replacement of primary minerals with greenschist-facies assemblages (Tempelman-Kluit, 2012). Primary minerals in coarse-grained, mafic intrusive rocks include clinopyroxene, plagioclase, and Fe-Ti oxide minerals. Pyroxene is replaced by chlorite in most samples, whereas plagioclase is typically replaced by sericite. These observations are consistent with high loss on ignition (LOI; up to 14 wt. %) values in some samples.

Immobile elements were used to classify Kechika group rocks because of the likelihood major element mobility (Spitz and Darling, 1978; MacLean and Barrett, 1993; Jenner, 1996; Piercey et al., 2002) as indicated by the lack of primary mineralogy in most samples. Elements that are usually immobile during hydrothermal alteration include Al, Ti, Th, Cr, HFSEs, and REEs (except La). Elements that are typically immobile include Sc, V, P, Co, and Ni (Pearce and Cann, 1973; Winchester and Floyd, 1977; Jenner, 1996; Pearce, 1996).

3.5 Results

3.5.1 CA-TIMS zircon U-Pb geochronology

Sheep Creek stock

The informally named Sheep Creek stock is an isolated, 1-km^2 body that intrudes Groundhog formation strata along the upper reaches of Sheep Creek, ~50 km southwest of Ross River. A sample of coarse-grained pyroxene gabbro (42LB14; Fig. 3-5B) contains equant to elongate zircons that range in size from 100-125 μm. The crystallization age of the Sheep Creek stock is derived from three concordant zircons that yield a weighted mean $^{206}Pb/^{238}U$ age of 488.25 ± 0.45 Ma (MSWD = 0.96; Fig. 3-6A). A fourth zircon gave a discordant age of ca. 486 Ma and likely reflects post-crystallization Pb loss.

Cloutier Creek stock

The informally named Cloutier Creek stock is a ca. 1-km^2 body that intrudes Groundhog formation strata on the south side of Cloutier Creek, ~40 km southeast of Ross River. Coarse-grained pyroxene gabbro (15RC14; Fig. 5) from this location contains opaque, high U zircons that dissolved completely during chemical abrasion leaching at standard conditions. Five zircons survived a relatively gentle leach and yielded strongly discordant data (20-23%) that define a linear array interpreted to result from Pb loss, with an upper intercept of 486 ± 19 Ma and lower intercept of 167 ± 17 Ma (MSWD = 1.14). Five additional zircons that survived the first step underwent a second, higher temperature leach to assess whether less disturbed, possibly concordant sectors of grains exist. One of these dissolved completely and only minor traces of material survived for the other four. The latter gave relatively imprecise results that lie along the same discordia array defined by gently leached grains. A discordia line constructed through results for all nine analyses yields intercepts of 487 ± 19 Ma and 167 ± 16 Ma (MSWD = 0.56). Based on these data a crystallization age of ca. 487 Ma is estimated for the Cloutier Creek stock.

Groundhog Creek sill complex

The informally named Groundhog Creek sill complex consists of well-exposed, 1 to >30 m-thick sills that intrude Groundhog formation strata along the north side of Groundhog Creek, ~40 km southwest of Ross River. The sills consist of fine- to coarse-grained mafic rocks that underlie an area of ~12 km^2. A sample of medium-grained pyroxene gabbro (24LB15; Fig. 3-5B) contains mostly equant zircons that range in size from 75-125 μm. The crystallization age of the Groundhog Creek sill complex is constrained by two concordant zircons that yield a weighted mean ^{206}Pb/^{238}U age of 472.99 ± 0.70 Ma (MSWD = 0.85; Fig. 3-6B). An upper intercept age of ca. 1742 Ma is estimated for the core of a third, highly discordant zircon.

Polymictic conglomerate

Cloutier formation strata to the east of the Ketza River Mine, ~50 km southeast of Ross River, mostly consist of vesicular to amygdaloidal massive basalt, pillow basalt, and associated volcanogenic rock units that were deposited in a submarine, vent proximal environment (Campbell and Beranek, 2017). Variably deformed shale, limestone, and polymictic (limestone, mafic-intermediate volcanic rock) conglomerate units immediately overlie these Cloutier formation strata but have uncertain contact relationships with the underlying volcanic sequence. Six detrital zircons analyzed from a sample of the polymictic conglomerate (20LB15; Fig. 3-5B) yielded concordant $^{206}Pb/^{238}U$ ages of 428.92 ± 0.87 Ma, 483.43 ± 0.65 Ma, 484.34 ± 0.89 Ma, 485.01 ± 1.12 Ma, 1820.29 ± 4.23 Ma, and 2687.25 ± 7.73 Ma (Fig. 3-6C). Two zircons yielded discordant ages of ca. 432 Ma and 1745 Ma.

Askin group tuff

Kechika group strata within the upper reaches of Ram Creek, ~30 km south-southeast of Ross River, consist of a lower section of well-exposed, Groundhog formation shale, silty limestone, mafic intrusions, and volcanic to sedimentary lithic breccia, and an upper section of poorly exposed, Magundy formation black shale (Campbell and Beranek, 2017). Mafic to intermediate lava flows and tuff of the basal Askin group (Orange Volcanics member of Tempelman-Kluit, 2012) overlie the Kechika group rocks. Four detrital zircons analyzed from a sample of orange-weathering Askin group tuff (44LB15; Fig. 3-5B) yielded concordant $^{206}Pb/^{238}U$ ages of 435.37 ± 0.86 Ma, 1375.99 ± 3.37 Ma, 1840.66 ± 4.26 Ma, and 2023.17 ± 9.20 Ma (Fig. 3-6D). Two zircons yielded discordant ages of ca. 1658 Ma and 2677 Ma.
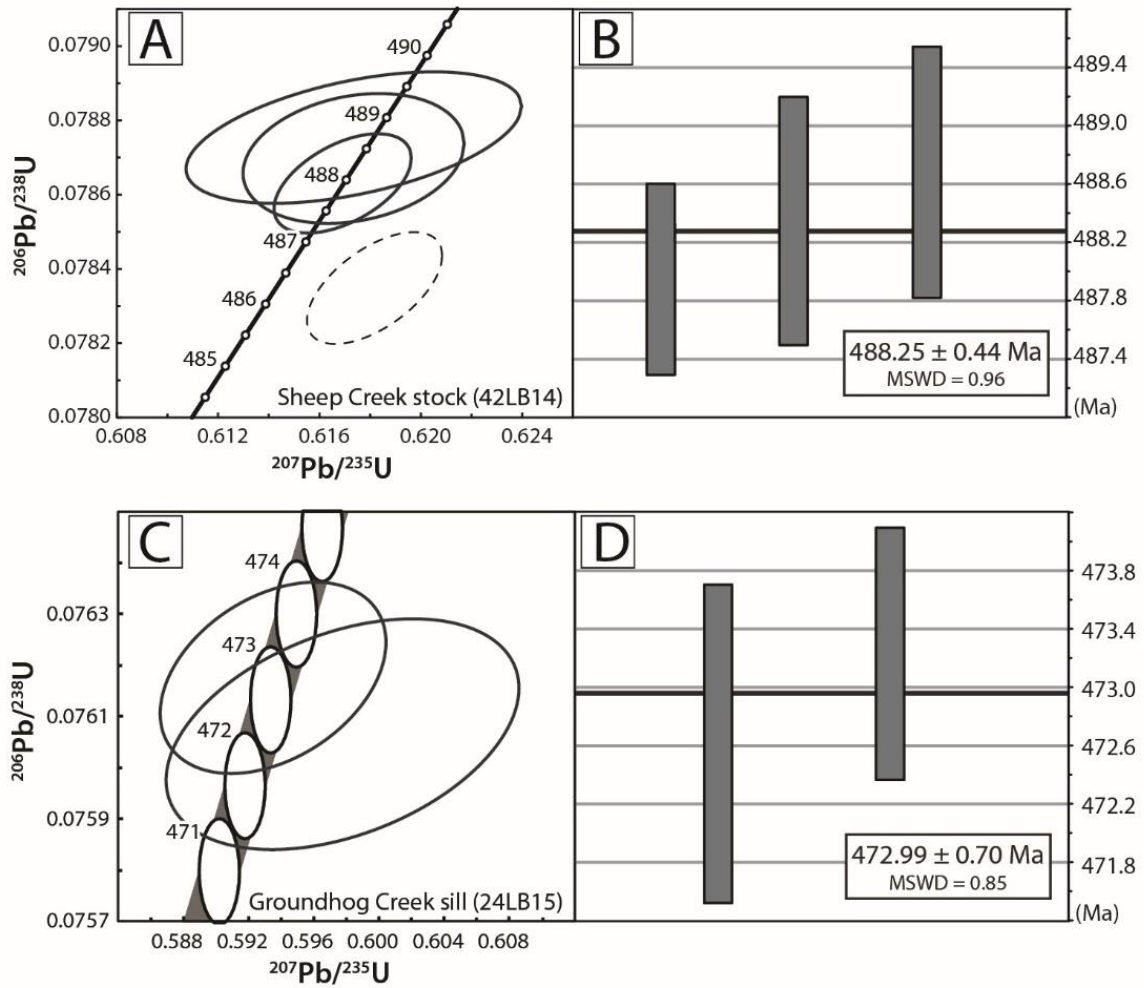
Figure 3-6 (A, C) Wetherill concordia plots of CA-TIMS U-Pb ages from samples 42LB14 (Sheep Creek stock) and 24LB15 (Groundhog Creek sill complex). Data are shown with 2σ error ellipses. Dashed ellipse is a data point not used for interpretation. **(B, D)** 206Pb/238U weighted mean plots for samples 42LB14 and 24LB15. See text for age interpretations. MSWD – mean square of weighted deviates.

3.5.2 Lithogeochemistry

Element mobility

Sodium, immobile element concentrations, and some incompatible element ratios used to signify magmatic processes were plotted against the Al_2O_3/Na_2O alteration index of Spitz and Darling (1978) to semi-quantitatively determine element mobility (Figs. 3-7A-I). Most samples have low Al_2O_3/Na_2O ratios (23 of 30 samples yield Al_2O_3/Na_2O <10) with the exception of four Cloutier formation rocks that have elevated Al_2O_3/Na_2O ratios (>25; Fig. 3-7A). Some elements such as Ni, Cr, and Y can be highly variable, however, but most immobile element ratios show no relationship to alteration.
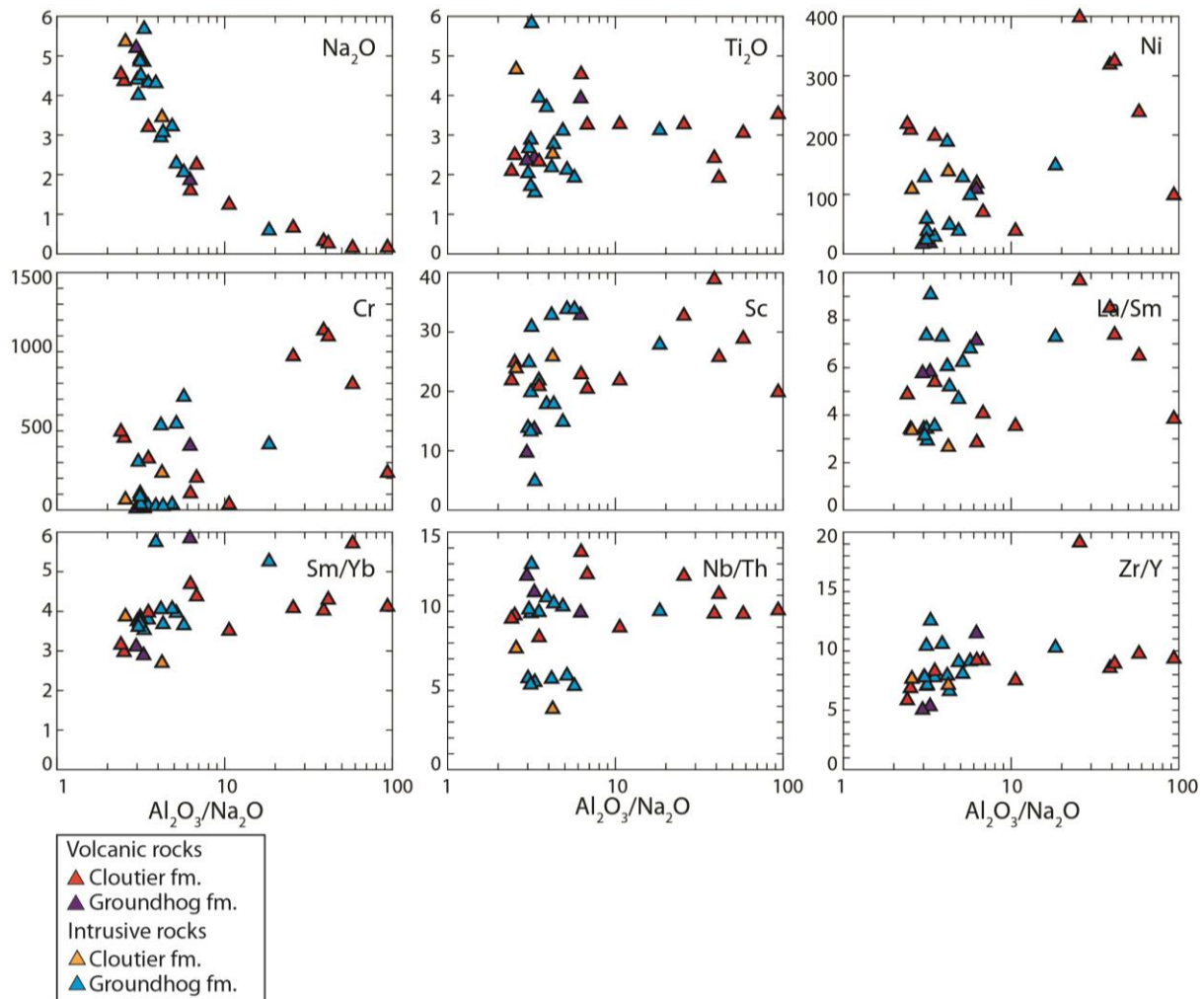
Figure 3-7 (a-i) *Key trace elements and elements ratios of the Kechika group rocks plotted*

against the Spitz-Darling Al_2O_3/Na_2O alteration index (Spitz and Darling, 1978). Most

elements and elemental ratios feature a lack of correlation with the alteration index

suggesting that elemental variation is independent of alteration. Five of the volcanic rock

samples feature a slight negative correlation for Ni, Cr, Sc and Y but this is not present in the

remaining samples. Red triangle = Cloutier fm. volcanic rocks, orange triangle = Cloutier

fm. intrusive rocks, blue triangle = Groundhog fm. intrusive rocks, and purple triangle =

Groundhog fm. volcanic rocks.

Cloutier and Groundhog formation volcanic rocks

Volcanic rock samples from the Cloutier formation ($n = 11$) and Groundhog formation ($n = 3$) consist of pillow basalt and massive vesicular to amygdaloidal basalt. Kechika group volcanic rocks have basaltic affinities (Zr/Ti = 0.011-0.013), are moderately to extremely alkalic (Nb/Y = 1.6-8.8) and classified as alkali basalts to foidites (Fig. 3-8). The Zr/Ti ratio may signify crystal fractionation analogous to silica in a total alkali-silica diagram (Pearce, 1996). Zr behaves in a highly incompatible manner up to "acid-intermediate" composition magmas, whereas the compatibility of Ti increases during fractional crystallisation of intermediate composition magmas (specifically due to crystallization of Fe-Ti oxide minerals; e.g., Cann, 1970; Pearce, 1996; Piercey et al., 2002).

Kechika group volcanic rocks display a broad range of transition metal contents such as Ni (18-400 ppm), Cr (15-1140 ppm), and Co (17-62 ppm) with moderate to low magnesium numbers (61 to 20; Fig. 3-9A). Aside from one basalt sample with high Ni and two with high Cr (400ppm, 1102ppm, and 1140 ppm respectively) the majority of Kechika group volcanic rocks have transition metal contents, and magnesium numbers, that are below the expected values of primary melts (e.g., Ni = 400-500 and Cr > 1000 ppm; Mg # > 70). The variability of these elements is most likely linked to olivine and clinopyroxene (+/- chromite) fractionation for Ni and Cr, respectively. A decreasing Cr/Ni ratio with increasing Zr is consistent with field and petrographic identification of clinopyroxene phenocrysts in volcanic rocks, and therefore clinopyroxene fractionation. Therefore, these values are consistent with high to moderate degrees of crystal fractionation and/or crustal assimilation. The Kechika group volcanic rocks are therefore unlikely to represent primary mantle melts.

TiO_2, Al_2O_3, V, and Eu show increasing trends with increasing Zr content, although samples with elevated Zr contents (>300 ppm) have significant variability. This is possibly related to crystal fractionation and/or accumulation of Fe-Ti oxide minerals and plagioclase

in more evolved samples. The Al_2O_3/TiO_2 ratio of the volcanic rocks (2.2-6.5; Fig. 3-9C) is relatively low, comparable to modern ocean-island basalts (OIB = ~5; Piercey et al., 2004) and enriched mid-ocean ridge basalts (E-MORB = ~10; Sun and McDonough, 1989; Piercey et al., 2004), and likely due to relatively elevated TiO_2 contents.

The Nb/Y ratio indicates the degree of alkalinity (broadly analogous to Na in the total alkali silica diagram) because the behaviour of Nb is broadly comparable to Na during anhydrous mantle melting (e.g., Pearce, 1996). Nb and Y become fractionated due to Y becoming more compatible during mantle melting in the presence of residual garnet (Pearce, 1996). The degree of alkalinity of basaltic magmas is controlled by factors including the enrichment of the mantle source area, degree of partial melting, and depth of melting (e.g., Pearce, 1996; Humphreys and Niu, 2009). The Ti/V ratio (46-85; Fig. 3-9D) is comparable to modern non-arc, transitional tholeiites to alkaline basaltic rocks (alkaline basalts = >50; Shervais, 1982).

Cloutier and Groundhog formation volcanic rocks have steep, negative sloping, primitive mantle–normalised trace-element patterns (Figs. 3-10A, 3-10B) that are characterized by light rare earth element (LREE) enrichment (La/Sm$_{mn}$ = 1.9-6.3) relative to heavy rare earth element (HREE) depletion (Sm/Yb$_{mn}$ = 3.3-6.5) and a flat to positive Nb anomaly (Nb/Th$_{mn}$ = 1.0-1.6). These geochemical signatures are broadly comparable to global average OIB (La/Sm$_{mn}$ = 2.4, Nb/Th$_{mn}$ = 1.4 and Sm/Yb$_{mn}$ = 5.14; Sun and McDonough, 1989) with more LREE-depleted samples approaching global E-MORB compositions (La/Sm$_{mn}$ = 1.6, Nb/Th$_{mn}$ = 1.6, and Sm/Yb$_{mn}$ = 1.2; Sun and McDonough, 1989).

The immobile element ratios (Zr/Yb, Nb/Yb and Nb/Th ratios; Figs. 3-11A, 3-11B) of some Cloutier and Groundhog formation volcanic rocks suggest derivation from a fertile, incompatible element-enriched mantle source (e.g., Sun and McDonough, 1989; Pearce and

Peate, 1995; Piercey and Colpron, 2009; Piercey et al., 2012). The Nb/Ta (13-17) and Zr/Hf

(36-48) ratios show evidence of fractionation relative to the chondritic uniform reservoir

(CHUR; Nb/Ta = 17.6; Zr/Hf = 36.3; Sun and McDonough, 1989), and composition of global

OIB and NMORB (Zr/Hf for OIB = 35.9 and NMORB = 36, and Nb/Ta for OIB = 17.8 and

NMORB = 17.7; Sun and McDonough, 1989). This process is consistent with low-degree

mantle partial melting processes (~1-3%; Green, 1995; David et al., 2000).

Cloutier and Groundhog formation intrusive rocks

Mafic intrusive rocks of the Groundhog formation (*n* =14) and Cloutier formation (*n*

= 2) consist of medium- to coarse-grained, >1 m-thick sills and stocks. Kechika group

intrusive rocks are mostly classified as alkali basalts (Fig. 3-8), however, these can range

from basaltic to intermediate affinities (Zr/Ti = 0.005-0.036) and be subalkalic to foiditic in

composition (Nb/Y = 0.56-3.8). The intrusive rocks show a greater degrees of fractionation

than comagmatic lava flows based on the increased variability within the Zr/Ti ratio.

The intrusive rocks show a broad range of Ni (<20-190 ppm), Cr (<20-720 ppm), and

Co (9-49 ppm) contents with moderate to low magnesium numbers (59 to 23; Fig. 3-9B). The

transition metal contents, and magnesium numbers are generally lower than those observed in

the volcanic rocks, and lower than the expected values from primary mantle melts. Some of

the more fractionated gabbros (Zr >300 ppm) have Ni concentrations below the limit of

detection (<20 ppm). Kechika group intrusive rocks therefore do not represent primary

mantle melts. The range of Cr contents and steep Cr vs. Ni ratios with increasing

fractionation provide evidence for clinopyroxene fractionation, which is consistent with field

and petrographic observations of clinopyroxene phenocrysts.

The elevated levels of magma evolution in some intrusive rocks (e.g., Zr contents

>250 ppm) are associated with either a relative depletion or enrichment in Ti, Eu, V, and

Al_2O_3 contents. Gabbro samples with enrichments in Ti, Eu, V, and Al_2O_3 relative to Zr are associated with field and petrographic observations of plagioclase and skeletal to interstitial Fe-Ti oxides. The Al_2O_3/TiO_2 ratio (2.5-12; Fig. 3-9C) is greater than that of volcanic rocks, but comparable to modern OIB to E-MORB.

Nb/Y values are consistent with Kechika group volcanic rocks values and imply similar mantle source regions and mantle melting processes. Elevated Ti/V (46-154) ranges from the values associated with modern alkaline basalts (alkaline array) to transitional tholeiites (Fig. 3-9D; Shervais, 1982).

Kechika group intrusive rocks have steep, negative sloping, primitive-mantle normalized multi-element patterns with high to moderate LREE enrichment (La/Sm_{mn} = 1.7-5.9) and relatively steep HREE profiles (Sm/Yb_{mn} = 3.0-6.4) that are comparable to the Kechika group volcanic rocks and modern OIB to E-MORB (Figs. 3-10A, 3-10B). Some of the samples (n = 8) have a negative Nb/Th_{mn} ratio (0.46-1.6) in addition to reduced LREE enrichment compared to other Kechika group rocks.

Zr/Yb and Nb/Yb ratios reflect derivation from a fertile, incompatible element-enriched mantle source (Figs. 3-11A, 3-11B). The Nb/La vs. Nb/Th plot indicates the significance of crustal contamination in many of these rocks (Fig. 3-11A). Fractionation of the Nb/Ta and Zr/Hf ratio relative to CHUR is also present in the intrusive rocks of the Kechika group (e.g., Nb/Ta = 13 to 6.5; Zr/Hf = 39 to 48; Sun and McDonough, 1989; Green, 1995).
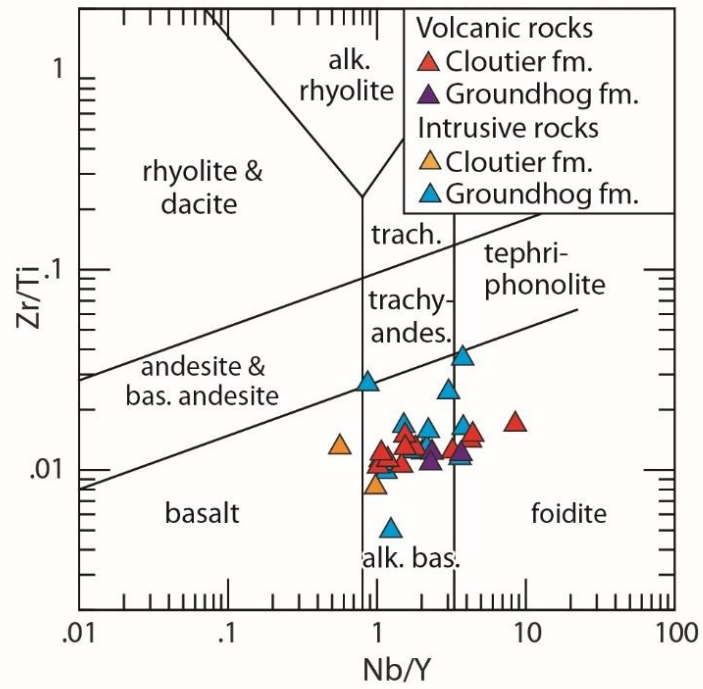
Figure 3-8 *Nb/Y vs. Zr/Ti plot of Winchester and Floyd (1977) as modified by Pearce (1996) for Kechika group rocks.*
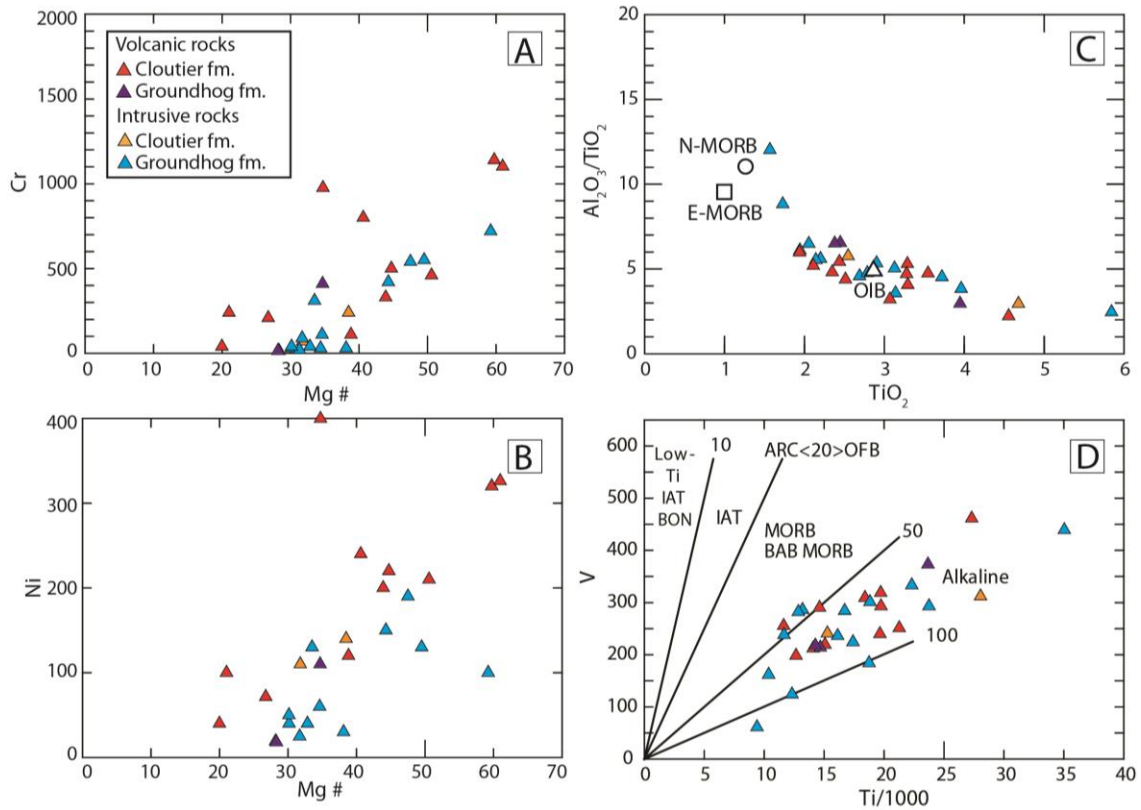
Figure 3-9 (a) Mg number vs. Cr, (b) Mg number vs. Ni, (c) *Al₂O₃/TiO₂ vs. TiO₂ plot after*

Piercey et al. (2012). Included in this diagram are global average values for normal mid-

ocean ridge basalt (MORB), enriched mid-ocean ridge basalt (E-MORB), and ocean-island

basalt (OIB) from Sun and McDonough (1989). ***(d)*** *The Ti-V discrimination diagram of*

Shervais (1982) indicating the alkaline to transitional tholeiite character of the Kechika

group rocks.
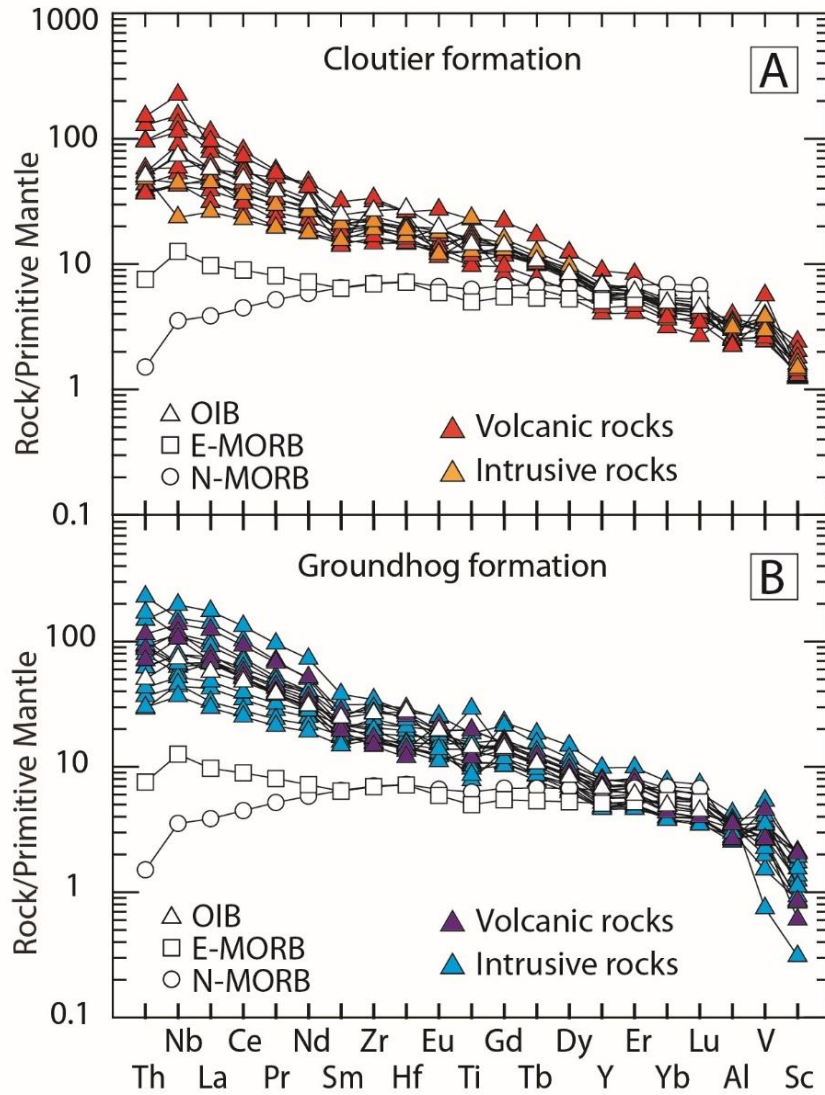
Figure 3-10 *Primitive-mantle–normalized multi-element plots of the Kechika group volcanic*

(a) and intrusive rocks (b) with modern analogues for comparison. Primitive-mantle

normalisation values, modern N-MORB, E-MORB, and OIB are from Sun and McDonough

(1989).
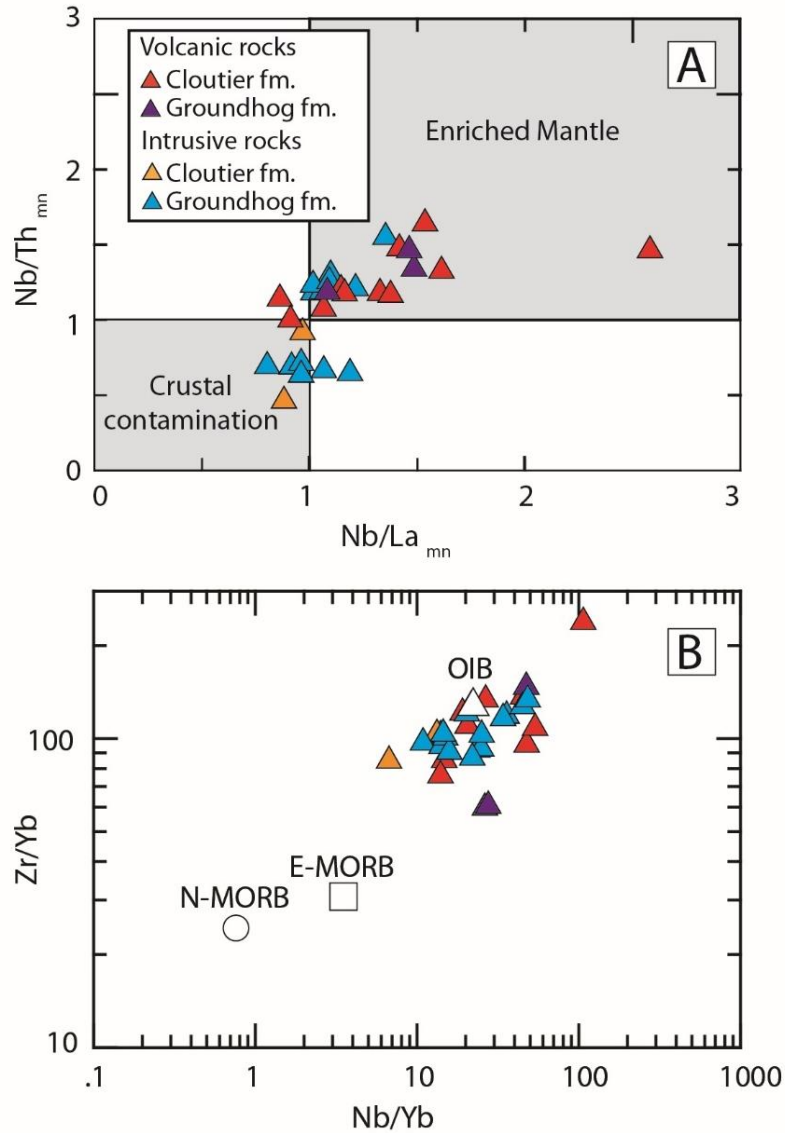
Figure 3-11 (a) *Nb/Th$_{mn}$ vs. Nb/La$_{mn}$ diagram for Kechika group rocks. Diagram adapted*

from Piercey et al. (2006) which in turn was based on the concept of Niu et al. (1999) (e.g.,

Ta/U$_{mn}$ vs. Nb/Th$_{mn}$ diagram), $_{mn}$ = mantle normalised with primitive-mantle normalisation

*values from Sun and McDonough (1989). **(b)** Zr/Yb vs. Nb/Yb diagram of Pearce and Peate*

(1995). The Kechika group rocks plot between enriched mid-ocean ridge basalt (E-MORB)

and ocean island basalt (OIB) end members and are therefore consistent with derivation

from an incompatible element–enriched mantle.

Nd-Hf isotope geochemistry

Initial epsilon values were calculated using the crystallization ages of 488 Ma and 473 Ma for the newly dated gabbros and an intermediate age of 480 Ma was used for undated rocks. Kechika group volcanic rocks have ε_{Ndt} values that range from +2.9 to +5.5 and ε_{Hft} values that range from +2.9 to +6.6 (Fig. 3-12A). These values are lower than expected for rocks sourced from the depleted mantle reservoir at 480 Ma, with ε_{Ndt} values ranging between +7.8 and +9.3 based on the models of DePaolo (1981) and Goldstein et al. (1984), respectively, and ε_{Hft} values at +15.6 based on the model of Vervoort and Blichert-Toft (1999). This implies that the mantle source underwent relative enrichment in LREE, resulting in a Sm/Nd ratio < CHUR (Goldstein et al., 1984; DePaolo, 1988). Kechika group intrusive rocks have ε_{Ndt} values that range from -4.2 to +1.0 and ε_{Hft} values that range from –9.8 to +0.6. The negative values are comparable to an evolved crustal source (e.g., DePaolo, 1988), including shale units of the Kechika group that have ε_{Ndt} values that range from to -11.6 to -13.9 and ε_{Hft} values that range from -13.5 and -21.0 (Figs. 3-12A-C; L. Beranek, unpublished data). Depleted mantle model ages for the volcanic rocks range from T_{DM} (Nd) = 670 Ma to 1000 Ma and T_{DM} (Hf) = 840 to 1030 Ma. The model ages for the intrusive rocks range from T_{DM} (Nd) = 1220 to 1450 Ma and T_{DM} (Hf) = 1150 to 1620 Ma. Rocks with strongly negative ε_{Ndt} and ε_{Hft} compositions also have low Nb/Th ratios (Figs. 3-13A, 3-13B).
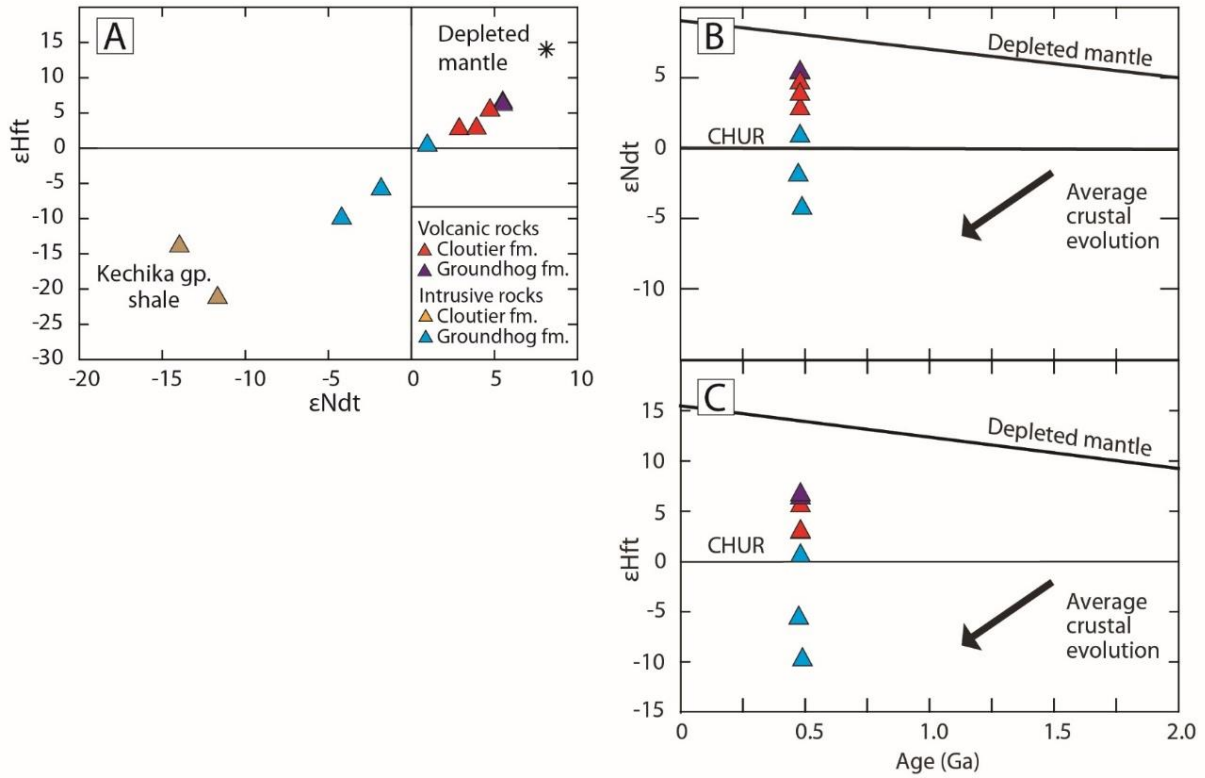
Figure 3-12 (a) *Initial εHf$_t$ vs. εNd$_t$ for the Kechika group volcanic, intrusive and fine-grained clastic rocks. The value of depleted mantle at 480 Ma is also shown (based on the model of DePaolo, 1981, and Vervoort and Blichert-Toft, 1999).* ***(b)*** *εNd$_t$ against time for the Kechika volcanic, and intrusive rocks. The depleted mantle evolution line is based on DePaolo (1981).* ***(c).*** *εHf$_t$ against time for the Kechika volcanic, and intrusive rocks. The depleted mantle evolution line is based on Vervoort and Blichert-Toft (1999).*
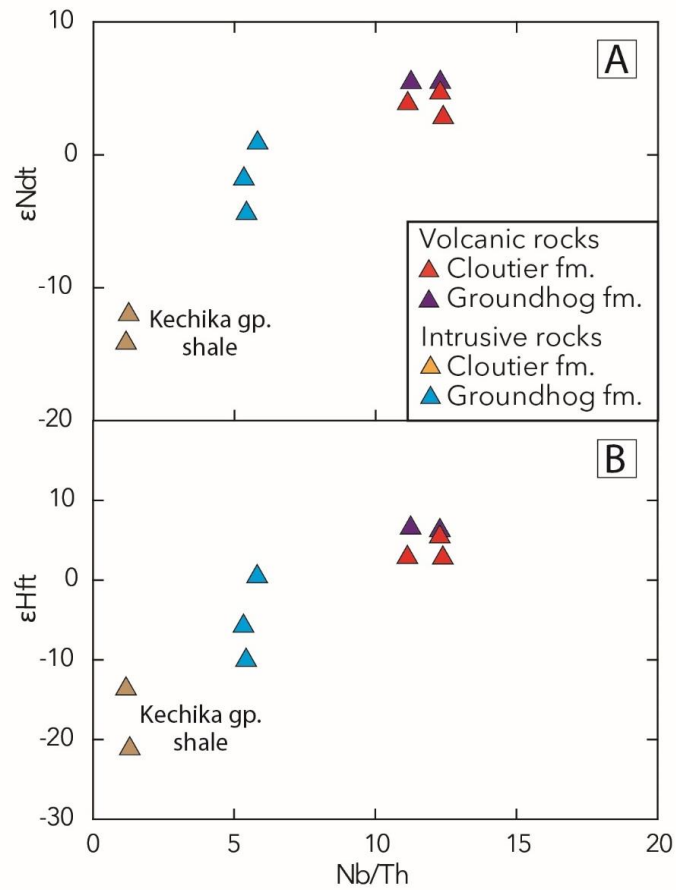
Figure 3-13 (a) *Initial εNd$_t$ vs. Nb/Th, and **(b)** Initial εHf$_t$ vs. Nb/Th for the Kechika group*

volcanic, intrusive and fine-grained clastic rocks. This demonstrates that the chemical and

isotopic values of the intrusive rocks can be modelled as a mixture between the fine-grained

clastic rocks, and the volcanic rocks.

3.6 Discussion

3.6.1 Timing and emplacement history of the Kechika group

The Sheep Creek and Cloutier Creek stocks, Groundhog Creek sill complex, and other Kechika group intrusive rocks likely originated as sill-sediment complexes (Campbell and Beranek, 2017) that were periodically emplaced into the outer Cordilleran margin during the latest Cambrian (ca. 488-487 Ma) to Early Ordovician (473 Ma). The sill-sediment complexes represent syn-sedimentary volcanism in sediment-rich basins that formed during the rifting of thinned continental crust and are spatially associated with transform-transfer zones like the Liard line (e.g., Einsele, 1986; Naylor et al., 1999). The geochemistry and observed field relationships strongly suggest that these crystallization ages are also appropriate for the overlying and comagmatic extrusive rocks, which originated at subaqueous volcanic centers. These U-Pb dates confirm the limited Cambrian to Ordovician fossil ages for the upper Kechika group (Tempelman-Kluit, 2012). Silurian detrital zircons within the polymictic conglomerate and Askin group tuff samples provide an upper age limit for Kechika group deposition. The presence of 485, 484, and 483 Ma detrital zircons in the polymictic conglomerate sample is consistent with local uplift and erosion of Kechika group rocks during the early Silurian (Tempelman-Kluit, 2012).

3.6.2 Petrogenesis and magma source components

The non-arc primitive mantle-normalized signatures of the Kechika group rocks (Fig. 3-10) indicates that melt generation was likely associated with decompression melting associated with upwelling mantle. The OIB- to E-MORB-like primitive mantle-normalized signatures and alkaline geochemistry of Kechika group rocks indicates the enrichment of incompatible elements during mantle melting (e.g., Pearce, 1996). This enrichment is a

function of both the mantle source, as indicated by Nd-Hf isotopic compositions, and melting processes, as indicated by trace element data (e.g., Fitton, 1987; Pearce, 1996; MacDonald et al., 2001; Niu et al., 2011, 2012). Similar incompatible element-enriched basalts are found in extensional settings, including continental rifts (e.g., Furman, 2007), attenuated continental margins (e.g., Pe-Piper et al., 2013), exhumed continental mantle lithosphere (e.g. Merle et al., 2009; Miranda et al., 2009), and areas with thickened oceanic lithosphere (e.g., Sun and McDonough, 1989; Niu et al., 2011). An increase in lithospheric thickness can inhibit asthenospheric mantle upwelling and therefore increase the overall depth of the melting interval. This increase in depth will increase the pressure of melting and reduce the volume of melt (the lid effect; e.g., McKenzie and Bickle, 1988; Niu and O'Hara, 2007; Humphrey and Niu, 2009). A reduction in melt volume will therefore further concentrate incompatible elements and volatiles, such as Na, Nb, HFSE, Ti, P, H_2O, and CO_2 present in the mantle source region (e.g., Edgar 1987; Pearce, 1996; Kogiso et al., 2003; Niu et al., 2011). Melting at sufficient depth produces the characteristic OIB signature with LREE enrichment relative to HREE. This signature likely reflects the melting of clinopyroxene in the presence of residual garnet (e.g., Ionov et al., 1993; Hirschmann et al., 2003; Sobolev et al., 2005) and implies that some amount of melting occurred within or below the garnet-spinel transition zone.

Kechika group volcanic rocks yield moderately juvenile ε_{Ndt} and ε_{Hft} values that are lower than those of the depleted mantle array at ~480 Ma, but greater than CHUR. Published Nd isotope datasets from OIB- and E-MORB-like mafic rocks along the Cordilleran margin similarly indicate mantle sources with a long history of incompatible element enrichment (e.g., Piercey et al., 2006; Piercey and Colpron, 2009). Kechika group intrusive rocks, however, yield moderately juvenile to evolved ε_{Ndt} and ε_{Hft} values that imply the involvement of an evolved crustal source. In addition to the negative Nb/Th ratios, relative Ti depletions,

and relatively high Zr/Ti ratios, these gabbroic rocks have broadly similar incompatible element-enrichment as the volcanic rocks. Whilst the Kechika volcanic rocks could be slightly older than the intrusive rocks, there is no observed field relationship that supports a significant difference in age, the available stratigraphic data (e.g., Tempelman-Kluit, 2012) agrees with the U-Pb dates of the gabbroic rocks, and the strong similarities in trace-element support a comagmatic relationship between the volcanic and intrusive rocks. A plot of ε_{Ndt} and ε_{Hft} composition versus Nb/Th ratio (Figs. 3-13A, 3-13B) forms a mixing line between volcanic, intrusive, and coeval sedimentary rocks and is therefore consistent with magma chamber or emplacement processes such as crustal assimilation (e.g., Pearce, 1996; Piercey et al., 2006; Meade et al., 2009).

There are several mantle sources that could explain the Nd-Hf isotopic compositions and incompatible element-enrichment of Kechika group volcanic rocks, including a mantle plume (e.g., Morgan, 1971), enriched 'blobs' within the asthenospheric mantle (Fitton, 2007), and metasomatised mantle in the subcontinental lithosphere (Lloyd and Bailey, 1975; Halliday et al., 1995; Pearce, 1996) and/or within the lithosphere-asthenosphere boundary (e.g., Green et al., 2010; Niu et al., 2011; Schmerr, 2012). A plume origin for early Paleozoic volcanism along the Cordilleran margin has been discounted previously (Goodfellow et al., 1995) due to the margin-length scale of magmatism, duration and minor volume of magmatism, and proximity of volcanic rocks to major lineaments or faults.

The repeated melting of a metasomatised subcontinental lithospheric mantle source is consistent with the highly incompatible element-enriched composition of early to mid-Paleozoic lavas (including ultrapotassic melts) along the inner Cordilleran margin (e.g., Foley, 1992; Goodfellow et al., 1995; Leslie, 2009; Millonig et al., 2012) and is presumably a significant contributor to the incompatible element-enriched nature of mafic alkalic volcanic rocks in more outboard regions (e.g., Piercey et al., 2006; Piercey and Colpron, 2009).

Metasomatism of Cordilleran lithospheric mantle could be linked with prolonged rifting and magmatic episodes that affected western North America during the Mesoproterozoic to Neoproterozoic (Piercey et al., 2006). For example, the Tonian (780 Ma) Muncho Lake dykes form part of the Gunbarrel magmatic event in British Columbia and are spatially associated with the Liard line (LeCheminant and Heaman, 1994; Ross et al., 2001; Harlan et al., 2003).

Metasomatism at the lithosphere-asthenosphere boundary by melt and/or volatiles may explain the incompatible element-enrichment of off-axis alkaline rocks and geophysical signature of the low velocity zone (Niu et al., 2011; Keller et al., 2017). This melt and/or volatile rich region occurs at depths of <90 km along the eastern North American margin (Rychert et al., 2005). This depth is at or below the spinel-garnet transition in peridotite (~85 km; Wood et al., 2013), which consistent with the formation of the OIB-like signature. Goodfellow et al. (1995) concluded that potassic-ultrapotassic rocks in the northwestern Selwyn basin were sourced from the lithospheric mantle, whereas alkali basalts in the central Selwyn basin partially sampled an OIB-like asthenospheric domain.

3.6.3 Syn- to post-breakup volcanism along the Cordilleran margin

The high-precision zircon U-Pb ages reported from the Pelly Mountains provide unequivocal evidence for continued volcanic activity at least 40 m.y. after lithospheric breakup along western North America. From a stratigraphic perspective, post-breakup rocks in the Pelly Mountains are analogous to other Cambrian-Ordovician volcano-sedimentary successions in British Columbia, Yukon, Washington, Idaho, and Nevada. For example, sediment-sill complexes similarly underlie the Menzie Creek and Crow Formations in central and southeastern Yukon, respectively (Pigage, 2004; Pigage et al., 2015; Cobbett, 2016). The principal lithofacies of these volcanic successions are akin to those of Kechika group and consist of pillow basalt, basalt breccia, lapilli tuff, and epiclastic sandstone (Pigage, 2004,

2009). At the margin-scale, there is evidence for middle Cambrian to Ordovician normal faults to be related to mafic volcanism throughout the Selwyn basin, Meilleur River embayment, Misty Creek embayment, Kechika trough, and Roberts Mountain allochthon (Cecile et al., 1982; Turner et al., 1989; MacIntyre, 1998; Pigage, 2004; Pigage et al., 2015). From central Yukon to northern British Columbia, Cambrian-Ordovician volcanism was coincident with shale deposition in relatively anoxic conditions (Fig. 3-3; Cecile et al., 1982; Abbott et al., 1986; Cecile and Norford, 1991; MacIntyre, 1998; Pyle and Barnes, 2000; Pigage, 2009; Gordey, 2013), suggesting that at least some sedimentation occurred in deep-marine environments (e.g., Goodfellow et al., 1995; MacIntyre, 1998). Farther south in the Roberts Mountain allochthon of Nevada, Middle to Late Ordovician greenstone and faulting are associated with a chert-argillite basinal sequence (Madrid, 1987; Turner et al., 1989).

Field evidence for Cambrian-Ordovician faults in the Pelly Mountains is lacking (Tempelman-Kluit, 2012) although the lithofacies, stratigraphic trends, and geochemical signatures of the Kechika group are analogous to extension-related depocenters in the Selwyn basin, Meilleur River embayment, and Misty Creek embayment. The similarities between these coeval volcanic centers suggest that analogous post-breakup, rift-related processes occurred throughout the early Paleozoic development of the Cordilleran margin. In the Gataga district of northern British Columbia, MacIntyre (1998) inferred that major facies boundaries between lower Paleozoic rock units formed through the reactivation of listric normal faults that originally bounded tilted fault blocks. It is therefore plausible that the basal units of the Kechika group (Cloutier, Groundhog, Gray Creek formations), now separated by Mesozoic thrust faults, may have originally been deposited in an analogous setting.

3.6.4 Implications for Cordilleran rift models

The Cordilleran margin has a protracted rift evolution that includes >300 m.y. of crustal stretching and thinning, lithospheric breakup, and pre-, syn-, and post-breakup magmatism (e.g., Stewart, 1972; Colpron et al., 2002; Yonkee et al., 2014; Strauss et al., 2015). Although post-breakup, early Paleozoic magmatism has long been recognized in western North America (e.g., Goodfellow et al., 1995; Lund, 2008), there are many open questions about the tectonic significance of Cambrian-Ordovician volcanic strata assigned to the Cordilleran passive margin. New CA-TIMS zircon U-Pb age and whole-rock geochemical data from south-central Yukon, in concert with published studies from western Canada and United States, allow us to test the three end-member rift models for the Cordilleran margin.

Pure-shear rift models

Pure-shear rift models propose that Cordilleran lithosphere underwent uniform, homogeneous extension as per McKenzie (1978). Within this framework, Bond et al. (1985) used thermal subsidence curves to conclude that the final development of the Cordilleran passive margin occurred during a short-lived rift phase at the Ediacaran-Cambrian boundary. Christie-Blick and Levy (1989), however, noted the lack of evidence for late Ediacaran-early Cambrian crustal extension in locations with significant early Paleozoic subsidence. It follows that the field localities of Bond et al. (1985) were either inboard of the hinge zone between stretched and unstretched lithosphere or that pure-shear thinning is inappropriate and heterogeneous deformation and/or detachment faults may be important (Christie-Blick and Levy, 1989).

The timing of Cambrian-Ordovician magmatism, extension, and tectonic subsidence along the length of the Cordilleran margin, including that recorded by Kechika group, is not consistent with that predicted by pure-shear rift models. For example, there is no obvious mechanism to explain the timing of Tonian-Cryogenian rifting and basin development with

respect to late Ediacaran and younger lithospheric breakup and magmatism (e.g., Yonkee et al., 2014). The marked asymmetry of the Cordilleran margin is also problematic for pure-shear rift models (Cecile et al., 1997), which typically predict symmetrical rift settings.

Simple-shear rift models

Simple-shear or asymmetric rift models (Lister et al., 1986, 1991) assume that crustal-scale detachment faults result in upper- and lower-plate segments along continental margins. Cecile et al. (1997) and Lund (2008) used these ideas to conclude that Ediacaran-early Paleozoic subsidence trends and alkaline magmatism across lithospheric-scale lineaments in western Canada and United States were consistent with such asymmetric rifting models. For example, Ediacaran alkaline rocks associated with inboard (platformal) siliciclastic strata and erosional unconformities in British Columbia, Idaho, and Utah (e.g., Yonkee et al., 2014), are consistent with igneous underplating in an upper-plate margin setting. Lower Cambrian tholeiitic rocks in the outboard (basinal) regions of southern British Columbia (e.g. Kootenay terrane, Paradis et al., 2006) are furthermore consistent with lithospheric thinning and asthenospheric upwelling during lithospheric breakup (e.g., Lister et al., 1991; Lund, 2008). The spatial proximity of these mafic volcanic rocks with Cordilleran transfer-transform zones is consistent with the role of inherited lineaments in modern rifts which can accommodate along-axis flow of asthenospheric mantle-derived melts (Georgen and Lin, 2003; Bronner et al., 2011).

There are several outstanding problems in Cordilleran margin development that are not fully explained by simple-shear rift models. Firstly, simple-shear scenarios do not adequately explain how Tonian-Cryogenian rifting along western North America is related to the timing of Ediacaran-early Cambrian lithospheric breakup, similar to pure-shear rift models. Secondly, simple-shear rift models do not provide a mechanism to generate

Cambrian-Ordovician alkaline magmas and accommodate coeval extension along the length of the margin after Ediacaran-early Cambrian lithospheric breakup and the onset of seafloor spreading. As a result, rift models for the Cordilleran margin must propose how post-breakup, lithospheric-scale processes occurred simultaneously in both upper- and lower-plate regions.

Magma-poor rift models

Modern passive margins are subdivided into magma-rich and magma-poor rift systems based on the volume of syn-rift magmatism, timing and location of lithospheric rupture, and lithospheric architecture (e.g., Franke, 2013; Doré and Lundin, 2015). Magma-poor rift margins have low volumes of syn-rift magmatism and undergo significant thinning through depth-dependent extension and necking of the crust and lithospheric mantle. The Newfoundland-Iberia system is the type example of a magma-poor rift and comprises a conjugate set of hyperextended, asymmetric margins that formed during the protracted opening of the North Atlantic Ocean (e.g., Fig. 3-14; 3-15A-D; Peron-Pinvidic et al., 2007, 2013; Peron-Pinvidic and Manatschal, 2009; Brune et al., 2014). Our preferred rift model follows the magma-poor rift framework for the modern Newfoundland-Iberia system; below, we first present a comprehensive overview of North Atlantic rift evolution and then secondly propose ancient corollaries along the Cordilleran margin using modern analogues (Fig. 3-15E, F).

The initial Late Triassic to Early Jurassic crustal stretching phase of North Atlantic rift evolution resulted in half-graben basins within the Grand Banks (offshore Newfoundland) and Lusitanian basin (onshore and offshore Portugal) platforms in the so-called proximal domain (e.g., Peron-Pinvidic et al., 2013). These basins formed part of a major rift system that developed between Europe, Africa, and North America prior to the opening of the North and Central Atlantic (Klitgord and Schouten, 1986). South of the Newfoundland-Iberia rift

system, the Central Atlantic Magmatic Province was emplaced at the Triassic-Jurassic boundary after initial rifting, but prior to seafloor spreading (e.g., Marzoli et al., 1999; Nomade et al., 2007). The Central Atlantic Magmatic Province mostly consists of dikes and sills in Atlantic Canada, Iberia, and Morocco (e.g., Dunn et al., 1998; Verati et al., 2007).

After a brief hiatus, renewed Late Jurassic-Early Cretaceous rifting and detachment faulting resulted in a necking zone or a region of major lithospheric thinning (e.g., Unternehr et al., 2010; Peron-Pinvidic et al., 2013). The development of the necking zone was coincident Middle Jurassic-Early Cretaceous alkaline and ultrapotassic magmatism within the proximal zone, including alkaline volcanic rocks in the Lusitanian basin (ca. 145 Ma; Grange et al., 2008) and Budgell Harbour Stock and related dikes in central Newfoundland (ca. 139-135 Ma; Helwig et al., 1974; Strong and Harris, 1974). Depth-dependent extension occurred as a result of shear zones in the weak middle crust (e.g., Wernicke, 1985; Lister et al., 1986; Lavier and Manatschal, 2006). These detachment faults likely reactivated long-lived basement weaknesses, such as rheological boundaries along pre-existing basins (Masini et al., 2013; Manatschal et al., 2015). Detachment faulting within necking zones leads to the formation of a wedge of lesser extended crust, termed the H-block (hanging-wall) or keystone block, that is underlain by ductile lower lithosphere (e.g., Lavier and Manatschal, 2006; Peron-Pinvidic and Manatschal, 2010). One of the H-block-bounding conjugate faults becomes preferentially weakened during strain softening and leads to the domination of one shear-zone (Huismans and Beaumont, 2014). This process results in asymmetric, simple-shear rifting within the necking and distal zones and broadly resembles the upper- and lower-plate rift scenarios of Lister et al. (1986, 1991). Such rifting within relatively hot, pliable lithosphere widens the necking zone and leads to a complicated crustal configuration that includes failed rift or offset basins (Chenin and Beaumont, 2013; Manatschal et al., 2015). These v-shaped to margin-parallel basins (e.g., Orphan, Galician, and Porcupine basins)

overlie thinned to locally ruptured lithosphere, are bounded by high-angle faults, and

associated with major lineaments such as the Charlie Gibbs Fracture Zone (e.g., Whitmarsh et

al., 1996; O'Reilly et al., 2006; Dafoe et al., 2017). These basins can result in partial or

complete separation of the continental margin from outboard areas of thick crust, such as the

Flemish Cap and Galicia Bank continental ribbons (Peron-Pinvidic and Manatschal, 2010).

The failure of these rift basins to proceed to lithospheric breakup has been linked to various

causes including the role of depleted zones of subcontinental lithospheric mantle restricting

the supply of magma (e.g., Manatschal et al., 2015), reduced mantle temperature, and as a

function of the spreading rate (e.g., Dore and Lundin, 2015). Early Cretaceous thinning led to

hyperextended (<10 km thick) crust and penetration of faults into the continental lithospheric

mantle (e.g., Peron-Pinvidic et al., 2013). This resulted in coupled extension and Valanginian

(ca. 140 Ma) and younger exhumation of continental lithospheric mantle along detachment

faults (e.g., Boillot et al., 1980; Whitmarsh et al., 2001; Tucholke et al., 2007). The ocean-

continent transition region is termed the distal domain and variably composed of

hyperextended crust, exhumed lithospheric mantle, embryonic oceanic crust, and magmatic

intrusions (e.g., Peron-Pinvidic et al., 2013). Mantle exhumation was accompanied by the

progressive emplacement of Lower Cretaceous (138-121 Ma) magmatic rocks towards the

future site of breakup in the Gorringe and Galicia Bank areas, offshore Portugal (Schärer et

al., 2000; Bronner et al., 2011; Eddy et al., 2017). Lower Cretaceous alkaline and tholeiitic

rocks with N-MORB- to E-MORB-like signatures yield ε_{Hft} values that range from +12 to

+20, comparable to modern rocks along this segment of the Mid-Atlantic ridge (+14 to +21;

Blichert-Toft et al., 2005), suggesting derivation from the depleted asthenospheric mantle

(e.g., Cornen et al., 1999; Schärer et al. 2000, Eddy et al., 2017). Coeval tholeiitic and lesser

alkalic volcanic rocks in the Fogo Seamounts, offshore Newfoundland, have ε_{Ndt} values that

range from +1 to +6 and were emplaced along the Grand Banks leaky transform margin (e.g.,

Pe-Piper et al., 2007). These Nd isotope values are lower than MORB along this segment of the Mid-Atlantic ridge (e.g. +7.5 to +11.5; Blichert-Toft et al., 2005). Pe-Piper et al. (2007) concluded that Upper Jurassic-Lower Cretaceous volcanic rocks were generated by edge-driven convection along the Grand Banks transform margin.

Aptian-Albian lithospheric breakup was time-transgressive and occurred first in the south and migrated north (e.g., Bronner et al., 2011). Breakup was associated with the generation of a lithospheric breakup surface and overlying Albian-Cenomanian breakup succession that records the transition from breakup tectonism to thermal subsidence (Soares et al., 2012). Syn-breakup activity included a large pulse of mafic magmatism in the distal domain (J-anomaly; Bronner et al., 2011) that was likely derived from the depleted mantle (Eddy et al., 2017). The delayed melt extraction may indicate that the lithospheric mantle acted as a sponge to melts derived from the upwelling asthenosphere (e.g., Müntener et al., 2010). Evidence for mafic magma emplacement within exhumed lithospheric mantle of the Newfoundland-Iberia rift system (e.g., Cornen et al., 1999; Müntener and Manatschal, 2006) and Alpine ophiolites (e.g., Müntener et al., 2010) supports this hypothesis.

Alkaline volcanic rocks with OIB-like signatures were emplaced along the Newfoundland-Iberia margins for at least 30 m.y. after Aptian-Albian lithospheric breakup, prior to the first seafloor spreading magnetic anomaly ca. 84 Ma (Schärer et al. 2000; Hart and Blusztajn, 2006; Jagoutz et al., 2007). Widespread alkalic magmatism is a seemingly consistent component of the post-breakup stratigraphy of magma-poor rift margins (e.g., Manatschal and Müntener, 2009; Bronner et al., 2011). Post-breakup volcanism along the Newfoundland margin probably consisted of volcanic centers and sills that were spatially associated with transform-transfer faults and related margin-parallel faults. This includes the Newfoundland seamounts in the Newfoundland basin (Sullivan and Keen, 1977) and Charlie Gibbs Volcanic Province (Keen et al., 2014), and Orphan seamount (Pe-Piper et al., 2013) in

the Orphan basin. The Charlie Gibbs Volcanic Province formed during the Late Cretaceous and was associated with extensional strain during oblique strike-slip movement along the Charlie Gibbs Fracture Zone (Keen et al., 2014). This structure likely allowed the upward migration of magma and acted as a transform margin separating the northern Orphan basin and volcanic-rich Rockall basin (Keen et al., 2014). The alkaline rocks of the Cretaceous Orphan Knoll seamount formed along a margin-parallel fault that provided a pathway for magmatism (Pe-Piper et al., 2013). Along the Iberian margin, mafic alkaline rocks of the Tore-Madeira Rise and onshore Portugal have positive ε_{Hft} values that range from +4 to +12 (Merle et al., 2006, 2009; Miranda et al., 2009; Grange et al., 2010). These rocks formed through melting of an enriched mantle source that mixed with the subcontinental lithospheric mantle (e.g., Grange et al., 2010). Post-breakup volcanism generally consists of alkaline, incompatible element-enriched melts with intermediate isotopic values, in contrast to pre-breakup volcanic rocks, which suggests that lithospheric breakup exerted a significant control on the mantle sources and melting processes of subsequent magmatism along the continental margin.

The cause of post-breakup magmatism is uncertain, but the distribution of stress throughout the distal continental margin during the initiation of seafloor spreading (e.g. Jagoutz et al., 2007), continued thinning of the lithospheric mantle in distal basins (e.g., Dafoe et al., 2017), and influence of oblique-slip displacement along transfer-transform zones (e.g., Keen et al., 2014) are likely important factors. Within the Newfoundland-Iberia rift system, the lack of sufficient available melt prior to lithospheric breakup allowed the build-up of in-plane tensile stress along the nascent plate boundary (Tucholke et al., 2007). When this stress is suddenly released, termed tectonic spreading, it triggers a basin wide extensional event leading to low-degree decompression melting and resultant off-axis magmatism (Jagoutz et al., 2007). A comparable process likely occurs during the initial production of

oceanic crust and prior to the first seafloor-spreading magnetic anomaly (e.g., Bronner et al., 2011).

Modelling results from modern mid-ocean ridge systems suggest that some volatile- and trace element-rich melts sourced from upwelling asthenosphere undergo along-axis flow beneath the adjacent lithosphere (Keller et al., 2017). This would be consistent with seismic interpretations of melt at the lithosphere-asthenosphere boundary and provide an enriched metasomatised mantle source for alkalic, off-axis seamounts in modern margins (e.g., Niu et al., 2012; Keller et al., 2017). Although these ideas are developed on modern mid-ocean ridges it is not inconceivable that similar metasomatic processes occur along highly attenuated continental margins, especially during periods with evidence for tholeiitic magmatism. This would be consistent with post-breakup magmatic rocks in Portugal that resulted from the mixing of the subcontinental lithospheric mantle and an enriched asthenospheric mantle component (Grange et al., 2010).

The Neoproterozoic-early Paleozoic Cordilleran margin may have developed in a manner not unlike that of the modern North Atlantic rift system (Yonkee et al., 2014, Hayward, 2015; Beranek, 2017). Although no two margins develop in an identical manner, the major aim of our comparison here is to recognize analogous processes that occurred during Cordilleran and Newfoundland-Iberia rift evolution (Fig. 3-14). The early or Tonian-Cryogenian rift phase of Cordilleran development included magmatism (Gunbarrel event), intracratonic basin deposition (Windermere Supergroup), and pure-shear stretching that weakened an initially strong lithosphere relative to the cratonic interior (Yonkee et al., 2014). We propose that this initial rift event is analogous to the Triassic-Jurassic stretching phase in the North Atlantic, including that of the Grand Banks and Lusitanian basins. The failure to proceed to breakup in the North Atlantic has been suggested to relate to a heterogeneous

lithospheric mantle that was unable to produce sufficient melt during these early rift stages (Manatschal et al., 2015).
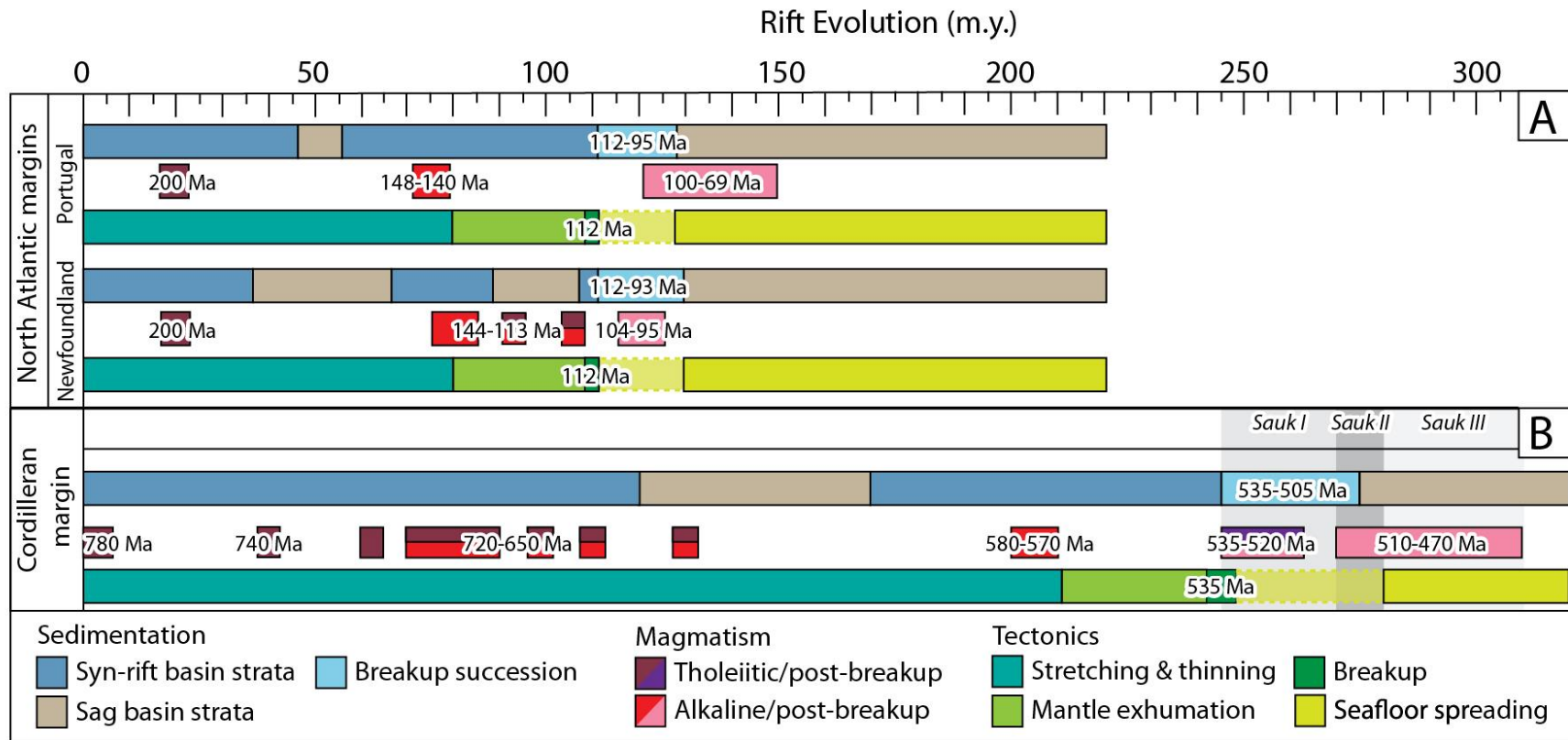
Figure 3-14 Rift evolution model modified from Beranek (2017); A: Magma-poor rift model for the North Atlantic margins (Péron-Pinvidic et al., 2013 and references therein). B: Existing rift models for the Cordilleran margin (Lund, 2008 and references therein).

Ediacaran and early Cambrian rifting led to the initial development of the Kechika trough, Selwyn basin, Lardeau trough, and other basins with intermittent extensional histories (Gordey and Anderson, 1993; Logan and Colpron, 2006; Post and Long, 2008). This rift stage was probably related to formation of the necking zone and significant lithospheric thinning, analogous to the development of outboard Jurassic-Cretaceous basins in the North Atlantic Ocean (e.g., Orphan basin; Dafoe et al., 2017). Cordilleran basins also likely evolved along transform-transfer zones and some outboard areas with periodic shallow-water deposition. Such outboard platforms, including the Cassiar platform, reflect lesser-extended crust and are likely analogous to continental ribbons like the Flemish Cap. This is consistent with published observations for minimally extended, outboard crustal blocks in the northern Cordillera (Hansen et al., 1993; Cecile et al., 1997). Ediacaran alkaline volcanic rocks of the Hamill Group in British Columbia (Colpron et al., 2002), Browns Hole Formation in Utah (Crittenden and Wallace, 1973) and lower Cambrian Quartet Mountain lamprophyre suite in northern Yukon (Milidragovic et al., 2006) are proposed equivalents to Jurassic alkaline and ultrapotassic volcanic rocks in the North Atlantic.

Lithospheric breakup along western Laurentia is widely thought to have occurred by the early Cambrian (e.g., Bond et al., 1984, 1985). Recent studies have furthermore proposed that late Ediacaran-early Cambrian rift evolution involved mantle exhumation (Yonkee et al. 2014; Hayward, 2015) and the deposition of breakup successions like those along the modern North Atlantic margins (Beranek, 2017). Exhumed continental mantle blocks and hyperextended crust produced during late rift evolution are now located beneath accreted Cordilleran terranes (Fig. 3-15E, F; e.g., Hayward, 2015). Beranek (2017) predicted that a sequence boundary at the base of the Sauk I megasequence represents a lithospheric breakup surface along western North America. The breakup succession includes early Fortunian to Cambrian Stage 5 strata (ca. 535-505 Ma) that from bottom to top consist of lowstand,

transgressive, and highstand system tract deposits, analogous to the Albian-Cenomanian depositional histories of offshore Portugal and Newfoundland (Soares et al., 2012).

Lower Cambrian volcanic rocks that were deposited in distal margin settings range in composition from tholeiitic to alkalic and broadly overlap with the inferred timing of breakup. Tholeiites in the Kootenay terrane near Shuswap Lake, southern British Columbia, yield N-MORB-like signatures and ε_{Ndt} values (+8; unit EBG of the Eagle Bay assemblage, Paradis et al., 2006) that are close to the predicted values for the Cambrian depleted mantle (ε_{Nd540} = +9.1; Goldstein et al., 1984). Kootenay terrane strata that comprise sediment-sill complexes in the northern Selkirk Mountains (Index Formation) yield intermediate E-MORB- to N-MORB-like signatures and are locally associated with chlorite schist and serpentinized ultramafic rocks (e.g., Zwanzig, 1973; Logan and Colpron, 2006). Similar fault-bounded mafic and ultramafic units are associated with lower Cambrian volcanic and sedimentary rocks in the northern Kootenay terrane (Showshoe Group; e.g., Ferri and Schiarizza, 2006) and southern Kootenay terrane (e.g., Smith and Gehrels, 1992; Logan and Colpron, 2006). The juvenile mafic volcanic rocks, sediment-sill complexes, and association with Cu-rich base metal deposits led Logan and Colpron (2002) to suggest a Gulf of California analogue for the Lardeau trough, implying that these rocks were emplaced during rift-related lithospheric thinning. Lardeau trough tholeiitic rocks are probably analogous to the depleted mantle-derived rocks that erupted during mantle exhumation and lithospheric breakup in the Gorringe, Galicia, and Grand Banks regions. Tholeiitic volcanism in the Kootenay terrane continued into the middle to late Cambrian (Ferri and Schiarizza, 2006; Logan and Colpron, 2006). Analogous to Early Cretaceous tholeiites in the Newfoundland-Iberia rift system, the emplacement of these Cambrian volcanic rocks and associated mafic to ultramafic intrusive rocks may have contributed to lithospheric heating and weakening. Other pre- to syn-breakup rocks that crop out between Ediacaran volcanic and clastic strata and

lower Cambrian archaeocyathid horizons are expected to show depleted asthenospheric mantle contributions (e.g., Paradis et al., 2006). Lower Cambrian volcanic strata, however, are mostly exposed in the eastern or inboard regions of the Cordillera that may not have undergone sufficient lithospheric attenuation to expect only depleted mantle inputs. Example rock units include the Fish Lake volcanics (Donald Formation) of southern British Columbia (Kubli and Simony, 1992) and olivine basalt flows within the Prospect Mountain and Tintic Quartzites of Nevada and Utah (Morris and Lovering, 1961; Kellogg, 1963).

Upper Cambrian to Middle Ordovician volcanic strata form parts of the Sauk II, III, and Tippecanoe sequences and their syn- to post-breakup nature is therefore consistent with a magma-poor rift origin (e.g., Fig. 3-15E; Cecile et al., 1997; Beranek, 2017). Most Cambrian Series 2 to Ordovician volcanic rocks in Yukon and western United States are alkali basalts with OIB-like to E-MORB-like signatures (Fig. 3-16A). Post-breakup volcanic rocks of the Kootenay terrane have lower overall LREE-enrichment than volcanic rocks in other parts of the Cordilleran margin (Fig. 3-16A), however, they display geochemical trends consistent with increasing LREE-enrichment and alkalinity following breakup. This is shown in British Columbia by the contrast between the Index Formation and overlying alkali basalts of the Jowett Formation (Logan and Colpron, 2006) and lower and upper parts of the Eagle Bay assemblage (Paradis et al., 2006), although this transition appears slightly more complex within Cambrian volcanic strata of the Snowshoe Group (e.g., Ferri and Schiarizza, 2006). Within the upper section of the Eagle Bay assemblage, Cambrian Series 2 alkali basalts yield intermediate ε_{Ndt} values (range from +4 to +6; Paradis et al., 2006), which suggests the involvement of incompatible element-enriched mantle following breakup. The generation of syn- to post-breakup alkaline volcanic rocks along western North America is akin to the emplacement of post-Aptian magmatic rocks on both sides of the Newfoundland-Iberia (Fig. 3-16B; e.g., Jagoutz et al., 2007; Bronner et al., 2011) and other magma-poor rift systems

(e.g., Manatschal and Müntener, 2009). Notably, many occurrences of post-breakup magmatic rocks along the Cordilleran and Newfoundland-Iberia margins are spatially associated with leaky transfer-transform lineaments and extensional faults. These structures are likely important for localizing basin-wide extension and associated off-axis magmatism (Jagoutz et al., 2007). Therefore, the lack of sufficient melt to enable breakup, and initiate seafloor spreading within a magma-poor rift system, could directly explain the wide distribution and longevity of syn- to post-breakup magmatism along both rifted margins. The major distinction in magmatism that follows lithospheric breakup is an increase in the proportion of alkaline volcanic rocks with contributions from an enriched mantle source. Whilst the overall length of rifting varies from the Cordilleran to Atlantic margin (Fig. 3-14; e.g. >150 Ma in the Atlantic margin to ~ 300 Ma) this is not inconsistent with the length of time for the evolution of the Carboniferous–Paleocene magma-poor, East Greenland–Mid-Norwegian rift system (~ 300Ma; e.g. Peron-Pinvidic et al., 2013). Furthermore, the length of time suggested for individual components of the Cordilleran rift system such as the period of Ediacaran-early Cambrian rifting prior to breakup (~80 Ma), and the subsequent breakup to post-breakup period (~65 Ma) strongly compares to the length of time for the comparable process in the Newfoundland-Iberia rift system (Fig. 3-14; e.g., ~60Ma, and ~40 Ma respectively; e.g., Peron-Pinvidic et al., 2013).

Figure 3-15 *Continental margin maps, and schematic cross sections of the Newfoundland margin (a, b), and Iberian margin (c, d) with crustal architectural adapted from Peron-Pinvidic et al. (2013), and extent of volcanic rocks, and structures from Pe-Piper et al. (2013). Solid grey line shows necking domain; dashed black line shows outer domain; CGVP = Charlie Gibbs volcanic province; FZ = fracture zone; (e) Schematic*

diagram of the northwestern North American ancestral margin during late Cambrian to Early Ordovician time. Lithospheric structures based on Cecile et al. (1997), platformal, and basinal strata from Cecile and Norford (1993), and Pyle (2012), and with inferred restoration of the Tintina fault based on ~400 km of dextral displacement from Gabrielse et al. (2006). See Figure 1, and Appendix 1 for data on volcanic rocks. RT = Richardson Trough; OA = Ogilvie Arch; MCE = Misty Creek embayment; MRE = Meilleur River embayment; YTT = Yukon Tanana terrane; GSSZ; Great Slavelake Shear Zone; KT = Kootenay trough; OE = Ospika embayment; CT = Cassiar terrane; KP = Kakwa platform; PA = Purcell arch; WRE = White River embayment; (f) Magma-poor rift model after Beranek (2017) with elements in the Canadian Cordillera. CT—Cassiar platform, KT—Kechika trough, MP—MacDonald platform.
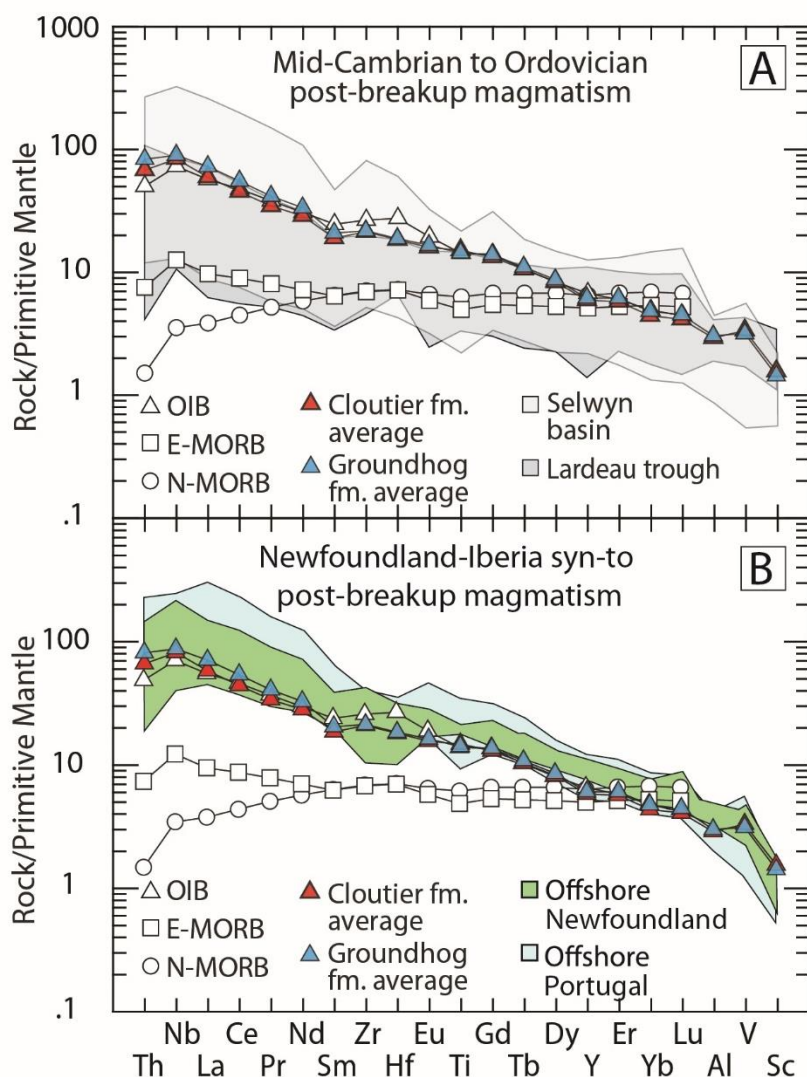
Figure 3-16 *Primitive mantle-normalized multi-element plots of mafic rock units. (a) Kechika*

group average (this study), Middle Cambrian to Ordovician rocks of the Lardeau trough and

Selwyn basin, and the global averages for ocean-island basalt (OIB) and normal and

enriched mid-ocean ridge basalt (E-MORB and N-MORB). Primitive-mantle values and

global averages are from Sun and McDonough (1989) and McDonough and Sun (1995). The

Lardeau trough units include the Index and Jowett Formations (Logan and Colpron, 2006),

Frank Creek volcanics (Ferri and Schiarizza, 2006), and Eagle Bay assemblage rocks that

overlie the early Cambrian Tshinakin limestone (Paradis et al., 2006). The Selwyn basin

units include the Marmot Formation (Leslie, 2009), Menzie Creek formation (Pigage, 2004),

and Crow, Rabbitkettle, and Sunblood Formations (Pigage et al., 2015). (b) The Cretaceous syn- to post-breakup volcanic rocks of the Newfoundland margin include the ODP site 1276 (Hart and Blusztajn, 2006), and Orphan Knoll seamount (Pe-Piper et al., 2013). The range of values from Cretaceous syn- to post-breakup volcanic rocks of the Iberian margin include volcanic rocks from the western Iberian continental margin (Miranda et al., 2009), and the Tore–Madeira Rise (Merle et al., 2009).

3.6.5 Future work

Many key observations of the North Atlantic Ocean basin, including the presence of hyperextended crust and exhumed lithospheric mantle, are preserved in deep-water regions that represent the necking and distal domains of the Newfoundland-Iberia rift (Fig. 3-15B, D). In the North American Cordillera, such elements are structurally beneath accreted allochthons (Hayward, 2015; Beranek, 2017), but we propose that outer continental margin remnants may be preserved in both parautochthonous and allochthonous fragments with ties to the western Laurentian margin (Fig. 3-15F). For example, the Yukon-Tanana terrane is demonstrably of northwest Laurentian margin affinity, but its pre-Devonian magmatic and tectonic histories are uncertain (e.g., Colpron et al., 2007). In central Yukon, the exposed metasedimentary basement of Yukon-Tanana (Snowcap assemblage) includes amphibolite units with OIB- to E-MORB-like signatures, ε_{Ndt} and ε_{Hft} values that indicate an enriched mantle source, and Proterozoic depleted mantle model ages (Piercey and Colpron, 2009). These amphibolites are analogous to Neoproterozoic to lower Paleozoic mafic rocks of the Cordilleran margin (Piercey and Colpron, 2009), including alkaline to tholeiitic rocks of the parautochthonous Kootenay terrane and Kechika group. The chondritic to juvenile Nd-Hf isotope signatures of metamorphosed carbonate rocks intercalated with the amphibolites have been used to infer emplacement during a major magmatic pulse such as the Gunbarrel magmatic event (e.g., Piercey et al., 2006). If early Cambrian lithospheric breakup along western Laurentia was accompanied by a significant outboard magmatic pulse, comparable to that of the Aptian-Albian magmatic pulse along the outboard Newfoundland-Iberia rift system, then an argument could be made to correlate Yukon-Tanana basement rocks with lower Cambrian syn-breakup successions of northwestern Laurentia.

3.7 Conclusions

Cambrian-Ordovician igneous rocks of the Pelly Mountains, south-central Yukon, have zircon U-Pb crystallization ages and geochemical compositions that provide new constraints on the tectonic significance of post-breakup magmatism in western North America. Comagmatic gabbro and basalt units of the Kechika group that post-date lithospheric breakup by >40 m.y. were generated by the low-degree partial melting of enriched mantle and emplaced within submarine volcanic centers and sill-sediment complexes during margin-scale extension. The Liard line, a long-lived basement feature that defines a transfer-transform zone in the northern Canadian Cordillera, likely accommodated Cambrian-Ordovician magmatism in the Pelly Mountains and adjacent areas of southeastern Yukon and northern British Columbia. Our preferred model for Cordilleran rift evolution features a magma-poor rift scenario not unlike that of the Newfoundland-Iberia system and includes Tonian-Cryogenian stretching and thinning, late Ediacaran-early Cambrian mantle exhumation and tholeiitic-dominated breakup magmatism, and middle Cambrian to Ordovician alkaline-dominated post-breakup magmatism. The Kechika group likely originated in a manner akin to mid- to Late Cretaceous sills and seamounts within the distal margins of Newfoundland (e.g., Orphan and Newfoundland basins) and Portugal (e.g., Tore-Madeira Rise). Following the models of Tucholke et al. (2007) and Jagoutz et al. (2007), it is predicted that the Kechika group and related off-axis volcanic units were generated during the release of in-plane tensile stresses after lithospheric breakup, but prior the establishment of a spreading ridge and formation of new ocean crust along northwestern Laurentia.

3.8 Acknowledgments

3.9 References

Abbott, G., 1997, Geology of the Upper Hart River Area, Eastern Ogilvie Mountains, Yukon Territory 9116A/10, 116A/11: Exploration and Geological Services Division, Yukon, Indian and Northern Affairs Canada, Bulletin 9, 92 p.

Abbott, J.G., Gordey, S.P., and Tempelman-Kluit, D.J., 1986, Setting of stratiform, sediment-hosted lead-zinc deposits in Yukon and northeastern British Columbia: Geological Survey of Canada Open File 2169, p. 69-98, doi:10.4095/132329.

Aitken, J.D., 1993, Cambrian and lower Ordovician-Sauk sequence, *in* Stott, D.F., and Aitken, J.D., eds., Sedimentary Cover of the North American Craton in Canada: Geological Survey of Canada, Geology of Canada, v. 5, p. 96-124, doi:10.1130/dnag-gna-d1.96.

Allen, T.L., Pigage, L.C., and MacNaughton, R.B., 2000, Preliminary geology of the Pool Creek map area (95C/5), southeastern Yukon: Yukon Exploration and Geology, p. 53-72.

Armin, R.A., and Mayer, L., 1983, Subsidence analysis of the Cordilleran miogeocline: Implications for timing of late Proterozoic rifting and amount of extension: Geology, v. 11, p. 702-705, doi:10.1130/0091-7613(1983)11<702:saotcm>2.0.co;2.

Audet, P., Sole, C. and Schaeffer, A.J., 2016, Control of lithospheric inheritance on neotectonic activity in northwestern Canada?: Geology, v. 44, p. 807-810, doi:10.1130/G38118.1

Beranek, L.P., 2017, A magma-poor rift model for the Cordilleran margin of western North America: Geology, v. 45, p. 1115-1118, doi:10.1130/G39265.1.

Black, R., Gladwin, K., and Johnston, S.T., 2003, Geology and metamorphic conditions in rocks of the Cassiar terrane, Glenlyon map area (105L/1), south-central Yukon, *in* Emond, D.S., and Lewis, L.L., eds., Yukon Exploration and Geology 2002: Exploration and Geological Services Division, Yukon Region, Indian and Northern Affairs Canada, p. 65-76.

Blichert-Toft, J., Agranier, A., Andres, M., Kingsley, R., Schilling, J.G., and Albarède, F., 2005, Geochemical segmentation of the Mid-Atlantic Ridge north of Iceland and ridge-hot spot interaction in the North Atlantic: Geochemistry, Geophysics, Geosystems, v. 6, p. 1-27, doi:10.1029/2004gc000788.

Boillot, G., Grimaud, S., Mauffret, A., Mougenot, D., Kornprobst, J., Mergoil-Daniel, J., and Torrent, G., 1980, Ocean-continent boundary off the Iberian margin: a serpentinite diapir west of the Galicia Bank: Earth and Planetary Science Letters, v. 48, p. 23-34, doi:10.1029/2004gc000788.

Bond, G.C., and Kominz, M.A., 1984, Construction of tectonic subsidence curves for the early

    Paleozoic miogeocline, southern Canadian Rocky Mountains: Implications for subsidence

    mechanisms, age of breakup, and crustal thinning: Geological Society of America Bulletin, v.

    95, p. 155-173, doi:10.1130/0016-7606(1984)95<155:cotscf>2.0.co;2.

Bond, G.C., Nickeson, P.A., and Kominz, M.A., 1984, Breakup of a supercontinent between 625 Ma

    and 555 Ma: new evidence and implications for continental histories: Earth and Planetary

    Science Letters, v. 70, p. 325-345, doi:10.1016/0012-821x(84)90017-7.

Bond, G.C., Christie-Blick, N., Kominz, M.A., and Devlin, W.J., 1985, An Early Cambrian rift to

    post-rift transition in the Cordillera of western North America: Nature, v. 315, p. 742-746,

    doi:10.1038/315742a0.

Braun, J., and Beaumont, C., 1989, A physical explanation of the relation between flank uplifts and

    the breakup unconformity at rifted continental margins: Geology, v. 17, p. 760-764,

    doi:10.1130/0091-7613(1989)017<0760:apeotr>2.3.co;2.

Bronner, A., Sauter, D., Manatschal, G., Peron-Pinvidic, G., and Munschy, M., 2011, Magmatic

    breakup as an explanation for magnetic anomalies at magma-poor rifted margins: Nature

    Geoscience, v. 4, p. 549-553, doi:10.1038/ngeo1201.

Brune, S., Heine, C., Pérez-Gussinyé, M., and Sobolev, S.V., 2014, Rift migration explains

    continental margin asymmetry and crustal hyper-extension: Nature Communications, v. 5, p.

    1-9, doi:10.1038/ncomms5014.

Buck, W.R., 2004, Consequences of asthenospheric variability on continental rifting, *in* Karner, G.D., Taylor, B., Driscoll, N.W., and Kohlstedt, D.L., eds., Rheology and deformation of the lithosphere at continental margins: Columbia University Press, New York, v. 62, p. 1-30, doi:10.7312/karn12738-002.

Campbell, R.W., and Beranek, L.P., 2017, Volcanic stratigraphy of the Cambrian-Ordovician Kechika group, Pelly Mountains, south-central Yukon, *in* MacFarlane, K.E., and Weston, L.H., eds., Yukon Exploration and Geology 2016: Yukon Geological Survey, p. 25-45.

Cann, J.R., 1970, Rb, Sr, Y, Zr and Nb in some ocean floor basaltic rocks: Earth and Planetary Science Letters, v. 10, p. 7-11, doi:10.1016/0012-821x(70)90058-0.

Cecile, M.P., 2000, Geology of the northeastern Niddery Lake map area, east-central Yukon and adjacent Northwest Territories: Geological Survey of Canada Bulletin, v. 553, 120 p, doi:10.4095/211664.

Cecile, M.P., Fritz, W.H., Norford, B.S., and Tipnis, R.S., 1982, The Lower Paleozoic Misty Creek embayment, Selwyn Basin, Yukon and Northwest Territories: Geological Survey of Canada, Bulletin 335, 78 p, doi:10.4095/111346.

Cecile, M.P., and Norford, B.S., 1991, Ordovician and Silurian assemblages, in Cambrian to Middle Devonian Assemblages, *in* Gabrielse, H., and Yorath, C.J., eds., Geology of the Cordilleran Orogen in Canada: Geological Survey of Canada, Geology of Canada series, no. 4, p. 184-196, doi:10.4095/134069.

Cecile, M.P., Norford, B.S., Stott, D.F., and Aitken, J.D., 1993, Ordovician and Silurian, *in* Stott, D.F., and Aitken, J.D., eds., Sedimentary cover of the craton in Canada: Geology of Canada: Geological Survey of Canada, v.5, p.125-149, doi:10.1130/dnag-gna-d1.125.

Cecile, M.P., Morrow, D.W., and Williams, G.K., 1997, Early Paleozoic (Cambrian to Early Devonian) tectonic framework, Canadian Cordillera: Bulletin of Canadian Petroleum Geology, v. 45, p. 54-74.

Chenin, P., and Beaumont, C., 2013, Influence of offset weak zones on the development of rift basins: Activation and abandonment during continental extension and breakup: Journal of Geophysical Research: Solid Earth, v. 118, p. 1698–1720, doi:10.1002/jgrb.50138.

Christie-Blick, N., 1997, Neoproterozoic sedimentation and tectonics in west-central Utah: Brigham Young University Geological Studies, v. 42, p. 1-30.

Christie-Blick, N., and Levy, M., 1989, Stratigraphic and tectonic framework of upper Proterozoic and Cambrian rocks in the western United States, *in* Christie-Blick, N., and Levy, M., eds., Late Proterozoic and Cambrian Tectonics, Sedimentation, and Record of Metazoan Radiation in the western United States: American Geophysical Union, 28th International Geological Congress Field Trip Guidebook T33, p. 7–22, doi:10.1029/FT331p0007.

Cobbett, R., 2016, Preliminary observations on the geology of Tay Mountain Area (parts of NTS 105K/12 and 13, 105L/09 and 16), central Yukon, *in* MacFarlane, K.E., and Nordling, M.G., eds., Yukon Exploration and Geology 2015: Yukon Geological Survey, p. 79-98.

Cohen, K.M., Finney, S.C., Gibbard, P.L., and Fan, J.-X., 2013 (updated): The ICS International Chronostratigraphic Chart: Episodes, 36, 199-204.

Colpron, M., Logan, J.M., and Mortensen, J.K., 2002, U-Pb zircon age constraint for late Neoproterozoic rifting and initiation of the lower Paleozoic passive margin of western Laurentia: Canadian Journal of Earth Sciences, v. 39, p. 133-143, doi:10.1139/E01-069.

Colpron, M., Nelson, J.L., and Murphy, D.C., 2007, Northern Cordilleran terranes and their interactions through time: GSA Today, v. 17, p. 4-10, doi:10.1130/gsat01704-5a.1.

Colpron, M., and Nelson, J.L., 2009, A Palaeozoic Northwest Passage: Incursion of Caledonian, Baltican, and Siberian terranes into eastern Panthalassa, and the early evolution of the North American Cordillera, *in* Cawood, P.A., and Kroner, A., eds., Earth accretionary systems in space and time: Geological Society, London, Special Publication 318, p. 273–307, doi:10.1144 /SP318.10.

Cornen, G., Girardeau, J., and Monnier, C., 1999, Basalts, underplated gabbros and pyroxenites record the rifting process of the West Iberian margin: Mineralogy and Petrology, v. 67, p. 111-142, doi:10.1007/BF01161518

Crittenden, M.D., Jr., and Wallace, C.A., 1973, Possible equivalents of the Belt Supergroup in Utah, Belt Symposium 1973, Volume 1: Moscow, Idaho, Idaho Bureau of Mines and Geology, p. 116–138.

Dafoe, L.T., Keen, C.E., Dickie, K., and Williams, G.L., 2017, Regional stratigraphy and subsidence of Orphan Basin near the time of breakup and implications for rifting processes: Basin Research, v. 29, p. 233-254, doi:10.1111/bre.12147.

David, K., Schiano, P., and Allegre, C.J., 2000, Assessment of the Zr/Hf fractionation in oceanic basalts and continental materials during petrogenetic processes: Earth and Planetary Science Letters, v. 178, p. 285–301, doi: 10.1016/S0012-821X(00)00088-1.

Davis, M., and Kusznir, N. J., 2004, Depth-Dependent Lithospheric Stretching at Rifted Continental Margins, *in* G. D. Karner., ed., Proceedings of NSF Rifted Margins Theoretical Institute: New York, Columbia University Press. p. 92-136, doi:10.7312/karn12738-005

DePaolo, D.J., 1981, Neodymium isotopes in the Colorado Front Range and crust–mantle evolution in the Proterozoic: Nature, v. 291, p. 193-196, doi:10.1038/291193a0

Devlin, W.J., 1989, Stratigraphy and Sedimentology of the Hamill Group in the northern Selkirk Mountains, British Columbia: evidence for latest Proterozoic-Early Cambrian extensional tectonism: Canadian Journal of Earth Sciences, v. 26, p. 515-533, doi:10.1139/e89-044.

Devlin, W.J., and Bond, G.C., 1988, The initiation of the early Paleozoic Cordilleran miogeocline: evidence from the uppermost Proterozoic-Lower Cambrian Hamill Group of southeastern British Columbia: Canadian Journal of Earth Sciences, v. 25, p. 1-19, doi:10.1139/e88-001.

Doré, T., and Lundin, E., 2015, Research focus: Hyperextended continental margins—knowns and unknowns: Geology, v. 43, p. 95-96, doi:10.1130/focus012015.1.

Douglas, R.J.W., Gabrielse, H., Wheeler, J.O., Stott, D.F., and Belyea, H.R., 1970, Geology of Western Canada, *in* Douglas, R.J.W., ed., Geology and Economic Minerals of Canada: Geological Survey of Canada, Economic Geology Report 1, 5th edition, p. 367-546, doi:10.4095/106151.

Dunn, A.M., Reynolds, P.H., Clarke, D.B., and Ugidos, J.M., 1998, A comparison of the age and composition of the Shelburne dyke, Nova Scotia, and the Messejana dyke, Spain: Canadian Journal of Earth Sciences, v. 35, p. 1110-1115, doi:10.1139/e98-058.

Eddy, M.P., Jagoutz, O., and Ibañez-Mejia, M., 2017, Timing of initial seafloor-spreading in the Newfoundland-Iberia rift: Geology, v. 45, p. 527-530, doi:10.1130/G38766.1.

Edgar, A.D., 1987, The genesis of alkaline magmas with emphasis on their source regions: inferences from experimental studies, *in* Fitton, J.G., and Upton B.G.J., eds., Alkaline Igneous Rocks:, Geological Society, London, Special Publications, v. 30, p. 29-52, doi:10.1144/gsl.sp.1987.030.01.04.

Einsele, G., 1986, Interaction between sediments and basalt injections in young Gulf of California-type spreading centers: Geologische Rundschau, v. 75, p. 197-208, doi:10.1007/bf01770188.

Eyster, A., Ferri, F., Schmitz, M.D., and Macdonald, F.A., 2018, One diamictite and two rifts: stratigraphy and geochronology of the Gataga Mountain of northern British Columbia: American Journal of Science, v. 318, p. 167-207, doi:10.2475/02.2018.1.

Fanning, C.M., and Link, P.K., 2004, U-Pb SHRIMP ages of Neoproterozoic (Sturtian) glaciogenic

    Pocatello Formation, southeastern Idaho: Geology, v. 32, p. 881-884, doi:10.1130/G20609.1.

Ferri, F., Rees, C., Nelson, J., and Legun, A., 1999, Geology and Mineral Deposits of the Northern

    Kechika Trough between Gataga River and the 60th Parallel: Geological Survey Branch,

    Mineral Resources Division, British Columbia Ministry of Energy and Mines Bulletin 107,

    122 p.

Ferri, F., and Schiarizza, P., 2006, Re-interpretation of Snowshoe group stratigraphy across a

    southwest-verging nappe structure and its implications for regional correlations within the

    Kootenay terrane, *in* Colpron, M., and Nelson, J.L., eds., Paleozoic Evolution and

    Metallogeny of Pericratonic Terranes at the Ancient Pacific Margin of North America,

    Canadian and Alaskan Cordillera: Geological Association of Canada, Special Paper, 45, p.

    415-432.

Fitton, J.G., 1987, The Cameroon line, West Africa: a comparison between oceanic and continental

    alkaline volcanism, *in* Fitton, J.G., and Upton B.G.J., eds., Alkaline Igneous Rocks:

    Geological Society, London, Special Publications, v. 30, p. 273-291,

    doi:10.1144/gsl.sp.1987.030.01.13.

Fitton, J.G., 2007, The OIB paradox, *in* Foulger, G.R., and Jurdy, D.M., eds., Plates, Plumes, and

    Planetary Processes: Geological Society of America Special Papers 430, p. 387-412,

    doi:10.1130/2007.2430(20)

Fitton, J.G., James, D., Kempton, P.D., Ormerod, D.S., and Leeman W.P., 1988, The Role of

    Lithospheric Mantle in the Generation of Late Cenozoic Basic Magmas in the Western

    United States: *Journal of Petrology,* Special Lithosphere Issue, v. 1, p. 331–349,

    doi:10.1093/petrology/Special_Volume.1.331

Foley, S., 1992, Vein-plus-wall-rock melting mechanisms in the lithosphere and the origin of

    potassic alkaline magmas: Lithos, v. 28, p. 435-453, doi:10.1016/0024-4937(92)90018-t.

Franke, D., 2013, Rifting, lithosphere breakup and volcanism: Comparison of magma-poor and

    volcanic rifted margins: Marine and Petroleum Geology, v. 43, p. 63-87,

    doi:10.1016/j.marpetgeo.2012.11.003.

Fritz, W.H., Cecile, M.P., Norford, B.S., Morrow, D.W., and Geldsetzer, H.H.J., 1991, Cambrian to

    Middle Devonian assemblages, *in* Gabrielse, H., and Yorath, C.J., eds., The Cordilleran

    Orogen: Canada: Geological Survey of Canada, Geology of Canada, no. 4, p. 151-218,

    doi:10.4095/134087

Furman, T., 2007, Geochemistry of East African Rift basalts: an overview: Journal of African Earth

    Sciences, v. 48, p. 147-160, doi:10.1016/j.jafrearsci.2006.06.009.

Gabrielse, H., 1963, McDame map area, Cassiar District, British Columbia: Geological Survey of

    Canada, Memoir 319, 138 p, doi:10.4095/100546.

Gabrielse, H., 1967, Tectonic evolution of the northern Canadian Cordillera: Canadian Journal of

    Earth Sciences, v. 4, p. 271-298, doi:10.1139/e67-013.

Gabrielse, H., 1998, Geology of the Cry Lake and Dease Lake map areas, north-central British

    Columbia: Geological Survey of Canada, Bulletin 504, 147 p, doi:10.4095/210074.

Gabrielse, H., Blusson, S.L., and Roddick, J.A., 1973, Geology of Flat River, Glacier Lake, and

    Wrigley Lake map-areas, District of Mackenzie and Yukon Territory: Geological Survey of

    Canada, Memoir 366, 153 p, doi:10.4095/100705.

Gabrielse, H., and Yorath, C.J., 1991, Tectonic synthesis, *in* Gabrielse, H., and Yorath, C.J., eds.,

    Geology of the Cordilleran Orogen in Canada: Geological Survey of Canada, Geology of

    Canada, no. 4, p. 677-705, doi:10.4095/134069.

Gabrielse, H., Murphy, D.C., and Mortensen, J.K., 2006, Cretaceous and Cenozoic dextral orogen-

    parallel displacements, magmatism, and paleogeography, northcentral Canadian Cordillera, *in*

    Haggart, J.W., Enkin, R.J., and Monger, J.W.H., eds., Paleogeography of the North American

    Cordillera: evidence for and against large-scale displacements: Geological Association of

    Canada, Special Paper, 46, p. 255-276.

Georgen, J.E., and Lin, J., 2003, Plume-transform interactions at ultra-slow spreading ridges:

    Implications for the Southwest Indian Ridge: Geochemistry, Geophysics, Geosystems, v. 4,

    doi:10.1029/2003GC000542.

Gladwin, K., Colpron, M., Black, R., and Johnston, S.T., 2003, Bedrock geology at the boundary

    between Yukon-Tanana and Cassiar terranes, Truitt Creek map area (NTS 105L/1), south

    central Yukon, *in* Emond, D.S., and Lewis, L.L., eds., Yukon Exploration and Geology 2002:

Exploration and Geological Services Division, Yukon Region, Indian and Northern Affairs Canada, p. 135-148.

Godwin, C.I., and Price, B.J., 1986, Geology of the Mountain diatreme kimberlite, north-central Mackenzie Mountains, District of Mackenzie, Northwest Territories, *in* Morin, J.A., ed., Mineral Deposits of Northern Cordillera Symposium: Canadian Institute of Mining and Metallurgy, Special Paper, v. 37, p. 87-99.

Goldstein, S.L., O'Nions, R.K., and Hamilton, P.J., 1984, A Sm-Nd isotopic study of atmospheric dusts and particulates from major river systems: Earth and Planetary Science letters, v. 70, p. 221-236, doi:10.1016/0012-821x(84)90007-4.

Goodfellow, W.D., and Jonasson, I.R., 1986, Environment of formation of the Howards Pass (XY) Zn-Pb deposit, Selwyn Basin, Yukon, *in* Morin, J.A., ed., Mineral Deposits of Northern Cordillera Symposium: Canadian Institute of Mining and Metallurgy, Special Paper, v. 37, p. 19-50.

Goodfellow, W.D., Cecile, M.P., and Leybourne, M.I., 1995, Geochemistry, petrogenesis, and tectonic setting of lower Paleozoic alkalic and potassic volcanic rocks, Northern Canadian Cordilleran Miogeocline: Canadian Journal of Earth Sciences, v. 32, p. 1236-1254, doi:10.1139/e95-101.

Gordey, S.P., 1981, Stratigraphy, structure, and tectonic evolution of the southern Pelly Mountains in the Indigo Lake area, Yukon Territory: Geological Survey of Canada, Bulletin 318, 44 p, doi:10.4095/111359.

Gordey, S.P., 2013, Evolution of the Selwyn Basin region, Sheldon Lake and Tay River map areas, central Yukon: Geological Survey of Canada, Bulletin 599, 176 p, doi:10.4095/293034.

Gordey, S.P., and Anderson, R.G., 1993, Evolution of the northern Cordilleran miogeocline, Nahanni map area (105 I), Yukon and Northwest Territories: Geological Survey of Canada, Memoir 428, 214 p, doi:10.4095/183983.

Grange, M., Schärer, U., Cornen, G., and Girardeau, J., 2008, First alkaline magmatism during Iberia–Newfoundland rifting: Terra Nova, v. 20, p. 494-503, doi:10.1111/j.1365-3121.2008.00847.x.

Grange, M., Schärer, U., Merle, R., Girardeau, J., and Cornen, G., 2010, Plume–lithosphere interaction during migration of Cretaceous alkaline magmatism in SW Portugal: evidence from U–Pb ages and Pb–Sr–Hf isotopes: Journal of Petrology, v. 51, p. 1143-1170, doi:10.1093/petrology/egq018.

Green, T.H., 1995, Significance of Nb/Ta as an indicator of geochemical processes in the crust-mantle system: Chemical Geology, v. 120, p. 347-359, doi:10.1016/0009-2541(94)00145-x.

Green, D.H., Hibberson, W.O., Kovács, I., and Rosenthal, A., 2010, Water and its influence on the lithosphere-asthenosphere boundary: Nature, v. 467, p. 448-451, doi:10.1038/nature09369.

Halliday, A.N., Lee, D.C., Tommasini, S., Davies, G.R., Paslick, C.R., Fitton, J.G., and James, D.E., 1995, Incompatible trace elements in OIB and MORB and source enrichment in the sub-

oceanic mantle: Earth and Planetary Science Letters, v. 133, p. 379-395, doi:10.1016/0012-821x(95)00097-v.

Hansen, V.L., Goodge, J.W., Keep, M., and Oliver, D.H., 1993, Asymmetric rift interpretation of the western North American margin: Geology, v. 21, p. 1067–1070, doi:10.1130/0 091-7613(1993)021<1067:ARIOTW>2.3.CO;2.

Harlan, S.S., Heaman, L., LeCheminant, A.N., and Premo, W.R., 2003, Gunbarrel mafic magmatic event: A key 780 Ma time marker for Rodinia plate reconstructions: Geology, v. 31, p. 1053-1056, doi:10.1130/G19944.1.

Hart, J.R.C., 1986, Geology of the Old Cabin Creek Massif, Selwyn Basin, Yukon Territory [Ph.D. thesis]: McMaster University, 135 p.

Hart, S.R., and Blusztajn, J., 2006, Age and geochemistry of the mafic sills, ODP site 1276, Newfoundland margin: Chemical Geology, v. 235, p. 222-237, doi:0.1016/j.chemgeo.2006.07.001.

Hayward, N., 2015, Geophysical investigation and reconstruction of lithospheric structure and its control on geology, structure, and mineralization in the Cordillera of northern Canada and eastern Alaska: Tectonics, v. 34, doi:10.1002/2015TC003871.

Heaman, L.M., LeCheminant, A.N., and Rainbird, R.H., 1992, Nature and timing of Franklin igneous events, Canada: implications for a Late Proterozoic mantle plume and the break-up

of Laurentia: Earth and Planetary Science Letters, v. 109, p.117-131, doi:10.1016/0012-821X(92)90078-A.

Hein, F.J., and McMechan, M.E., 1994, Proterozoic and Lower Cambrian strata of the Western Canada sedimentary basin, *in* Mossop, G.D., and Shetsen, I., eds., Geological Atlas of the Western Canada Sedimentary Basin: Canadian Society of Petroleum Geologists and Alberta Research Council, p. 57-67.

Helwig, J., Aronson, J., and Day, D.S., 1974, A Late Jurassic mafic pluton in Newfoundland: Canadian Journal of Earth Sciences, v. 11, p. 1314-1319, doi:10.1139/e74-123.

Hirschmann, M.M., Kogiso, T., Baker, M.B. and Stolper, E.M., 2003, Alkalic magmas generated by partial melting of garnet pyroxenite: Geology, v. 31, p. 481-484, doi:10.1130/0091-7613(2003)031.

Huismans, R.S., and Beaumont, C., 2014, Rifted continental margins: The case for depth-dependent extension: Earth and Planetary Science Letters, v. 407, p. 148-162, doi:10.1016/j.epsl.2014.09.032.

Humphreys, E.R., and Niu, Y., 2009, On the composition of ocean island basalts (OIB): The effects of lithospheric thickness variation and mantle metasomatism: Lithos, v. 112, p. 118-136, doi:10.1016/j.lithos.2009.04.038.

Ionov, D.A., Ashchepkov, I.V., Stosch, H.G., Witt-Eickschen, G., and Seck, H.A., 1993, Garnet peridotite xenoliths from the Vitim Volcanic Field, Baikal Region: the nature of the garnet—

spinel peridotite transition zone in the continental mantle: Journal of Petrology, v. 34, p. 1141-1175, doi:10.1093/petrology/34.6.1141.

Jagoutz, O., Munterer, O., Manatschal, G., Rubatto, D., Peron-Pinvidic, G., Turrin, B.D., and Villa, I.M., 2007, The rift-to-drift transition in the North Atlantic: A stuttering start of the MORB machine?: Geology, v. 35, p. 1087-1090, doi:10.1130/G23613A.1.

Jenner, G.A., 1996, Trace element geochemistry of igneous rocks: geochemical nomenclature and analytical geochemistry, *in* Wyman, D.A., ed., Trace element geochemistry of volcanic rocks: applications for massive sulfide exploration. Geological Association of Canada, Short Course Notes, v. 12, p. 51-77.

Jennings, D.S., and Jilson, G.A., 1986, Geology and sulfide deposits of Anvil Range, Yukon, *in* Morin, J.A., ed., Mineral Deposits of Northern Cordillera Symposium: Canadian Institute of Mining and Metallurgy, Special Paper, v. 37, p. 319–371.

Keen, C. E., Dafoe, L. T., and Dickie, K., 2014, A volcanic province near the western termination of the Charlie-Gibbs Fracture Zone at the rifted margin, offshore northeast Newfoundland: Tectonics, v. 33, p.1133–1153, doi:10.1002/2014TC003547.

Keller, T., Katz, R.F., and Hirschmann, M.M., 2017, Volatiles beneath mid-ocean ridges: Deep melting, channelised transport, focusing, and metasomatism: Earth and Planetary Science Letters, v. 464, p. 55–68, doi:10.1016/j.epsl.2017.02.006.

Kellogg, H.E., 1963, Paleozoic stratigraphy of the southern Egan Range, Nevada: Geological Society of America Bulletin, v. 74, p. 685-708, doi:10.1130/0016-7606(1963)74[685:psotse]2.0.co;2.

Klitgord, K.D., and Schouten, H., 1986, Plate kinematics of the central Atlantic, *in* Vogt, P.R., and Tucholke, B. E., eds., The Western North Atlantic Region: The Geology of North America: The Geological Society of America, p. 351–378, doi:10.1130/dnag-gna-m.351.

Kogiso, T., Hirschmann, M.M., and Frost, D.J., 2003, High-pressure partial melting of garnet pyroxenite: possible mafic lithologies in the source of ocean island basalts: Earth and Planetary Science Letters, v. 216, p. 603-617, doi:10.1016/S0012-821X(03)00538-7.

Kubli, T.E., and Simony, P.S., 1992, The Dogtooth High, northern Purcell Mountains, British Columbia: Bulletin of Canadian Petroleum Geology, v. 40, p. 36-51.

Lavier, L.L., and Manatschal, G., 2006, A mechanism to thin the continental lithosphere at magma-poor margins: Nature, v. 440, p. 324-328, doi:10.1038/nature04608.

LeCheminant, A.N., and Heaman, L.M., 1994, 779 Ma mafic magmatism in the northwestern Canadian Shield and northern Cordillera: a new regional time-marker: Eighth International Conference on Geochronology, Cosmochronology and Isotope Geology, US Geological Survey Circular, Berkeley, California, Abstracts, v. 1107, 197 p.

Leslie, C.D., 2009, Detrital zircon geochronology and rift-related magmatism: central Mackenzie Mountains, Northwest Territories [M.Sc. thesis] University of British Columbia, 224 p.

Levy, M, and Christie-Blick, N., 1991, Tectonic subsidence of the early Paleozoic passive

    continental margin in eastern California and southern Nevada: Geological Society of America

    Bulletin, v. 103, p. 1590-1606, doi:10.1130/0016-7606(1991)103<1590:tsotep>2.3.co;2.

Li, Z.X., Bogdanova, S.V., Collins, A.S., Davidson, A., De Waele, B., Ernst, R.E., Fitzsimmons,

    I.C.W., Fuck, R.A., Gladkochub, D.P., Jacobs, J., Karlstrom, K.E., Lu, S., Natapov, L.M.,

    Pease, V., Pisarevsky, S.A., Thrane, K., and Vernikovsky, V., 2008, Assembly,

    configuration, and break-up history of Rodinia: A synthesis: Precambrian Research, v. 160, p.

    179-210, doi:10.1016/j.precamres.2007.04.021.

Lickorish, W.H., and Simony, P.S., 1995, Evidence for late rifting of the Cordilleran margin outlined

    by stratigraphic division of the Lower Cambrian Gog Group, Rocky Mountain Main Ranges,

    British Columbia and Alberta: Canadian Journal of Earth Sciences, v. 32, p. 860-874,

    doi:10.1139/e95-072.

Link, P.K., Christie-Blick, N., Devlin, W.J., Elston, D.P., Horodyski, R.J., Levy, M., Miller, J.M.G.,

    Pearson, R.C., Prave, A., Stewart, J.H., Winston, D., Wright, L.A., and Wrucke, C.T., 1993,

    Middle and Late Proterozoic stratified rocks of the western U.S. Cordillera, Colorado Plateau,

    and Basin and Range Province, *in* Reed, J.C., Jr., Bickford, M.E., Houston, R.S., Link, P.K.,

    Rankin, D.W., Sims, P.K., and Van Schmus, W.R., eds., Precambrian: Conterminous U.S.:

    Boulder, Colorado, Geological Society of America, The Geology of North America, v. C-2,

    p. 463-595, doi:10.1130/dnag-gna-c2.463.

Link, P.K., Todt, M.K., Pearson, D.M., and Thomas, R.C., 2017, 500–490 Ma detrital zircons in

    Upper Cambrian Worm Creek and correlative sandstones, Idaho, Montana, and Wyoming:

Magmatism and tectonism within the passive margin: Lithosphere, v. 9, p. 910-926, doi:10.1130/l671.1.

Lister, G.S., Etheridge, M.A., and Symonds, P.A., 1986, Detachment faulting and the evolution of passive continental margins: Geology, v. 14, p. 246-250, doi:10.1130/0091-7613(1986)14<246:dfateo>2.0.co;2.

Lister, G.S., Etheridge, M.A., and Symonds, P.A., 1991, Detachment models for the formation of passive continental margins: Tectonics, v. 10, p. 1038-1064, doi:10.1029/90tc01007.

Lloyd, F.E., and Bailey, D., 1975, Light element metasomatism of the continental mantle: the evidence and the consequences: Physics and Chemistry of the Earth, v. 9, p. 389-416, doi:10.1016/b978-0-08-018017-5.50033-x.

Logan, J.M., and Colpron, M., 2006, Stratigraphy, geochemistry, syngenetic sulphide occurrences and tectonic setting of the lower Paleozoic Lardeau Group, northern Selkirk Mountains, British Columbia, *in* Colpron, M., and Nelson, J.L., eds., Paleozoic Evolution and Metallogeny of Pericratonic Terranes at the Ancient Pacific Margin of North America, Canadian and Alaskan Cordillera: Geological Association of Canada, Special Paper 45, p. 361-382, doi:10.2113/gsecongeo.102.3.534.

Ludwig, K.R., 2003, User's manual for Isoplox/Ex, version 3.00, a geochronological toolkit for Microsoft Excel: Berkeley Geochronology Center Special Publication 4, 77 p.

Lund, K., 2008, Geometry of the Neoproterozoic and Paleozoic rift margin of western Laurentia: Implications for mineral deposit settings: Geosphere, v. 4, p. 429-444, doi:10.1130/GES00121.1.

Lund, K., Aleinikoff, J.N., Evans, K.V., and Fanning, C.M., 2003, SHRIMP U-Pb geochronology of Neoproterozoic Windermere Supergroup, central Idaho: Implications for rifting of western Laurentia and synchroneity of Sturtian glacial deposits: Geological Society of America Bulletin, v. 115, p. 349-372, doi:10.1130/0016-7606(2003)115.

Lund, K., Aleinikoff, J.N., Evans, K.V., Dewitt, E.H., and Unruh, D.M., 2010, SHRIMP U-Pb dating of recurrent Cryogenian and Late Cambrian–Early Ordovician alkalic magmatism in central Idaho: Implications for Rodinian rift tectonics: Geological Society of America Bulletin, v. 122, p. 430-453, doi:10.1130/B26565.1.

MacDonald, R., Rogers, N.W., Fitton, J.G., Black, S., and Smith, M., 2001, Plume–lithosphere interactions in the generation of the basalts of the Kenya Rift, East Africa: Journal of Petrology, v. 42, p. 877-900, doi:10.1093/petrology/42.5.877.

Macdonald, F.A., Halverson, G.P., Strauss, J.V., Smith, E.F., Cox, G., Sperling, E.A., and Roots, C.F., 2012, Early Neoproterozoic Basin Formation in Yukon, Canada: Implications for the make-up and break-up of Rodinia: Geoscience Canada, v. 39, p. 77–97.

MacIntyre, D.G., 1998, Geology, geochemistry and mineral deposits of the Akie River Area, northeast British Columbia: British Columbia, Ministry of Energy and Mines, Bulletin 103, p. 1-91.

MacLean, W.H., and Barrett, T.J., 1993, Lithogeochemical techniques using immobile elements: Journal of Geochemical Exploration, v. 48, p. 109-133, doi:10.1016/0375-6742(93)90002-4.

Madrid, R.J., 1987, Stratigraphy of the Roberts Mountain allochthon in north-central Nevada [Ph. D. thesis]: Stanford University, 336 p.

Magwood, J.P.A., and Pemberton, S.G., 1988, Trace fossils of the Gog Group, a lower Cambrian tidal sand body, Lake Louise, Alberta, *in* Landing, E., Narbonne, G.M., and Myrow, P., eds., Trace fossils, small shelly fossils and the Precambrian-Cambrian boundary-proceedings: New York State Museum Bulletin 463, 14 p.

Manatschal, G., and Müntener, O., 2009, A type sequence across an ancient magma-poor ocean–continent transition: the example of the western Alpine Tethys ophiolites: Tectonophysics, v. 473, p. 4-19, doi:10.1016/j.tecto.2008.07.021.

Manatschal, G., Lavier, L., and Chenin, P., 2015, The role of inheritance in structuring hyperextended rift systems: Some considerations based on observations and numerical modeling: Gondwana Research, v. 27, p. 140-164, doi:10.1016/j.gr.2014.08.006.

Marzoli, A., Renne, P.R., Piccirillo, E.M., Ernesto, M., Bellieni, G., and De Min, A., 1999, Extensive 200-million-year-old continental flood basalts of the Central Atlantic Magmatic Province: Science, v. 284, p. 616-618, doi:10.1126/science.284.5414.616.

Masini, E., Manatschal, G., and Mohn, G., 2013, The Alpine Tethys rifted margins: reconciling old and new ideas to understand the stratigraphic architecture of magma-poor rifted margins: Sedimentology, v. 60, 174–196, doi:10.1111/sed.12017.

McDonough, W.F., and Sun, S.S., 1995, The composition of the Earth: Chemical Geology, vol. 120, p. 223-253, doi:10.1016/0009-2541(94)00140-4.

McKenzie, D., 1978, Some remarks on the development of sedimentary basins: Earth and Planetary Science Letters, v. 40, p. 25-32, doi:10.1016/0012-821x(78)90071-7.

McKenzie, D., and Bickle, M.J., 1988, The volume and composition of melt generated by extension of the lithosphere: Journal of Petrology, v. 29, p. 625-679, doi:10.1093/petrology/29.3.625.

McMechan, M.E. 1990, Upper Proterozoic to Middle Cambrian history of the Peace River Arch: evidence from the Rocky Mountains, *in* O' Connell, S.C., and Bell, J.S., eds., Geology of the Peace River Arch: Bulletin of Canadian Petroleum Geology, Special Volume 38A, p. 36-44.

McMechan, M.E., 2012, Deep transverse basement structural control of mineral systems in the southeastern Canadian Cordillera: Canadian Journal of Earth Sciences, v. 49, p. 693-708, doi:10.1139/e2012-013.

Meade, F.C., Chew, D.M., Troll, V.R., Ellam, R.M., and Page, L.M., 2009, Magma ascent along a major terrane boundary: crustal contamination and magma mixing at the Drumadoon Intrusive complex, Isle of Arran, Scotland: Journal of Petrology, v. 50, p. 2345-2374, doi:10.1093/petrology/egp081.

Merle, R., Schärer, U., Girardeau, J., and Cornen, G., 2006, Cretaceous seamounts along the continent–ocean transition of the Iberian margin: U–Pb ages and Pb–Sr–Hf isotopes: Geochimica et Cosmochimica Acta, v. 70, p. 4950-4976, doi:10.1016/j.gca.2006.07.004.

Merle, R., Jourdan, F., Marzoli, A., Renne, P.R., Grange, M., and Girardeau, J., 2009, Evidence of multi-phase Cretaceous to Quaternary alkaline magmatism on Tore–Madeira Rise and neighbouring seamounts from ^{40}Ar/^{39}Ar ages: Journal of the Geological Society, v. 166, p. 879-894, doi:10.1144/0016-76492008-060.

Milidragovic, D., Thorkelson, D.J., and Marshall, D.D., 2006, Geology of the Quartet Mountain lamprophyre suite, Wernecke Mountains, Yukon, *in* Emond, D.S., Bradshaw, G.D., Lewis, L.L., and Weston, L.H., eds., Yukon Exploration and Geology 2005: Yukon Geological Survey, p. 231-245.

Millonig, L.J., Gerdes, A., and Groat, L.A., 2012, U–Th–Pb geochronology of meta-carbonatites and meta-alkaline rocks in the southern Canadian Cordillera: a geodynamic perspective: Lithos, v. 152, p. 202-217, doi:10.1016/j.lithos.2012.06.016.

Miranda, R., Valadares, V., Terrinha, P., Mata, J., do Rosario Azevedo, M., Gaspar, M., Kullberg, J.C., and Ribeiro, C., 2009, Age constraints on the Late Cretaceous alkaline magmatism on the West Iberian Margin: Cretaceous Research, v. 30, p. 575-586, doi:10.1016/j.cretres.2008.11.002.

Morgan, W.J., 1971, Convection plumes in the lower mantle: Nature, v. 230, p. 42-43, doi:10.1038/230042a0.

Morris, H.T., and Lovering, T.S., 1961, Stratigraphy of the east Tintic Mountains, Utah: United States Geological Survey Professional Paper 361, 145 p.

Mott, J.A., 1989, Structural and stratigraphic relations in the White River region, eastern Main Ranges, southern Rocky Mountains, British Columbia [Ph.D. thesis]: Queen's University, 404 p.

Müntener, O., and Manatschal, G., 2006, High degrees of melt extraction recorded by spinel harzburgite of the Newfoundland margin: The role of inheritance and consequences for the evolution of the southern North Atlantic: Earth and Planetary Science Letters, v. 252, p. 437-452, doi:10.1016/j.epsl.2006.10.009.

Müntener, O., Manatschal, G., Desmurs, L., and Pettke, T., 2010, Plagioclase peridotites in ocean–continent transitions: refertilized mantle domains generated by melt stagnation in the shallow mantle lithosphere: Journal of Petrology, v. 51, p. 255-294, doi:10.1093/petrology/egp087.

Murphy, D.C., 1997, Geology of the McQuesten River Region, northern McQuesten and Mayo Map Areas, Yukon Territory (115P/14, 15, 16; 105M/13, 14): Yukon Geological Survey, Bulletin 6, 95 p.

Murton, B.J., Peate, D.W., Arculus, R.J., Pearce, J.A., and Van der Laan, S., 1992, Trace-element geochemistry of volcanic rocks from site 786: The Izu-Bonin Forearc: Proceedings of the

Ocean Drilling Program Scientific Results, v. 125, p. 211-235,

doi:10.2973/odp.proc.sr.125.133.1992.

Narbonne, G. M., and Aitken, J. D., 1995, Neoproterozoic of the Mackenzie Mountains,

northwestern Canada: Precambrian Research, v. 73, p, 101-121, doi:10.1016/0301-

9268(94)00073-Z.

Naylor, P.H., Bell, B.R., Jolley, D.W., Durnall, P., and Fredsted, R., 1999, Palaeogene magmatism in

the Faeroe–Shetland Basin: influences on uplift history and sedimentation, *in* Fleet, A.J., and

Boldy, S.A.R., eds., Petroleum Geology of Northwest Europe: Proceedings of the 5th

Conference: Geological Society, London, p. 545-558, doi:10.1144/0050545

Nelson, J.L., Colpron, M., and Israel, S., 2013, The Cordillera of British Columbia, Yukon, and

Alaska: Tectonics and metallogeny, *in* Colpron, M., Bissing, T., Rusk, B.G., and Thompson,

J.F.H., eds., Tectonics, Metallogeny, and Discovery: The North American Cordillera and

Similar Accretionary Settings: Society of Economic Geologists Special Publication 17, p. 53-

109.

Niu, Y., and O'Hara, M.J., 2007, Global correlations of ocean ridge basalt chemistry with axial

depth: a new perspective: Journal of Petrology, v. 49, p.633-664,

doi:10.1093/petrology/egm051.

Niu, Y., Wilson, M., Humphreys, E.R., and O'Hara, M.J., 2011, The origin of intra-plate ocean

island basalts (OIB): the lid effect and its geodynamic implications: Journal of Petrology, v.

52, p. 1443-1468, doi:10.1093/petrology/egr030.

Niu, Y., Wilson, M., Humphreys, E.R., and O'Hara, M.J., 2012, A trace element perspective on the source of ocean island basalts (OIB) and fate of subducted ocean crust (SOC) and mantle lithosphere (SML): Episodes, v. 35, p. 310-327, doi:10.1093/petrology/egr030.

Nomade, S., Knight, K.B., Beutel, E., Renne, P.R., Verati, C., Féraud, G., Marzoli, A., Youbi, N., and Bertrand, H., 2007, Chronology of the Central Atlantic Magmatic Province: Implications for the Central Atlantic rifting processes and the Triassic–Jurassic biotic crisis: Palaeogeography, Palaeoclimatology, Palaeoecology, v. 244, p. 326-344, doi:10.1016/j.palaeo.2006.06.034.

Norford, B.S., 1990, Ordovician and Silurian stratigraphy, paleogeography and depositional history in the Peace River Arch area, Alberta and British Columbia: Bulletin of Canadian Petroleum Geology, v. *38*, p. 45-54.

Norford, B.S., and Cecile, M.P., 1994, Ordovician emplacement of the Mount Dingley Diatreme, western ranges of the Rocky Mountains, southeastern British Columbia: Canadian Journal of Earth Sciences, v. 31, p. 1491-1500, doi:10.1139/e94-132.

O'Reilly, B.M., Hauser, F., Ravaut, C., Shannon, P.M., and Readman, P.W., 2006, Crustal thinning, mantle exhumation and serpentinization in the Porcupine Basin, offshore Ireland: evidence from wide-angle seismic data: Journal of the Geological Society, v. 163, p. 775-787, doi:10.1144/0016-76492005-079.

O'Nions, R.K., Evensen, N.M., and Hamilton, P.J., 1979, Geochemical modeling of mantle
  differentiation and crustal growth: Journal of Geophysical Research, Solid Earth, v.84, p.
  6091-6101, doi:10.1029/jb084ib11p06091.

Ootes, L., Gleeson, S.A., Turner, E., Rasmussen, K., Gordey, S., Falck, H., Martel, E., and Pierce,
  K., 2013, Metallogenic evolution of the Mackenzie and eastern Selwyn Mountains of
  Canada's Northern Cordillera, Northwest Territories: A compilation and review: Geoscience
  Canada, v. 40, p. 40–69, doi:10.12789/geocanj.2013.40.005.

Paradis, S., Bailey, S.L., Creaser, R.A., Piercey, S.J., Schiarizza, P., Colpron, M., and Nelson, J.L.,
  2006, Paleozoic magmatism and syngenetic massive sulphide deposits of the Eagle Bay
  assemblage, Kootenay terrane, southern British Columbia, *in* Colpron, M., and Nelson, J.L.,
  eds., Paleozoic evolution and metallogeny of pericratonic terranes at the ancient Pacific
  margin of North America, Canadian and Alaskan Cordillera: Geological Association of
  Canada Special Paper, 45, p. 383-414, doi:10.2113/gsecongeo.102.3.534.

Parrish, R.R., and Reichenbach, I., 1991, Age of xenocrystic zircon from diatremes of western
  Canada: Canadian Journal of Earth Sciences, v. 28, p. 1232-1238, doi:10.1139/e91-110.

Patchett, P.J., and Tatsumoto, M., 1981, A routine high-precision method for Lu-Hf isotope
  geochemistry and chronology: Contributions to Mineralogy and Petrology, v. 75, p. 263-267,
  doi:10.1007/bf01166766.

Pe-Piper, G., Piper, D.J.W., Jansa, L.F., and de Jonge, A., 2007, Early Cretaceous opening of the
  North Atlantic Ocean: Implications of the petrology and tectonic setting of the Fogo

Seamounts off the SW Grand Banks, Newfoundland: Geological Society of America
Bulletin, v. 119, p. 712-724, doi:10.1130/B26008.1.

Pe-Piper, G., Meredyk, S., Zhang, Y., Piper, D.J., and Edinger, E., 2013, Petrology and tectonic
significance of seamounts within transitional crust east of Orphan Knoll, offshore eastern
Canada: Geo-Marine Letters, v. 33, p. 433-447, doi:10.1007/s00367-013-0342-2.

Pearce, J.A., 1996, A user's guide to basalt discrimination diagrams. Trace element geochemistry of
volcanic rocks: applications for massive sulphide exploration: Geological Association of
Canada, Short Course Notes, v. 12, 113 p.

Pearce, J.A., and Cann, J.R., 1973, Tectonic setting of basic volcanic rocks determined using trace
element analyses: Earth and Planetary Science Letters, v. 19, p. 290-300, doi:10.1016/0012-
821x(73)90129-5.

Pearce, J.A., and Peate, D.W., 1995, Tectonic implications of the composition of volcanic arc
magmas: Annual Review of Earth and Planetary Sciences, v. 23, p. 251-285,
doi:10.1146/annurev.ea.23.050195.001343.

Pecha, M.E., Gehrels, G.E., McClelland, W.C., Giesler, D., White, C., and Yokelson, I., 2016,
Detrital zircon U-Pb geochronology and Hf isotope geochemistry of the Yukon-Tanana
terrane, Coast Mountains, southeast Alaska: *Geosphere*, v. 12, p. 1556–1574,
doi:10.1130/GES01303.1.

Pell, J. 1987, Alkaline ultrabasic rocks in British Columbia: carbonatites, nepheline syenites, kimberlites, ultramafic lamprophyres and related rocks: British Columbia Ministry of Energy, Mines, and Petroleum Resources, Geological Survey Branch, Open File 1987-17, p. 259-272.

Pell, J. 1994, Carbonatites, nepheline syenites, kimberlites and related rocks in British Columbia: British Columbia Ministry of Energy, Mines and Petroleum Resources, Geological Survey Branch, Bulletin 88, 136 p.

Peron-Pinvidic, G., and Manatschal, G., 2009, The final rifting evolution at deep magma-poor passive margins from Iberia-Newfoundland: a new point of view: International Journal of Earth Sciences, v. 98, p. 1581-1597, doi:10.1007/s00531-008-0337-9.

Peron-Pinvidic, G., and Manatschal, G., 2010, From microcontinents to extensional allochthons: witnesses of how continents rift and break apart?: Petroleum Geoscience, v. 16, p. 189-197, doi:10.1144/1354-079309-903.

Peron-Pinvidic, G., Manatschal, G., Minshull, T.A., and Sawyer, D.S., 2007, Tectonosedimentary evolution of the deep Iberia-Newfoundland margins: Evidence for a complex breakup history: Tectonics, v. 26, doi:10.1029/2006TC001970.

Peron-Pinvidic, G., Manatschal, G., and Osmundsen, P.T., 2013, Structural comparison of archetypal Atlantic rifted margins: A review of observations and concepts: Marine and Petroleum Geology, v. 43, p. 21-47, doi:10.1016/j.marpetgeo.2013.02.002.

Piercey, S.J., and Colpron, M., 2009, Composition and provenance of the Snowcap assemblage, basement to the Yukon-Tanana terrane, northern Cordillera: Implications for Cordilleran crustal growth: Geosphere, v. 5, p. 439-464, doi:10.1130/GES00505.1.

Piercey, S.J., Mortensen, J.K., Murphy, D.C., Paradis, S., and Creaser, R.A., 2002, Geochemistry and tectonic significance of alkalic mafic magmatism in the Yukon-Tanana terrane, Finlayson Lake region, Yukon: Canadian Journal of Earth Sciences, v. 39, p. 1729-1744, doi:10.1139/e02-090.

Piercey, S.J., Murphy, D.C., Mortensen, J.K., and Creaser, R.A., 2004, Mid-Paleozoic initiation of the northern Cordilleran marginal backarc basin: Geologic, geochemical, and neodymium isotope evidence from the oldest mafic magmatic rocks in the Yukon-Tanana terrane, Finlayson Lake district, southeast Yukon, Canada: Geological Society of America Bulletin, v. 116, p. 1087-1106, doi:10.1130/B25162.1.

Piercey, S.J., Nelson, J.L., Colpron, M., Dusel-Bacon, C., Simard, R.L., and Roots, C.F., 2006, Paleozoic magmatism and crustal recycling along the ancient Pacific margin of North America, northern Cordillera, *in* Colpron, M., and Nelson, J.L., eds., Paleozoic evolution and metallogeny of pericratonic terranes at the ancient Pacific margin of North America, Canadian and Alaskan Cordillera: Geological Association of Canada Special Paper, 45, p. 281-322, doi:10.2113/gsecongeo.102.3.534.

Piercey, S.J., Murphy, D.C., and Creaser, R.A., 2012, Lithosphere-asthenosphere mixing in a transform-dominated late Paleozoic backarc basin: Implications for northern Cordilleran crustal growth and assembly: Geosphere, v. 8, p. 716–739, doi:10.1130/GES00757.1

Pigage, L.C., 2004, Bedrock geology compilation of the Anvil District (parts of NTS 105K/2, 3, 4, 5, 6, 7 and 11), central Yukon: Yukon Geological Survey, Bulletin 15, 103 p.

Pigage, L.C., 2009, Bedrock geology of NTS 95C/5 (Pool Creek) and NTS 95D/8 map sheets, southeast Yukon: Yukon Geological Survey, Bulletin 16, 150 p.

Pigage, L.C., and Mortensen, J.K., 2004, Superimposed Neoproterozoic and early Tertiary alkaline magmatism in the La Biche River area, southeast Yukon Territory: Bulletin of Canadian Petroleum Geology, v. 52, p. 325-342, doi:10.2113/52.4.325.

Pigage, L.C., Crowley, J.L., Pyle, L.J., Abbott, J.G., Roots, C.F., and Schmitz, M.D., 2012, U–Pb zircon age of an Ordovician tuff in southeast Yukon: implications for the age of the Cambrian–Ordovician boundary: Canadian Journal of Earth Sciences, v. 49, p. 732-741, doi:10.1139/e2012-017.

Pigage, L.C., Roots, C.F., and Abbott, J.G., 2015, Regional bedrock geology for Coal River map area (NTS 95D), southeast Yukon: Yukon Geological Survey, Bulletin 17, 155 p.

Post, R.T., and Long, D.G., 2008, The middle Cambrian Mount Roosevelt Formation (new) of northeastern British Columbia: evidence for rifting and development of the Kechika graben system: Canadian Journal of Earth Sciences, v. 45, p. 483-498, doi:10.1139/E08-014.

Prave, A.R., 1999, Two diamictites, two cap carbonates, two δ13C excursions, two rifts: the
   Neoproterozoic Kingston Peak Formation, Death Valley, California: Geology, v. 27, p. 339-
   342, doi:10.1130/0091-7613(1999)027<0339:tdtcct>2.3.co;2.

Price, R.C., Gray, C.M., Wilson, R.E., Frey, F.A., and Taylor, S.R., 1991, The effects of weathering
   on rare-earth element, Y and Ba abundances in Tertiary basalts from southeastern Australia:
   Chemical Geology, v. 93, p. 245-265, doi:10.1016/0009-2541(91)90117-a.

Pyle, L.J., 2012, Cambrian and Lower Ordovician Sauk Megasequence of northwestern Canada,
   northern Rocky Mountains to the Beaufort Sea: American Association of Petroleum
   Geologists Memoir, v. 98, p. 675–723, doi:10.1306/13331661M983511.

Pyle, L.J., and Barnes, C.R., 2000, Upper Cambrian to Lower Silurian stratigraphic framework of
   platform-to-basin facies, northeastern British Columbia: Bulletin of Canadian Petroleum
   Geology, v. 48, p. 123-149, doi:10.2113/48.2.123.

Pyle, L.J., and Barnes, C.R., 2001, Conodonts from the Kechika Formation and Road River Group
   (Lower to Upper Ordovician) of the Cassiar Terrane, northern British Columbia: Canadian
   Journal of Earth Sciences, v. 38, p. 1387-1401, doi:10.1139/e01-033.

Pyle, L.J., and Barnes, C.R., 2003, Lower Paleozoic stratigraphic and biostratigraphic correlations in
   the Canadian Cordillera: implications for the tectonic evolution of the Laurentian margin:
   Canadian Journal of Earth Sciences, v. 40, p. 1739-1753, doi:10.1139/e03-049.

Read, B.C., 1980, Lower Cambrian archaeocyathid buildups, Pelly Mountains, Yukon: Geological
Survey of Canada, Paper 78, 54 p, doi:10.4095/106346.

Roots, C.F. 1988, Cambro-Ordovician volcanic rocks in the eastern Dawson map area, Ogilvie
mountains, Yukon, *in* Abbott, G., ed., Yukon Geology, v. 2: Indian and Northern Affairs
Canada, Geology Section, Whitehorse, Yukon. p. 81-87.

Roots, C.F., and Thompson, R.I., 1992, Long-lived basement weak zones and their role in
extensional magmatism in the Ogilvie Mountains, Yukon Territory, *in* Bartholomew, M.J.,
Hyndman, D.W., Mogk, D.W., and Mason, R., eds., Basement Tectonics and
Characterization of Ancient and Mesozoic Continental Margins: Proceedings of the 8th
International Conference in Basement Tectonics: Dordrecht, Kluwer Academic Publishers, p.
359-372, doi:10.1007/978-94-011-1614-5_24.

Ross, G.M., Villeneuve, M.E., and Theriault, R.J., 2001, Isotopic provenance of the lower Muskwa
assemblage (Mesoproterozoic, Rocky Mountains, British Columbia): New clues to
correlation and source areas: Precambrian Research, v. 111, p. 57-77, doi:10.1016/s0301-
9268(01)00156-5.

Rychert, C.A., Fischer, K.M., and Rondenay, S., 2005, A sharp lithosphere–asthenosphere boundary
imaged beneath eastern North America: Nature, v. 436, p. 542-545, doi:10.1038/nature03904.

Sandeman, H.A., Ootes, L., Cousens, B., and Kilian, T., 2014, Petrogenesis of Gunbarrel magmatic
rocks: Homogeneous continental tholeiites associated with extension and rifting of

Neoproterozoic Laurentia: Precambrian Research, v. 252, p. 166-179, doi:10.1016/j.precamres.2014.07.007.

Schärer, U., Girardeau, J., Cornen, G., and Boillot, G., 2000, 138–121 Ma asthenospheric magmatism prior to continental break-up in the North Atlantic and geodynamic implications: Earth and Planetary Science Letters, v. 181, p. 555-572, doi:10.1016/S0012-821X(00)00220-X.

Schmerr, N., 2012, The Gutenberg discontinuity: Melt at the lithosphere-asthenosphere boundary: Science, v. 335, p. 1480-1483: doi:10.1126/science.1215433.

Schmitz, M.D., and Schoene, B., 2007, Derivation of isotope ratios, errors, and error correlations for U-Pb geochronology using 205Pb-235U-(233U)-spiked isotope dilution thermal ionization mass spectrometric data: Geochemistry, Geophysics, Geosystems, v. 8, doi:10.1029/2006GC001492.

Scoates, J.S., and Friedman, R.M., 2008, Precise age of the platiniferous Merensky Reef, Bushveld Complex, South Africa, by the U-Pb zircon chemical abrasion ID-TIMS technique: Economic Geology, v. 103, p. 465-471, doi:0.2113/gsecongeo.103.3.465.

Shervais, J.W., 1982, Ti-V plots and the petrogenesis of modern and ophiolitic lavas: Earth and Planetary Science Letters, v. 59, p. 101-118, doi:10.1016/0012-821x(82)90120-0.

Smith, M.T., and Gehrels, G.E., 1992, Stratigraphic comparison of the Lardeau and Covada groups: implications for revision of stratigraphic relations in the Kootenay Arc: Canadian Journal of Earth Sciences, v. 29, p. 1320-1329, doi:10.1139/e92-105.

Soares, D.M., Alves, T.M., and Terrinha, P., 2012, The breakup sequence and associated lithospheric breakup surface: Their significance in the context of rifted continental margins (West Iberia and Newfoundland margins, North Atlantic): Earth and Planetary Science Letters, v. 355, p. 311-326, doi:10.1016/j.epsl.2012.08.036.

Sobolev, A.V., Hofmann, A.W., Sobolev, S.V., and Nikogosian, I.K., 2005, An olivine-free mantle source of Hawaiian shield basalts: Nature, v. 434, p. 590-597, doi:10.1038/nature03411.

Souther, J.G., 1991, Volcanic regimes, *in* Gabrielse, H., and Yorath, C.J., eds., Geology of the Cordilleran orogen in Canada: Geological Survey of Canada, Geology of Canada, no. 4, p. 459–490, doi:10.4095/134069.

Spitz, G., and Darling, R., 1978, Major and minor element lithogeochemical anomalies surrounding the Louvem copper deposit, Val d'Or, Quebec: Canadian Journal of Earth Sciences, v. 157, p. 1161-1169, doi:10.1139/e78-122.

Stewart, J.H., 1972, Initial deposits in the Cordilleran geosyncline: Evidence of a late Precambrian (< 850 my) continental separation: Geological Society of America Bulletin, v. 83, p. 1345-1360, doi:10.1130/0016-7606(1972)83[1345:iditcg]2.0.co;2.

Stewart, J.H., and Suczek, C.A., 1977, Cambrian and latest Precambrian paleogeography and tectonics in the western United States, *in* Stewart, J.H., Stevens, C.H., and Fritsche, A.E., eds., Paleozoic Paleogeography of the Western United States: Society of Economic Paleontologists and Mineralogists, Pacific section, Pacific Coast Paleogeography Symposium l, p. 1-17.

Strauss, J.V., Macdonald, F.A., Halverson, G.P., Tosca, N.J., Schrag, D.P., and Knoll, A.H., 2015. Stratigraphic evolution of the Neoproterozoic Callison Lake Formation: Linking the break-up of Rodinia to the Islay carbon isotope excursion: American Journal of Science, v. 315, p. 881-944, doi:10.2475/10.2015.01

Strong, D.F., and Harris, A., 1974, The petrology of Mesozoic alkaline intrusives of central Newfoundland: Canadian Journal of Earth Sciences, v. 11, p. 1208-1219, doi:10.1139/e74-114.

Sullivan, K.D., and Keen, C.E., 1977, Newfoundland Seamounts: Petrology and geochemistry, *in* Baragar, W.R.A., Coleman, L.C., and Hall, J.M., eds., Volcanic Regimes in Canada: Geological Association of Canada Special Paper 16, p. 461–476.

Sun, S.S., and McDonough, W.S., 1989, Chemical and isotopic systematics of oceanic basalts: implications for mantle composition and processes: Geological Society, London, Special Publications, v. 42, p. 313-345, doi:10.1144/gsl.sp.1989.042.01.19.

Taylor, G.C., and Stott, D.F., 1973, Tuchodi Lakes map-area, British Columbia (94K): Geological Survey of Canada, Memoir 373. 37 p, doi:10.4095/102437.

Tempelman-Kluit, D.J., 2012, Geology of Quiet Lake and Finlayson Lake map areas, south-central

    Yukon: An early interpretation of bedrock stratigraphy and structure: Geological Survey of

    Canada, Open File 5487, 103 p, doi:10.4095/291931.

Thirwall, M.F., 2000, Inter-laboratory and other errors in Pb isotope analyses investigated using a

    ^{207}Pb-^{204}Pb double spike: Chemical Geology, v. 163, p. 299-322, doi:10.1016/S0009-

    2541(99)00135-7.

Thomas, W.A., 2006, Tectonic inheritance at a continental margin: GSA Today, v. 16, p. 4-11,

    doi:10.1130/1052-5173(2006)016[4:tiaacm]2.0.co;2.

Thompson, R.I., and Roots, C.F., 1982, Ogilvie Mountains project, Yukon: a new regional mapping

    program: Current Research, Part A, Geological Survey of Canada Paper, p. 403-411,

    doi:10.4095/111324.

Thorkelson, D.J., Laughton, J.R., Hunt, J.A., and Baker, T., 2003, Geology and mineral occurrences

    of the Quartet Lakes map area (NTS 106E/1), Wernecke and Mackenzie mountains, Yukon,

    in Emond D.S., and Lewis L.L., eds., Yukon Exploration and Geology 2002: Exploration and

    Geological Services Division, Yukon Region, Indian and Northern Affairs Canada, p. 223-

    239.

Tosdal, R.M., Wooden, J.L., and Kistler, R.W., 2000, Inheritance of Nevadan mineral belts from

    Neoproterozoic continental breakup, *in* Cluer, J.K., Price, J.G., Struhsacker, E.M., Hardyman,

    R.F., and Morris, C.L., eds., Geology and ore deposits 2000: The Great Basin and beyond:

Geological Society of Nevada Symposium Proceedings, May 15–18, 2000: Reno, Nevada, Geological Society of Nevada: v. 1, p. 451–466.

Tucholke, B.E., Sawyer, D.S., and Sibuet, J.C., 2007, Breakup of the Newfoundland-Iberia rift, *in* Karner, G.D., Manatschal, G., and Pinheiro, L.M., eds., Imaging, Mapping, and Modelling Continental Lithosphere Extension and Breakup: Geological Society, London, Special Publication 282, p. 9–46, doi:10.1144 /SP282.2.

Turner, R.J., Madrid, R.J., and Miller, E.L., 1989, Roberts Mountains allochthon: Stratigraphic comparison with lower Paleozoic outer continental margin strata of the northern Canadian Cordillera: Geology, v. 17, p. 341-344, doi:10.1130/0091-7613(1989)017<0341:rmascw>2.3.co;2.

Unternehr, P., Peron-Pinvidic, G., Manatschal, G., and Sutra E., 2010, Hyper-extended crust in the South Atlantic: in search of a model: *Petroleum Geoscience*, v.16 p. 207–215, doi:10.1144/1354-079309-904.

Verati, C., Rapaille, C., Féraud, G., Marzoli, A., Bertrand, H., and Youbi, N., 2007, 40 Ar/39 Ar ages and duration of the Central Atlantic Magmatic Province volcanism in Morocco and Portugal and its relation to the Triassic–Jurassic boundary: Palaeogeography, Palaeoclimatology, Palaeoecology, v. 244, p. 308-325, doi:10.1016/j.palaeo.2006.06.033.

Vervoort, J.D., and Blichert-Toft, J., 1999, Evolution of the depleted mantle: Hf isotope evidence from juvenile rocks through time: Geochimica et Cosmochimica Acta, v. 63, p. 533-556, doi:10.1016/s0016-7037(98)00274-9.

Yonkee, W.A., Dehler, C.D., Link, P.K., Balgord, E.A., Keeley, J.A., Hayes, D.S., Wells, M.L., Fanning, C.M., and Johnston, S.M., 2014, Tectono-stratigraphic framework of Neoproterozoic to Cambrian strata, west-central US: Protracted rifting, glaciation, and evolution of the North American Cordilleran margin: Earth-Science Reviews, v. 136, p. 59-95, doi:10.1016/j.earscirev.2014.05.004.

Warren, M.J., 1997, Crustal extension and subsequent crustal thickening along the Cordilleran rifted margin of ancestral North America, western Purcell Mountains, southeastern British Columbia [Ph.D. thesis]: Queen's University, 361 p.

Watkins, R., and Browne, Q.J., 1989, An Ordovician continental-margin sequence of turbidite and seamount deposits in the Roberts Mountain allochthon, Independence Range, Nevada: Geological Society of America Bulletin, v. 101, p. 731-741, doi:10.1130/0016-7606(1989)101<0731:AOCMSO>2.3.CO;2.

Weis, D., Kieffer, B., Maerschalk, C., Barling, J., de Jong, J., Williams, G.A., Hanano, D., Pretorius, W., Mattielli, N., Scoates, J.S., and Goolaerts, A., 2006, High-precision isotopic characterization of USGS reference materials by TIMS and MC-ICP-MS: Geochemistry, Geophysics, Geosystems, v. 7, doi:10.1029/2006GC001283.

Weis, D., Kieffer, B., Hanano, D., Nobre Silva, I., Barling, J., Pretorius, W., Maerschalk, C., and Mattielli, N., 2007, Hf isotope compositions of US Geological Survey reference materials: Geochemistry, Geophysics, Geosystems, v. 8, doi:10.1029/2006GC001473.

Wernicke, B., 1985, Uniform-sense normal simple shear of the continental lithosphere: Canadian Journal of Earth Sciences, v. 22, p. 108-125, doi:10.1139/e85-009.

Whitmarsh, R.B., White, R.S., Horsefield, S.J., Sibuet, J.C., Recq, M., and Louvel, V., 1996, The ocean-continent boundary off the western continental margin of Iberia: Crustal structure west of Galicia Bank: Journal of Geophysical Research: Solid Earth, v. 101, p. 28291-28314, doi:10.1029/96jb02579.

Winchester, J.A., and Floyd, P.A., 1977, Geochemical discrimination of different magma series and their differentiation products using immobile elements: Chemical Geology, v. 20, p. 325-343, doi:10.1016/0009-2541(77)90057-2.

Whitmarsh, R.B., Manatschal, G., and Minshull, T.A., 2001, Evolution of magma-poor continental margins from rifting to seafloor-spreading: Nature, v. 413, p. 150-154, doi:10.1038/35093085.

Wood, B.J., Kiseeva, E.S., and Matzen, A.K., 2013, Garnet in the Earth's Mantle: Elements, v. 9, p. 421-426, doi:10.2113/gselements.9.6.421.

Zwanzig, H.V., 1973, Structural transition between the foreland zone and the core zone of the Columbian orogen, Selkirk Mountains, British Columbia [Ph.D. thesis]: Kingston, Ontario, Queen's University, 158 p.

Chapter 4 Summary and Future Research

4.1 Summary

The Kechika group forms part of a suite of syn- to post-breakup magmatic rocks that was emplaced following Tonian to early Cambrian rifting and the initiation of subsidence along the ancestral margin of western North America. This study presents new data that provide constraints on the precise timing of Kechika group magmatism and related Cambrian-Ordovician marine depositional environments within the Cassiar terrane. In particular, this thesis produced one of the most extensive whole-rock (major element, trace element, Nd-Hf isotopes) datasets to date for the Canadian sector of the North American Cordillera. The following conclusions are based on these new data:

- Kechika group basaltic and volcanogenic sedimentary lithofacies include pillow lava, sediment-matrix basalt breccia, and monomictic basalt breccia. Pillowed lava flows are consistent with subaqueous volcanism (Moore, 1975). Sediment-matrix basalt breccia lithofacies are interpreted as fluidal peperite units (e.g., Skilling et al., 2002). Monomictic volcanic breccia units likely represent resedimented hyaloclastite units (e.g., Batiza and White, 2000; Simpson and McPhie, 2001). Hyaloclastite units with bomb-sized fragments occur adjacent to pillow basalt and are inferred to represent pillow breccia (e.g., Batiza and White, 2000; Simpson and McPhie, 2001). Kechika group basaltic and volcanogenic sedimentary lithofacies are indicative of submarine volcanic centres. Associated mafic sills are likely comagmatic sediment-sill complexes.

- New CA-TIMS zircon U-Pb results have identified at least two episodes of mafic magmatism during the latest Cambrian and Early Ordovician (ca. 488-483 Ma, and 473 Ma), respectively. Silurian (435 and 428 Ma) detrital zircons provide a maximum depositional age for rock units of the basal Askin group.

- Kechika group lavas were generated by the low-degree partial melting of an enriched mantle source as indicated by high Nb/Y and Ti/V, OIB-like geochemical signatures, and superchondritic to chondritic Nd-Hf isotope compositions. Some comagmatic intrusive rocks show broadly similar results with the exception of lower Nb/Th values and subchrondritic Nd-Hf isotope compositions that suggest crustal contamination.

- The observed lithofacies and alkaline geochemistry of the Kechika group magmatic rocks are comparable to coeval Cambrian Series 2 to Ordovician syn- to post-breakup volcanic rocks that occur throughout the passive margin successions of western North America.

- The continuation of periodic extension after Ediacaran-Cambrian lithospheric breakup is supported by the occurrences of lower Paleozoic volcanic rocks, normal faults, base-metal deposits, and basinal shale units that are representative of deep-marine rift environments. Volcanic rocks typically occur along the trace of lithospheric-scale structures such as the Liard line and Snake River transfer, many of which underwent oblique-slip faulting during the early Paleozoic.

- Magma-poor scenarios with rift processes comparable to the modern Newfoundland-Iberia rift system may more accurately explain the timing and tectonic evolution of the early Paleozoic Cordilleran margin (e.g., Yonkee et al., 2014; Hayward, 2015; Beranek, 2017) than previously published simple- and pure-shear models (e.g., Bond et al., 1984; Cecile et al., 1997; Lund, 2008). Post-breakup extensional tectonism and volcanism within the Newfoundland-Iberia rift system continued within outboard basins during the initial ~30 m.y. of seafloor spreading (e.g., Keen et al., 2014; Dafoe et al., 2017). These syn- to post-breakup volcanic rocks include those within the Orphan Knoll of offshore Newfoundland (e.g., Pe-Piper et al., 2013) and alkaline massifs of Portugal (e.g., Grange et al., 2010), providing potential modern analogues for post-breakup volcanism along the Cordilleran margin.

- An outstanding question in Cordilleran geology concerns the considerable evidence for Cryogenian rifting and contrasting limited evidence for Ediacaran-early Cambrian rifting associated with lithospheric breakup (e.g., Christie-Blick and Levy, 1989). Early Paleozoic post-breakup magmatism indicates that extensional tectonism in the outer continental margin persisted beyond the early Cambrian likely due to the build-up and subsequent release of in-plane tensile stresses during the transition between lithospheric breakup and the generation of oceanic crust. This would suggest that the Ediacaran-Cambrian rift event associated with breakup was a more significant, prolonged, and geographically varied event than previously suggested.

4.2 Future Research

There are several unanswered questions that relate to the origins of lower Paleozoic strata in the Pelly Mountains and ancient Pacific margin of western North America. Future investigations in the Pelly Mountains may include: 1) detailed (1:50 000) mapping of lower Paleozoic strata to revisit the regional stratigraphy defined by Tempelman-Kluit (2012), determine the locations of type sections, and employ modern rules of the North American Stratigraphic Code; 2) re-examine the structural geology and potential role of early Paleozoic normal faults on Kechika group deposition; 3) examine the tectonic significance of Silurian volcanism in the Pelly Mountains and its relationship to late Ordovician-Silurian magmatism in the peri-Laurentian terranes of the northern Cordillera.

New high-precision zircon U-Pb and Nd-Hf geochemical studies in regions outside the Pelly Mountains would be hugely beneficial for understanding temporal or along-strike variations in pre-, syn- and post-breakup volcanism along the Cordilleran margin. Although magma-poor rift scenarios provide several new hypotheses on the likely timing and composition of these rocks, this hypothesis would benefit from further investigations. Specific examples that require further examination include Cambrian tholeiitic volcanic rocks in the Kootenay terrane and pre-Late Devonian magmatic rocks within the Snowcap assemblage of Yukon-Tanana terrane.

4.3 References

Abbott, G., 1997, Geology of the Upper Hart River Area, Eastern Ogilvie Mountains, Yukon Territory 9116A/10, 116A/11: Exploration and Geological Services Division, Yukon, Indian and Northern Affairs Canada, Bulletin 9, 92 p.

Abbott, J.G., Gordey, S.P., and Tempelman-Kluit, D.J., 1986, Setting of stratiform, sediment-hosted lead-zinc deposits in Yukon and northeastern British Columbia: Geological Survey of Canada Open File 2169, p. 69-98, doi:10.4095/132329.

Aitken, J. D., 1993a, Proterozoic sedimentary rocks, *in* Stott, D.F., and Aitken, J.D., eds., Sedimentary Cover of the North American Craton in Canada: Geological Survey of Canada, Geology of Canada, v. 5, p. 81-95, doi:10.1130/dnag-gna-d1.79.

Aitken, J.D., 1993b, Cambrian and lower Ordovician-Sauk sequence, *in* Stott, D.F., and Aitken, J.D., eds., Sedimentary Cover of the North American Craton in Canada: Geological Survey of Canada, Geology of Canada, v. 5, p. 96-124, doi:10.4095/192360.

Allen, T.L., Pigage, L.C., and MacNaughton, R.B., 2000, Preliminary geology of the Pool Creek map area (95C/5), southeastern Yukon: Yukon Exploration and Geology, p. 53-72.

Armin, R.A., and Mayer, L., 1983, Subsidence analysis of the Cordilleran miogeocline: Implications for timing of late Proterozoic rifting and amount of extension: Geology, v. 11, p. 702-705, doi:10.1130/0091-7613(1983)11<702:saotcm>2.0.co;2.

Audet, P., Sole, C. and Schaeffer, A.J., 2016, Control of lithospheric inheritance on neotectonic activity in northwestern Canada?: Geology, v. 44, p. 807-810, doi:10.1130/G38118.1

Batiza, R., and White, J.D.L., 2000, Submarine lavas and hyaloclastite, *in* Sigurdsson, H., ed., Encyclopedia of Volcanics: Academic, San Diego, California, p. 361-381.

Beranek, L.P., 2017, A magma-poor rift model for the Cordilleran margin of western North America: Geology, v. 45, p. 1115-1118, doi:10.1130/G39265.1.

Beranek, L.P., Piercey, S.J., Campbell, R., and Wawrzonkowski, P., 2016, Paleozoic stratigraphy, tectonics and metallogeny of the Pelly Mountains, Quiet Lake and Finlayson Lake map areas (NTS 105F and G), central Yukon: Project outline and preliminary field results, *in* MacFarlane, K.E., and Nordling, M.G., eds., Yukon Exploration and Geology 2015: Yukon Geological Survey, p. 17-28.

Black, R., Gladwin, K., and Johnston, S.T., 2003, Geology and metamorphic conditions in rocks of the Cassiar terrane, Glenlyon map area (105L/1), south-central Yukon, *in* Emond, D.S., and Lewis, L.L., eds., Yukon Exploration and Geology 2002: Exploration and Geological Services Division, Yukon Region, Indian and Northern Affairs Canada, p. 65-76.

Blichert-Toft, J., Agranier, A., Andres, M., Kingsley, R., Schilling, J.G., and Albarède, F., 2005, Geochemical segmentation of the Mid-Atlantic Ridge north of Iceland and ridge-hot spot interaction in the North Atlantic: Geochemistry, Geophysics, Geosystems, v. 6, p. 1-27, doi:10.1029/2004gc000788.

Boillot, G., Grimaud, S., Mauffret, A., Mougenot, D., Kornprobst, J., Mergoil-Daniel, J., and Torrent, G., 1980, Ocean-continent boundary off the Iberian margin: a serpentinite diapir west of the Galicia Bank: Earth and Planetary Science Letters, v. 48, p. 23-34, doi:10.1029/2004gc000788.

Bond, G.C., and Kominz, M.A., 1984, Construction of tectonic subsidence curves for the early

    Paleozoic miogeocline, southern Canadian Rocky Mountains: Implications for subsidence

    mechanisms, age of breakup, and crustal thinning: Geological Society of America Bulletin, v.

    95, p. 155-173, doi:10.1130/0016-7606(1984)95<155:cotscf>2.0.co;2.

Bond, G.C., Nickeson, P.A., and Kominz, M.A., 1984, Breakup of a supercontinent between 625 Ma

    and 555 Ma: new evidence and implications for continental histories: Earth and Planetary

    Science Letters, v. 70, p. 325-345, doi:10.1016/0012-821x(84)90017-7.

Bond, G.C., Christie-Blick, N., Kominz, M.A., and Devlin, W.J., 1985, An Early Cambrian rift to

    post-rift transition in the Cordillera of western North America: Nature, v. 315, p. 742-746,

    doi:10.1038/315742a0.

Braun, J., and Beaumont, C., 1989, A physical explanation of the relation between flank uplifts and

    the breakup unconformity at rifted continental margins: Geology, v. 17, p. 760-764,

    doi:10.1130/0091-7613(1989)017<0760:apeotr>2.3.co;2.

Bronner, A., Sauter, D., Manatschal, G., Peron-Pinvidic, G., and Munschy, M., 2011, Magmatic

    breakup as an explanation for magnetic anomalies at magma-poor rifted margins: Nature

    Geoscience, v. 4, p. 549-553, doi:10.1038/ngeo1201.

Brune, S., Heine, C., Pérez-Gussinyé, M., and Sobolev, S.V., 2014, Rift migration explains

    continental margin asymmetry and crustal hyper-extension: Nature Communications, v. 5, p.

    1-9, doi:10.1038/ncomms5014.

Buck, W.R., 2004, Consequences of asthenospheric variability on continental rifting, *in* Karner, G.D., Taylor, B., Driscoll, N.W., and Kohlstedt, D.L., eds., Rheology and deformation of the lithosphere at continental margins: Columbia University Press, New York, v. 62, p. 1-30, doi:10.7312/karn12738-002.

Campbell, R.W., and Beranek, L.P., 2017, Volcanic stratigraphy of the Cambrian-Ordovician Kechika group, Pelly Mountains, south-central Yukon, *in* MacFarlane, K.E., and Weston, L.H., eds., Yukon Exploration and Geology 2016: Yukon Geological Survey, p. 25-45.

Cann, J.R., 1970, Rb, Sr, Y, Zr and Nb in some ocean floor basaltic rocks: Earth and Planetary Science Letters, v. 10, p. 7-11, doi:10.1016/0012-821x(70)90058-0.

Cas, R.A.F., and Wright, J.V., 1988, Volcanic successions, Modern and Ancient: A geological approach to processes, products and successions: Allen and Unwin, London 528 p.

Cecile, M.P., 2000, Geology of the northeastern Niddery Lake map area, east-central Yukon and adjacent Northwest Territories: Geological Survey of Canada Bulletin, v. 553, 120 p, doi:10.4095/211664.

Cecile, M.P., Fritz, W.H., Norford, B.S., and Tipnis, R.S., 1982, The Lower Paleozoic Misty Creek embayment, Selwyn Basin, Yukon and Northwest Territories: Geological Survey of Canada, Bulletin 335, 78 p, doi:10.4095/111346.

Cecile, M.P., and Norford, B.S., 1991, Ordovician and Silurian assemblages, in Cambrian to Middle Devonian Assemblages, *in* Gabrielse, H., and Yorath, C.J., eds., Geology of the Cordilleran

Orogen in Canada: Geological Survey of Canada, Geology of Canada series, no. 4, p. 184-196, doi:10.4095/134069.

Cecile, M.P., Norford, B.S., Stott, D.F., and Aitken, J.D., 1993, Ordovician and Silurian, *in* Stott, D.F., and Aitken, J.D., eds., Sedimentary cover of the craton in Canada: Geology of Canada: Geological Survey of Canada, v.5, p.125-149, doi:10.1130/dnag-gna-d1.125.

Cecile, M.P., Morrow, D.W., and Williams, G.K., 1997, Early Paleozoic (Cambrian to Early Devonian) tectonic framework, Canadian Cordillera: Bulletin of Canadian Petroleum Geology, v. 45, p. 54-74.

Chenin, P., and Beaumont, C., 2013, Influence of offset weak zones on the development of rift basins: Activation and abandonment during continental extension and breakup: Journal of Geophysical Research: Solid Earth, v. 118, p. 1698–1720, doi:10.1002/jgrb.50138.

Christie-Blick, N., 1997, Neoproterozoic sedimentation and tectonics in west-central Utah: Brigham Young University Geological Studies, v. 42, p. 1-30.

Christie-Blick, N., and Levy, M., 1989, Stratigraphic and tectonic framework of upper Proterozoic and Cambrian rocks in the western United States, *in* Christie-Blick, N., and Levy, M., eds., Late Proterozoic and Cambrian Tectonics, Sedimentation, and Record of Metazoan Radiation in the western United States: American Geophysical Union, 28th International Geological Congress Field Trip Guidebook T33, p. 7–22, doi:10.1029/FT331p0007.

Cobbett, R., 2016, Preliminary observations on the geology of Tay Mountain Area (parts of NTS 105K/12 and 13, 105L/09 and 16), central Yukon, *in* MacFarlane, K.E., and Nordling, M.G., eds., Yukon Exploration and Geology 2015: Yukon Geological Survey, p. 79-98.

Cohen, K.M., Finney, S.C., Gibbard, P.L., and Fan, J.-X., 2013 (updated): The ICS International Chronostratigraphic Chart: Episodes, 36, 199-204.

Colpron, M., Logan, J.M., and Mortensen, J.K., 2002, U-Pb zircon age constraint for late Neoproterozoic rifting and initiation of the lower Paleozoic passive margin of western Laurentia: Canadian Journal of Earth Sciences, v. 39, p. 133-143, doi:10.1139/E01-069.

Colpron, M., Nelson, J.L., and Murphy, D.C., 2007, Northern Cordilleran terranes and their interactions through time: GSA Today, v. 17, p. 4-10, doi:10.1130/gsat01704-5a.1.

Colpron, M., and Nelson, J.L., 2009, A Palaeozoic Northwest Passage: Incursion of Caledonian, Baltican, and Siberian terranes into eastern Panthalassa, and the early evolution of the North American Cordillera, *in* Cawood, P.A., and Kroner, A., eds., Earth accretionary systems in space and time: Geological Society, London, Special Publication 318, p. 273–307, doi:10.1144 /SP318.10.

Colpron, M., and Nelson, J.L., 2011, A Digital Atlas of Terranes for the Northern Cordillera. Yukon Geological Survey, <www.geology.gov.yk.ca> [accessed November 2016].

Cornen, G., Girardeau, J., and Monnier, C., 1999, Basalts, underplated gabbros and pyroxenites record the rifting process of the West Iberian margin: Mineralogy and Petrology, v. 67, p. 111-142, doi:10.1007/BF01161518

Corti, G., Bonini, M., Mazzarini, F., Boccaletti, M., Innocenti, F., Manetti, P., Mulugeta, G., and Sokoutis, D., 2002, Magma-induced strain localization in centrifuge models of transfer zones: Tectonophysics, vol. 348, p. 205-218, doi:/10.1016/s0040-1951(02)00063-x.

Crittenden, M.D., Jr., and Wallace, C.A., 1973, Possible equivalents of the Belt Supergroup in Utah, Belt Symposium 1973, Volume 1: Moscow, Idaho, Idaho Bureau of Mines and Geology, p. 116–138.

Dafoe, L.T., Keen, C.E., Dickie, K., and Williams, G.L., 2017, Regional stratigraphy and subsidence of Orphan Basin near the time of breakup and implications for rifting processes: Basin Research, v. 29, p. 233-254, doi:10.1111/bre.12147.

David, K., Schiano, P., and Allegre, C.J., 2000, Assessment of the Zr/Hf fractionation in oceanic basalts and continental materials during petrogenetic processes: Earth and Planetary Science Letters, v. 178, p. 285–301, doi: 10.1016/S0012-821X(00)00088-1.

Davis, M., and Kusznir, N. J., 2004, Depth-Dependent Lithospheric Stretching at Rifted Continental Margins, *in* G. D. Karner., ed., Proceedings of NSF Rifted Margins Theoretical Institute: New York, Columbia University Press. p. 92-136, doi:10.7312/karn12738-005

DePaolo, D.J., 1981, Neodymium isotopes in the Colorado Front Range and crust–mantle evolution in the Proterozoic: Nature, v. 291, p. 193-196, doi:10.1038/291193a0

Devlin, W.J., 1989, Stratigraphy and Sedimentology of the Hamill Group in the northern Selkirk Mountains, British Columbia: evidence for latest Proterozoic-Early Cambrian extensional tectonism: Canadian Journal of Earth Sciences, v. 26, p. 515-533, doi:10.1139/e89-044.

Devlin, W.J., and Bond, G.C., 1988, The initiation of the early Paleozoic Cordilleran miogeocline: evidence from the uppermost Proterozoic-Lower Cambrian Hamill Group of southeastern British Columbia: Canadian Journal of Earth Sciences, v. 25, p. 1-19, doi:10.1139/e88-001.

Doré, T., and Lundin, E., 2015, Research focus: Hyperextended continental margins—knowns and unknowns: Geology, v. 43, p. 95-96, doi:10.1130/focus012015.1.

Douglas, R.J.W., Gabrielse, H., Wheeler, J.O., Stott, D.F., and Belyea, H.R., 1970, Geology of Western Canada, *in* Douglas, R.J.W., ed., Geology and Economic Minerals of Canada: Geological Survey of Canada, Economic Geology Report 1, 5th edition, p. 367-546, doi:10.4095/106151.

Dunn, A.M., Reynolds, P.H., Clarke, D.B., and Ugidos, J.M., 1998, A comparison of the age and composition of the Shelburne dyke, Nova Scotia, and the Messejana dyke, Spain: Canadian Journal of Earth Sciences, v. 35, p. 1110-1115, doi:10.1139/e98-058.

Eddy, M.P., Jagoutz, O., and Ibañez-Mejia, M., 2017, Timing of initial seafloor-spreading in the Newfoundland-Iberia rift: Geology, v. 45, p. 527-530, doi:10.1130/G38766.1.

Edgar, A.D., 1987, The genesis of alkaline magmas with emphasis on their source regions: inferences from experimental studies, *in* Fitton, J.G., and Upton B.G.J., eds., Alkaline Igneous Rocks, Geological Society, London, Special Publications, v. 30, p. 29-52, doi:10.1144/gsl.sp.1987.030.01.04.

Einsele, G., 1986, Interaction between sediments and basalt injections in young Gulf of California-type spreading centers: Geologische Rundschau, v. 75, p. 197-208, doi:10.1007/bf01770188.

Eyster, A., Ferri, F., Schmitz, M.D., and Macdonald, F.A., 2018, One diamictite and two rifts: stratigraphy and geochronology of the Gataga Mountain of northern British Columbia: American Journal of Science, v. 318, p. 167-207, doi:10.2475/02.2018.1.

Fanning, C.M., and Link, P.K., 2004, U-Pb SHRIMP ages of Neoproterozoic (Sturtian) glaciogenic Pocatello Formation, southeastern Idaho: Geology, v. 32, p. 881-884, doi:10.1130/G20609.1.

Ferri, F., Nelson, J., and Rees, C., 1995, Geology and mineralization of the Gataga River Area, northern Rocky Mountains (94l/7,8,9 and 10): Geological fieldwork 1994: British Columbia Ministry of Energy, Mines and Petroleum Resources, Paper 1995-1, p. 277–295.

Ferri, F., Rees, C., Nelson, J., and Legun, A., 1999, Geology and Mineral Deposits of the Northern Kechika Trough between Gataga River and the 60th Parallel: Geological Survey Branch, Mineral Resources Division, British Columbia Ministry of Energy and Mines Bulletin 107, 122 p.

Ferri, F., and Schiarizza, P., 2006, Re-interpretation of Snowshoe group stratigraphy across a southwest-verging nappe structure and its implications for regional correlations within the Kootenay terrane, *in* Colpron, M., and Nelson, J.L., eds., Paleozoic Evolution and Metallogeny of Pericratonic Terranes at the Ancient Pacific Margin of North America, Canadian and Alaskan Cordillera: Geological Association of Canada, Special Paper, 45, p. 415-432.

Fisher, R.V., and Schmincke, H.U., 1984, Pyroclastic rocks: Springer-Verlag, Berlin, 472 p, doi:10.1007/978-3-642-74864-6.

Fitton, J.G., 1987, The Cameroon line, West Africa: a comparison between oceanic and continental alkaline volcanism, *in* Fitton, J.G., and Upton B.G.J., eds., Alkaline Igneous Rocks: Geological Society, London, Special Publications, v. 30, p. 273-291, doi:10.1144/gsl.sp.1987.030.01.13.

Fitton, J.G., 2007, The OIB paradox, *in* Foulger, G.R., and Jurdy, D.M., eds., Plates, Plumes, and Planetary Processes: Geological Society of America Special Paper 430, p. 387-412, doi:10.1130/2007.2430(20)

Fitton, J.G., James, D., Kempton, P.D., Ormerod, D.S., and Leeman W.P., 1988, The Role of Lithospheric Mantle in the Generation of Late Cenozoic Basic Magmas in the Western United States: *Journal of Petrology,* Special Lithosphere Issue, v. 1, p. 331–349, doi:10.1093/petrology/Special_Volume.1.331

Foley, S., 1992, Vein-plus-wall-rock melting mechanisms in the lithosphere and the origin of

    potassic alkaline magmas: Lithos, v. 28, p. 435-453, doi:10.1016/0024-4937(92)90018-t.

Franke, D., 2013, Rifting, lithosphere breakup and volcanism: Comparison of magma-poor and

    volcanic rifted margins: Marine and Petroleum Geology, v. 43, p. 63-87,

    doi:10.1016/j.marpetgeo.2012.11.003.

Fritz, W.H., Cecile, M.P., Norford, B.S., Morrow, D.W., and Geldsetzer, H.H.J., 1991, Cambrian to

    Middle Devonian assemblages, *in* Gabrielse, H., and Yorath, C.J., eds., The Cordilleran

    Orogen: Canada: Geological Survey of Canada, Geology of Canada, no. 4, p. 151-218,

    doi:10.4095/134087

Furman, T., 2007, Geochemistry of East African Rift basalts: an overview: Journal of African Earth

    Sciences, v. 48, p. 147-160, doi:10.1016/j.jafrearsci.2006.06.009.

Gabrielse, H., 1963, McDame map area, Cassiar District, British Columbia: Geological Survey of

    Canada, Memoir 319, 138 p, doi:10.4095/100546.

Gabrielse, H., 1967, Tectonic evolution of the northern Canadian Cordillera: Canadian Journal of

    Earth Sciences, v. 4, p. 271-298, doi:10.1139/e67-013.

Gabrielse, H., 1998, Geology of the Cry Lake and Dease Lake map areas, north-central British

    Columbia: Geological Survey of Canada, Bulletin 504, 147 p, doi:10.4095/210074.

Gabrielse, H., and Taylor, G.C., 1982, Geological maps and cross-sections of the Cordillera

    from near Fort Nelson, British Columbia to Gravina Island, southeastern Alaska:

    Geological Survey of Canada, Open File 864, doi:10.4095/129756.

Gabrielse, H., Blusson, S.L., and Roddick, J.A., 1973, Geology of Flat River, Glacier Lake, and

    Wrigley Lake map-areas, District of Mackenzie and Yukon Territory: Geological Survey of

    Canada, Memoir 366, 153 p, doi:10.4095/100705.

Gabrielse, H., and Yorath, C.J., 1991, Tectonic synthesis, *in* Gabrielse, H., and Yorath, C.J., eds.,

    Geology of the Cordilleran Orogen in Canada: Geological Survey of Canada, Geology of

    Canada, no. 4, p. 677-705, doi:10.4095/134069.

Gabrielse, H., Murphy, D.C., and Mortensen, J.K., 2006, Cretaceous and Cenozoic dextral orogen-

    parallel displacements, magmatism, and paleogeography, northcentral Canadian Cordillera, *in*

    Haggart, J.W., Enkin, R.J., and Monger, J.W.H., eds., Paleogeography of the North American

    Cordillera: evidence for and against large-scale displacements: Geological Association of

    Canada, Special Paper, 46, p. 255-276.

Georgen, J.E., and Lin, J., 2003, Plume-transform interactions at ultra-slow spreading ridges:

    Implications for the Southwest Indian Ridge: Geochemistry, Geophysics, Geosystems, v. 4,

    doi:10.1029/2003GC000542.

Gladwin, K., Colpron, M., Black, R., and Johnston, S.T., 2003, Bedrock geology at the boundary

    between Yukon-Tanana and Cassiar terranes, Truitt Creek map area (NTS 105L/1), south

    central Yukon, *in* Emond, D.S., and Lewis, L.L., eds., Yukon Exploration and Geology 2002:

Exploration and Geological Services Division, Yukon Region, Indian and Northern Affairs Canada, p. 135-148.

Godwin, C.I., and Price, B.J., 1986, Geology of the Mountain diatreme kimberlite, north-central Mackenzie Mountains, District of Mackenzie, Northwest Territories, *in* Morin, J.A., ed., Mineral Deposits of Northern Cordillera Symposium: Canadian Institute of Mining and Metallurgy, Special Paper, v. 37, p. 87-99.

Goldstein, S.L., O'Nions, R.K., and Hamilton, P.J., 1984, A Sm-Nd isotopic study of atmospheric dusts and particulates from major river systems: Earth and Planetary Science letters, v. 70, p. 221-236, doi:10.1016/0012-821x(84)90007-4.

Goodfellow, W., 2007, Base metal metallogeny of the Selwyn basin, Canada, *in* Goodfellow, W. D., ed., Mineral Deposits of Canada: A Synthesis of Major Deposit Types, District Metallogeny, the Evolution of Geological Provinces, and Exploration Methods: Mineral Deposit Division: Geological Association of Canada, Special Publication 5, p. 553–580.

Goodfellow, W.D., and Jonasson, I.R., 1986, Environment of formation of the Howards Pass (XY) Zn-Pb deposit, Selwyn Basin, Yukon, *in* Morin, J.A., ed., Mineral Deposits of Northern Cordillera Symposium: Canadian Institute of Mining and Metallurgy, Special Paper, v. 37, p. 19-50.

Goodfellow, W.D., Cecile, M.P., and Leybourne, M.I., 1995, Geochemistry, petrogenesis, and tectonic setting of lower Paleozoic alkalic and potassic volcanic rocks, Northern Canadian

Cordilleran Miogeocline: Canadian Journal of Earth Sciences, v. 32, p. 1236-1254, doi:10.1139/e95-101.

Gordey, S.P., 1981, Stratigraphy, structure, and tectonic evolution of the southern Pelly Mountains in the Indigo Lake area, Yukon Territory: Geological Survey of Canada, Bulletin 318, 44 p, doi:10.4095/111359.

Gordey, S.P., 2013, Evolution of the Selwyn Basin region, Sheldon Lake and Tay River map areas, central Yukon: Geological Survey of Canada, Bulletin 599, 176 p, doi:10.4095/293034.

Gordey, S.P., and Anderson, R.G., 1993, Evolution of the northern Cordilleran miogeocline, Nahanni map area (105 I), Yukon and Northwest Territories: Geological Survey of Canada, Memoir 428, 214 p, doi:10.4095/183983.

Grange, M., Schärer, U., Cornen, G., and Girardeau, J., 2008, First alkaline magmatism during Iberia–Newfoundland rifting: Terra Nova, v. 20, p. 494-503, doi:10.1111/j.1365-3121.2008.00847.x.

Grange, M., Schärer, U., Merle, R., Girardeau, J., and Cornen, G., 2010, Plume–lithosphere interaction during migration of Cretaceous alkaline magmatism in SW Portugal: evidence from U–Pb ages and Pb–Sr–Hf isotopes: Journal of Petrology, v. 51, p. 1143-1170, doi:10.1093/petrology/egq018.

Green, T.H., 1995, Significance of Nb/Ta as an indicator of geochemical processes in the crust-mantle system: Chemical Geology, v. 120, p. 347-359, doi:10.1016/0009-2541(94)00145-x.

Green, D.H., Hibberson, W.O., Kovács, I., and Rosenthal, A., 2010, Water and its influence on the lithosphere-asthenosphere boundary: Nature, v. 467, p. 448-451, doi:10.1038/nature09369.

Halliday, A.N., Lee, D.C., Tommasini, S., Davies, G.R., Paslick, C.R., Fitton, J.G., and James, D.E., 1995, Incompatible trace elements in OIB and MORB and source enrichment in the sub-oceanic mantle: Earth and Planetary Science Letters, v. 133, p. 379-395, doi:10.1016/0012-821x(95)00097-v.

Hansen, V.L., Goodge, J.W., Keep, M., and Oliver, D.H., 1993, Asymmetric rift interpretation of the western North American margin: Geology, v. 21, p. 1067–1070, doi:10.1130/0 091-7613(1993)021<1067:ARIOTW>2.3.CO;2.

Harlan, S.S., Heaman, L., LeCheminant, A.N., and Premo, W.R., 2003, Gunbarrel mafic magmatic event: A key 780 Ma time marker for Rodinia plate reconstructions: Geology, v. 31, p. 1053-1056, doi:10.1130/G19944.1.

Hart, C.J.R., 1986, Geology of the Old Cabin Creek Massif, Selwyn Basin, Yukon Territory [B.Sc. thesis]: McMaster University, 135 p.

Hart, S.R., and Blusztajn, J., 2006, Age and geochemistry of the mafic sills, ODP site 1276, Newfoundland margin: Chemical Geology, v. 235, p. 222-237, doi:0.1016/j.chemgeo.2006.07.001.

Hayward, N., 2015, Geophysical investigation and reconstruction of lithospheric structure and its control on geology, structure, and mineralization in the Cordillera of northern Canada and eastern Alaska: Tectonics, v. 34, doi:10.1002/2015TC003871.

Heaman, L.M., LeCheminant, A.N., and Rainbird, R.H., 1992, Nature and timing of Franklin igneous events, Canada: implications for a Late Proterozoic mantle plume and the break-up of Laurentia: Earth and Planetary Science Letters, v. 109, p.117-131, doi:10.1016/0012-821X(92)90078-A.

Hein, F.J., and McMechan, M.E., 1994, Proterozoic and Lower Cambrian strata of the Western Canada sedimentary basin, *in* Mossop, G.D., and Shetsen, I., eds., Geological Atlas of the Western Canada Sedimentary Basin: Canadian Society of Petroleum Geologists and Alberta Research Council, p. 57-67.

Helwig, J., Aronson, J., and Day, D.S., 1974, A Late Jurassic mafic pluton in Newfoundland: Canadian Journal of Earth Sciences, v. 11, p. 1314-1319, doi:10.1139/e74-123.

Hirschmann, M.M., Kogiso, T., Baker, M.B. and Stolper, E.M., 2003, Alkalic magmas generated by partial melting of garnet pyroxenite: Geology, v. 31, p. 481-484, doi:10.1130/0091-7613(2003)031.

Hoffman, P. F., 1988, United plates of America, the birth of a craton: Annual Review of Earth and Planetary Science, v. 16, p. 543-603, doi:10.1146/annurev.earth.16.1.543.

Huismans, R.S., and Beaumont, C., 2014, Rifted continental margins: The case for depth-dependent extension: Earth and Planetary Science Letters, v. 407, p. 148-162, doi:10.1016/j.epsl.2014.09.032.

Humphreys, E.R., and Niu, Y., 2009, On the composition of ocean island basalts (OIB): The effects of lithospheric thickness variation and mantle metasomatism: Lithos, v. 112, p. 118-136, doi:10.1016/j.lithos.2009.04.038.

Ionov, D.A., Ashchepkov, I.V., Stosch, H.G., Witt-Eickschen, G., and Seck, H.A., 1993, Garnet peridotite xenoliths from the Vitim Volcanic Field, Baikal Region: the nature of the garnet—spinel peridotite transition zone in the continental mantle: Journal of Petrology, v. 34, p. 1141-1175, doi:10.1093/petrology/34.6.1141.

Jagoutz, O., Munterer, O., Manatschal, G., Rubatto, D., Peron-Pinvidic, G., Turrin, B.D., and Villa, I.M., 2007, The rift-to-drift transition in the North Atlantic: A stuttering start of the MORB machine?: Geology, v. 35, p. 1087-1090, doi:10.1130/G23613A.1.

Jenner, G.A., 1996, Trace element geochemistry of igneous rocks: geochemical nomenclature and analytical geochemistry, *in* Wyman, D.A., ed., Trace element geochemistry of volcanic rocks: applications for massive sulfide exploration. Geological Association of Canada, Short Course Notes, v. 12, p. 51-77.

Jennings, D.S., and Jilson, G.A., 1986, Geology and sulfide deposits of Anvil Range, Yukon, *in* Morin, J.A., ed., Mineral Deposits of Northern Cordillera Symposium: Canadian Institute of Mining and Metallurgy, Special Paper, v. 37, p. 319–371.

Keen, C. E., Dafoe, L. T., and Dickie, K., 2014, A volcanic province near the western termination of the Charlie-Gibbs Fracture Zone at the rifted margin, offshore northeast Newfoundland: Tectonics, v. 33, p.1133–1153, doi:10.1002/2014TC003547.

Keller, T., Katz, R.F., and Hirschmann, M.M., 2017, Volatiles beneath mid-ocean ridges: Deep melting, channelised transport, focusing, and metasomatism: Earth and Planetary Science Letters, v. 464, p. 55–68, doi:10.1016/j.epsl.2017.02.006.

Kellogg, H.E., 1963, Paleozoic stratigraphy of the southern Egan Range, Nevada: Geological Society of America Bulletin, v. 74, p. 685-708, doi:10.1130/0016-7606(1963)74[685:psotse]2.0.co;2.

Klitgord, K.D., and Schouten, H., 1986, Plate kinematics of the central Atlantic, *in* Vogt, P.R., and Tucholke, B. E., eds., The Western North Atlantic Region: The Geology of North America: The Geological Society of America, p. 351–378, doi:10.1130/dnag-gna-m.351.

Kogiso, T., Hirschmann, M.M., and Frost, D.J., 2003, High-pressure partial melting of garnet pyroxenite: possible mafic lithologies in the source of ocean island basalts: Earth and Planetary Science Letters, v. 216, p. 603-617, doi:10.1016/S0012-821X(03)00538-7.

Kubli, T.E., and Simony, P.S., 1992, The Dogtooth High, northern Purcell Mountains, British Columbia: Bulletin of Canadian Petroleum Geology, v. 40, p. 36-51.

Lavier, L.L., and Manatschal, G., 2006, A mechanism to thin the continental lithosphere at magma-poor margins: Nature, v. 440, p. 324-328, doi:10.1038/nature04608.

LeCheminant, A.N., and Heaman, L.M., 1994, 779 Ma mafic magmatism in the northwestern

    Canadian Shield and northern Cordillera: a new regional time-marker: Eighth International

    Conference on Geochronology, Cosmochronology and Isotope Geology, US Geological

    Survey Circular, Berkeley, California, Abstracts, v. 1107, 197 p.

Leslie, C.D., 2009, Detrital zircon geochronology and rift-related magmatism: central Mackenzie

    Mountains, Northwest Territories [M.Sc. thesis] University of British Columbia, 224 p.

Levy, M, and Christie-Blick, N., 1991, Tectonic subsidence of the early Paleozoic passive

    continental margin in eastern California and southern Nevada: Geological Society of America

    Bulletin, v. 103, p. 1590-1606, doi:10.1130/0016-7606(1991)103<1590:tsotep>2.3.co;2.

Li, Z.X., Bogdanova, S.V., Collins, A.S., Davidson, A., De Waele, B., Ernst, R.E., Fitzsimmons,

    I.C.W., Fuck, R.A., Gladkochub, D.P., Jacobs, J., Karlstrom, K.E., Lu, S., Natapov, L.M.,

    Pease, V., Pisarevsky, S.A., Thrane, K., and Vernikovsky, V., 2008, Assembly,

    configuration, and break-up history of Rodinia: A synthesis: Precambrian Research, v. 160, p.

    179-210, doi:10.1016/j.precamres.2007.04.021.

Lickorish, W.H., and Simony, P.S., 1995, Evidence for late rifting of the Cordilleran margin outlined

    by stratigraphic division of the Lower Cambrian Gog Group, Rocky Mountain Main Ranges,

    British Columbia and Alberta: Canadian Journal of Earth Sciences, v. 32, p. 860-874,

    doi:10.1139/e95-072.

Link, P.K., Christie-Blick, N., Devlin, W.J., Elston, D.P., Horodyski, R.J., Levy, M., Miller, J.M.G., Pearson, R.C., Prave, A., Stewart, J.H., Winston, D., Wright, L.A., and Wrucke, C.T., 1993, Middle and Late Proterozoic stratified rocks of the western U.S. Cordillera, Colorado Plateau, and Basin and Range Province, *in* Reed, J.C., Jr., Bickford, M.E., Houston, R.S., Link, P.K., Rankin, D.W., Sims, P.K., and Van Schmus, W.R., eds., Precambrian: Conterminous U.S.: Boulder, Colorado, Geological Society of America, The Geology of North America, v. C-2, p. 463-595, doi:10.1130/dnag-gna-c2.463.

Link, P.K., Todt, M.K., Pearson, D.M., and Thomas, R.C., 2017, 500–490 Ma detrital zircons in Upper Cambrian Worm Creek and correlative sandstones, Idaho, Montana, and Wyoming: Magmatism and tectonism within the passive margin: Lithosphere, v. 9, p. 910-926, doi:10.1130/l671.1.

Lister, G.S., Etheridge, M.A., and Symonds, P.A., 1986, Detachment faulting and the evolution of passive continental margins: Geology, v. 14, p. 246-250, doi:10.1130/0091-7613(1986)14<246:dfateo>2.0.co;2.

Lister, G.S., Etheridge, M.A., and Symonds, P.A., 1991, Detachment models for the formation of passive continental margins: Tectonics, v. 10, p. 1038-1064, doi:10.1029/90tc01007.

Lloyd, F.E., and Bailey, D., 1975, Light element metasomatism of the continental mantle: the evidence and the consequences: Physics and Chemistry of the Earth, v. 9, p. 389-416, doi:10.1016/b978-0-08-018017-5.50033-x.

Logan, J.M., and Colpron, M., 2006, Stratigraphy, geochemistry, syngenetic sulphide occurrences

    and tectonic setting of the lower Paleozoic Lardeau Group, northern Selkirk Mountains,

    British Columbia, *in* Colpron, M., and Nelson, J.L., eds., Paleozoic Evolution and

    Metallogeny of Pericratonic Terranes at the Ancient Pacific Margin of North America,

    Canadian and Alaskan Cordillera: Geological Association of Canada, Special Paper 45, p.

    361-382, doi:10.2113/gsecongeo.102.3.534.

Ludwig, K.R., 2003, User's manual for Isoplox/Ex, version 3.00, a geochronological toolkit for

    Microsoft Excel: Berkeley Geochronology Center Special Publication 4, 77 p.

Lund, K., 2008, Geometry of the Neoproterozoic and Paleozoic rift margin of western Laurentia:

    Implications for mineral deposit settings: Geosphere, v. 4, p. 429-444,

    doi:10.1130/GES00121.1.

Lund, K., Aleinikoff, J.N., Evans, K.V., and Fanning, C.M., 2003, SHRIMP U-Pb geochronology of

    Neoproterozoic Windermere Supergroup, central Idaho: Implications for rifting of western

    Laurentia and synchroneity of Sturtian glacial deposits: Geological Society of America

    Bulletin, v. 115, p. 349-372, doi:10.1130/0016-7606(2003)115.

Lund, K., Aleinikoff, J.N., Evans, K.V., Dewitt, E.H., and Unruh, D.M., 2010, SHRIMP U-Pb dating

    of recurrent Cryogenian and Late Cambrian–Early Ordovician alkalic magmatism in central

    Idaho: Implications for Rodinian rift tectonics: Geological Society of America Bulletin, v.

    122, p. 430-453, doi:10.1130/B26565.1.

MacDonald, R., Rogers, N.W., Fitton, J.G., Black, S., and Smith, M., 2001, Plume–lithosphere
interactions in the generation of the basalts of the Kenya Rift, East Africa: Journal of
Petrology, v. 42, p. 877-900, doi:10.1093/petrology/42.5.877.

Macdonald, F.A., Schmitz, M.D., Crowley, J.L., Roots, C.F., Jones, D.S., Maloof, A.C., Strauss,
J.V., Cohen, P.A., Johnston, D.T., and Schrag, D.P., 2010, Calibrating the Cryogenian:
Science, v. 327, p. 1241-1243, doi: 10.1126/science.1183325.

Macdonald, F.A., Halverson, G.P., Strauss, J.V., Smith, E.F., Cox, G., Sperling, E.A., and Roots,
C.F., 2012, Early Neoproterozoic Basin Formation in Yukon, Canada: Implications for the
make-up and break-up of Rodinia: Geoscience Canada, v. 39, p. 77–97.

MacIntyre, D.G., 1998, Geology, geochemistry and mineral deposits of the Akie River Area,
northeast British Columbia: British Columbia, Ministry of Energy and Mines, Bulletin 103,
p. 1-91.

MacLean, W.H., and Barrett, T.J., 1993, Lithogeochemical techniques using immobile elements:
Journal of Geochemical Exploration, v. 48, p. 109-133, doi:10.1016/0375-6742(93)90002-4.

Madrid, R.J., 1987, Stratigraphy of the Roberts Mountain allochthon in north-central Nevada [Ph. D.
thesis]: Stanford University, 336 p.

Magwood, J.P.A., and Pemberton, S.G., 1988, Trace fossils of the Gog Group, a lower Cambrian
tidal sand body, Lake Louise, Alberta, *in* Landing, E., Narbonne, G.M., and Myrow, P., eds.,

Trace fossils, small shelly fossils and the Precambrian-Cambrian boundary-proceedings: New York State Museum Bulletin 463, 14 p.

Manatschal, G., and Müntener, O., 2009, A type sequence across an ancient magma-poor ocean–continent transition: the example of the western Alpine Tethys ophiolites: Tectonophysics, v. 473, p. 4-19, doi:10.1016/j.tecto.2008.07.021.

Manatschal, G., Lavier, L., and Chenin, P., 2015, The role of inheritance in structuring hyperextended rift systems: Some considerations based on observations and numerical modeling: Gondwana Research, v. 27, p. 140-164, doi:10.1016/j.gr.2014.08.006.

Marzoli, A., Renne, P.R., Piccirillo, E.M., Ernesto, M., Bellieni, G., and De Min, A., 1999, Extensive 200-million-year-old continental flood basalts of the Central Atlantic Magmatic Province: Science, v. 284, p. 616-618, doi:10.1126/science.284.5414.616.

Masini, E., Manatschal, G., and Mohn, G., 2013, The Alpine Tethys rifted margins: reconciling old and new ideas to understand the stratigraphic architecture of magma-poor rifted margins: Sedimentology, v. 60, 174–196, doi:10.1111/sed.12017.

McDonough, W.F., and Sun, S.S., 1995, The composition of the Earth: Chemical Geology, vol. 120, p. 223-253, doi:10.1016/0009-2541(94)00140-4.

McKenzie, D., 1978, Some remarks on the development of sedimentary basins: Earth and Planetary Science Letters, v. 40, p. 25-32, doi:10.1016/0012-821x(78)90071-7.

McKenzie, D., and Bickle, M.J., 1988, The volume and composition of melt generated by extension

    of the lithosphere: Journal of Petrology, v. 29, p. 625-679, doi:10.1093/petrology/29.3.625.

McMechan, M.E. 1990, Upper Proterozoic to Middle Cambrian history of the Peace River Arch:

    evidence from the Rocky Mountains, *in* O' Connell, S.C., and Bell, J.S., eds., Geology of the

    Peace River Arch: Bulletin of Canadian Petroleum Geology, Special Volume 38A, p. 36-44.

McMechan, M.E., 2012, Deep transverse basement structural control of mineral systems in the

    southeastern Canadian Cordillera: Canadian Journal of Earth Sciences, v. 49, p. 693-708,

    doi:10.1139/e2012-013.

McPhie, J., and Cas, R., 2015, Volcanic Successions Associated with Ore Deposits: Facies

    Characteristics and Ore–Host Relationships, Chapter 49, *in* Sigurdsson, H., ed., The

    Encyclopedia of Volcanoes (Second Edition): Academic Press, Amsterdam, p. 865-879,

    doi:10.1016/b978-0-12-385938-9.00049-3.

Meade, F.C., Chew, D.M., Troll, V.R., Ellam, R.M., and Page, L.M., 2009, Magma ascent along a

    major terrane boundary: crustal contamination and magma mixing at the Drumadoon

    Intrusive complex, Isle of Arran, Scotland: Journal of Petrology, v. 50, p. 2345-2374,

    doi:10.1093/petrology/egp081.

Merle, R., Schärer, U., Girardeau, J., and Cornen, G., 2006, Cretaceous seamounts along the

    continent–ocean transition of the Iberian margin: U–Pb ages and Pb–Sr–Hf isotopes:

    Geochimica et Cosmochimica Acta, v. 70, p. 4950-4976, doi:10.1016/j.gca.2006.07.004.

Merle, R., Jourdan, F., Marzoli, A., Renne, P.R., Grange, M., and Girardeau, J., 2009, Evidence of multi-phase Cretaceous to Quaternary alkaline magmatism on Tore–Madeira Rise and neighbouring seamounts from $^{40}Ar/^{39}Ar$ ages: Journal of the Geological Society, v. 166, p. 879-894, doi:10.1144/0016-76492008-060.

Milidragovic, D., Thorkelson, D.J., and Marshall, D.D., 2006, Geology of the Quartet Mountain lamprophyre suite, Wernecke Mountains, Yukon, *in* Emond, D.S., Bradshaw, G.D., Lewis, L.L., and Weston, L.H., eds., Yukon Exploration and Geology 2005: Yukon Geological Survey, p. 231-245.

Millonig, L.J., Gerdes, A., and Groat, L.A., 2012, U–Th–Pb geochronology of meta-carbonatites and meta-alkaline rocks in the southern Canadian Cordillera: a geodynamic perspective: Lithos, v. 152, p. 202-217, doi:10.1016/j.lithos.2012.06.016.

Miranda, R., Valadares, V., Terrinha, P., Mata, J., do Rosario Azevedo, M., Gaspar, M., Kullberg, J.C., and Ribeiro, C., 2009, Age constraints on the Late Cretaceous alkaline magmatism on the West Iberian Margin: Cretaceous Research, v. 30, p. 575-586, doi:10.1016/j.cretres.2008.11.002.

Moore, J.G., 1975, Mechanism of formation of pillow lava: pillow lava, produced as fluid lava cools underwater, is the most abundant volcanic rock on earth, but only recently have divers observed it forming: American Scientist, vol. 63, no. 3, p. 269-277.

Morgan, W.J., 1971, Convection plumes in the lower mantle: Nature, v. 230, p. 42-43, doi:10.1038/230042a0.

Morris, H.T., and Lovering, T.S., 1961, Stratigraphy of the east Tintic Mountains, Utah: United States Geological Survey Professional Paper 361, 145 p.

Mott, J.A., 1989, Structural and stratigraphic relations in the White River region, eastern Main Ranges, southern Rocky Mountains, British Columbia [Ph.D. thesis]: Queen's University, 404 p.

Moynihan, D., 2014, Bedrock Geology of NTS 106B/04, Eastern Rackla Belt, *in* MacFarlane, K.E., Nordling, M.G., and Sack, P.J., eds., Yukon Exploration and Geology 2013: Yukon Geological Survey, p. 147-167.

Müntener, O., and Manatschal, G., 2006, High degrees of melt extraction recorded by spinel harzburgite of the Newfoundland margin: The role of inheritance and consequences for the evolution of the southern North Atlantic: Earth and Planetary Science Letters, v. 252, p. 437-452, doi:10.1016/j.epsl.2006.10.009.

Müntener, O., Manatschal, G., Desmurs, L., and Pettke, T., 2010, Plagioclase peridotites in ocean–continent transitions: refertilized mantle domains generated by melt stagnation in the shallow mantle lithosphere: Journal of Petrology, v. 51, p. 255-294, doi:10.1093/petrology/egp087.

Murphy, D.C., 1997, Geology of the McQuesten River Region, northern McQuesten and Mayo Map Areas, Yukon Territory (115P/14, 15, 16; 105M/13, 14): Yukon Geological Survey, Bulletin 6, 95 p.

Murton, B.J., Peate, D.W., Arculus, R.J., Pearce, J.A., and Van der Laan, S., 1992, Trace-element geochemistry of volcanic rocks from site 786: The Izu-Bonin Forearc: Proceedings of the Ocean Drilling Program Scientific Results, v. 125, p. 211-235, doi:10.2973/odp.proc.sr.125.133.1992.

Narbonne, G. M., and Aitken, J. D., 1995, Neoproterozoic of the Mackenzie Mountains, northwestern Canada: Precambrian Research, v. 73, p, 101-121, doi:10.1016/0301-9268(94)00073-Z.

Naylor, P.H., Bell, B.R., Jolley, D.W., Durnall, P., and Fredsted, R., 1999, Palaeogene magmatism in the Faeroe–Shetland Basin: influences on uplift history and sedimentation, *in* Fleet, A.J., and Boldy, S.A.R., eds., Petroleum Geology of Northwest Europe: Proceedings of the 5th Conference: Geological Society, London, p. 545-558, doi:10.1144/0050545

Nelson, J.L., Colpron, M., and Israel, S., 2013, The Cordillera of British Columbia, Yukon, and Alaska: Tectonics and metallogeny, *in* Colpron, M., Bissing, T., Rusk, B.G., and Thompson, J.F.H., eds., Tectonics, Metallogeny, and Discovery: The North American Cordillera and Similar Accretionary Settings: Society of Economic Geologists Special Publication 17, p. 53-109.

Niu, Y., and O'Hara, M.J., 2007, Global correlations of ocean ridge basalt chemistry with axial depth: a new perspective: Journal of Petrology, v. 49, p.633-664, doi:10.1093/petrology/egm051.

Niu, Y., Wilson, M., Humphreys, E.R., and O'Hara, M.J., 2011, The origin of intra-plate ocean island basalts (OIB): the lid effect and its geodynamic implications: Journal of Petrology, v. 52, p. 1443-1468, doi:10.1093/petrology/egr030.

Niu, Y., Wilson, M., Humphreys, E.R., and O'Hara, M.J., 2012, A trace element perspective on the source of ocean island basalts (OIB) and fate of subducted ocean crust (SOC) and mantle lithosphere (SML): Episodes, v. 35, p. 310-327, doi:10.1093/petrology/egr030.

Nomade, S., Knight, K.B., Beutel, E., Renne, P.R., Verati, C., Féraud, G., Marzoli, A., Youbi, N., and Bertrand, H., 2007, Chronology of the Central Atlantic Magmatic Province: Implications for the Central Atlantic rifting processes and the Triassic–Jurassic biotic crisis: Palaeogeography, Palaeoclimatology, Palaeoecology, v. 244, p. 326-344, doi:10.1016/j.palaeo.2006.06.034.

Norford, B.S., 1990, Ordovician and Silurian stratigraphy, paleogeography and depositional history in the Peace River Arch area, Alberta and British Columbia: Bulletin of Canadian Petroleum Geology, v. *38*, p. 45-54.

Norford, B.S., and Cecile, M.P., 1994, Ordovician emplacement of the Mount Dingley Diatreme, western ranges of the Rocky Mountains, southeastern British Columbia: Canadian Journal of Earth Sciences, v. 31, p. 1491-1500, doi:10.1139/e94-132.

O'Reilly, B.M., Hauser, F., Ravaut, C., Shannon, P.M., and Readman, P.W., 2006, Crustal thinning, mantle exhumation and serpentinization in the Porcupine Basin, offshore Ireland: evidence

from wide-angle seismic data: Journal of the Geological Society, v. 163, p. 775-787, doi:10.1144/0016-76492005-079.

O'Nions, R.K., Evensen, N.M., and Hamilton, P.J., 1979, Geochemical modeling of mantle differentiation and crustal growth: Journal of Geophysical Research, Solid Earth, v.84, p. 6091-6101, doi:10.1029/jb084ib11p06091.

Ootes, L., Gleeson, S.A., Turner, E., Rasmussen, K., Gordey, S., Falck, H., Martel, E., and Pierce, K., 2013, Metallogenic evolution of the Mackenzie and eastern Selwyn Mountains of Canada's Northern Cordillera, Northwest Territories: A compilation and review: Geoscience Canada, v. 40, p. 40–69, doi:10.12789/geocanj.2013.40.005.

Paradis, S., Bailey, S.L., Creaser, R.A., Piercey, S.J., Schiarizza, P., Colpron, M., and Nelson, J.L., 2006, Paleozoic magmatism and syngenetic massive sulphide deposits of the Eagle Bay assemblage, Kootenay terrane, southern British Columbia, *in* Colpron, M., and Nelson, J.L., eds., Paleozoic evolution and metallogeny of pericratonic terranes at the ancient Pacific margin of North America, Canadian and Alaskan Cordillera: Geological Association of Canada Special Paper, 45, p. 383-414, doi:10.2113/gsecongeo.102.3.534.

Parrish, R.R., and Reichenbach, I., 1991, Age of xenocrystic zircon from diatremes of western Canada: Canadian Journal of Earth Sciences, v. 28, p. 1232-1238, doi:10.1139/e91-110.

Patchett, P.J., and Tatsumoto, M., 1981, A routine high-precision method for Lu-Hf isotope geochemistry and chronology: Contributions to Mineralogy and Petrology, v. 75, p. 263-267, doi:10.1007/bf01166766.

Pe-Piper, G., Piper, D.J.W., Jansa, L.F., and de Jonge, A., 2007, Early Cretaceous opening of the North Atlantic Ocean: Implications of the petrology and tectonic setting of the Fogo Seamounts off the SW Grand Banks, Newfoundland: Geological Society of America Bulletin, v. 119, p. 712-724, doi:10.1130/B26008.1.

Pe-Piper, G., Meredyk, S., Zhang, Y., Piper, D.J., and Edinger, E., 2013, Petrology and tectonic significance of seamounts within transitional crust east of Orphan Knoll, offshore eastern Canada: Geo-Marine Letters, v. 33, p. 433-447, doi:10.1007/s00367-013-0342-2.

Pearce, J.A., 1996, A user's guide to basalt discrimination diagrams. Trace element geochemistry of volcanic rocks: applications for massive sulphide exploration: Geological Association of Canada, Short Course Notes, v. 12, 113 p.

Pearce, J.A., and Cann, J.R., 1973, Tectonic setting of basic volcanic rocks determined using trace element analyses: Earth and Planetary Science Letters, v. 19, p. 290-300, doi:10.1016/0012-821x(73)90129-5.

Pearce, J.A., and Peate, D.W., 1995, Tectonic implications of the composition of volcanic arc magmas: Annual Review of Earth and Planetary Sciences, v. 23, p. 251-285, doi:10.1146/annurev.ea.23.050195.001343.

Pecha, M.E., Gehrels, G.E., McClelland, W.C., Giesler, D., White, C., and Yokelson, I., 2016, Detrital zircon U-Pb geochronology and Hf isotope geochemistry of the Yukon-Tanana

terrane, Coast Mountains, southeast Alaska: *Geosphere*, v. 12, p. 1556–1574, doi:10.1130/GES01303.1.

Pell, J. 1987, Alkaline ultrabasic rocks in British Columbia: carbonatites, nepheline syenites, kimberlites, ultramafic lamprophyres and related rocks: British Columbia Ministry of Energy, Mines, and Petroleum Resources, Geological Survey Branch, Open File 1987-17, p. 259-272.

Pell, J. 1994, Carbonatites, nepheline syenites, kimberlites and related rocks in British Columbia: British Columbia Ministry of Energy, Mines and Petroleum Resources, Geological Survey Branch, Bulletin 88, 136 p.

Peron-Pinvidic, G., and Manatschal, G., 2009, The final rifting evolution at deep magma-poor passive margins from Iberia-Newfoundland: a new point of view: International Journal of Earth Sciences, v. 98, p. 1581-1597, doi:10.1007/s00531-008-0337-9.

Peron-Pinvidic, G., and Manatschal, G., 2010, From microcontinents to extensional allochthons: witnesses of how continents rift and break apart?: Petroleum Geoscience, v. 16, p. 189-197, doi:10.1144/1354-079309-903.

Peron-Pinvidic, G., Manatschal, G., Minshull, T.A., and Sawyer, D.S., 2007, Tectonosedimentary evolution of the deep Iberia-Newfoundland margins: Evidence for a complex breakup history: Tectonics, v. 26, doi:10.1029/2006TC001970.

Peron-Pinvidic, G., Manatschal, G., and Osmundsen, P.T., 2013, Structural comparison of archetypal
Atlantic rifted margins: A review of observations and concepts: Marine and Petroleum
Geology, v. 43, p. 21-47, doi:10.1016/j.marpetgeo.2013.02.002.

Piercey, S.J., and Colpron, M., 2009, Composition and provenance of the Snowcap assemblage,
basement to the Yukon-Tanana terrane, northern Cordillera: Implications for Cordilleran
crustal growth: Geosphere, v. 5, p. 439-464, doi:10.1130/GES00505.1.

Piercey, S.J., Mortensen, J.K., Murphy, D.C., Paradis, S., and Creaser, R.A., 2002, Geochemistry
and tectonic significance of alkalic mafic magmatism in the Yukon-Tanana terrane, Finlayson
Lake region, Yukon: Canadian Journal of Earth Sciences, v. 39, p. 1729-1744,
doi:10.1139/e02-090.

Piercey, S.J., Murphy, D.C., Mortensen, J.K., and Creaser, R.A., 2004, Mid-Paleozoic initiation of
the northern Cordilleran marginal backarc basin: Geologic, geochemical, and neodymium
isotope evidence from the oldest mafic magmatic rocks in the Yukon-Tanana terrane,
Finlayson Lake district, southeast Yukon, Canada: Geological Society of America Bulletin, v.
116, p. 1087-1106, doi:10.1130/B25162.1.

Piercey, S.J., Nelson, J.L., Colpron, M., Dusel-Bacon, C., Simard, R.L., and Roots, C.F., 2006,
Paleozoic magmatism and crustal recycling along the ancient Pacific margin of North
America, northern Cordillera, *in* Colpron, M., and Nelson, J.L., eds., Paleozoic evolution and
metallogeny of pericratonic terranes at the ancient Pacific margin of North America,
Canadian and Alaskan Cordillera: Geological Association of Canada Special Paper, 45, p.
281-322, doi:10.2113/gsecongeo.102.3.534.

Piercey, S.J., Murphy, D.C., and Creaser, R.A., 2012, Lithosphere-asthenosphere mixing in a

transform-dominated late Paleozoic backarc basin: Implications for northern Cordilleran

crustal growth and assembly: Geosphere, v. 8, p. 716–739, doi:10.1130/GES00757.1

Pigage, L.C., 2004, Bedrock geology compilation of the Anvil District (parts of NTS 105K/2, 3, 4, 5,

6, 7 and 11), central Yukon: Yukon Geological Survey, Bulletin 15, 103 p.

Pigage, L.C., 2009, Bedrock geology of NTS 95C/5 (Pool Creek) and NTS 95D/8 map sheets,

southeast Yukon: Yukon Geological Survey, Bulletin 16, 150 p.

Pigage, L.C., and Mortensen, J.K., 2004, Superimposed Neoproterozoic and early Tertiary alkaline

magmatism in the La Biche River area, southeast Yukon Territory: Bulletin of Canadian

Petroleum Geology, v. 52, p. 325-342, doi:10.2113/52.4.325.

Pigage, L.C., Crowley, J.L., Pyle, L.J., Abbott, J.G., Roots, C.F., and Schmitz, M.D., 2012, U–Pb

zircon age of an Ordovician tuff in southeast Yukon: implications for the age of the

Cambrian–Ordovician boundary: Canadian Journal of Earth Sciences, v. 49, p. 732-741,

doi:10.1139/e2012-017.

Pigage, L.C., Roots, C.F., and Abbott, J.G., 2015, Regional bedrock geology for Coal River map area

(NTS 95D), southeast Yukon: Yukon Geological Survey, Bulletin 17, 155 p.

Post, R.T., and Long, D.G., 2008, The middle Cambrian Mount Roosevelt Formation (new) of

    northeastern British Columbia: evidence for rifting and development of the Kechika graben

    system: Canadian Journal of Earth Sciences, v. 45, p. 483-498, doi:10.1139/E08-014.

Prave, A.R., 1999, Two diamictites, two cap carbonates, two δ13C excursions, two rifts: the

    Neoproterozoic Kingston Peak Formation, Death Valley, California: Geology, v. 27, p. 339-

    342, doi:10.1130/0091-7613(1999)027<0339:tdtcct>2.3.co;2.

Price, R.C., Gray, C.M., Wilson, R.E., Frey, F.A., and Taylor, S.R., 1991, The effects of weathering

    on rare-earth element, Y and Ba abundances in Tertiary basalts from southeastern Australia:

    Chemical Geology, v. 93, p. 245-265, doi:10.1016/0009-2541(91)90117-a.

Pyle, L.J., 2012, Cambrian and Lower Ordovician Sauk Megasequence of northwestern Canada,

    northern Rocky Mountains to the Beaufort Sea: American Association of Petroleum

    Geologists Memoir, v. 98, p. 675–723, doi:10.1306/13331661M983511.

Pyle, L.J., and Barnes, C.R., 2000, Upper Cambrian to Lower Silurian stratigraphic framework of

    platform-to-basin facies, northeastern British Columbia: Bulletin of Canadian Petroleum

    Geology, v. 48, p. 123-149, doi:10.2113/48.2.123.

Pyle, L.J., and Barnes, C.R., 2001, Conodonts from the Kechika Formation and Road River Group

    (Lower to Upper Ordovician) of the Cassiar Terrane, northern British Columbia: Canadian

    Journal of Earth Sciences, v. 38, p. 1387-1401, doi:10.1139/e01-033.

Pyle, L.J., and Barnes, C.R., 2003, Lower Paleozoic stratigraphic and biostratigraphic correlations in the Canadian Cordillera: implications for the tectonic evolution of the Laurentian margin: Canadian Journal of Earth Sciences, v. 40, p. 1739-1753, doi:10.1139/e03-049.

Read, B.C., 1980, Lower Cambrian archaeocyathid buildups, Pelly Mountains, Yukon: Geological Survey of Canada, Paper 78, 54 p, doi:10.4095/106346.

Roots, C.F. 1988, Cambro-Ordovician volcanic rocks in the eastern Dawson map area, Ogilvie mountains, Yukon, *in* Abbott, G., ed., Yukon Geology, v. 2: Indian and Northern Affairs Canada, Geology Section, Whitehorse, Yukon. p. 81-87.

Roots, C.F., and Thompson, R.I., 1992, Long-lived basement weak zones and their role in extensional magmatism in the Ogilvie Mountains, Yukon Territory, *in* Bartholomew, M.J., Hyndman, D.W., Mogk, D.W., and Mason, R., eds., Basement Tectonics and Characterization of Ancient and Mesozoic Continental Margins: Proceedings of the 8th International Conference in Basement Tectonics: Dordrecht, Kluwer Academic Publishers, p. 359-372, doi:10.1007/978-94-011-1614-5_24.

Ross, G.M., Villeneuve, M.E., and Theriault, R.J., 2001, Isotopic provenance of the lower Muskwa assemblage (Mesoproterozoic, Rocky Mountains, British Columbia): New clues to correlation and source areas: Precambrian Research, v. 111, p. 57-77, doi:10.1016/s0301-9268(01)00156-5.

Rychert, C.A., Fischer, K.M., and Rondenay, S., 2005, A sharp lithosphere–asthenosphere boundary imaged beneath eastern North America: Nature, v. 436, p. 542-545, doi:10.1038/nature03904.

Sandeman, H.A., Ootes, L., Cousens, B., and Kilian, T., 2014, Petrogenesis of Gunbarrel magmatic

    rocks: Homogeneous continental tholeiites associated with extension and rifting of

    Neoproterozoic Laurentia: Precambrian Research, v. 252, p. 166-179,

    doi:10.1016/j.precamres.2014.07.007.

Schärer, U., Girardeau, J., Cornen, G., and Boillot, G., 2000, 138–121 Ma asthenospheric

    magmatism prior to continental break-up in the North Atlantic and geodynamic implications:

    Earth and Planetary Science Letters, v. 181, p. 555-572, doi:10.1016/S0012-821X(00)00220-

    X.

Schmerr, N., 2012, The Gutenberg discontinuity: Melt at the lithosphere-asthenosphere boundary:

    Science, v. 335, p. 1480-1483: doi:10.1126/science.1215433.

Schmitz, M.D., and Schoene, B., 2007, Derivation of isotope ratios, errors, and error correlations for

    U-Pb geochronology using 205Pb-235U-(233U)-spiked isotope dilution thermal ionization

    mass spectrometric data: Geochemistry, Geophysics, Geosystems, v. 8,

    doi:10.1029/2006GC001492.

Scoates, J.S., and Friedman, R.M., 2008, Precise age of the platiniferous Merensky Reef, Bushveld

    Complex, South Africa, by the U-Pb zircon chemical abrasion ID-TIMS technique:

    Economic Geology, v. 103, p. 465-471, doi:0.2113/gsecongeo.103.3.465.

Shervais, J.W., 1982, Ti-V plots and the petrogenesis of modern and ophiolitic lavas: Earth and

    Planetary Science Letters, v. 59, p. 101-118, doi:10.1016/0012-821x(82)90120-0.

Simpson, K., and McPhie, J., 2001, Fluidal-clast breccia generated by submarine fire fountaining, Trooper Creek Formation, Queensland, Australia: Journal of Volcanology and Geothermal research, vol. 109, p. 339-355, doi:10.1016/s0377-0273(01)00199-8.

Skilling, I.P., White, J.D.L., and McPhie, J., 2002, Peperite: a review of magma-sediment mingling: Journal of Volcanology and Geothermal Research, v. 114, p. 1-17, doi:10.1016/s0377-0273(01)00278-5.

Smith, M.T., and Gehrels, G.E., 1992, Stratigraphic comparison of the Lardeau and Covada groups: implications for revision of stratigraphic relations in the Kootenay Arc: Canadian Journal of Earth Sciences, v. 29, p. 1320-1329, doi:10.1139/e92-105.

Soares, D.M., Alves, T.M., and Terrinha, P., 2012, The breakup sequence and associated lithospheric breakup surface: Their significance in the context of rifted continental margins (West Iberia and Newfoundland margins, North Atlantic): Earth and Planetary Science Letters, v. 355, p. 311-326, doi:10.1016/j.epsl.2012.08.036.

Sobolev, A.V., Hofmann, A.W., Sobolev, S.V., and Nikogosian, I.K., 2005, An olivine-free mantle source of Hawaiian shield basalts: Nature, v. 434, p. 590-597, doi:10.1038/nature03411.

Souther, J.G., 1991, Volcanic regimes, *in* Gabrielse, H., and Yorath, C.J., eds., Geology of the Cordilleran orogen in Canada: Geological Survey of Canada, Geology of Canada, no. 4, p. 459–490, doi:10.4095/134069.

Spitz, G., and Darling, R., 1978, Major and minor element lithogeochemical anomalies surrounding

    the Louvem copper deposit, Val d'Or, Quebec: Canadian Journal of Earth Sciences, v. 157, p.

    1161-1169, doi:10.1139/e78-122.

Stewart, J.H., 1972, Initial deposits in the Cordilleran geosyncline: Evidence of a late Precambrian (<

    850 my) continental separation: Geological Society of America Bulletin, v. 83, p. 1345-1360,

    doi:10.1130/0016-7606(1972)83[1345:iditcg]2.0.co;2.

Stewart, J.H., and Suczek, C.A., 1977, Cambrian and latest Precambrian paleogeography and

    tectonics in the western United States, *in* Stewart, J.H., Stevens, C.H., and Fritsche, A.E.,

    eds., Paleozoic Paleogeography of the Western United States: Society of Economic

    Paleontologists and Mineralogists, Pacific section, Pacific Coast Paleogeography Symposium

    l, p. 1-17.

Strauss, J.V., Macdonald, F.A., Halverson, G.P., Tosca, N.J., Schrag, D.P., and Knoll, A.H., 2015.

    Stratigraphic evolution of the Neoproterozoic Callison Lake Formation: Linking the break-up

    of Rodinia to the Islay carbon isotope excursion: American Journal of Science, v. 315, p.

    881-944, doi:10.2475/10.2015.01

Strong, D.F., and Harris, A., 1974, The petrology of Mesozoic alkaline intrusives of central

    Newfoundland: Canadian Journal of Earth Sciences, v. 11, p. 1208-1219, doi:10.1139/e74-

    114.

Sullivan, K.D., and Keen, C.E., 1977, Newfoundland Seamounts: Petrology and geochemistry, *in* Baragar, W.R.A., Coleman, L.C., and Hall, J.M., eds., Volcanic Regimes in Canada: Geological Association of Canada Special Paper 16, p. 461–476.

Sun, S.S., and McDonough, W.S., 1989, Chemical and isotopic systematics of oceanic basalts: implications for mantle composition and processes: Geological Society, London, Special Publications, v. 42, p. 313-345, doi:10.1144/gsl.sp.1989.042.01.19.

Sykes, L.R., 1978, Intraplate seismicity, reactivation of preexisting zones of weakness, alkaline magmatism, and other tectonism postdating continental fragmentation: Reviews of Geophysics, v. 16, p. 621-688, doi:10.1029/rg016i004p00621.

Taylor, G.C., and Stott, D.F., 1973, Tuchodi Lakes map-area, British Columbia (94K): Geological Survey of Canada, Memoir 373. 37 p, doi:10.4095/102437.

Tempelman-Kluit, D.J., 2012, Geology of Quiet Lake and Finlayson Lake map areas, south-central Yukon: An early interpretation of bedrock stratigraphy and structure: Geological Survey of Canada, Open File 5487, 103 p, doi:10.4095/291931.

Thirwall, M.F., 2000, Inter-laboratory and other errors in Pb isotope analyses investigated using a ^{207}Pb-^{204}Pb double spike: Chemical Geology, v. 163, p. 299-322, doi:10.1016/S0009-2541(99)00135-7.

Thomas, W.A., 2006, Tectonic inheritance at a continental margin: GSA Today, v. 16, p. 4-11, doi:10.1130/1052-5173(2006)016[4:tiaacm]2.0.co;2.

Thompson, R.I., and Roots, C.F., 1982, Ogilvie Mountains project, Yukon: a new regional mapping

    program: Current Research, Part A, Geological Survey of Canada Paper, p. 403-411,

    doi:10.4095/111324.

Thorkelson, D. J., 2000, Geology and mineral occurrences of the Slats Creek, Fairchild Lake and

    "Dolores Creek" areas, Wernecke Mountains 106D/16, 106C/13, 106C/14, Yukon Territory:

    Exploration and Geological Services Division, Yukon, Indian and Northern Affairs

    Canada. Bulletin, v.10, 73 p.

Thorkelson, D.J., Laughton, J.R., Hunt, J.A., and Baker, T., 2003, Geology and mineral occurrences

    of the Quartet Lakes map area (NTS 106E/1), Wernecke and Mackenzie mountains, Yukon,

    in Emond D.S., and Lewis L.L., eds., Yukon Exploration and Geology 2002: Exploration and

    Geological Services Division, Yukon Region, Indian and Northern Affairs Canada, p. 223-

    239.

Tosdal, R.M., Wooden, J.L., and Kistler, R.W., 2000, Inheritance of Nevadan mineral belts from

    Neoproterozoic continental breakup, *in* Cluer, J.K., Price, J.G., Struhsacker, E.M., Hardyman,

    R.F., and Morris, C.L., eds., Geology and ore deposits 2000: The Great Basin and beyond:

    Geological Society of Nevada Symposium Proceedings, May 15–18, 2000: Reno, Nevada,

    Geological Society of Nevada: v. 1, p. 451–466.

Tucholke, B.E., Sawyer, D.S., and Sibuet, J.C., 2007, Breakup of the Newfoundland-Iberia rift, *in*

    Karner, G.D., Manatschal, G., and Pinheiro, L.M., eds., Imaging, Mapping, and Modelling

Continental Lithosphere Extension and Breakup: Geological Society, London, Special Publication 282, p. 9–46, doi:10.1144 /SP282.2.

Turner, E. C., 2011, Stratigraphy of the Mackenzie Mountains supergroup in the Wernecke Mountains, Yukon, *in* MacFarlane, K. E., Weston, L. H., and Relf, C., eds., Yukon Exploration and Geology 2010: Whitehorse, Yukon, Yukon Geological Survey, p. 207-231.

Turner, E. C., and Long, D. G. F., 2008, Basin architecture and syndepositional fault activity during deposition of the Neoproterozoic Mackenzie Mountains supergroup: Canadian Journal of Earth Sciences, v. 45, p. 1159-1184, doi:10.1139/e08-062.

Turner, R.J., Madrid, R.J., and Miller, E.L., 1989, Roberts Mountains allochthon: Stratigraphic comparison with lower Paleozoic outer continental margin strata of the northern Canadian Cordillera: Geology, v. 17, p. 341-344, doi:10.1130/0091-7613(1989)017<0341:rmascw>2.3.co;2.

Unternehr, P., Peron-Pinvidic, G., Manatschal, G., and Sutra E., 2010, Hyper-extended crust in the South Atlantic: in search of a model: *Petroleum Geoscience*, v.16 p. 207–215, doi:10.1144/1354-079309-904.

Verati, C., Rapaille, C., Féraud, G., Marzoli, A., Bertrand, H., and Youbi, N., 2007, 40 Ar/39 Ar ages and duration of the Central Atlantic Magmatic Province volcanism in Morocco and Portugal and its relation to the Triassic–Jurassic boundary: Palaeogeography, Palaeoclimatology, Palaeoecology, v. 244, p. 308-325, doi:10.1016/j.palaeo.2006.06.033.

Vervoort, J.D., and Blichert-Toft, J., 1999, Evolution of the depleted mantle: Hf isotope evidence

    from juvenile rocks through time: Geochimica et Cosmochimica Acta, v. 63, p. 533-556,

    doi:10.1016/s0016-7037(98)00274-9.

Yonkee, W.A., Dehler, C.D., Link, P.K., Balgord, E.A., Keeley, J.A., Hayes, D.S., Wells, M.L.,

    Fanning, C.M., and Johnston, S.M., 2014, Tectono-stratigraphic framework of

    Neoproterozoic to Cambrian strata, west-central US: Protracted rifting, glaciation, and

    evolution of the North American Cordilleran margin: Earth-Science Reviews, v. 136, p. 59-

    95, doi:10.1016/j.earscirev.2014.05.004.

Warren, M.J., 1997, Crustal extension and subsequent crustal thickening along the Cordilleran rifted

    margin of ancestral North America, western Purcell Mountains, southeastern British

    Columbia [Ph.D. thesis]: Queen's University, 361 p.

Watkins, R., and Browne, Q.J., 1989, An Ordovician continental-margin sequence of turbidite and

    seamount deposits in the Roberts Mountain allochthon, Independence Range, Nevada:

    Geological Society of America Bulletin, v. 101, p. 731-741, doi:10.1130/0016-

    7606(1989)101<0731:AOCMSO>2.3.CO;2.

Weis, D., Kieffer, B., Maerschalk, C., Barling, J., de Jong, J., Williams, G.A., Hanano, D., Pretorius,

    W., Mattielli, N., Scoates, J.S., and Goolaerts, A., 2006, High-precision isotopic

    characterization of USGS reference materials by TIMS and MC-ICP-MS: Geochemistry,

    Geophysics, Geosystems, v. 7, doi:10.1029/2006GC001283.

Weis, D., Kieffer, B., Hanano, D., Nobre Silva, I., Barling, J., Pretorius, W., Maerschalk, C., and Mattielli, N., 2007, Hf isotope compositions of US Geological Survey reference materials: Geochemistry, Geophysics, Geosystems, v. 8, doi:10.1029/2006GC001473.

Wernicke, B., 1981, Low-angle normal faults in the Basin and Range Province: nappe tectonics in an extending orogen: Nature, v. 291, p. 645-648, doi:10.1038/291645a0.

Wernicke, B., 1985, Uniform-sense normal simple shear of the continental lithosphere: Canadian Journal of Earth Sciences, v. 22, p. 108-125, doi:10.1139/e85-009.

Whitmarsh, R.B., White, R.S., Horsefield, S.J., Sibuet, J.C., Recq, M., and Louvel, V., 1996, The ocean-continent boundary off the western continental margin of Iberia: Crustal structure west of Galicia Bank: Journal of Geophysical Research: Solid Earth, v. 101, p. 28291-28314, doi:10.1029/96jb02579.

Winchester, J.A., and Floyd, P.A., 1977, Geochemical discrimination of different magma series and their differentiation products using immobile elements: Chemical Geology, v. 20, p. 325-343, doi:10.1016/0009-2541(77)90057-2.

Whitmarsh, R.B., Manatschal, G., and Minshull, T.A., 2001, Evolution of magma-poor continental margins from rifting to seafloor-spreading: Nature, v. 413, p. 150-154, doi:10.1038/35093085.

Wood, B.J., Kiseeva, E.S., and Matzen, A.K., 2013, Garnet in the Earth's Mantle: Elements, v. 9, p. 421-426, doi:10.2113/gselements.9.6.421.

Zwanzig, H.V., 1973, Structural transition between the foreland zone and the core zone of the

Columbian orogen, Selkirk Mountains, British Columbia [Ph.D. thesis]: Kingston, Ontario,

Queen's University, 158 p.

Appendices

Appendix 1 – Compilation of Ediacaran-early Paleozoic magmatic ages and stratigraphic

relationships

Appendix 2 – CA-TIMS zircon U-Pb isotopic results

Appendix 3 – Whole-rock major and trace element geochemical results

Appendix 4 – Whole-rock Nd-Hf isotope geochemical results

Appendix 1

Compilation of Ediacaran-early Paleozoic magmatic ages shown in Figure 1-1B and 3-1B.

Location 1

Dempster Volcanics (Rabbitkettle Fm.)

Middle Cambrian-Ordovician

Abbott, G., 1997, Geology of the Upper Hart River Area, Eastern Ogilvie Mountains, Yukon Territory 116A/10, 116A/11: Exploration and Geological Services Division, Yukon, Indian and Northern Affairs Canada, Bulletin 9, 92 p.

Green, L.H., 1972, Geology of Nash Creek, Larsen Creek, and Dawson map-areas, Yukon Territory: Geological Survey of Canada, Memoir 364, doi:10.4095/100697.

Pigage, L.C., Roots, C.F., and Abbott, J.G., 2015, Regional bedrock geology for Coal River map area (NTS 95D), southeast Yukon: Yukon Geological Survey, Bulletin 17, 155 p.

Roots, C.F. 1988, Cambro-Ordovician volcanic rocks in the eastern Dawson map area, Ogilvie mountains, Yukon, in Abbott, G., ed., Yukon Geology, Indian and Northern Affairs Canada, Geology Section, Whitehorse, Yukon. p. 81-87.

Strauss, J.V., Marmrol, P.J., Crowley, J.L., Colpron, M., King, J.D., Kamerer, W.T., and Taylor, J.F., 2016, Middle Cambrian extensional tectonism in Yukon, Canada: New age constraints and lithogeochemistry from the Dempster volcanics: American Geophysical Union Fall Meeting Abstracts, http://adsabs.harvard.edu/abs/2016AGUFM.T11B2612S

Location 2

Gull Lake Formation mafic volcanic mbr.

Cambrian

Abbott, G., 1997, Geology of the Upper Hart River Area, Eastern Ogilvie Mountains, Yukon Territory 9116A/10, 116A/11: Exploration and Geological Services Division, Yukon, Indian and Northern Affairs Canada, Bulletin 9, 92 p.

Nash volcanics

Middle Ordovician-Silurian

Abbott, G., 1997, Geology of the Upper Hart River Area, Eastern Ogilvie Mountains, Yukon Territory 9116A/10, 116A/11: Exploration and Geological Services Division, Yukon, Indian and Northern Affairs Canada, Bulletin 9, 92 p.

Green, L.H., 1972, Geology of Nash Creek, Larsen Creek, and Dawson map-areas, Yukon Territory: Geological Survey of Canada, Memoir 364, doi:10.4095/100697.

Dempster Volcanics
Cambrian-Ordovician

Abbott, G., 1997, Geology of the Upper Hart River Area, Eastern Ogilvie Mountains, Yukon Territory 9116A/10, 116A/11: Exploration and Geological Services Division, Yukon, Indian and Northern Affairs Canada, Bulletin 9, 92 p.

Location 3

Quartet Mountain suite lamprophyre
Upper Cambrian (ca. 532-522 Ma)

Milidragovic, D., Thorkelson, D.J., and Marshall, D.D., 2006, Geology of the Quartet Mountain lamprophyre suite, Wernecke Mountains, Yukon, *in* Emond, D.S., Bradshaw, G.D., Lewis, L.L., and Weston, L.H., eds., Yukon Exploration and Geology 2005: Yukon Geological Survey, p. 231-245.

Location 4

Old Cabin Formation (Craig Volcanics)
Middle Cambrian-Silurian

Moynihan, D., 2014, Bedrock Geology of NTS 106B/04, Eastern Rackla Belt, *in* K.E. MacFarlane, M.G. Nordling, and P.J. Sack., eds., Yukon Exploration and Geology 2013: Yukon Geological Survey, p. 147-167.

Tempelman-Kluit, D.J., 1981, Description of the Craig claim: Yukon geology and exploration 1979 -80, Indian and Northern Affairs Canada, Geology Section, Whitehorse, Yukon, p. 225 - 230.

Location 5

Marmot Formation (Arctic Red Volcanics/Porter Puddle/Duo lakes Formation)

Middle to Upper Ordovician (ca. 460-444 Ma)

Cecile, M.P., Fritz, W.H., Norford, B.S., and Tipnis, R.S., 1982, The Lower Paleozoic Misty Creek Embayment, Selwyn Basin, Yukon and Northwest Territories: Geological Survey of Canada, Bulletin 335, 78 p.

Goodfellow, W.D., Cecile, M.P., and Leybourne, M.I., 1995, Geochemistry, petrogenesis, and tectonic setting of lower Paleozoic alkalic and potassic volcanic rocks, Northern Canadian Cordilleran Miogeocline: Canadian Journal of Earth Sciences, v. 32, p. 1236-1254.

Leslie, C.D., 2009, Detrital zircon geochronology and rift-related magmatism: central Mackenzie Mountains, Northwest Territories [M.Sc. thesis] University of British Columbia, 224 p.

Location 6

Gull Lake Formation mafic volcanic mbr.

Upper Cambrian-Upper Ordovician

Abbott, G., 1997, Geology of the Upper Hart River Area, Eastern Ogilvie Mountains, Yukon Territory 9116A/10, 116A/11: Exploration and Geological Services Division, Yukon, Indian and Northern Affairs Canada, Bulletin 9, 92 p.

Murphy, D.C., 1997, Geology of the McQuesten River Region, northern McQuesten and Mayo Map Areas, Yukon Territory (115P/14, 15, 16; 105M/13, 14): Yukon Geological Survey, Bulletin 6, 95 p.

Pigage, L.C., Roots, C.F., and Abbott, J.G., 2015, Regional bedrock geology for Coal River map area (NTS 95D), southeast Yukon: Yukon Geological Survey, Bulletin 17, 155 p.

Location 7

Mountain Diatreme

Middle to Upper Ordovician (ca. 460-452 Ma)

McArthur, M.L., Tipnis, R.S., and Godwin, C.I., 1980, Early and Middle Ordovician conodont fauna from the Mountain diatreme, northern Mackenzie Mountains, District of Mackenzie: Geological Survey of Canada Paper 80-1A, p. 363–368.

Godwin, C.I., and Price, B.J., 1986, Geology of the Mountain diatreme kimberlite, north-central Mackenzie Mountains, District of Mackenzie, Northwest Territories, *in* Morin, J.A., ed., Mineral Deposits of Northern Cordillera Symposium: Canadian Institute of Mining and Metallurgy, Special Paper, v. 37, p. 87-99.

Leslie, C.D., 2009, Detrital zircon geochronology and rift-related magmatism: central Mackenzie Mountains, Northwest Territories [M.Sc. thesis] University of British Columbia, 224 p.

Location 8
Old Cabin Formation (Niddery volcanics/Gull Lake Formation mafic volcanic member)
Upper Cambrian-Silurian

Cecile, M.P., 2000, Geology of the northeastern Niddery Lake map area, east-central Yukon and adjacent Northwest Territories: Geological Survey of Canada Bulletin, v. 553, 120 p.

Cecile, M.P., and Abbott, J.G. 1992, Geology of the Niddery Lake Map-area (1 : 250000 scale): Geological Survey of Canada, Open File Report 2465.

Hart, C.J.R., 1986, Geology of the Old Cabin Creek Massif, Selwyn Basin, Yukon Territory [B.Sc. thesis]: McMaster University, 135 p.

Roots, C.F., Abbott, J.G., Cecile, M.P., Gordey, S.P., and Orchard, M.J., 1995, New stratigraphy and structures in eastern Lansing map area, central Yukon: Current Research, Part A; Geological Survey of Canada, Paper 1995A, p. 141-148

Roots, C.F., 2003, Bedrock geology of Lansing Range map area (NTS 105N), central Yukon: Yukon Geological Survey, Geoscience Map 2003-1.

Location 10
Old Cabin Formation (Plateau Mtn. volcanics/ Gull Lake Formation mafic volcanic member)
Middle Cambrian-Ordovician

Roots, C.F., 1997, Bedrock geology of Mayo map area, central Yukon (NTS 105M). Exploration and Geological Services Division, Indian and Northern Affairs Canada, Geoscience Map 1997-1, 1:250 000-scale.

Roots, C.F., 2003, Bedrock geology of Lansing Range map area (NTS 105N), central Yukon. Yukon Geological Survey, Geoscience Map 2003-1.

Location 11

Vulcan volcanics (Haywire Formation/Sapper volcanics)

Upper Cambrian-Middle Ordovician

Gordey, S.P., and Anderson, R.G., 1993, Evolution of the northern Cordilleran miogeocline, Nahanni map area (105 I), Yukon and Northwest Territories: Geological Survey of Canada, Memoir 428, 214 p.

Goodfellow, W.D., Cecile, M.P., and Leybourne, M.I., 1995, Geochemistry, petrogenesis, and tectonic setting of lower Paleozoic alkalic and potassic volcanic rocks, Northern Canadian Cordilleran Miogeocline: Canadian Journal of Earth Sciences, v. 32, p. 1236-1254.

Location 12

Menzie Creek Formation

Lower Ordovician-Lower Silurian

Gordey, S.P., 1983, Thrust faults in the Anvil Range and a new look at the Anvil Range Group, south-central Yukon Territory: Current research, part A. Geological Survey of Canada, Paper 83-lA, p. 225-227.

Pigage, L.C., 2004, Bedrock geology compilation of the Anvil District (parts of NTS 105K/2, 3, 4, 5, 6, 7 and 11), central Yukon: Yukon Geological Survey, Bulletin 15, 103 p.

Cobbett, R., 2016, Preliminary observations on the geology of Tay Mountain Area (parts of NTS 105K/12 and 13, 105L/09 and 16), central Yukon, *in* MacFarlane, K.E., and Nordling, M.G., eds., Yukon Exploration and Geology 2015: Yukon Geological Survey, p. 79-98.

Location 13

Itsi Lake

Lower Ordovician-Lower Silurian

Goodfellow, W.D., Cecile, M.P., and Leybourne, M.I., 1995, Geochemistry, petrogenesis, and tectonic setting of lower Paleozoic alkalic and potassic volcanic rocks, Northern Canadian Cordilleran Miogeocline: Canadian Journal of Earth Sciences, v. 32, p. 1236-1254.

Location 14

Headwaters Volcanics (Sekwi Formation)

Ediacaran-Ordovician

Blusson, S.L. 1966, Frances Lake, Yukon Territory: Geological Survey of Canada, Map 6-1966.

Blusson, S.L. 1968, Geology and tungsten deposits near the headwaters of Flat River, Yukon Territory and southwestern District of Mackenzie: Geological Survey of Canada, Paper 67-22.

Gabrielse, H., Blusson, S.L., and Roddick, J.A., 1973, Geology of Flat River, Glacier Lake, and Wrigley Lake map-areas, District of Mackenzie and Yukon Territory: Geological Survey of Canada, Memoir 366, 153 p.

Gordey, S.P., and Anderson, R.G., 1993, Evolution of the northern Cordilleran miogeocline, Nahanni map area (105 I), Yukon and Northwest Territories: Geological Survey of Canada, Memoir 428, 214 p.

Location 15

Groundhog and Cloutier Formations

Upper Cambrian-Lower Ordovician (ca. 488-473 Ma)

Gordey, S.P., 1981, Stratigraphy, structure, and tectonic evolution of the southern Pelly Mountains in the Indigo Lake area, Yukon Territory: Geological Survey of Canada, Bulletin 318, 44 p.

Tempelman-Kluit, D.J., 2012, Geology of Quiet Lake and Finlayson Lake map areas, south-central Yukon: An early interpretation of bedrock stratigraphy and structure: Geological Survey of Canada, Open File 5487, 103 p.

Beranek, L.P., Piercey, S.J., Campbell, R., and Wawrzonkowski, P., 2016, Paleozoic stratigraphy, tectonics and metallogeny of the Pelly Mountains, Quiet Lake and Finlayson Lake map areas (NTS105F and G), central Yukon: Project outline and preliminary field results, *in* MacFarlane, K.E., and Nordling, M.G., eds., Yukon Exploration and Geology 2015: Yukon Geological Survey, p. 17-28.

Campbell, R.W., and Beranek, L.P., 2017, Volcanic stratigraphy of the Cambrian-Ordovician Kechika group, Pelly Mountains, south-central Yukon, *in* MacFarlane, K.E., and Weston, L.H., eds., Yukon Exploration and Geology 2016: Yukon Geological Survey, p. 25-45.

Location 16

Askin group Orange Volcanics mbr.

Silurian

Tempelman-Kluit, D.J., 2012, Geology of Quiet Lake and Finlayson Lake map areas, south-central Yukon: An early interpretation of bedrock stratigraphy and structure: Geological Survey of Canada, Open File 5487, 103 p.

Beranek, L.P., Piercey, S.J., Campbell, R., and Wawrzonkowski, P., 2016, Paleozoic stratigraphy, tectonics and metallogeny of the Pelly Mountains, Quiet Lake and Finlayson Lake map areas (NTS105F and G), central Yukon: Project outline and preliminary field results, *in* MacFarlane, K.E., and Nordling, M.G., eds., Yukon Exploration and Geology 2015: Yukon Geological Survey, p. 17-28.

Campbell, R.W., and Beranek, L.P., 2017, Volcanic stratigraphy of the Cambrian-Ordovician Kechika group, Pelly Mountains, south-central Yukon, *in* MacFarlane, K.E., and Weston, L.H., eds., Yukon Exploration and Geology 2016: Yukon Geological Survey, p. 25-45.

Location 16

Crow Formation (Gusty Volcanics; Toobally Volcanics)

Upper Cambrian-Lower Ordovician

Gabrielse, H., and Blusson, S.L., 1969, Geology of Coal River map-area, Yukon Territory and District of Mackenzie (95 D): Geological Survey of Canada, Paper 68-38, 22 p.

Goodfellow, W.D., Cecile, M.P., and Leybourne, M.I., 1995, Geochemistry, petrogenesis, and tectonic setting of lower Paleozoic alkalic and potassic volcanic rocks, Northern Canadian Cordilleran Miogeocline: Canadian Journal of Earth Sciences, v. 32, p. 1236-1254.

Pigage, L.C., 2009, Bedrock geology of NTS 95C/5 (Pool Creek) and NTS 95D/8 map sheets, southeast Yukon: Yukon Geological Survey, Bulletin 16, 150 p.

Pigage, L.C., Crowley, J.L., Pyle, L.J., Abbott, J.G., Roots, C.F., and Schmitz, M.D., 2012, U–Pb zircon age of an Ordovician tuff in southeast Yukon: implications for the age of the Cambrian–Ordovician boundary. Canadian Journal of Earth Sciences, v. 49, p. 732-741, doi:10.1139/e2012-017.

Pigage, L.C., Roots, C.F., and Abbott, J.G., 2015, Regional bedrock geology for Coal River map area (NTS 95D), southeast Yukon: Yukon Geological Survey, Bulletin 17, 155 p.

Rabbitkettle Formation (Coal River Volcanics)
Upper Cambrian-Middle Ordovician

Gabrielse, H., and Blusson, S.L., 1969, Geology of Coal River map-area, Yukon Territory and District of Mackenzie (95 D): Geological Survey of Canada, Paper 68-38, 22 p.

Goodfellow, W.D., Cecile, M.P., and Leybourne, M.I., 1995, Geochemistry, petrogenesis, and tectonic setting of lower Paleozoic alkalic and potassic volcanic rocks, Northern Canadian Cordilleran Miogeocline: Canadian Journal of Earth Sciences, v. 32, p. 1236-1254.

Pigage, L.C., Roots, C.F., and Abbott, J.G., 2015, Regional bedrock geology for Coal River map area (NTS 95D), southeast Yukon: Yukon Geological Survey, Bulletin 17, 155 p.

Sunblood Formation
Middle Ordovician

Gabrielse, H., and Blusson, S.L., 1969, Geology of Coal River map-area, Yukon Territory and District of Mackenzie (95 D): Geological Survey of Canada, Paper 68-38, 22 p.

Gabrielse, H., Blusson, S.L., and Roddick, J.A., 1973, Geology of Flat River, Glacier Lake, and Wrigley Lake map-areas, District of Mackenzie and Yukon Territory: Geological Survey of Canada, Memoir 366, 153 p.

Goodfellow, W.D., Cecile, M.P., and Leybourne, M.I., 1995, Geochemistry, petrogenesis, and tectonic setting of lower Paleozoic alkalic and potassic volcanic rocks, Northern Canadian Cordilleran Miogeocline: Canadian Journal of Earth Sciences, v. 32, p. 1236-1254.

Pigage, L.C., Roots, C.F., and Abbott, J.G., 2015, Regional bedrock geology for Coal River map area (NTS 95D), southeast Yukon: Yukon Geological Survey, Bulletin 17, 155 p.

Location 17

Vampire-Narchilla Formation

Ediacaran-Upper Cambrian

Pigage, L.C., Roots, C.F., and Abbott, J.G., 2015, Regional bedrock geology for Coal River map area (NTS 95D), southeast Yukon: Yukon Geological Survey, Bulletin 17, 155 p.

Location 18

Rabbit intrusives (Kechika Formation)

Lower Cambrian-Silurian

Gabrielse, H., 1963, Geology of Rabbit River, British Columbia: Geological Survey of Canada, Map 46-1962

Location 19

Looncry Volcanics (Kechika Formation and Sandpile Group)

Upper Cambrian-Silurian

Gabrielse, H., 1963, McDame map-area, Cassiar District, British Columbia: Geological Survey of Canada, Memoir 3 19.

Location 20

Matulka group (Upper Gatatga volcanics)

Ediacaran-Middle Cambrian

Eyster, A., Ferri, F., Schmitz, M.D., and Macdonald, F.A., 2018, One diamictite and two rifts: Stratigraphy and geochronology of the Gataga Mountain of northern British Columbia: American Journal of Science, v. 318, p. 167-207.

Ferri, F., Rees, C., Nelson, J., and Legun, A., 1999, Geology and Mineral Deposits of the Northern Kechika Trough between Gataga River and the 60th Parallel: Geological Survey Branch, Mineral Resources Division, British Columbia Ministry of Energy and Mines Bulletin 107, 122 p.

Location 21

Ospika Volcanics (Kechika Formation)

Middle-Upper Ordovician

Gabrielse, H., 1975, Geology of Fort Grahame E 112 map-area, British Columbia: Geological Survey of Canada, Paper 75-33.

MacIntyre, D.G., 1998, Geology, geochemistry and mineral deposits of the Akie River Area, northeast British Columbia: British Columbia, Ministry of Energy and Mines, Bulletin 103, p. 1-91.

Pyle, L.J., and Barnes, C.R., 2003, Lower Paleozoic stratigraphic and biostratigraphic correlations in the Canadian Cordillera: implications for the tectonic evolution of the Laurentian margin: Canadian Journal of Earth Sciences, v. 40, p. 1739-1753, doi:10.1139/e03-049.

Location 22

Redfern Intrusives (Kechika Formation)

Upper Cambrian-Middle Ordovician

Taylor, G.C., and Stott, D.F., 1973, Tuchodi Lakes map-area, British Columbia (94K): Geological Survey of Canada, Memoir 373, 37 p.

Location 23

Lady Laurier Volcanics (Skoki Formation)

Middle-Upper Ordovician

Thompson, R.I., 1989, Stratigraphy, tectonic evolution and structural analysis of the Halfway River map-area (94 B), Northern Rocky Mountains, British Columbia. Geological Survey of Canada, Memoir 425.

Location 24

Golden Columbia icefield diatremes

Cambrian-Upper Devonian

Pell, J., 1987, Alkaline ultrabasic rocks in British Columbia: carbonatites, nepheline syenites, kimberlites, ultramafic lamprophyres and related rocks: British Columbia Ministry of Energy, Mines, and Petroleum Resources, Geological Survey Branch, Open File 1987-17, p. 259-272.

Blue River area diatremes (Felix and little Chicago Carbonatites, and alkalic intrusive rocks)

Upper Cambrian (ca. 498-490 Ma)

Millonig, L.J., Gerdes, A., and Groat, L.A., 2012, U–Th–Pb geochronology of meta-carbonatites and meta-alkaline rocks in the southern Canadian Cordillera: a geodynamic perspective: Lithos, v. 152, p. 202-217, doi:10.1016/j.lithos.2012.06.016.

Location 25

Snowshoe Group

Ediacaran-Upper Cambrian(?)

Ferri, F., and Schiarizza, P., 2006, Re-interpretation of Snowshoe group stratigraphy across a southwest-verging nappe structure and its implications for regional correlations within the Kootenay terrane, *in* Colpron, M., and Nelson, J.L., eds., Paleozoic Evolution and Metallogeny of Pericratonic Terranes at the Ancient Pacific Margin of North America, Canadian and Alaskan Cordillera: Geological Association of Canada, Special Paper, 45, p. 415-432.

Location 26

Eagle Bay Assemblage

Ediacaran-Cambrian(?)

Paradis, S., Bailey, S.L., Creaser, R.A., Piercey, S.J., Schiarizza, P., Colpron, M., and Nelson, J.L., 2006, Paleozoic magmatism and syngenetic massive sulphide deposits of the Eagle Bay assemblage, Kootenay terrane, southern British Columbia, *in* Colpron, M., and Nelson, J.L., eds., Paleozoic evolution and metallogeny of pericratonic terranes at the ancient Pacific margin of North America, Canadian and Alaskan Cordillera: Geological Association of Canada Special Paper, 45, p. 383-414.

Location 27

Jowett Formation

Upper Ordovician-Silurian

Logan, J.M., and Colpron, M., 2006, Stratigraphy, geochemistry, syngenetic sulphide occurrences and tectonic setting of the lower Paleozoic Lardeau Group, northern Selkirk Mountains, British Columbia, *in* Colpron, M., and Nelson, J.L., eds., Paleozoic Evolution and Metallogeny of Pericratonic Terranes at the Ancient Pacific Margin of North America, Canadian and Alaskan Cordillera: Geological Association of Canada, Special Paper 45, p. 361-382.

Index Formation (Lardeau volcanics)

Middle Cambrian-Lower Ordovician

Lane, L.S., 1977, Geology of the Gold-Stream River – Downie Creek area, Southeastern British Columbia: British Columbia Ministry of Mines and Petroleum Resources, Preliminary Map 25.

Logan, J.M., and Colpron, M., 2006, Stratigraphy, geochemistry, syngenetic sulphide occurrences and tectonic setting of the lower Paleozoic Lardeau Group, northern Selkirk Mountains, British Columbia, *in* Colpron, M., and Nelson, J.L., eds., Paleozoic Evolution and Metallogeny of Pericratonic Terranes at the Ancient Pacific Margin of North America, Canadian and Alaskan Cordillera: Geological Association of Canada, Special Paper 45, p. 361-382.

Hamill Group volcanics

Ediacaran (ca. 570 Ma)

Colpron, M., Logan, J.M., and Mortensen, J.K., 2002, U-Pb zircon age constraint for late Neoproterozoic rifting and initiation of the lower Paleozoic passive margin of western Laurentia: Canadian Journal of Earth Sciences, v. 39, no. 2, p. 133-143, doi:10.1139/E01-069.

Location 28

Southern Rocky Mountain diatremes (Mount Dingley diatreme, Summer diatreme, McKay volcanics, Bear Lake-Rualt lake volcanics and diatremes)

Upper Cambrian-Middle Ordovician

Helmstaedt, H.H., Mott, J.A., Hall, D.C., Schulze, D.J., and Dixon, J.M. 1988, Stratigraphic and structural setting of intrusive breccia diatremes in the White River - Bull River area, southeastern British Columbia: British Columbia Ministry of Energy, Mines and Petroleum Resources, Paper 1988-1, p. 363-368.

Norford, B.S., and Cecile, M.P, 1994a, Cambrian and Ordovician rocks in the McKay Group and Beaverfoot Formation, Western Ranges of the Rocky Mountains, Southern British Columbia, *in* Current research, part A. Geological Survey of Canada, Paper 94-lA, p. 83-90.

Norford, B.S., and Cecile, M.P., 1994b, Ordovician emplacement of the Mount Dingley Diatreme, Western Ranges of the Rocky Mountains, southeastern British Columbia: Canadian Journal of Earth Sciences, v. 31 p. 1491 - 1500.

Pell, J., 1987, Alkaline ultrabasic rocks in British Columbia: carbonatites, nepheline syenites, kimberlites, ultramafic lamprophyres and related rocks: British Columbia Ministry of Energy, Mines, and Petroleum Resources, Geological Survey Branch, Open File 1987-17, p. 259-272.

Fish Lake volcanics (Donald Formation)
Upper Cambrian
Kubli, T.E., and Simony, P.S., 1992, The Dogtooth High, northern Purcell Mountains, British Columbia: Bulletin of Canadian Petroleum Geology, v. 40, p. 36-51.

Location 29
Snowcap assemblage, Yukon-Tanana terrane
Neoproterozoic-Devonian
Piercey, S.J., and Colpron, M., 2009, Composition and provenance of the Snowcap assemblage, basement to the Yukon-Tanana terrane, northern Cordillera: Implications for Cordilleran crustal growth: Geosphere, v. 5, p. 439-464, doi:10.1130/GES00505.1.

Appendix 2. Table of CA-ID-TIMS results from the Pacific Centre of Isotopic and Geochemical Research, University of British Columbia

		Compositional Parameters								Radiogenic Isotope Ratios									Isotopic Ages				
	Wt.	U	Pb	Th/U	^{206}Pb*/	mol %	Pb*/	Pb$_c$	^{206}Pb/	^{208}Pb/	^{207}Pb/		^{207}Pb/		^{206}Pb/		corr.	^{207}Pb/		^{207}Pb/		^{206}Pb/	
Sample	mg	ppm	ppm		x10^{-13} mol	^{206}Pb*	Pb$_c$	(pg)	^{204}Pb	^{206}Pb	^{206}Pb	% err	^{235}U	% err	^{238}U	% err	coef.	^{206}Pb	±	^{235}U	±	^{238}U	±
(a)	(b)	(c)	(c)	(d)	(e)	(e)	(e)	(e)	(f)	(g)	(g)	(h)	(g)	(h)	(g)	(h)		(i)	(h)	(i)	(h)	(i)	(h)
42LB14: Groundhog formation pyroxene gabbro (Sheep Creek stock; 08V 615130E 6824768N NAD 83)																							
A	0.0005	1412	154.0	1.476	2.3190	97.83%	17	4.22	853	0.461	0.0569	0.805	0.6174	0.876	0.07875	0.184	0.477	485.9	17.8	488.2	3.4	488.68	0.86
B	0.0007	1169	122.4	1.523	2.6746	99.65%	111	0.76	5352	0.479	0.0572	0.291	0.6182	0.353	0.07835	0.157	0.583	500.2	6.4	488.7	1.4	486.26	0.74
C	0.0012	855	85.7	1.315	3.3665	99.73%	136	0.75	6858	0.411	0.0569	0.564	0.6173	0.577	0.07870	0.182	0.229	487.4	12.4	488.2	2.2	488.34	0.85
E	0.0006	776	78.2	1.312	1.5260	99.47%	69	0.67	3494	0.411	0.0569	0.312	0.6169	0.359	0.07863	0.139	0.511	487.8	6.9	487.9	1.4	487.94	0.65
24LB15: Groundhog formation pyroxene gabbro (Groundhog Creek sill complex; 08V 604846E 6843856N NAD 83)																							
A	0.0002	389	46.5	2.091	0.2105	97.44%	17	0.45	722	0.660	0.056991	1.393	0.597725	1.471	0.076066	0.241	0.399	491.19	30.72	475.79	5.59	472.60	1.10
B	0.0080	153	22.0	0.155	6.8493	97.62%	12	13.65	776	0.057	0.085550	0.675	1.594449	0.725	0.135173	0.172	0.401	1328.03	13.06	968.04	4.52	817.31	1.32
C	0.0004	208	25.2	2.255	0.2821	98.03%	22	0.46	940	0.706	0.056506	0.894	0.593487	0.948	0.076176	0.199	0.372	472.29	19.77	473.09	3.59	473.26	0.91
15RC14: Groundhog formation pyroxene gabbro (Cloutier Creek stock; 08V 645834E 6834843N NAD 83)																							
A	0.0029	637	44.4	1.816	3.795	99.80%	207	0.62	9380	0.574	0.05464	0.121	0.3722	0.211	0.04940	0.122	0.869	397.6	2.7	321.25	0.58	310.82	0.37
B	0.0081	564	38.2	1.783	9.129	99.58%	96	3.17	4394	0.564	0.05454	0.166	0.3613	0.243	0.04805	0.118	0.793	393.4	3.7	313.18	0.66	302.51	0.35
C	0.0022	830	56.1	1.967	3.543	99.73%	153	0.80	6748	0.622	0.05426	0.134	0.3474	0.208	0.04644	0.098	0.857	381.8	3.0	302.80	0.54	292.64	0.28
D	0.0062	528	40.0	2.287	6.681	99.75%	178	1.38	7391	0.723	0.05467	0.120	0.3706	0.200	0.04917	0.104	0.881	398.7	2.7	320.11	0.55	309.41	0.31
E	0.0018	1016	79.9	2.218	4.021	99.79%	205	0.71	8610	0.701	0.05491	0.139	0.3915	0.217	0.05170	0.110	0.835	408.6	3.1	335.43	0.62	324.98	0.35
F	0.0001	238	21.9	1.309	0.063	94.95%	7	0.28	366	0.412	0.05640	3.504	0.4938	3.770	0.06349	0.421	0.665	468.3	77.6	407.49	12.65	396.83	1.62
G	0.0001	170	14.9	1.565	0.041	95.46%	8	0.16	407	0.493	0.05625	4.703	0.4528	5.047	0.05839	0.464	0.762	462.1	104.2	379.26	15.97	365.83	1.65
H	0.0001	262	18.2	1.336	0.051	94.12%	6	0.26	315	0.423	0.05425	3.060	0.3500	3.280	0.04678	0.314	0.724	381.6	68.8	304.69	8.63	294.74	0.91
J	0.0001	260	28.0	1.405	0.076	93.29%	5	0.45	276	0.441	0.05680	6.473	0.5486	6.946	0.07006	0.533	0.896	483.7	142.9	444.09	24.99	436.49	2.25
20LB15: Polymictic conglomerate (08V 653904E 6828411N NAD 83)																							
A	0.005	98	7.8	0.850	1.2826	99.71%	115	0.30	6427	0.268	0.055662	0.158	0.528017	0.306	0.068800	0.210	0.876	438.92	3.53	430.49	1.07	428.92	0.87
B	0.0023	64	26.7	1.083	1.9895	98.83%	30	1.94	1575	0.316	0.112036	0.203	5.040132	0.375	0.326273	0.272	0.850	1832.71	3.68	1826.09	3.18	1820.29	4.32
C	0.0048	309	29.2	1.111	4.7947	99.87%	272	0.51	14299	0.348	0.056786	0.112	0.609741	0.231	0.077875	0.140	0.934	483.25	2.48	483.40	0.89	483.43	0.65
D	0.0038	30	2.7	0.683	0.3732	99.08%	34	0.28	2017	0.214	0.056878	0.361	0.611914	0.460	0.078027	0.190	0.673	486.80	7.96	484.77	1.77	484.34	0.89
E	0.0017	147	47.4	0.301	3.2466	99.72%	106	0.75	6562	0.089	0.108436	0.121	4.648161	0.260	0.310890	0.177	0.917	1773.31	2.20	1757.96	2.17	1745.08	2.70
F	0.0016	167	15.4	0.865	0.8642	98.91%	30	0.78	1702	0.272	0.057110	0.916	0.615290	0.965	0.078139	0.240	0.322	495.77	20.18	486.89	3.73	485.01	1.12
G	0.0017	90	7.6	0.845	0.4463	97.88%	15	0.79	873	0.272	0.057089	2.246	0.546186	2.392	0.069388	0.351	0.477	494.98	49.50	442.49	8.58	432.47	1.47
H	0.0015	49	30.9	0.740	1.6051	99.31%	50	0.91	2691	0.204	0.181592	0.536	12.949321	0.637	0.517190	0.352	0.541	2667.46	8.88	2675.97	6.01	2687.25	7.73
44LB15: Askin group tuff (08V 625978E 6845601N NAD 83)																							
A	0.0010	21	10.0	0.877	0.3373	97.71%	15	0.65	807	0.252	0.124222	0.424	6.314569	0.732	0.368677	0.530	0.821	2017.73	7.51	2020.48	6.42	2023.17	9.20
B	0.0007	124	10.0	0.661	0.2379	97.82%	14	0.44	847	0.208	0.055753	0.782	0.537105	0.874	0.069870	0.204	0.545	442.55	17.38	436.51	3.10	435.37	0.86
C	0.0006	92	31.3	0.736	0.6519	99.40%	55	0.33	3067	0.217	0.102766	0.159	4.154888	0.330	0.293229	0.240	0.891	1674.68	2.94	1665.17	2.70	1657.65	3.51
D	0.0008	64	46.6	1.562	1.0543	99.42%	70	0.50	3203	0.437	0.187845	0.119	13.326878	0.314	0.514551	0.249	0.936	2723.38	1.97	2703.09	2.97	2676.03	5.45
E	0.0013	38	9.8	0.344	0.4939	97.84%	13	0.90	855	0.102	0.087611	0.447	2.874289	0.582	0.237941	0.272	0.673	1373.97	8.60	1375.20	4.39	1375.99	3.37
F	0.0018	122	47.4	0.834	3.0828	99.66%	99	0.87	5395	0.242	0.112193	0.505	5.112101	0.617	0.330471	0.266	0.598	1835.24	9.14	1838.12	5.24	1840.66	4.26

(a) A, B etc. are labels for fractions composed of single zircon grains or fragments; all fractions annealed and chemically abraded after Mattinson (2005) and Scoates and Friedman (2008).

(b) Nominal fraction weights estimated from photomicrographic grain dimensions, adjusted for partial dissolution during chemical abrasion.

(c) Nominal U and total Pb concentrations subject to uncertainty in photomicrographic estimation of weight and partial dissolution during chemical abrasion.

(d) Model Th/U ratio calculated from radiogenic 208Pb/206Pb ratio and 207Pb/235U age.

(e) Pb* and Pbc represent radiogenic and common Pb, respectively; mol % 206Pb* with respect to radiogenic, blank and initial common Pb.

(f) Measured ratio corrected for spike and fractionation only. Mass discrimination of 0.30 ± 0.05%/amu based on analysis of NBS-982; all Daly analyses.

(g) Corrected for fractionation, spike, and all common Pb was assumed to be procedural blank: 206Pb/204Pb = 18.50 ± 1.0%; 207Pb/204Pb = 15.50 ± 1.0%; 208Pb/204Pb = 38.40 ± 1.0% (all uncertainties 1-sigma).

(h) Errors are 2-sigma, propagated using the algorithms of Schmitz and Schoene (2007) and Crowley et al. (2007).

(i) Calculations are based on the decay constants of Jaffey et al. (1971). 206Pb/238U and 207Pb/206Pb ages corrected for initial disequilibrium in 230Th/238U using Th/U [magma] = 3.

Campbell et al.
GSA Data Repository 2
Concordia plots for CA-TIMS zircon U-Pb samples

Sheep Creek stock (42LB14)
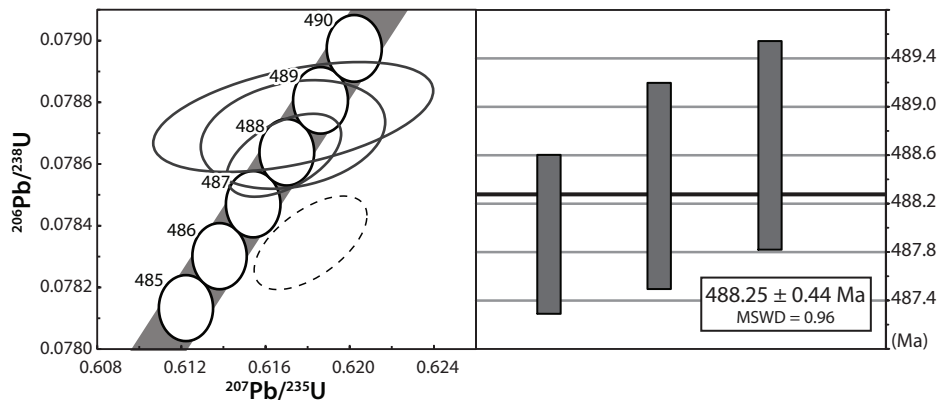
Cloutier Creek stock (15RC14)

Grains that underwent a single leach step only.

Intercepts at 167 ± 17 Ma
& 486 ± 19 Ma
MSWD = 1.14

All analyses
Four relatively large ellipses are associated with residual material that survived second leach step.

Intercepts at 167 ± 16 Ma
& 486 ± 19 Ma
MSWD = 0.56
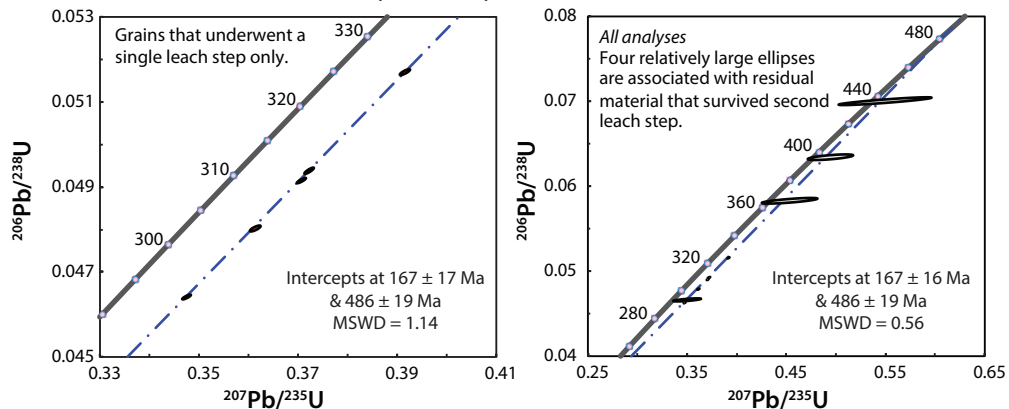
Groundhog Creek sill (24LB15)

488.25 ± 0.44 Ma
MSWD = 0.96

472.99 ± 0.70 Ma
MSWD = 0.85
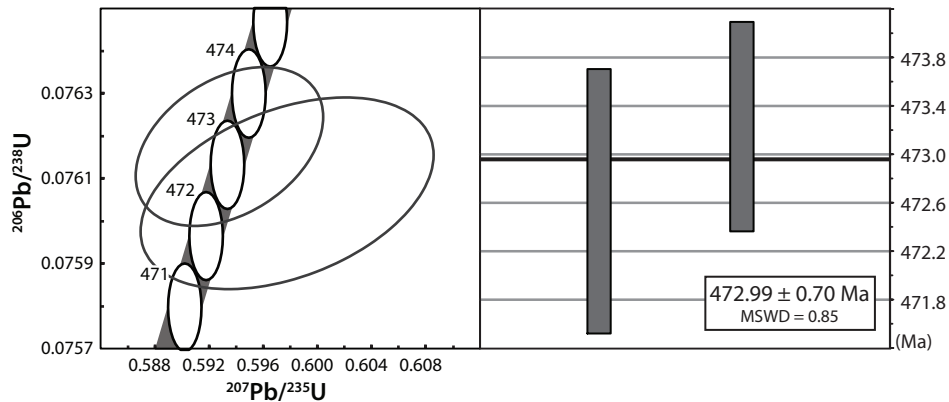
Campbell et al.
GSA Data Repository 2
Concordia plots for CA-TIMS zircon U-Pb samples

Polymictic conglomerate (20LB15)
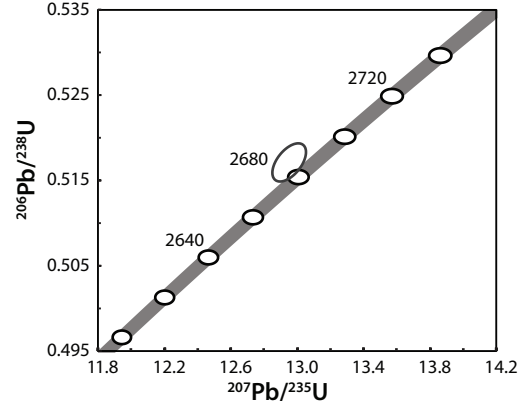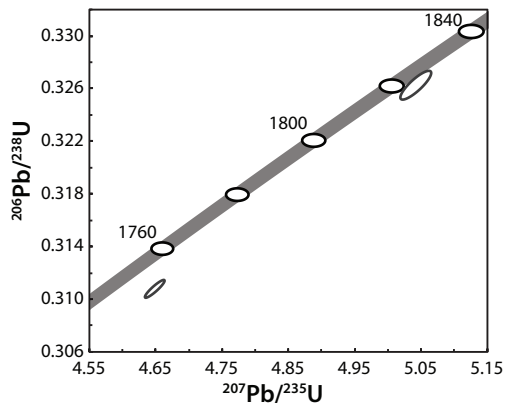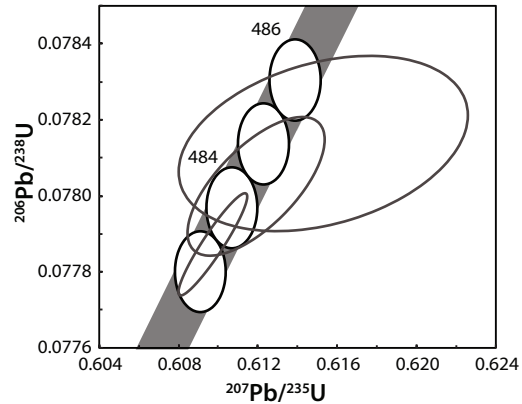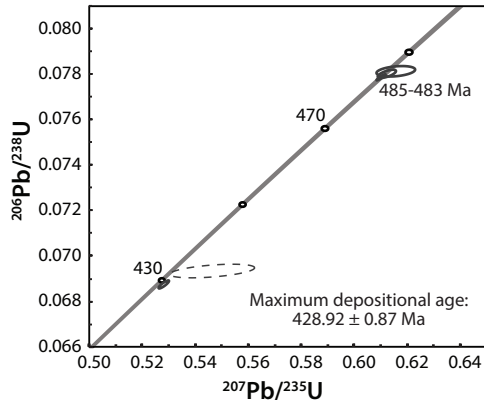
Maximum depositional age:
428.92 ± 0.87 Ma

Askin group tuff (44LB15)

Maximum depositional age:
435.37 ± 0.86 Ma
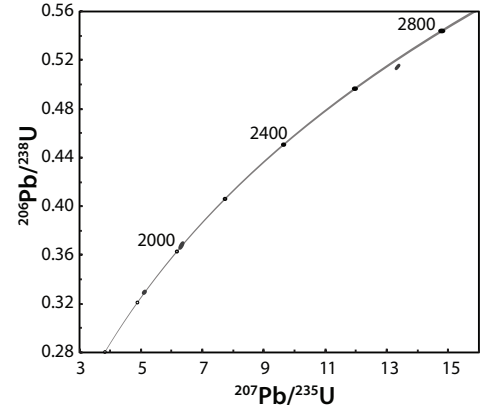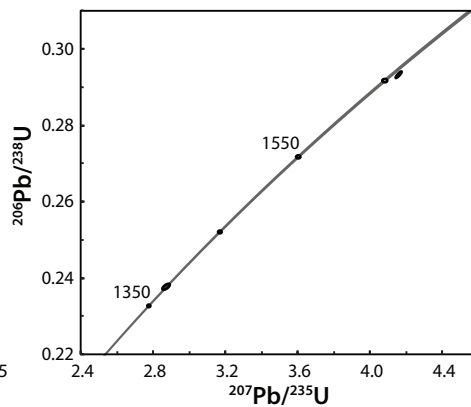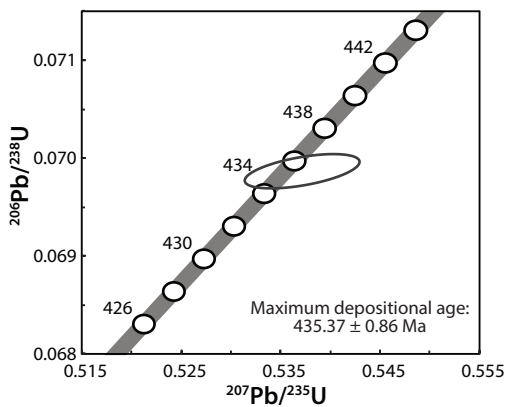
Appendix 3. Whole-rock geochemical data for basaltic rocks from the Kechika group

Sample	15RC 26	21LB14	25LB14	15RC 10	15RC 11	15RC 12	15RC 14	15RC 16	15RC 19	15RC 27	15RC 28	15RC 30	24LB15	42LB14	16RC23
Lithology	amygdaloidal basalt	basalt	basalt	gabbro sill	gabbro sill	gabbro sill	gabbroic stock	gabbro sill	gabbro sill	gabbro sill	gabbro sill	gabbro	pyroxene gabbro	Pyroxene gabbro	gabbro
UTM Zone	08V	08V	08V	08V	08V	08V	08V	08V	08V	08V	08V	08V	08V	08V	08V
Easting (NAD 83)	645297	626471	626414	604401	604503	605699	645712	645297	644934	626206	626012	625679	604846	615130	636380
Northing (NAD 83)	6835602	6836926	6836907	6843672	6843715	6844480	6834820	6835602	6835719	6844674	6844841	6845219	6843856	6824768	6842919
Formation	Groundhog	Groundhog	Groundhog	Groundhog	Groundhog	Groundhog	Groundhog	Groundhog	Groundhog	Groundhog	Groundhog	Groundhog	Groundhog	Groundhog	Groundhog
Location	Ram Creek	McConnell River headwaters	McConnell River headwaters	East of Lapie Lakes	East of Lapie Lakes	East of Lapie Lakes	Cloutier Creek area	Cloutier Creek area	Cloutier Creek area	Ram Creek	Ram Creek	Ram Creek	East of Lapie Lakes	Pass Peak area	South of Mount Green
SiO_2	38.50	46.61	44.89	45.61	46.83	56.48	55.59	49.90	48.60	37.78	41.71	47.26	50.14	54.98	48.66
Al_2O_3	11.68	16.02	15.48	12.33	11.85	18.86	13.33	15.51	15.19	11.22	16.82	14.33	11.87	15.26	12.31
$Fe_2O_{3(T)}$	11.22	11.73	11.37	11.59	10.97	6.73	12.18	11.19	11.44	12.54	13.97	13.12	7.66	8.07	10.50
MnO	0.12	0.17	0.20	0.21	0.14	0.07	0.09	0.12	0.11	0.17	0.15	0.17	0.16	0.11	0.12
MgO	5.36	4.14	4.04	9.44	9.68	2.76	3.25	5.33	6.34	8.97	6.59	5.77	10.01	3.37	4.76
CaO	12.80	5.98	7.24	8.65	7.59	1.83	2.88	3.73	3.73	11.66	4.97	3.77	11.33	4.14	7.71
Na_2O	1.88	4.87	5.22	2.96	2.30	5.70	4.42	4.95	4.34	0.61	4.33	4.53	2.08	4.88	4.03
K_2O	0.30	0.60	0.30	0.92	0.54	2.37	1.30	0.37	0.15	0.02	0.05	0.33	2.27	3.00	0.09
TiO_2	3.95	2.45	2.38	2.20	2.14	1.57	2.06	2.91	3.96	3.14	3.72	5.85	1.95	1.73	2.69
Ti	23668	14688	14268	13207	12853	9406	12336	17415	23758	18830	22313	35041	11660	10371	16133
P_2O_5	0.70	0.81	0.74	0.31	0.32	0.38	0.79	0.43	0.44	0.52	0.94	0.36	0.28	0.38	0.34
LOI	14.07	6.13	7.43	6.14	7.88	3.81	3.84	5.04	6.34	13.79	7.37	4.76	2.73	4.09	7.71
Total	101	100	99	100	100	101	100	99	101	100	101	100	101	100	99
Sc	33.00	13.74	9.79	33.00	34.00	5.00	14.00	20.00	22.00	28.00	18.00	31.00	34.00	13.38	25.00
Be	1.00	N.D.	N.D.	3.00	2.00	2.00	2.00	2.00	1.00	2.00	2.00	1.00	2.00		1.00
V	373	214	217	286	282	61	124	224	293	301	333	439	238	162	236
Cr	410	15	15	540	550	20	< 20	110	30	420	30	40	720	90	310
Co	48.00	30.99	28.22	48.00	43.00	9.00	21.00	30.00	33.00	49.00	37.00	46.00	35.00	19.52	38.00
Ni	110	19	18	190	130	< 20	< 20	60	30	150	< 20	40	100	25	130
Cu	120	10	28	20	30	< 10	30	80	100	100	20	230	30	15	110
Zn	100	118	98	260	70	30	130	200	130	110	180	120	80	87	110
Ga	18.00	19.45	17.64	20.00	17.00	23.00	26.00	25.00	24.00	18.00	24.00	23.00	16.00	19.76	19.00
Ge	2.00	N.D.	N.D.	2.00	1.80	1.50	1.60	1.60	1.40	1.80	1.60	1.60	1.70	N.D.	1.30
As	< 5	N.D.	N.D.	< 5	< 5	< 5	< 5	< 5	< 5	< 5	< 5	< 5	< 5	N.D.	< 5
Rb	10.00	10.64	3.70	12.00	9.00	79.00	19.00	6.00	3.00	< 1	1.00	7.00	51.00	106.33	2.00
Sr	560	210	264	204	289	190	179	382	484	619	444	456	272	246	547
Y	24.60	33.08	30.17	20.30	20.30	26.80	42.30	27.40	29.60	20.90	33.90	24.20	19.80	24.13	22.20
Zr	284	179	154	162	165	338	331	195	232	216	361	174	182	253	174
Nb	90.50	77.76	69.19	41.20	43.90	101.00	36.70	28.90	34.10	75.50	129.00	30.10	43.90	73.19	24.10
Mo	< 2	3.01	2.39	< 2	< 2	< 2	< 2	< 2	< 2	< 2	< 2	< 2	< 2	1.12	< 2
Ag	1.80	N.D.	N.D.	1.70	2.00	1.90	3.70	2.00	1.90	1.50	1.80	1.20	0.90	N.D.	0.50
In	< 0.1	N.D.	N.D.	< 0.1	< 0.1	< 0.1	0.10	< 0.1	< 0.1	< 0.1	< 0.1	< 0.1	< 0.1	N.D.	< 0.1
Sn	2.00	0.68	1.17	1.00	1.00	4.00	4.00	2.00	2.00	1.00	2.00	2.00	< 1	2.38	2.00
Sb	4.40	0.25	0.35	9.30	8.20	5.30	8.00	12.20	5.40	1.30	1.60	3.50	1.30	0.19	< 0.2
Cs	0.60	0.42	0.17	0.50	1.10	2.50	5.00	0.70	0.80	0.20	0.60	3.80	1.00	4.57	1.30
Ba	116	705	337	314	221	722	697	387	155	38	124	511	1207	484	114
La	80.40	50.39	45.51	43.20	43.90	91.10	43.90	27.30	31.00	65.00	113.00	21.40	43.90	59.25	19.10
Ce	155	95	86	85	88	171	94	58	65	123	222	47	85	116	42
Pr	17.20	11.21	10.10	9.72	9.76	17.90	11.40	7.22	8.12	13.30	24.40	6.10	9.50	12.37	5.39
Nd	64.60	44.88	40.57	36.70	37.80	62.60	49.30	31.20	34.90	50.20	90.80	27.20	35.20	46.85	23.90
Sm	11.20	8.61	7.85	7.09	7.00	10.00	12.70	7.90	8.69	8.87	15.40	7.23	6.42	8.02	6.02
Eu	2.99	3.35	2.97	1.88	1.94	2.39	3.80	2.65	3.02	2.32	3.91	2.35	1.87	2.01	1.71
Gd	8.48	8.21	7.38	5.77	5.86	7.50	12.30	8.06	8.35	7.13	11.60	7.11	5.51	6.39	6.37
Tb	1.18	1.21	1.07	0.84	0.85	1.07	1.82	1.16	1.32	1.02	1.53	1.05	0.76	0.85	0.95
Dy	6.21	6.45	5.87	4.38	4.67	5.79	9.94	6.30	6.81	5.04	7.90	5.62	4.23	4.96	5.07
Ho	1.02	1.25	1.10	0.79	0.83	1.08	1.68	1.09	1.17	0.85	1.34	0.98	0.74	0.87	0.87
Er	2.67	3.54	3.21	2.10	2.20	3.05	4.33	2.73	3.07	2.21	3.40	2.53	2.02	2.47	2.19
Tm	0.33	0.47	0.42	0.29	0.29	0.44	0.57	0.35	0.41	0.29	0.47	0.32	0.28	0.36	0.28
Yb	1.91	2.96	2.51	1.74	1.76	2.82	3.37	2.04	2.28	1.68	2.67	1.90	1.75	2.15	1.66
Lu	0.27	0.40	0.36	0.27	0.26	0.42	0.49	0.29	0.32	0.24	0.35	0.26	0.27	0.30	0.23
Hf	7.20	3.95	3.38	4.00	4.10	7.60	8.30	5.00	5.90	5.50	7.80	4.40	4.20	5.91	3.80
Ta	6.50	4.66	4.20	2.98	3.14	7.07	2.47	2.15	2.53	5.15	9.37	2.38	3.16	4.44	1.74
W	1.00	0.65	1.83	0.90	0.90	2.10	1.60	< 0.5	1.10	0.70	< 0.5	4.10	1.82		< 0.05
Tl	< 0.05	N.D.	N.D.	< 0.05	< 0.05	0.18	< 0.05	< 0.05	< 0.05	< 0.05	< 0.05	< 0.05	< 0.05	0.12	< 0.05
Pb	9.00	0.62	0.90	91.00	10.00	7.00	7.00	20.00	11.00	7.00	11.00	5.00	8.00	7.36	< 5
Bi	< 0.1	0.01	0.01	0.10	0.10	0.10	0.20	0.30	< 0.1	< 0.1	< 0.1	< 0.1	< 0.1	0.01	< 0.1
Th	9.08	6.91	5.63	7.12	7.33	18.10	6.31	2.91	3.41	7.50	11.80	2.31	8.23	13.49	2.37
U	2.35	4.97	3.17	1.83	1.90	3.91	1.50	0.76	0.81	1.84	2.82	0.58	2.00	2.61	0.59
Cd	N.D.	0.20	0.18	N.D.	N.D.	N.D.	N.D.	N.D.	N.D.	N.D.	N.D.	N.D.	N.D.	0.53	N.D.
Li	N.D.	21.55	14.76	N.D.	N.D.	N.D.	N.D.	N.D.	N.D.	N.D.	N.D.	N.D.	N.D.	N.D.	N.D.
Mg number	34.68	28.17	28.31	47.51	49.51	31.31	22.87	34.61	38.12	44.29	34.39	32.83	59.22	31.70	33.50

Mg number = MgO/(FeOt+MgO)*100 where FeO = Fe2O3*0.8998

Sample	15RC 26	21LB14	25LB14	15RC 10	15RC 11	15RC 12	15RC 14	15RC 16	15RC 19	15RC 27	15RC 28	15RC 30	24LB15	42LB14	16RC23
Al_2O_3/Na_2O	6.2	3.3	3.0	4.2	5.2	3.3	3.0	3.1	3.5	18.4	3.9	3.2	5.7	3.1	3.1
Al_2O_3/TiO_2	3.0	6.5	6.5	5.6	5.5	12.0	6.5	5.3	3.8	3.6	4.5	2.5	6.1	8.8	4.6
Zr/Ti	0.0	0.0	0.0	0.0	0.0	0.0	0.0	0.0	0.0	0.0	0.0	0.0	0.0	0.0	0.0
Zr/Y	11.5	5.4	5.1	8.0	8.1	12.6	7.8	7.1	7.8	10.3	10.6	7.2	9.2	10.5	7.8
Zr/Yb	148.7	60.4	61.3	93.1	93.8	119.9	98.2	95.6	101.8	128.6	135.2	91.6	104.0	117.7	104.8
Zr/Sm	25.4	20.8	19.6	22.8	23.6	33.8	26.1	24.7	26.7	24.4	23.4	24.1	28.3	31.6	28.9
Zr/Ni	2.6	9.4	8.5	0.9	1.3	<LOD	<LOD	3.3	7.7	1.4	N.D.	4.4	1.8	10.2	1.3
Cr/Ni	3.7	0.8	0.8	2.8	4.2	<LOD	<LOD	1.8	1.0	2.8	N.D.	1.0	7.2	3.6	2.4
Nb/Y	3.7	2.4	2.3	2.0	2.2	3.8	0.9	1.1	1.2	3.6	3.8	1.2	2.2	3.0	1.1
Ti/V	63.5	68.7	65.6	46.2	45.6	154.2	99.4	77.7	81.1	62.6	67.0	79.8	49.0	64.2	68.4
La/Sm $_{mn}$	4.6	3.8	3.7	3.9	4.1	5.9	2.2	2.2	2.3	4.7	4.7	1.9	4.4	4.8	2.1
Nb/Th $_{mn}$	1.2	1.3	1.5	0.7	0.7	0.7	0.7	1.2	1.2	1.2	1.3	1.6	0.6	0.6	1.2
Sm/Yb $_{mn}$	6.5	3.2	3.5	4.5	4.4	3.9	4.2	4.3	4.2	5.9	6.4	4.2	4.1	4.1	4.0
Zr/Nb	3.1	2.3	2.2	3.9	3.8	3.3	9.0	6.7	6.8	2.9	2.8	5.8	4.1	3.5	7.2
Nb/Yb	47.4	26.3	27.6	23.7	24.9	35.8	10.9	14.2	15.0	44.9	48.3	15.8	25.1	34.0	14.5
Nb/Th	10.0	11.3	12.3	5.8	6.0	5.6	5.8	9.9	10.0	10.1	10.9	13.0	5.3	5.4	10.2
Nb/Ta	13.9	16.7	16.5	13.8	14.0	14.3	14.9	13.4	13.5	14.7	13.8	12.6	13.9	16.5	13.9
Zr/Hf	39.4	45.3	45.5	40.5	40.2	44.5	39.9	39.0	39.3	39.3	46.3	39.5	43.3	42.8	45.8

Appendix 3. Whole-rock geochemical data for basaltic rocks from the Kechika group (continued)

Sample	16RC27	16RC29	15RC 01	15RC 02	15RC 30.5	15RC 31	15RC 32	48LB14	51LB14	52LB14	16RC05	16RC07
Lithology	gabbro	gabbro	basalt	basalt	amygdaloidal basalt	basalt	basalt	basalt	amygdaloidal basalt	basalt	pillow basalt	sheared mafic rock
UTM Zone	08V	08V	08V	08V	08V	09V	09V	08V	08V	08V	08V	08V
Easting (NAD 83)	637693	637566	654103	653996	625696	351363	351363	654215	654215	654215	654399	654448
Northing (NAD 83)	6829110	6829243	6828969	6828683	6845399	6811775	6811802	6828915	6828925	6828925	6823016	6822885
Formation	Groundhog	Groundhog	Cloutier	Cloutier	Cloutier/Magundy	Cloutier	Cloutier	Cloutier	Cloutier	Cloutier	Cloutier	Cloutier
Location	Northwest of Ketza River Mine	Northwest of Ketza River Mine	East of Ketza River Mine	East of Ketza River Mine	Ram Creek	McNeil Lake	McNeil Lake	East of Ketza River Mine	East of Ketza River Mine	East of Ketza River Mine	South of Ketza River Mine	South of Ketza River Mine
SiO_2	46.23	41.82	44.74	45.14	42.91	50.79	51.13	33.02	41.41	42.44	49.92	49.25
Al_2O_3	15.76	13.26	13.38	16.82	13.22	11.01	10.97	17.42	15.44	11.60	11.29	10.12
$Fe_2O_{3(T)}$	12.72	12.03	11.84	14.32	11.24	9.76	11.69	16.18	10.41	10.77	10.67	11.29
MnO	0.10	0.16	0.14	0.08	0.12	0.26	0.12	0.03	0.13	0.09	0.15	0.12
MgO	4.94	4.67	2.66	3.43	15.01	8.99	8.51	7.75	3.42	15.14	7.51	6.45
CaO	5.26	10.65	6.20	2.27	4.33	8.02	6.65	6.86	7.30	5.89	8.41	7.89
Na_2O	3.24	3.09	1.26	0.18	0.34	4.38	4.56	0.68	2.27	0.28	3.22	1.62
K_2O	0.49	0.03	3.07	6.82	0.95	0.34	0.26	2.39	4.04	0.02	1.60	0.67
TiO_2	3.13	2.79	3.29	3.55	2.44	2.52	2.11	3.29	3.28	1.94	2.35	4.56
Ti	18758	16714	19748	21270	14622	15077	12661	19724	19664	11630	14082	27319
P_2O_5	0.79	0.70	0.38	0.59	0.69	0.28	0.23	0.85	0.62	0.46	0.36	0.74
LOI	5.92	9.88	13.49	5.32	9.18	3.72	2.96	11.83	11.45	11.35	4.13	6.22
Total	99	99	100	99	100	100	99	101	100	100	100	99
Sc	15.00	18.00	22.00	20.00	39.00	25.00	22.00	32.86	20.58	25.92	21.00	23.00
Be	1.00	< 1	2.00	1.00	2.00	1.00	2.00	N.D.	N.D.	N.D.	2.00	3.00
V	184	284	293	251	290	219	198	319	240	255	212	461
Cr	40	30	40	240	1140	460	500	976	208	1101	330	110
Co	30.00	31.00	17.00	30.00	53.00	44.00	37.00	48.73	13.55	53.61	44.00	37.00
Ni	40	50	40	100	320	210	220	400	72	326	200	120
Cu	20	40	< 10	100	80	70	100	167	148	92	60	150
Zn	130	110	< 30	70	90	110	90	74	14	136	100	110
Ga	25.00	20.00	22.00	25.00	15.00	16.00	13.00	20.72	23.65	13.14	18.00	20.00
Ge	2.20	1.70	0.90	1.10	1.60	1.70	1.30	N.D.	N.D.	N.D.	1.50	1.80
As	< 5	< 5	< 5	< 5	< 5	< 5	< 5	N.D.	N.D.	N.D.	< 5	< 5
Rb	17.00	< 1	48.00	81.00	13.00	4.00	5.00	34.65	65.86	0.31	18.00	15.00
Sr	203	421	167	67	237	99	73	116	129	221	174	268
Y	34.10	31.00	27.00	23.70	23.80	24.40	25.90	17.32	27.17	19.36	25.00	38.00
Zr	311	207	205	223	205	169	153	332	251	174	209	352
Nb	51.80	51.90	27.70	34.80	101.00	28.90	27.80	147.20	49.45	85.32	38.60	58.90
Mo	< 2	< 2	< 2	< 2	< 2	< 2	< 2	0.84	1.54	1.67	< 2	< 2
Ag	1.10	0.60	0.70	0.90	1.40	4.30	3.20	N.D.	N.D.	N.D.	0.60	1.20
In	< 0.1	< 0.1	< 0.1	< 0.1	< 0.1	< 0.1	< 0.1	N.D.	N.D.	N.D.	< 0.1	< 0.1
Sn	2.00	2.00	2.00	2.00	1.00	1.00	1.00	2.19	2.50	1.58	2.00	2.00
Sb	0.20	0.40	3.00	4.50	0.50	2.40	2.00	0.08	0.12	0.15	< 0.2	< 0.2
Cs	0.80	0.20	3.60	10.40	1.60	0.40	0.50	1.68	4.27	1.04	1.00	8.90
Ba	128	23	3042	3651	1282	109	100	1350	4975	73	899	830
La	49.00	45.70	25.00	29.20	73.20	20.20	31.00	54.91	33.57	50.90	40.70	36.90
Ce	103	92	53	63	135	43	52	100	68	96	74	89
Pr	12.30	10.80	6.60	7.49	14.20	5.13	5.76	9.90	8.33	10.60	8.54	12.40
Nd	50.00	42.10	28.30	33.00	51.10	22.00	24.50	36.90	36.09	40.97	34.00	56.30
Sm	10.40	8.72	6.99	7.53	8.56	5.86	6.32	5.66	8.18	6.86	7.50	12.80
Eu	2.77	2.13	2.25	2.01	2.60	1.96	2.08	1.75	2.77	1.88	2.96	4.18
Gd	8.89	7.96	7.36	6.98	6.89	6.38	6.37	4.46	8.07	5.21	7.59	11.90
Tb	1.31	1.16	1.09	1.00	0.97	0.98	1.03	0.63	1.13	0.76	1.07	1.68
Dy	7.10	6.38	5.91	5.56	5.06	5.45	5.69	3.66	6.14	4.16	5.65	8.34
Ho	1.25	1.16	1.07	0.96	0.92	0.95	0.99	0.66	1.03	0.74	0.96	1.40
Er	3.27	3.02	2.68	2.34	2.52	2.48	2.52	1.78	2.65	2.03	2.48	3.65
Tm	0.44	0.39	0.34	0.30	0.34	0.32	0.33	0.25	0.34	0.29	0.31	0.47
Yb	2.55	2.36	1.98	1.82	2.12	1.96	1.99	1.38	1.86	1.59	1.88	2.72
Lu	0.37	0.36	0.29	0.29	0.26	0.31	0.27	0.29	0.18	0.25	0.25	0.28	0.40
Hf	6.70	4.30	5.00	5.30	4.60	4.10	4.20	7.34	5.84	4.18	4.50	7.40
Ta	3.51	3.50	2.06	2.70	6.85	1.84	1.70	8.74	2.87	5.00	2.64	4.34
W	0.80	< 0.05	0.16	0.36	< 0.05	< 0.05	< 0.05	1.36	1.03	1.61	1.80	0.50
Tl	< 0.05	< 0.05	0.16	0.36	< 0.05	2.20	< 0.05	N.D.	N.D.	N.D.	0.09	0.11
Pb	< 5	< 5	< 5	< 5	< 5	5.00	13.00	1.65	1.26	8.46	< 5	< 5
Bi	< 0.1	< 0.1	< 0.1	< 0.1	< 0.1	< 0.1	< 0.1	0.00	0.00	0.02	< 0.1	< 0.1
Th	5.00	4.92	3.07	3.44	10.20	2.95	2.90	11.98	3.99	7.66	4.59	4.27
U	1.32	1.26	0.70	0.68	2.34	0.79	0.76	2.27	0.97	3.64	1.18	1.00
Cd	N.D.	N.D.	N.D.	N.D.	N.D.	N.D.	N.D.	0.28	0.20	0.26	N.D.	N.D.
Li	N.D.	N.D.	N.D.	N.D.	N.D.	N.D.	N.D.	145.23	20.13	150.55	N.D.	N.D.
Mg number	30.15	30.14	19.98	21.02	59.74	50.59	44.72	34.74	26.75	60.97	43.89	38.83

Sample	16RC27	16RC29	15RC 01	15RC 02	15RC 30.5	15RC 31	15RC 32	48LB14	51LB14	52LB14	16RC05	16RC07
Al_2O_3/Na_2O	4.9	4.3	10.6	93.4	38.9	2.5	2.4	25.6	6.8	41.4	3.5	6.2
Al_2O_3/TiO_2	5.0	4.8	4.1	4.7	5.4	4.4	5.2	5.3	4.7	6.0	4.8	2.2
Zr/Ti	0.0	0.0	0.0	0.0	0.0	0.0	0.0	0.0	0.0	0.0	0.0	0.0
Zr/Y	9.1	6.7	7.6	9.4	8.6	6.9	5.9	19.2	9.3	9.0	8.4	9.3
Zr/Yb	122.0	87.7	103.5	122.5	96.7	86.2	76.9	240.9	135.2	109.5	111.2	129.4
Zr/Sm	29.9	23.7	29.3	29.6	23.9	28.8	24.2	58.7	30.7	25.4	27.9	27.5
Zr/Ni	7.8	4.1	5.1	2.2	0.6	0.8	0.7	0.8	3.5	0.5	1.0	2.9
Cr/Ni	1.0	0.6	1.0	2.4	3.6	2.2	2.3	2.4	2.9	3.4	1.7	0.9
Nb/Y	1.5	1.7	1.0	1.5	4.2	1.2	1.1	8.5	1.8	4.4	1.5	1.6
Ti/V	101.9	58.9	67.4	84.7	50.4	68.8	63.9	61.9	82.0	45.6	66.4	59.3
La/Sm_{mn}	3.0	3.4	2.3	2.5	5.5	2.2	3.2	6.3	2.7	4.8	3.5	1.9
Nb/Th_{mn}	1.2	1.3	1.1	1.2	1.2	1.2	1.1	1.5	1.5	1.3	1.0	1.6
Sm/Yb_{mn}	4.5	4.1	3.9	4.6	4.5	3.3	3.5	4.6	4.9	4.8	4.4	5.2
Zr/Nb	6.0	4.0	7.4	6.4	2.0	5.8	5.5	2.3	5.1	2.0	5.4	6.0
Nb/Yb	20.3	22.0	14.0	19.1	47.6	14.7	14.0	106.7	26.6	53.7	20.5	21.7
Nb/Th	10.4	10.5	9.0	10.1	9.9	9.8	9.6	12.3	12.4	11.1	8.4	13.8
Nb/Ta	14.8	14.8	13.4	12.9	14.7	15.7	16.4	16.8	17.2	17.1	14.6	13.6
Zr/Hf	46.4	48.1	41.0	42.1	44.6	41.2	36.4	45.3	43.1	41.6	46.4	47.6

Appendix 3. Whole-rock geochemical data for basaltic rocks from the Kechika group (continued)

Sample	16RC12	16RC02	16RC04
Lithology	vesicular basalt sill	gabbro	gabbro
UTM Zone	08V	08V	08V
Easting (NAD 83)	652074	654314	654386
Northing (NAD 83)	6831774	6823099	6823055
Formation	Cloutier	Cloutier	Cloutier
Location	Northeast of Ketza River Mine	South of Ketza River Mine	South of Ketza River Mine
SiO_2	38.10	53.60	49.87
Al_2O_3	9.84	14.67	13.78
$Fe_2O_{3(T)}$	13.68	12.79	11.78
MnO	0.13	0.11	0.17
MgO	8.42	7.20	4.94
CaO	13.23	1.65	4.10
Na_2O	0.17	3.47	5.38
K_2O	0.06	0.03	0.32
TiO_2	3.07	2.55	4.68
Ti	18411	15275	28051
P_2O_5	0.52	0.27	0.50
LOI	11.22	4.42	4.19
Total	98	101	100
Sc	29.00	26.00	24.00
Be	1.00	1.00	2.00
V	309	241	312
Cr	800	240	70
Co	62.00	45.00	37.00
Ni	240	140	110
Cu	100	70	100
Zn	100	140	120
Ga	17.00	24.00	22.00
Ge	1.90	1.80	1.40
As	< 5	< 5	< 5
Rb	2.00	< 1	22.00
Sr	549	94	383
Y	23.20	27.50	29.80
Zr	228	198	230
Nb	74.70	15.50	29.20
Mo	< 2	< 2	< 2
Ag	0.60	0.60	0.70
In	< 0.1	< 0.1	< 0.1
Sn	2.00	2.00	2.00
Sb	< 0.2	< 0.2	< 0.2
Cs	0.50	0.20	12.20
Ba	73	58	451
La	61.80	16.90	29.00
Ce	120	38	60
Pr	13.50	4.95	7.51
Nd	51.40	22.10	32.80
Sm	9.46	6.27	8.55
Eu	2.98	1.85	2.75
Gd	7.54	7.07	8.63
Tb	1.00	1.10	1.23
Dy	5.19	6.26	6.53
Ho	0.85	1.10	1.11
Er	2.26	2.88	2.79
Tm	0.29	0.39	0.37
Yb	1.65	2.31	2.20
Lu	0.23	0.33	0.31
Hf	5.60	4.70	5.30
Ta	4.96	1.14	2.18
W	8.80	0.50	< 0.5
Tl	< 0.05	< 0.05	0.15
Pb	< 5	< 5	< 5
Bi	< 0.1	< 0.1	< 0.1
Th	7.56	4.00	3.79
U	1.88	0.94	0.95
Cd	N.D.	N.D.	N.D.
Li	N.D.	N.D.	N.D.
Mg number	40.62	38.49	31.79

Sample	16RC12	16RC02	16RC04
Al_2O_3/Na_2O	57.9	4.2	2.6
Al_2O_3/TiO_2	3.2	5.8	2.9
Zr/Ti	0.0	0.0	0.0
Zr/Y	9.8	7.2	7.7
Zr/Yb	138.2	85.7	104.5
Zr/Sm	24.1	31.6	26.9
Zr/Ni	1.0	1.4	2.1
Cr/Ni	3.3	1.7	0.6
Nb/Y	3.2	0.6	1.0
Ti/V	59.6	63.4	89.9
La/Sm $_{mn}$	4.2	1.7	2.2
Nb/Th $_{mn}$	1.2	0.5	0.9
Sm/Yb $_{mn}$	6.4	3.0	4.3
Zr/Nb	3.1	12.8	7.9
Nb/Yb	45.3	6.7	13.3
Nb/Th	9.9	3.9	7.7
Nb/Ta	15.1	13.6	13.4
Zr/Hf	40.7	42.1	43.4

Total Alkali silica plot
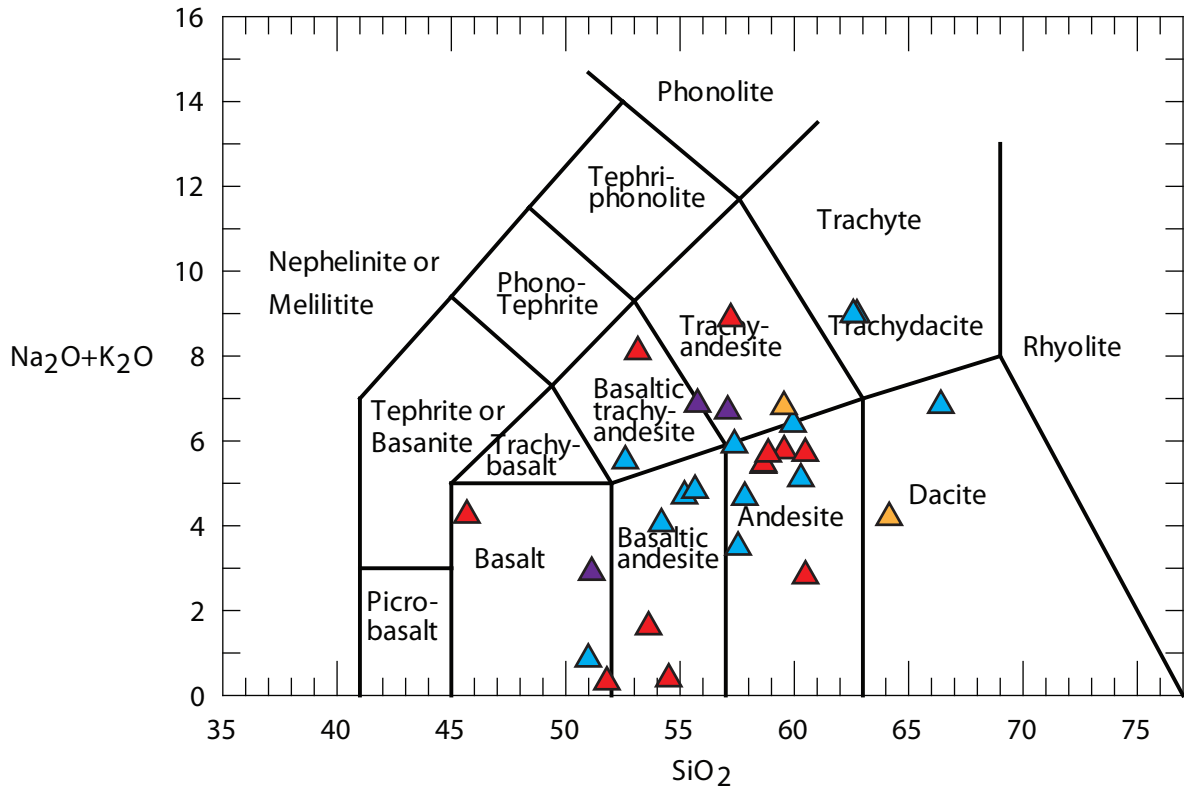
AFM plot
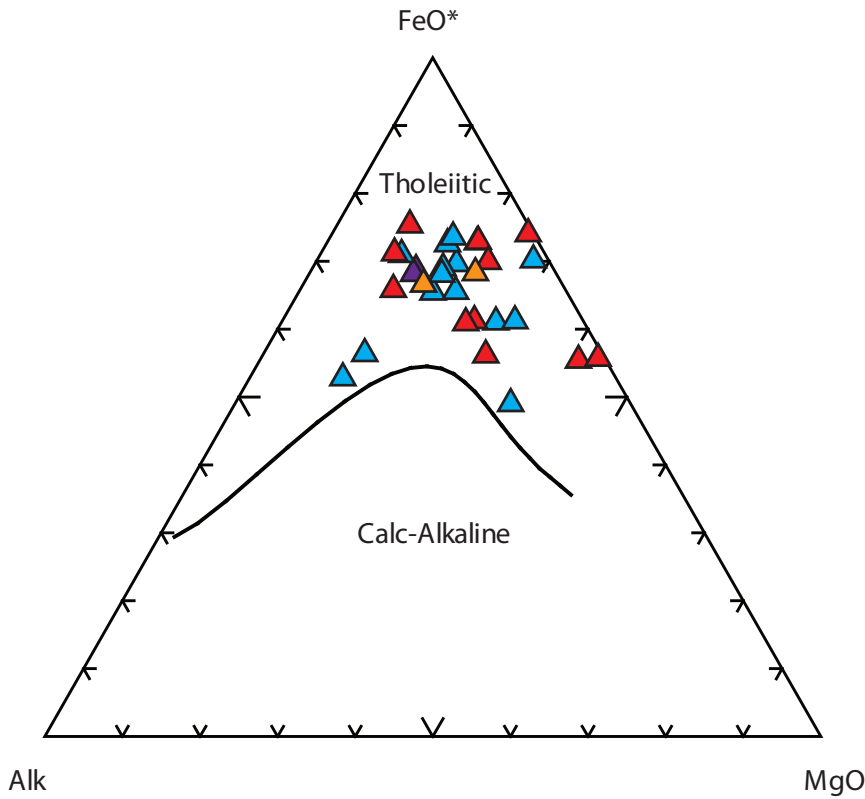
Appendix 4. Nd-Hf isotope results from the Pacific Centre of Isotopic and Geochemical Research, University of British Columbia

Sample	Lithology	Formation	Age (m.y.)	Sm (ppm)	Nd (ppm)	Lu (ppm)	Hf (ppm)	$^{147}Sm/^{144}Nd$	$^{143}Nd/^{144}Nd$	Uncertainty $\pm2s_m$	ε_{Ndt0}	ε_{Ndti}	$T_{DM}(Nd)$	$^{176}Lu/^{177}Hf$	$^{176}Hf/^{177}Hf$	Uncertainty $\pm2s_m$	$\varepsilon_{Hf(t=0)}$	$\varepsilon_{Hf(t)}$	$T_{DM}(Hf)$
21LB14	basalt	Groundhog	480	8.61	44.88	0.40	3.95	0.1160	0.512660	0.000006	0.6	5.5	672 Ma	0.0144	0.282800	0.000004	0.5	6.6	936 Ma
25LB14	basalt	Groundhog	480	7.85	40.57	0.36	3.38	0.1170	0.512665	0.000008	0.7	5.5	672 Ma	0.0153	0.282799	0.000003	0.5	6.3	975 Ma
42LB14	pyroxene gabbro	Groundhog	488	8.02	46.85	0.30	5.91	0.1034	0.512117	0.000007	-10.0	-4.2	1359 Ma	0.0073	0.282268	0.000004	-18.3	-9.8	1618 Ma
48LB14	basalt	Cloutier	480	5.66	36.90	0.18	7.34	0.0928	0.512548	0.000007	-1.6	4.7	685 Ma	0.0034	0.282670	0.000005	-4.1	5.5	841 Ma
51LB14	amygdaloidal basalt	Cloutier	480	8.18	36.09	0.25	5.84	0.1369	0.512592	0.000006	-0.7	2.9	1000 Ma	0.0061	0.282619	0.000005	-5.9	2.9	992 Ma
52LB14	basalt	Cloutier	480	6.86	40.97	0.25	4.18	0.1012	0.512533	0.000007	-1.9	3.9	758 Ma	0.0087	0.282644	0.000004	-5.0	3.0	1032 Ma
15RC14	gabbro	Groundhog	480	12.70	49.30	0.49	8.30	0.1557	0.512553	0.000006	-1.5	1.0	1445 Ma	0.0084	0.282574	0.000005	-7.5	0.6	1145 Ma
24LB15	gabbro	Groundhog	473	6.42	35.20	0.27	4.20	0.1102	0.512271	0.000005	-7.0	-1.8	1219 Ma	0.0090	0.282404	0.000005	-13.5	-5.8	1469 Ma